

VOLUME XLIV

GEMS & GEMOLOGY

WINTER 2008



*Color Grading
D-to-Z Diamonds*

THE QUARTERLY JOURNAL OF THE GEMOLOGICAL INSTITUTE OF AMERICA

EDITORIAL STAFF

Editor-in-Chief

Alice S. Keller
akeller@gia.edu

Managing Editor

Thomas W. Overton
tom.overton@gia.edu

Technical Editor

Emily V. Dubinsky
emily.dubinsky@gia.edu

Consulting Editor

Carol M. Stockton

Contributing Editor

James E. Shigley

Editor

Brendan M. Laurs
GIA, The Robert Mouawad Campus
5345 Armada Drive
Carlsbad, CA 92008
(760) 603-4503
blaurs@gia.edu

Associate Editor

Stuart D. Overlin
soverlin@gia.edu

Circulation Coordinator

Mary Navarro
(760) 603-4000, ext. 7142
mary.navarro@gia.edu

Editors, Lab Notes

Thomas M. Moses
Shane F. McClure

Editor, Gem News International

Brendan M. Laurs

Editors, Book Reviews

Susan B. Johnson
Jana E. Miyahira-Smith
Thomas W. Overton

Editors, Gemological Abstracts

Brendan M. Laurs
Thomas W. Overton

PRODUCTION STAFF

Art Director

Karen Myers

Production Assistant

Suzan Pearman

G&G Online:

gia.metapress.com

EDITORIAL REVIEW BOARD

Shigeru Akamatsu
Tokyo, Japan

Edward W. Boehm
Solana Beach, California

James E. Butler
Washington, DC

Alan T. Collins
London, United Kingdom

John Emmett
Brush Prairie, Washington

Emmanuel Fritsch
Nantes, France

Henry A. Hänni
Basel, Switzerland

Jaroslav Hyršl
Prague, Czech Republic

A. J. A. (Bram) Janse
Perth, Australia

Alan Jobbins
Caterham, United Kingdom

Mary L. Johnson
San Diego, California

Anthony R. Kampf
Los Angeles, California

Robert E. Kane
Helena, Montana

Lore Kiefert
New York, New York

Thomas M. Moses
New York, New York

Mark Newton
Coventry, United Kingdom

George Rossman
Pasadena, California

Kenneth Scarratt
Bangkok, Thailand

James E. Shigley
Carlsbad, California

Christopher P. Smith
New York, New York

Christopher M. Welbourn
Reading, United Kingdom

SUBSCRIPTIONS

Online subscriptions, and print subscriptions sent to addresses in the U.S., are priced as follows: \$74.95 for one year (4 issues), \$194.95 for three years (12 issues). Print subscriptions sent elsewhere are \$85.00 for one year, \$225.00 for three years. Combination print/online subscriptions are \$99.95 in the U.S. and \$110.00 elsewhere for one year, and \$269.95 in the U.S. and \$300.00 elsewhere for three years. Canadian subscribers should add GST. Discounts of \$10 (one year) and \$15 (three years) are available for renewals, GIA alumni, and current GIA students. Please have your student or alumni number ready when ordering.

Electronic (PDF) versions of all articles and sections from Spring 1981 forward can be purchased at gia.metapress.com for \$10 each. Full issue access can be purchased for \$20.

To purchase subscriptions and print back issues, visit www.gia.edu/gemsandgemology or contact the Circulation Coordinator.

To obtain a Japanese translation of *Gems & Gemology*, contact GIA Japan, Okachimachi Cy Bldg., 5-15-14 Ueno, Taitoku, Tokyo 110, Japan. Our Canadian goods and service registration number is 126142892RT.

Gems & Gemology's impact factor is 1.227 (ranking 11th out of the 26 journals in the Mineralogy category), according to Thomson Scientific's 2007 Journal Citation Reports (issued July 2008). *Gems & Gemology* is abstracted in Thompson Scientific products (*Current Contents: Physical, Chemical & Earth Sciences* and *Science Citation Index—Expanded*, including the Web of Knowledge) and other databases. For a complete list, see www.gia.edu/gemsandgemology.

Gems & Gemology welcomes the submission of articles on all aspects of the field. Please see the Guidelines for Authors on our Website, or contact the Managing Editor. Letters on articles published in *Gems & Gemology* are also welcome.

Abstracting is permitted with credit to the source. Libraries are permitted to photocopy beyond the limits of U.S. copyright law for private use of patrons. Instructors are permitted to photocopy isolated articles for noncommercial classroom use without fee. Copying of the photographs by any means other than traditional photocopying techniques (Xerox, etc.) is prohibited without the express permission of the photographer (where listed) or author of the article in which the photo appears (where no photographer is listed). For other copying, reprint, or republication permission, please contact the Managing Editor.

Gems & Gemology is published quarterly by the Gemological Institute of America, a nonprofit educational organization for the gem and jewelry industry, The Robert Mouawad Campus, 5345 Armada Drive, Carlsbad, CA 92008.

Postmaster: Return undeliverable copies of *Gems & Gemology* to GIA, The Robert Mouawad Campus, 5345 Armada Drive, Carlsbad, CA 92008.

Any opinions expressed in signed articles are understood to be the opinions of the authors and not of the publisher.

DATABASE COVERAGE

MANUSCRIPT SUBMISSIONS

COPYRIGHT AND REPRINT PERMISSIONS

ABOUT THE COVER



FSC

Mixed Sources
Product group from well-managed
forests, controlled sources and
recycled wood or fiber

Cert no. SW-COC-002272
www.fsc.org
© 1996 Forest Stewardship Council

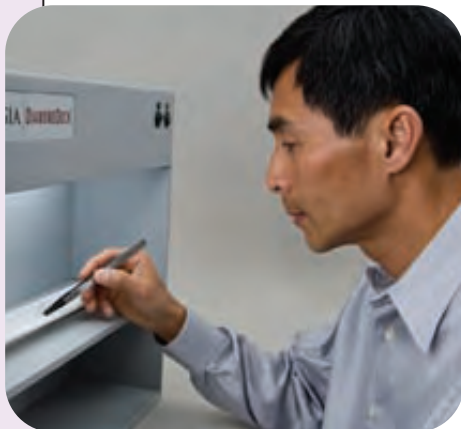
The GIA D-to-Z color grading system revolutionized the manufacture of diamond jewelry because it allowed for tighter control over the quality of the diamonds used in individual pieces. At the same time, an important market developed for the finest, D-color, diamonds, as represented by the rings shown here. The D color, VVS2 round brilliant in the ring on the right weighs 7.12 ct; courtesy of Harry Winston Inc. The D color, VVS2 heart-shaped diamond in the other ring weighs 10 ct; from Mona Lee Nesselth, Custom Estate Jewels (courtesy of a private collector). The diamonds in the pin have colors ranging from F to I, and their total weight is 21.10 carats; courtesy of Louis Glick & Co. The necklace is a diamond sautoir by Van Cleef & Arpels, Paris, circa 1925; courtesy of a private collector.

Photo © GIA and Harold & Erica Van Pelt.

Color separations for *Gems & Gemology* are by Pacific Plus, Carlsbad, California.

Printing is by Allen Press, Lawrence, Kansas.

© 2008 Gemological Institute of America All rights reserved. ISSN 0016-626X



pg. 310



pg. 323

EDITORIAL

295 Challenges, Changes, and New Directions

Alice S. Keller

FEATURE ARTICLES

296 Color Grading "D-to-Z" Diamonds at the GIA Laboratory



John M. King, Ron H. Geurts, Al M. Gilbertson, and James E. Shigley

Examines the history and current methodology of the GIA Laboratory's system for color grading colorless to light yellow polished diamonds, which is a critical component in the valuation of these gems.

322 Rubies and Sapphires from Winza, Central Tanzania

Dietmar Schwarz, Vincent Pardieu, John M. Saul, Karl Schmetzer, Brendan M. Laurs, Gaston Giuliani, Leo Klemm, Anna-Kathrin Malsy, Eric Erel, Christoph Hauzenberger, Garry Du Toit, Anthony E. Fallick, and Daniel Ohnenstetter

Describes the mining and geology of this new source of untreated rubies, and characterizes the gem corundum produced there, which arrived on the market in early 2008.

348 The Wittelsbach Blue

Rudolf Dröschel, Jürgen Evers, and Hans Ottomeyer

Reviews the colorful past of this 35.56 ct gem, the former crown jewel of Bavaria and one of the largest historic blue diamonds ever fashioned, and presents the results of known gemological investigations.



pg. 353

REGULAR FEATURES

364 Lab Notes

Fancy dark brown-yellow zoned type IIa/IIb diamond • HPHT-treated CVD synthetic diamond submitted for Dossier grading • Quartz with secondary covellite dendrites • Induced copper contamination of tourmaline

369 Gem News International

Andesine from Tibet and Inner Mongolia • Vivid kunzite from Pala, California • Natural pearls of the Veneridae family • Synthetic citrine with abundant nail-head spicules • "Neptunian" beads from Asia • Purplish blue synthetic quartz • Dyed chalcedony resembling chrysocolla

S1 Book Reviews

S4 Gemological Abstracts

S12 Annual Index



pg. 366



Challenges, Changes and New Directions

The current global economic downturn has affected every industry, and ours is no exception. As one consequence, GIA has decided to postpone the second Gemological Research Conference, originally scheduled for August 21–23, 2009. Our foremost concern is that many people who had hoped to participate are now facing significant budget and travel restrictions, so—rather than risk the success of this important event—the conference will wait until the economy improves. Our heartfelt thanks go to everyone who was involved with the 2009 GRC, and we look forward to the time when preparations can be resumed.

To better continue delivering comprehensive research and exceptional gem photography, *Gems & Gemology* will be shifting a portion of its content online, starting with this issue. The Book Reviews and Gemological Abstracts sections are now available (in their entirety) only in electronic form, as are our year-end subject and author indexes, traditionally part of the Winter issue. The annual indexes will also be combined with our online cumulative index, which covers the years 1981–2008. Additional content, such as supplemental tables, spectra, and images, will be featured online in the *G&G* Data Depository. To use these resources, all of them available free of charge, just visit us at www.gia.edu/gemsandgemology.

This issue also marks the long-awaited launch of *Gems & Gemology* Online, which will offer electronic (PDF format) issues concurrently with the printed issue. Subscribers now have the option of receiving their issues in either print or PDF format, or selecting a combination of the two versions for a nominal additional fee of \$25 per year. The online issue will go live the day the printed issue mails (in the case of the present issue, for example, the online version went live Friday, January 16). Those of you, especially overseas, who may have had to wait weeks for your issue to arrive by post will now be able to see it on the Internet the moment it becomes available. Note that we cannot guarantee that the color of the photos seen on

your computer monitor will be the same as that verified by art director Karen Myers while the journal is on press. However, the online version uses the same electronic files that are used for the printed version.

G&G Online is hosted by MetaPress, a division of the world's largest subscription agency, EBSCO, at gia.metapress.com. There you will find electronic versions of every article and journal section from 1981 through the present. Editorials, Letters, Book Reviews, and Gemological Abstracts (as well as all the articles on our Free Downloads page) are available without charge. For a limited time, we are also offering a free look at the entire Fall 2008 issue online. Other articles and sections can be purchased for just \$10 each, and entire issues for \$20 each. (The smaller-format, predominately black-and-white issues from 1934 to 1980 can still be downloaded from the *G&G* web site at no cost.) If you're interested in upgrading your subscription to include online access, please contact our circulation coordinator.

Gems & Gemology is no stranger to challenges and change. When Robert Shipley published the first issue in 1934, the world was in the throes of the Great Depression. When the current large-format version was launched in 1981, the diamond industry was still recovering from the speculative boom and bust of the late 1970s. Now, as we implement these new initiatives in the midst of another period of economic uncertainty, we're confident we can continue to support GIA's mission to ensure the public trust in gems and jewelry by upholding the highest standards of professionalism in one of our industry's most important sectors: gemological research. *G&G* looks forward to maintaining excellence in print and online in 2009 and for many years to come.

Alice S. Keller • Editor-in-Chief • akeller@gia.edu

COLOR GRADING “D-TO-Z” DIAMONDS AT THE GIA LABORATORY

John M. King, Ron H. Geurts, Al M. Gilbertson, and James E. Shigley

Since its introduction in the early 1950s, GIA’s D-to-Z scale has been used to color grade the overwhelming majority of colorless to light yellow gem-quality polished diamonds on which laboratory reports have been issued. While the use of these letter designations for diamond color grades is now virtually universal in the gem and jewelry industry, the use of GIA color grading standards and procedures is not. This article discusses the history and ongoing development of this grading system, and explains how the GIA Laboratory applies it. Important aspects of this system include a specific color grading methodology for judging the absence of color in diamonds, a standard illumination and viewing environment, and the use of color reference diamonds (“master stones”) for the visual comparison of color.

Historically, the evaluation of most gem diamonds focused on the absence of color (Feuchtwanger, 1867; figure 1). Today, this lack of color is expressed virtually worldwide in a grading system introduced by GIA more than 50 years ago that ranges from D (colorless) to Z (light yellow). With the acceptance of this system, color grade has become a critical component in the valuation of diamonds, leading to historic highs at the top end of the scale. In May 2008, the diamond in figure 2 (a 16.04 ct round brilliant that GIA graded D color, VVS2 [potentially Flawless]) sold at Christie’s Hong Kong for a record US\$208,500 per carat for a colorless diamond. At the same auction, a 101.27 ct shield-shaped diamond sold for \$61,500 per carat, a vivid reminder of the impact of even minor differences in grade; it was F color, VVS1. At auction, and throughout the marketplace, differences between adjacent color grades can result in substantial differences in asking price. For example, on December 5, 2008, the *Rapaport Diamond Report* noted an approximately 32% (and *IDEX* about 33%) difference between D and E color for a one carat Internally Flawless round-brilliant diamond. Important price distinctions based on color are not limited to high-end colors and clarities. On the same date, the differ-

ence between G and H color for a one carat round-brilliant diamond of VS1 clarity was about 16% in both *IDEX* and *Rapaport*.

As part of its educational program, GIA has taught the basics of color grading D-to-Z diamonds since the early 1950s. And in the more than five decades since the GIA Laboratory issued its first diamond grading report in 1955 (Shuster, 2003), it has issued reports for millions of diamonds using the D-to-Z system. Throughout this period, GIA has experienced increased demand for its diamond grading services over a growing range of diamond sizes, cutting styles, and color appearances. This has required a continual evolution in the equipment and methods used in the GIA Laboratory, while maintaining the integrity of the grading system itself. At the core of the system’s development has been an ongoing assessment of how best to observe a diamond in order to describe its color consistently. At times, the resulting adjustments have appeared to conflict with earlier statements.

This article reviews the history of the system’s

See end of article for About the Authors and Acknowledgments.
GEMS & GEMOLOGY, Vol. 44, No. 4, pp. 296–321.
© 2008 Gemological Institute of America



Figure 1. Although historically absence of color has been important in selecting diamonds for jewelry, only with the global acceptance of GIA's D-to-Z color grading system has the industry been able to refine that selection to tight tolerances. This contemporary brooch is one example, with all the diamonds in the D-E-F range. Prior to the broad acceptance of the system, as with the 1955 necklace, pieces typically had a greater color range. The brooch, courtesy of Harry Winston Inc., is 21.93 carats total weight. The necklace is about 24 carats total; gift of Harriet B. Cocomo, GIA Collection no. 14188. Photo by Robert Weldon.

development to help clarify the various modifications that have taken place over the years in the color grading equipment and practices used at the GIA Laboratory. We then describe how D-to-Z diamonds are currently graded in the lab, that is, the procedures that have resulted from these years of evolution and refinement. Last, we discuss special considerations in D-to-Z color grading, such as the grading of brown and gray diamonds, the selection process for master color comparison diamonds (“master stones”), and the impact of adopting advanced instrumentation.

BACKGROUND

While there has been evaluation of diamond color (or absence of color) throughout history, the systems and methods used for this purpose were not clearly defined, standardized, or consistently applied before the 1950s. In the late 19th century, color was considered a diamond's most important value factor, but the naming conventions in use at the time placed color in a variety of categories that were general at best. For example, the color appearance of gem diamonds was often described using metaphoric terms (e.g., “River” or “Water” for the most colorless diamonds), or by association with a geographic location from which similarly colored diamonds were commonly seen (e.g., “Wesselton” and “Top Wesselton” for near-colorless diamonds traditionally associated with the Wesselton mine, “Cape” for pale yellow

diamonds from the Cape of Good Hope region, and “Jager” for colorless diamonds with strong fluorescence such as those typically recovered from the “Jagersfontein” mine in South Africa (Shipley, 1950b; Liddicoat, 1993). In the case of *blue white*, abuse of the term eventually prompted action by the U.S. Federal Trade Commission to ban its misuse in diamond marketing (Shipley, 1938).

Recognizing the importance of objective, consistent color communication, GIA—in conjunction with the American Gem Society (AGS)—began work on color grading standards in the 1930s (“Diamond grading instrument . . .,” 1934), and by 1941 had developed a color scale for evaluating diamonds (see following section; Barton, 1941; Shipley and Liddicoat, 1941; AGS, 1955; Shuster, 2003). The development of this “color yardstick,” as it was then described, evolved over the next decade and became the basis for what is known today as the D-to-Z color grading scale.

While color grading was introduced in the early 1940s for AGS members, the general trade was not familiar with the GIA/AGS standard. Richard Liddicoat, who became the executive director of GIA in 1952, created a full diamond grading system that he taught for the first time in 1953 to jewelers in classes around the United States (Shuster, 2003). Soon, other GIA instructors such as Bert Krashes and G. Robert Crowningshield became part of the traveling team that taught this new grading system, which greatly expanded interest in—and use of—this approach.



Figure 2. This 16.04 ct D-color, VVS2 (potentially Flawless) round brilliant set an auction record for per-carat price for a colorless diamond when it sold for US\$208,500 per carat in May 2008. Courtesy of Christie's.

Attracted by the system's ability to generate a diamond's market value based on the new quality grades and other concepts regarding diamond proportions and appearance (Gilbertson, 2007), jewelers flocked to GIA to get a better understanding of diamond valuation. GIA's new system launched the scale of "D to Z" for color grading. Regarding the unusual starting point (the letter *D*), Richard Liddicoat (Liddicoat, n.d.; *Gem Talk*, 1981) stated the choice was made to differentiate the GIA system from other less clearly defined ones that used designations such as "A," "AA," or metaphoric terms like those noted above.

As jewelers went home to grade their own diamonds, they started to question some of their decisions and sent the diamonds to GIA for checking by their instructors. Over time, this informal practice led to GIA's diamond grading laboratory service, with the first formal reports issued in 1955.

For more than 50 years, this grading system has been taught by GIA Education and used in the GIA Laboratory. The combination of understandable letter designations for color grades, the availability of a standardized grading environment and sets of diamonds as color references, and GIA's ability to teach the basics of this system to others provided a new level of stability and confidence in diamond commerce. In the decades since its introduction, the D-to-Z nomenclature has been adopted virtually worldwide for the sale, purchase, and evaluation of pol-

ished diamonds. Consequently, other grading laboratories also use this nomenclature, sometimes in combination with their own. While most claim to use the GIA system, however, it is not likely that it is applied as it is at the GIA Laboratory. *Using the same color grading terms does not constitute adhering to the conditions or methodology of the GIA system.* The reasons for this should be evident by the end of this article.

The Origin of GIA's Viewing and Comparator Standards. In 17th century India, Tavernier (1676) noted, diamonds were color "graded" at night by lamplight. By the 19th century, however, daylight was the worldwide standard in which gemstones were observed to discern their color (Chester, 1910; Cattelle, 1911; Wade, 1915, 1916; Ferguson, 1927). Unfortunately, the characteristics of daylight vary (throughout the day, in different locations around the globe, and at different times of the year), and these differences in light quality can significantly affect the color appearance of gemstones (Cattelle, 1911; Wade, 1915; Sersen and Hopkins, 1989).

The historical methods used to observe and compare diamond color were just as variable as the type of illumination itself. Observers held diamonds in the palms of their hands or between their fingers, typically examining them against a range of different backgrounds (Tavernier, 1676; Mawe, 1823; Feuchtwanger, 1867; Morton, 1878; Wodiska, 1886; "On diamonds," 1902; Wade, 1916). For most of history, of course, diamonds were so rare that very fine color distinctions among them were not needed, so the trade could function using such simple evaluation techniques.

With the discovery of large deposits in southern Africa in the late 19th century, more diamonds entered the marketplace than ever before. This influx generated a greater desire (more specifically, a commercial need) for finer color distinctions. By the early 20th century, certain minimal standards for color grading had evolved, as summarized from Wade (1916):

1. Use "good north light unobstructed by buildings or other objects. There must not be any coloured surface nearby to reflect tinted light, as a false estimate might easily result."
2. Color grade diamonds only between 10 a.m. and 2 p.m.
3. Do not use artificial light.
4. Always use the same location for color grading.

5. Use comparison diamonds.
6. Dim the “fire” (i.e., dispersion) of the diamond, perhaps by breathing on the stone.
7. View the stone on edge as well as face-up (face-up only can yield a false color).
8. Use magnification (aplanatic triplet lens).

Even with these standards, color grading among dealers and retailers was inconsistent; the result in the trade was chaos. Cattelle (1911, p. 134) noted that “Color in diamonds is the opportunity of many dealers, and the despair of others, for it is very deceptive.”

By the mid-20th century, advances in lighting technology and vision science paralleled the jewelry industry’s increasing desire for improvements in diamond color analysis. GIA began one of the earliest efforts to address this desire in the mid-1930s (“Diamond-grading instrument . . .,” 1934; AGS Research Service, 1936), which culminated in a 1941 article by GIA founder Robert Shipley and Richard Liddicoat. Among their concerns was the need for a grading scale with uniform comparators (i.e., color references) that could be used throughout the industry.

Although jewelers commonly kept a few reference diamonds to use for color comparison, there was no standard for such comparators, so the color grade given to a diamond by one jeweler could easily differ from the grade assigned to it by another. Moreover, different jewelers used different sources of light, both artificial and natural, which further complicated their interactions with one another. To address this situation, Shipley and Liddicoat’s 1941 article announced the development of: (1) a visual color comparison instrument (the GIA Colorimeter), (2) a color scale (the “color yardstick”) that represented grade categories, (3) a standardized light source and viewing environment for use by jewelers (the Diamolite), and (4) a service to grade “reference” or “master” diamonds for AGS jewelers to use as comparators.

The GIA Colorimeter and Color Yardstick. Notes and drawings from Shipley in the 1940s indicate that the GIA Colorimeter was adapted from the Duboscq Colorimeter made by Bausch & Lomb, which was widely used in the medical field up to the early 1960s (Warner, 2006). Shipley and Liddicoat’s colorimeter (figure 3) consisted of a small box with an indirect light source and a split-image magnifier that allowed a grader to compare a diamond placed in a tray to a movable, transparent glass wedge that var-

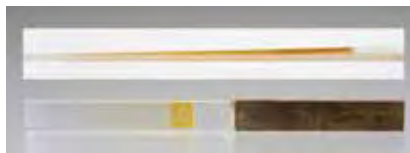


Figure 3. The GIA Colorimeter, introduced in 1941, was developed to select master stones by visually comparing a diamond to a repeatable standard called the “color yardstick” (inset, top)—a graduated wedge of glass that transitioned from colorless to yellow. When a diamond being graded matched a section of the wedge in the colorimeter, the corresponding Roman numeral expressed the grade. Lighting, viewing geometry, and the comparison standards were all controlled with this box. Although modified over time, these three factors continue to be at the heart of consistent color grading. Photos by Robert Weldon.

ied (and was graduated into ranges) from colorless at the thin end to yellow at the thick end (Shipley and Liddicoat, 1941). This first system had 13 grade ranges: The glass wedge had markings for seven categories, which were labeled “0” followed by Roman numerals “I” to “VI,” with these latter six further separated by half-division marks (see figure 3, inset). These 13 grades equated to the D-to-P range in GIA’s later system.

With this colorimeter, the color determination was made by visual comparison, with the diamond placed in three different positions (table-up, girdle-up, culet-up), and 10 observations in each position. The results obtained for each position were then averaged to reach the overall color grade. It is interesting to note that this early form of color grading at GIA was done with magnification (about 4×) and through the comparison of the diamond to a flat transparent wedge of graduated colored glass rather

than other diamonds. The box in which the diamond was viewed against the glass wedge housed a light source for observing the diamond and eliminated influences from outside lighting. The light source used was a blue-coated incandescent bulb that was intended to mimic the color appearance of daylight.

When Shipley's son, Robert Shipley Jr., felt the colorimeter was ready to use for color grading, he wrote to his father in a letter dated April 2, 1941: "I have run thirty reading checks on four stones on which Dick [Liddicoat] has made thirty reading averages. Neither of us had any reference to the others (sic) work, and in no case were we off more than .125 of a division!" Nevertheless, to the best of our knowledge, the GIA Colorimeter was never manufactured commercially (apparently only two were made) or used for any purpose other than the grading of AGS master stones by GIA staff.

The GIA Diamolite. While the GIA Colorimeter allowed for the visual comparison of a diamond to a color standard to develop sets of master stones, jewelers still needed a standard viewing environment when comparing other diamonds to these masters. Although some jewelers had stores situated such that they could effectively use north daylight, many did not, so they used whatever light source they had available. Up to this point, artificial light had proved problematic because it was not close enough in color appearance to natural north daylight (the accepted trade standard). And, again, "north daylight" varied depending on the time of year, time of day, weather, and geographic location; the color of the diamond was also influenced by colors in the viewing area. Ultimately, the Diamolite was the first step toward providing a solution to this problem (figure 4).

From the development of their colorimeter, GIA researchers knew that controlling the light source would be critical, but they also realized that an environment to compare diamonds to one another would have different requirements from that of the colorimeter. Shipley Sr. had been working on this issue ("Diamond-grading instrument . . .," 1934), but it was Shipley Jr. who carried it to its next step. He and others at GIA examined every new light source on the market; they tried argon bulbs (AGS Research Service, 1936) and filtered incandescent bulbs, as well as the relatively new fluorescent lamps ("Instrument research . . .," 1937). Even though GIA was selling the "Da-Grade" fluorescent light source, made by General Electric (GE), for use in displaying diamonds ("At last . . .," 1938), they



Figure 4. The GIA Diamolite was introduced to AGS members in 1941 and, for the first time, offered jewelers a controlled lighting and viewing environment for comparing "master" diamonds to other diamonds. The Diamolite measured $13\frac{3}{4}$ in. high \times 12 in. wide \times 6 in. deep (34.4 \times 30 \times 15 cm) and housed an incandescent bulb with a blue filter (inset) designed to make the light output better simulate daylight. Photos by Robert Weldon.

realized an observer could not use it to distinguish fine nuances of faint yellow color, so the search continued for a better light source for grading.

Shipley Jr. also looked to other industries in which fine color distinctions were critical and found a filtered incandescent light source used as a standard for oil colorimetry and cotton grading. The Shipleys and Liddicoat worked with the color technology company Macbeth (Shuster, 2003) to counterbalance the overabundance of the long rays (i.e., "redder" light) of this tungsten bulb with a special blue filter (figure 4, inset). This adjusted the color temperature (i.e., appearance) of the light output to be closer to that of daylight.

Shipley Jr. also recognized that color grading needed an enclosed viewing environment: "Preliminary research shows that the greatest single handicap in accurate color grading is the difficulty of securing a light absolutely free from colored reflections from adjacent objects" (AGS Research Service, 1936, p. 77). The following excerpt from an article about changes to the *Gemology* textbook ("A note on diamonds," 1938, p. 174) expresses GIA observations at the time on the effect of external lighting on diamond color appearance and defines "body color" for the trade:

The color of a diamond, as it is seen by the eye, may be affected (1) by the comparative amount of the various spectrum colors which it disperses, and (2) by the color of the light reflected from sky, walls, ceiling or other objects. Upon examination by transmitted light against a white, neutral gray, or black background, the true color of the diamond itself is observable, and the resulting appearance is known as the *body color*. However, if colored reflections fall upon those surfaces of the diamond which are toward the eye, the true body color may not be observable. (If colored reflections fall upon a white background against which the diamond is being examined, they will also affect the body color.)

Some in the trade already understood this effect of the lighting environment. By the late 1800s, diamond dealers were very aware of how the surrounding environment affected the appearance of color in a diamond. In the New York jewelry district on Maiden Lane, neighboring buildings were painted yellow—and these faced the windows from which dealers judged color in the north daylight. The dealers pooled their funds and offered to repaint the offending buildings. *Jewelers' Circular* reported: "Several [dealers] stated that it is impossible to sell diamonds in their offices, and unless the colors of [buildings] No. 5 and 7 are changed, they will be forced to vacate their offices" ("Dealers object . . .," 1894, p. 16).

GIA researchers ultimately determined that a box made of translucent white matte paper, open on one side for observation, furnished a much more satisfactory environment for judging color (AGS Research Service, 1936). Not only was the direction of the light that fell on the diamond controlled, but the light was also diffused, which subdued surface reflections from facets that might obscure the bodycolor. In 1941, the Institute introduced a commercial version, the GIA Diamolite, for use in color grading (again, see figure 4; Shipley and Liddicoat, 1941). The accompanying brochure stated that this viewing box (small enough for the display counter in a retail store) allowed a jeweler to observe diamonds under a standardized light source in any physical location at any time of the day or night.

Grading Master Stones. Now that it had a light source and an environment in which to visually compare diamond color, as well as an instrument that related the color to an established scale, in the early 1940s

GIA began to collect diamonds graded with the colorimeter to use as its own "master" comparators.

After leadership review, the AGS membership voted in 1941 to recommend the use of the GIA Colorimeter for master stones, the scale as the standard for color distinctions in diamonds, the GIA Diamolite, and the new grading service for master stones (see, e.g., Shipley and Liddicoat, 1941). For the AGS master stones, two of the averaged colorimeter grades were reported to the AGS member jeweler—for the table-up and girdle-up positions. The "0-VI" numerical scale of the colorimeter was promoted as the color grade nomenclature to be used for diamonds (Shipley and Liddicoat, 1941) and was strictly for AGS members. Consequently, when GIA chose to develop a diamond grading system available to everyone, it had to use new terms. The choice for color grading colorless to near-colorless diamonds, as previously noted, was the letter grade scale beginning with D.

GIA had offered other technical services, such as pearl identification, to the trade since the 1930s, but the master diamonds service (started in 1941) was the first one related to diamond grading. In fact, this service preceded the 1949 creation of the laboratory as its own division within GIA.

The 1950s to '80s: The Continued Evolution of Lighting and Viewing Environments. The last known mention of the name *Diamolite* was in the January 1950 issue of *Jeweler's Circular Keystone (JCK)* magazine. *Gems & Gemology* first cited the new name, *DiamondLite*, in 1949 (Schlossmacher, 1949). This change in name accompanied an updated filter from Macbeth that was still used with an incandescent bulb (Shipley, 1950a). We do not know if the physical proportions of the viewing environment changed at that time.

This period saw the continuation of GIA's investigation into alternative light sources for the assessment of diamonds. By the 1950s, Liddicoat and his contemporaries had apparently developed a comfort level with the fluorescent lamps available at that time. GIA began teaching that jewelers could use a modified fluorescent lamp for color grading when they didn't have access to a (still incandescent bulb) *DiamondLite*: "a reasonable substitute may be secured by adapting a simple fluorescent tube desk lamp . . . lined with flat-white paper . . . enclosed on the back and two sides so as to exclude as nearly as possible all reflections from surroundings" (Shipley, 1955, p. 5). A sheet of

white tissue paper between the fluorescent tubes and the diamond further diffused the light.

Depending on the evenness, thickness, and type of phosphor coating, however, the early generations of fluorescent lamps had considerable variation in the wavelengths and intensities of their light output. This included an inconsistent—and, at times, relatively high—amount of ultraviolet (UV) emission, in contrast to the extremely low UV content in incandescent bulbs commonly used at that time. Realizing that some fluorescent diamonds appeared different when observed under lights with UV content (fluorescent lamps as well as the former Diamolite with its UV source, added in 1947, turned on), GIA made a number of statements related to this with each accompanying modification. In 1955 course material, GIA advised that “This factor should not cause too much difficulty, however, since only a very small percentage of stones fluoresce strongly enough to modify the body color under this light source” (Shipley, 1955, p. 5). Nevertheless, contemporary course materials advocated the grading properties of the (low-UV) incandescent bulb grading light, even to the disavowal of the historical standard, (relatively higher UV) daylight. GIA Assignment 2-31 (Shipley, 1957, p. 8) stated that “Fluorescent stones should be graded at their poorer color [as seen] in artificial light devoid of ultraviolet radiation [i.e., the incandescent bulb of the DiamondLite], rather than at their daylight grade [i.e., the grade they would receive if viewed against a comparison stone in daylight].”

In the mid-1960s, GIA introduced the GIA Diamond Color Grader tray to their Mark IV gemological microscope, which allowed color grading under the overhead diffused fluorescent source attached to the microscope. However, Gem Instruments advised that “Highly fluorescent stones cannot be graded in the GIA Color Grader” (GIA, 1966), due to the proximity of the diamond to the lamps.

In 1974, Ken Moore (director of Gem Instruments Corp.) introduced a DiamondLite (figure 5) that used 6-watt fluorescent lamps made by Verilux, with a new coating that minimized UV emission as compared to similar lamps and especially as compared to earlier fluorescent lamps. GIA often promoted the minimized UV emission in these lamps. For example, in 1979 course materials, GIA described these new lamps as “practically devoid of ultraviolet waves” (GIA, 1979, p. 9). Later course material (GIA, 1995, p. 9) claimed that “Filtered,



Figure 5. This version of GIA's early fluorescent viewing environment, the DiamondLite, was introduced in 1974 and used Verilux 6-watt lamps. It measured 9 in. high, 13 in. wide, and 8 in. deep (22.5 × 32.5 × 20 cm). Photo by Robert Weldon.

cool white balanced fluorescent light is best: unlike sunlight, it is nearly free of ultraviolet.” As frequent as such statements were, it is important to remember that no fluorescent lamp is truly “UV free.”

From the 1990s to the Present: Lighting and Viewing Refinements. Research in the 1990s and the first decade of the new millennium led to refinements in the equipment and processes used to color grade diamonds that are reflected in the grading methods in place today.

Light Source Testing. Since at least the 1970s, millions of diamonds have been graded using fluorescent lighting, at GIA and throughout the industry. It has become the standard in the diamond industry. To ensure consistency in GIA's grading, proposed changes in lighting must be thoroughly tested to balance the potential benefits to the grading methodology against the very real damage that would be caused if subsequent color grades were inconsistent with earlier ones. (The success the laboratory has had in this regard can be tracked in very real terms through its update service. Today we occasionally see diamonds graded in the 1970s that have been submitted for updated grading reports; after they have undergone a full grading process using contemporary equipment and procedures, the vast majority are returned with the same grade determinations.) With that as a guideline, GIA began researching options for fluorescent “daylight equivalent” lighting. In part, this research was driv-

en by the fact that the Verilux 6-watt lamps used in the DiamondLite were no longer readily available, and other manufacturers' lamps of the same size did not consistently meet GIA lighting standards.

Researchers compiled a list of factors to be considered in selecting an alternative lamp: worldwide availability, suitable illumination levels, uniform distribution across the work area, a spectrum that mimics International Commission on Illumination (known as CIE) D55-to-D65 specifications, a color temperature in the 5500–6500 K range, and a color rendering index of at least 90 (for details, see box A). Data collection began in January 1998, with 40 different lamps from various manufacturers. The 6-watt Verilux lamp used in the DiamondLite at that time was included for comparison. For each manufacturer, four different sizes of fluorescent lamps were tested: 4 watt (134 mm/5–6 in.), 6 watt (210 mm/8–9 in.), 15 watt (435 mm/17–18 in.), and 18/20 watt (590 mm/23–24 in.). Spectra were collected when the lamps were first turned on and after “burn in” times of 50, 100, 500, 1,000, and 2,000 hours, so that the evolution of each spectrum could be analyzed (see, e.g., figure 6). Data were collected using a Photo Research PR-704 Spectrascan spectroradiometer, an Ocean Optics SD2000 spectrometer, and a Gossen Mavolux digital lightmeter.

In late 1998, GIA researchers did additional testing on three of these lamps: an 18-watt Osram Biolux, a 20-watt Verilux, and a 20-watt Macbeth. For comparative visual observations, choices were narrowed to the Verilux and Macbeth lamps. The former was selected because researchers felt that continuity with the Verilux lamp characteristics was important, and the latter was chosen because GIA had been using the Macbeth lamp successfully to color grade colored diamonds for a number of years. After weighing all the factors and completing data analysis, GIA decided that the Verilux lamp was the best lighting source for the purpose of color grading D-to-Z diamonds.

Viewing Environment. The decision to use the longer (23–24 in.) 20-watt lamps required the design of a new and much larger viewing environment to house them. From its research on color grading colored diamonds (see, e.g., King et al., 1994), GIA recognized that a larger viewing box would also better shield the observer from distracting visual clutter in the surrounding environment, give a larger neutral background for the field of vision, and be more comfortable for the observer. These factors contributed

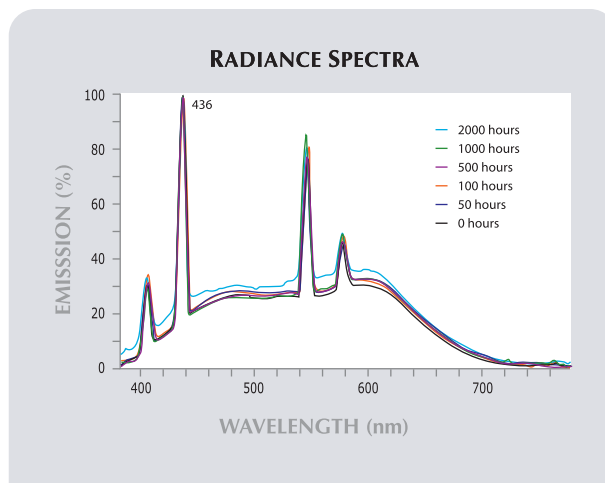


Figure 6. In characterizing light sources, it is important to know the consistency of their properties over time. To accomplish this, the lights are left on for extended periods and a number of radiance spectra are taken at specified times; in this case after 50, 100, 500, 1,000, and 2,000 hours. The plot shows the captured radiance spectra of the Verilux 6-watt fluorescent lamp (used for comparison with potential new selections) normalized for the 436 nm peak at 100%. The minor deviations seen here are typical and do not result in noticeable differences in performance for color grading.

to our decision to make the height of the box 18.5 in. (47 cm), which is similar to the Judge II used for colored diamonds (20 in.; illustrated in King et al., 1994, p. 230). Recognizing that the depth of environments used for D-to-Z color grading had traditionally been shallow (approximately 8 in. in the DiamondLite to 6 in. in the Diamolite), we decided to make the prototype viewing box 6 in. (15.24 cm) deep. As mentioned above, the width was determined by the length of the two lamps being used. In practice, we found that the wider environment was better for handling the diamonds. To improve the consistency and life cycle of the lamps, we successfully experimented with electronic high-frequency ballasts. Although the walls of the DiamondLite were coated dull white, GIA staff members had found that medium to light gray walls reduced eye fatigue (at the same time, various standards organizations also recommended a neutral gray surround for color grading environments; ASTM, 2003; ISO, 2005).

Subtle modifications were made to the design of the box over the next five years, as a prototype was formalized for use in the laboratory in the early 2000s. At the same time, we also developed a product for commercial release, a viewing environment that incorporates two 15-watt Verilux lamps into a slightly smaller (more retailer friendly) box, which is market-

BOX A: CHARACTERISTICS OF THE STANDARDIZED FLUORESCENT LIGHT SOURCE GIA USES FOR D-TO-Z COLOR GRADING

Proper illumination is critical when performing tasks requiring subtle color comparisons, as is the case with color grading D-to-Z diamonds. There must be enough light to view the subtle differences, but not so much that color perception is affected by surface glare or that the light causes eye fatigue. We have found the acceptable range for light output to be between 2000 and 4500 lux. The light output needs to be stable (which is accomplished with an efficient, high-frequency ballast) so there is no variation in intensity (e.g., flickering), and it should be consistent across the entire viewing surface. It should take very little time for the lamps to become stable once they are turned on. The light emitted also must be diffuse, since point or spot lighting can cause bright surface reflections, more obvious dispersion, and strong contrasts in polished diamonds.

There are a number of characteristics of daylight that are valued in diamond color grading and were considered in choosing the standard light. These include, for example, daylight's overall spectrum, its color appearance in the northern hemisphere, and its ability to render colors. While the full emission spectrum should be considered when choosing lamps, it is also important to note the output in the areas that can affect the predominant task at hand, in this case the grading of colorless to light yellow diamonds. In particular, there must be enough output in the blue region of the spectrum, as it is the

absorption area of wavelengths in this region that allows yellow diamonds to be perceived at optimum visual acuity. Fluorescent lamps have "spikes" in their emission spectra (see again figures 6 and 8): narrow ranges of wavelengths that have much greater intensity. The positions of these spikes and their potential effect on color grading were important to our choice of a light source. In addition, the spectrum of a lamp used for color grading should not emit short- and mid-wave UV, as these emissions can be harmful to the eyes of the observer over extended periods of time. However, the lamp should emit long-wave UV, which is an important characteristic of daylight. The CIE standards for D55 to D65 light also specify a UV component.

Regarding the UV component, we have learned that for some fluorescent diamonds the distance between the lamps and the grading tray can influence the final color grade. For consistency, we use a distance of 8–10 in. (20–25 cm) between the lamps and the diamond. Bringing a fluorescent diamond closer to the lamps may result in a stronger fluorescence impact. For instance, a yellow diamond with strong blue fluorescence could appear less yellow (i.e., to have a higher color grade) as it gets closer to the lamps. Moving the same diamond more than 10 in. from the lamps will have the opposite effect; that is, the color will appear more yellow (a lower color grade).

The relative amount of UV versus visible light

ed for both D-to-Z color grading and round-brilliant-cut evaluation as the GIA DiamondDock (figure 7). It is also used in the laboratory.

With each modification to the viewing environment, experienced color grading staff in the New

Figure 7. This viewing box, the DiamondDock, provides a good surround for making visual comparisons of diamonds, both for color grading D-to-Z stones and observing round brilliant cuts. When the raised platform is inserted in the box as seen here, a viewing tray of master diamonds is at the appropriate height for color grading. When the platform is removed (and the auxiliary LED lights turned on), cut can be observed with the diamonds placed in a tray on the base of the unit. The box measures about 18 in. high × 21 in. wide × 6½ in. deep (45 × 52.5 × 16.25 cm). Photo by Robert Weldon.



emission in the spectrum remains the same regardless of the distance to the light source. However, if the stone is observed close to the light source, the blue fluorescence emission in diamond may become more obvious than its absorption of yellow.

The “correlated color temperature” (CCT; or just “color temperature”) is another important aspect of a light source. This term is used to describe the overall color of “white” light sources, and the “temperature” is most commonly expressed in units of kelvin (K). Incandescent lighting has color temperatures around 2000–3000 K and is generally referred to as being “warm” light. Common fluorescent lighting in general, with a CCT of 4500 K or higher, is considered “cool.” The use of *warm* and *cool* with regard to lights refers to the color appearance of the light; the temperature designations could lead one to think the reverse. To simulate north daylight, a light source should be much “cooler” or “whiter” and have a color temperature in the 5500–6500 K range.

Lighting manufacturers often refer to the light’s color rendering index (CRI) as an important criterion as well. In general, CRI is a quantitative measure of a specific light source’s ability to reproduce colors faithfully in comparison with an ideal or natural light source (CIE and IEC, 1987). On a scale of 0 to 100, lights with 90 or higher are generally preferred for tasks requiring color differentiation.

When choosing a lamp, GIA uses the CRI and the color temperature of the light source in conjunction with both its complete spectrum and the specific regions that can affect D-to-Z color grading.

In researching practical solutions for the laboratory and the trade, GIA requires that the lamp be energy efficient, widely available in the marketplace, and reasonably priced. (Information on lighting criteria and explanations of these and other terms used regarding lighting can be found on many lighting websites. One example is www.lightsearch.com/resources/lightguides/colormetrics.html.)

In summary, the basic technical specifications for the lighting used for D-to-Z color grading at GIA are:

- Stable, fluorescent lamps 17 in. (43 cm) or longer
- An intensity of light in the range of 2000–4500 lux at the surface of the grading tray
- An 8-to-10 in. distance between the lamps and the grading tray
- A color spectrum close to CIE D55–D65
- A color temperature between 5500 K and 6500 K
- A color rendering index of 90 or above
- A high-frequency (>20,000 Hz) electronic ballast
- A light ballast with efficiency (power factor) above 0.5 (50%)
- No noticeable output in the short- or medium-wave UV range (or a filter available to eliminate UV in this range)
- An emission for long-wave UV (between 315 and 400 nm, close to the reference spectrum of D55–D65)

York and Carlsbad laboratories independently color graded the same diamonds in the DiamondLite and the two new viewing environments to verify the consistency of grading results. Our findings showed that overall results were within tolerances recorded in the history of GIA’s D-to-Z color grading. Spectral analysis of the three lamps showed consistency as well (figure 8).

THE UV CONTENT IN LIGHT SOURCES USED FOR D-TO-Z COLOR GRADING

The potential effect of lighting on diamond fluorescence (and therefore color appearance) has long been a subject of discussion, although the UV component in a light source only impacts color appearance in some obviously fluorescent diamonds. In the 1930s and before, there was general agreement that diamonds should be observed in north daylight, which

contains UV. Yet the first widely accepted standard viewing environment, the Diamolite, contained a filtered incandescent bulb, which had low UV content compared to daylight. As noted earlier, fluorescent lamps of that era were neither stable enough nor consistent enough to meet the requirements of diamond color grading.

During the 1940s, the appearance of a highly fluorescent diamond in daylight was considered a positive attribute. Recognizing the inherent limitations of the Diamolite’s incandescent bulb in this regard, GIA introduced a stand-alone long-wave ultraviolet light source in 1945 (Shannon, 1945) and in 1946 updated the Diamolite by adding a UV source. When used alone, this UV lamp revealed the presence and strength of fluorescence in a diamond and, when used in conjunction with the filtered tungsten lamp of the Diamolite, created a condition that was felt to better simulate daylight and “show the

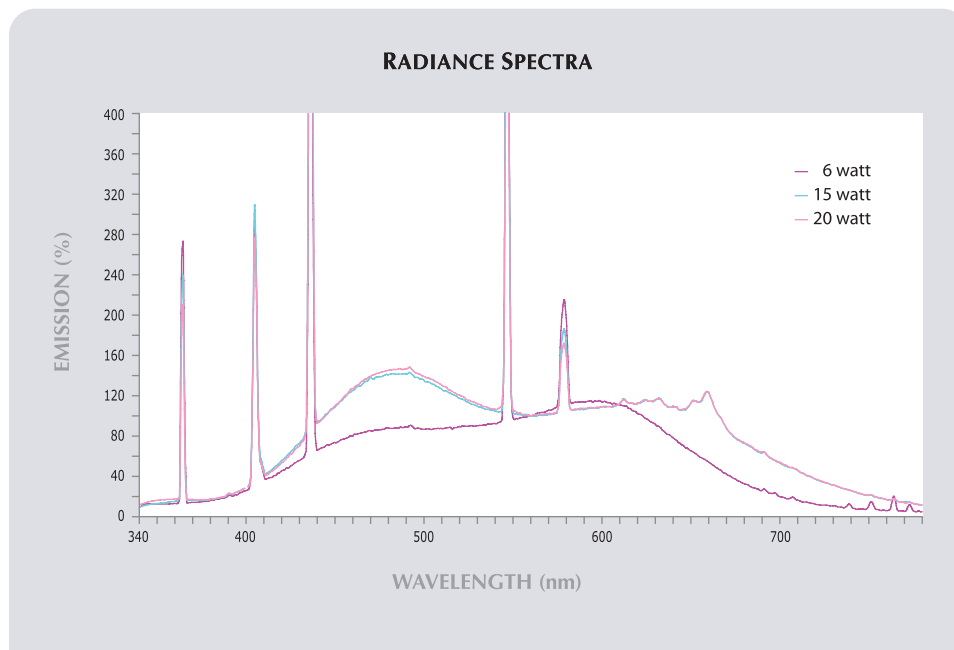


Figure 8. The 15- and 20-watt Verilux lamps chosen for the new viewing environments produce results that are within tolerance for color grading and compatible with the 6-watt lamps used in the past. Here, the UV region shows good agreement between the three lamps. Note that the 15- and 20-watt lamps have a phosphor layer that results in an additional emission in the red region between 620 and 700 nm that does not have a noticeable influence on D-to-Z color grading. Spectra normalized at 560 nm.

diamond off under the most attractive and favorable conditions” (Collison, 1947, p. 431).

As noted earlier, GIA continued to experiment with different lighting sources throughout the 1950s and ‘60s, and began moving toward the use of fluorescent lamps, both in conjunction with the incandescent bulb of the DiamondLite and separately in the overhead light source of their microscopes.

Eventually, the use of different phosphors, phosphor layer thicknesses, and new ignition technologies reduced the amount of UV emitted by fluorescent lamps. Research that GIA began in the early 1970s revealed that the lower UV content helped reduce the extreme appearance differences in diamonds that had been encountered with earlier lamps. To market the new DiamondLite, with its 6-watt Verilux lamps, some GIA literature implied that little to no UV content was preferable for D-to-Z color grading. Actually, the low UV content of these lamps was preferable to the UV content of earlier fluorescent lamps, which was higher or inconsistent. Indeed, the lamps chosen in the ‘70s had a small, but not negligible, UV component. And we continue to see this UV component in lamps chosen since then.

We recognize, however, that language used and certain statements made by GIA in the past several decades have led to confusion about the presence and, therefore, perceived desirability of the UV component in lighting used for D-to-Z diamond color grading. As mentioned above, course materials from the late 1970s to mid ‘90s described the lamps as “practically devoid” or “nearly free” of UV (GIA,

1979, p. 8; 1995). Even in the GIA Laboratory, an internal manual published in 1989 (p. IH-1) noted “Use a cool white, filtered, *ultraviolet free* fluorescent light [in the lab, the DiamondLite] in an area of consistent, subdued light.”

“Filtered” referred (incorrectly) to the coatings used on the lamps to control output *across the spectrum*; this could be confused with using a filter to block UV. Again, these fluorescent lamps were not UV free.

In the late 1990s, referring to lamps with essentially the same UV content as their predecessor, laboratory staff spoke of the appropriateness of that UV component. As one of the authors [JMK] commented in an interview (Roskin, 1998, p. 149), “Yes, you can create an environment devoid of UV but it’s a false situation . . . It may sound like the ideal, but it steps outside the practical world. It’s not relevant because it doesn’t really exist anywhere. We try to be sensitive to the practical gemological issues.” Tom Moses corroborated this position at GIA by stating, “we found that the Verilux bulbs used in GIA’s diamond-grading units, standard cool-white fluorescent light bulbs, and northern hemisphere daylight (even filtered through a glass window) all have a certain amount of UV radiation. Hence the Verilux sources are similar—in terms of UV exposure—to grading environments throughout the world” (Moses, 1998, p. 21). The light source GIA uses for color grading has continued to be discussed in the trade (Tashey, 2000, 2001; Haske, 2002; Cowing, 2008).

The fact is that since the 1974 implementation

of new coatings on fluorescent lamps, GIA has promoted using a daylight-equivalent fluorescent lamp with a non-negligible amount of emitted UV. GIA will continue to study the subject as new lighting technology and research become available, with the goal of maintaining existing color grading standards. In fact, one of the authors (RG) was recently informed by CIE (Peter Hanselaer, pers. comm., 2008) that the UV content of the proposed new reference illuminant for “Indoor Daylight” (e.g., ID65) that CIE is working on will define the daylight specifications indoors under standardized conditions regarding glass thickness and absorption of the windows and standard angles of incidence of the light. This “Indoor” reference illuminant will have a noticeably reduced UV content compared to the regular CIE Daylight standard D65 because of the typical absorption of glass in the UV region, so its resulting spectrum will be even closer to the Verilux lamps GIA is using in the lab.

THE GIA D-TO-Z COLOR GRADING SYSTEM

The equipment and methods used today at GIA to color grade D-to-Z diamonds have come from the experience gained through the observation of millions of diamonds, as well as from continuous research into advances in lighting technology and vision science. *Even though there have been modifications, such as changes to the viewing environment, it is important to recognize that the GIA standard—the spacing of the key historical grade markers—has remained unchanged since the system’s inception more than 65 years ago.*

D-to-Z color grading is based on the observations of a trained observer, who compares a diamond to color master stones of known position on the grading scale (see box B for a discussion of the selection and care of master stones for clients and the laboratory). To achieve repeatable results, graders use a standard light source and a controlled viewing environment. Also important are the proper maintenance of equipment and consistency in the set-up of references, viewing geometry, and methodology. In addition, the observer must have been tested and shown to have normal color vision.

Screening, Training, and Monitoring of GIA Color Graders. Controlling all the conditions would be of little value without the proper screening and training of staff. At GIA, eligible staff members must pass tests such as the Dvorine Color Test, the

Matchpoint Metameric Color Rule Test, and the Farnsworth-Munsell 100 Hue Test to ensure that they have normal color vision, discrimination, and acuity. Other tests are designed to gauge visual and verbal understanding of the color grading process.

Training sessions with experienced graders allow those staff members who are accepted as new color graders to gain first-hand knowledge over a period of weeks. All staff members are routinely monitored through the data collection of “blind” observations on control stones as well, to help insure color grading consistency.

To control for potential perception differences from individual to individual, GIA’s grading process requires a minimum of two or three random, independent opinions (depending on the size of the stone). A consensus is required before a color grade is finalized. For larger or potentially D-color stones, the laboratory’s computer operating system identifies the need for the most experienced graders. Last, to avoid the potential of reduced accuracy due to eye fatigue, color grading sessions are limited to approximately one hour, at which point a minimum break of one hour must be taken.

Routine Calibration and Maintenance. Since the viewing environment (e.g., the DiamondDock) is the neutral surround for the observer’s field of vision, its care and cleaning is the first priority before grading even begins. If it is soiled it can distract the observer just as objects in the field of vision would. In the laboratory, the viewing environments are cleaned with a mild soap and soft cloth every week. Prior to placing new lamps in a unit, we capture their spectra with an Ocean Optics spectrometer equipped with an integrating sphere to make sure they are within tolerances. The light output at the surface of observation is checked monthly using a Gossen Mavolux Digital 5032B lux meter. Our testing has shown that the average life of a lamp is around 5,000 hours; from our experience, the “useful” life of the lamp for color grading purposes is half that, 2,500 hours. To avoid any deterioration in the illumination, we replace the lamps even sooner, at approximately 1,800 hours, unless some problem is noted earlier (i.e., discoloration at the ends of the lamps or a prominent drop in the lux meter readings). In the color grading area of the laboratory, ambient lighting is also controlled. Overall, the lighting is subdued, with no influence from natural daylight.

Again, see box B for the routine cleaning and care of master stones.

BOX B: SELECTION AND CARE OF MASTER STONES AT THE GIA LABORATORY

Since the advent of its first colorimeter in 1941, GIA has received requests from members of the trade to evaluate diamonds that would serve as master comparators for color grading (figure B-1). This service continues to this day, although the selection process is accomplished through visual comparison supported by instrumentation, not a colorimeter.

Acceptance of one stone as a master is sufficient to start a set for a client and the issuance of a GIA Master Color Comparison Report. This report contains basic identifying information on the diamonds selected as masters and can be expanded with new master stone selections over time. There are several criteria for the selection of diamonds for a master set. These include cut, size, inclusions, fluorescence, and color. In creating a set of diamond color masters, the laboratory's overriding goal is to reduce as many visual variables as possible for the greatest consistency in all but color from one master stone to the next. Therefore, GIA will only grade round brilliant diamonds for masters. Besides being the most common cut, the round brilliant yields the most consistent color appearance (and shape) of any cut. In addition, master stones must meet good proportion standards.

Members of the trade decide the best size for the diamonds in their set of master stones, based on their typical stock (understanding that GIA will not grade diamonds under 0.25 ct for master stones). If, for example, a manufacturer or jeweler typically works with half-carat diamonds, the master stones should also be approximately half a carat. Over the years, we have found that sets larger than one carat are not necessary, as masters in the one-carat range can accommodate comparisons to larger diamonds. At the laboratory, we have compared masters of this size to diamonds 50 ct and more. When such diamonds have been observed on more than one occasion, we have

come to the same color grading results. Within a given set (up to about one carat), master stones should not vary more than 10 points from one another. There can be no eye-visible inclusions, and they cannot exhibit "off-colors" such as having a subtle brown or gray cast.

Fluorescence is also an important consideration. For the E-to-J range, GIA only accepts diamonds as masters that have no observable (reported as "none") fluorescence. For K and lower, a "faint" fluorescence reaction is acceptable. While a more strongly fluorescent diamond might be used as a master if strict laboratory conditions were always to be used (i.e., standardized methodology, lighting, and environment), GIA has no way of determining whether client master stones will be used in these conditions. With regard to the acceptance of faint fluorescence for masters K and lower, our experience has shown that, as the amount of color increases, the impact of faint fluorescence on color appearance is less noticeable. Also, we have found that diamonds in the lower color grades commonly fluoresce, so it would be difficult to locate stones with no fluorescence in this color range.

A diamond selected as a master stone is not necessarily an exact duplicate of the GIA master of the same color grade designation. A diamond is an acceptable master when it falls in the range of repeatable visual tolerance as established by the laboratory over the years. Consequently, a diamond may be acceptable as a master if it is very close to the GIA master, but is very slightly to the higher or lower side. Our research has shown that skilled graders reach a point of visual tolerance (i.e., the range of repeatability) for D-to-Z color discrimination at slightly less than one-fifth of a grade at best. While this fraction may appear large, it is important to remember that even between whole grades the differences are extremely subtle. For example, it is common for untrained observers to see no dif-

Locations of Master Stones in the Grade Ranges.

Every individual grade designation on the D-to-Z scale is actually a range of colors within that grade. *The GIA master stones are located at the highest boundary of each grade range* (figure 9), that is, at that end of their respective grade range that has the least color. Therefore, a diamond with less color than the G master stone (but not less than the F) would receive a grade of F. If the diamond appears to have the same amount of color as the G master, it would receive a grade of G. When a diamond has

slightly more color than the G master stone but less than the H master stone, it will be called a G color. Any diamond, no matter how colorless in appearance, receives a D grade if it appears to have less color than the E master stone. Thus, no D master stone is necessary.

Set-Up of References in the Viewing Environment.

At the laboratory, a "working master set" of the 10 master stones needed to grade the most commonly submitted diamonds, D through M range, is typical-



Figure B-1. For almost 70 years, GIA has been building diamond “master sets” as comparators for use in color grading. Since the mid-1950s, such sets have been at the core of the GIA diamond grading system for colorless to light yellow diamonds. The diamonds in the set above range from E to Z. There is no D master; a D-color diamond is one that has less color than the E master. Photo by Robert Weldon.

ference between two or three adjacent masters (e.g., the E, F, and G masters or the I and J masters). To overcome this challenge, GIA has multiple graders independently grade diamonds submitted for master stone reports (as is the practice for regular grading, too) and uses instrumentation for support. In assembling a new master set, our goal is to create a group of stones that meet this visual tolerance. Such subtle appearance differences relative to a GIA master have not been found to adversely affect the use of sets within the laboratory or by our clients.

Note that there may be differences in the color grade indicated on a GIA Diamond Grading Report and a Master Color Comparison Report; that is, if the diamond was within visual tolerance to the slightly higher side, it could receive a different grade than its master designation. For example, a diamond accepted as an L on a Master Color Comparison Report might be perceived during random grading to be slightly to the high side in the visual tolerance range of a GIA master. In that case, the diamond could be graded K on a Diamond Grading Report (see, e.g., figure B-2).

As a final note, master stones require special care and maintenance. It is particularly important to clean them regularly. The GIA Laboratory routinely boils master stones in sulfuric acid every two to four weeks, depending on the frequency with which they are used, to minimize the potential influence of foreign surface material. Boiling is an especially critical part of master stone maintenance for diamonds with bruted girdles. When outside sources have returned sets for us to

review or supplement, the laboratory has seen up to four grade shifts in appearance for diamonds with bruted girdles that have not been boiled for some time.

Constant handling of diamonds can result in minor damage, so this must also be monitored. If a master stone has noticeable chips or is badly worn, its color appearance may be affected. The laboratory uses rubber-tipped tweezers to greatly reduce the risk of damage (these tweezers also reduce the accumulation of surface material mentioned above).

Figure B-2. Master stones are always at the high side of the grade range. The shaded area here indicates the visual tolerance range surrounding a master diamond designated as L on a GIA Master Color Comparison Report. The vertical line represents the location of an ideal L master diamond. If the stone is randomly graded toward the high end of the tolerance range, it could receive a K on a GIA Diamond Grading Report.

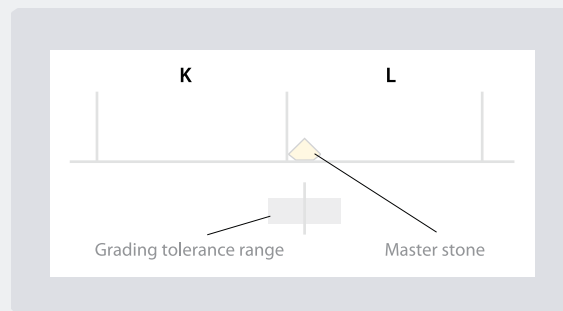


Figure 9. GIA master stones are located at the highest point in their respective grade range. A diamond equal to the G master is graded a G. If it has slightly less color, it would receive a grade of F. A diamond with more color than the G master and less than the H master would receive a G grade. A diamond with less color than the E master is graded a D. A diamond with more color than the Y-Z master is graded face-up as a fancy color.





Figure 10. To speed production and facilitate comparison, all the E-to-N masters are kept in the grading tray throughout a grading session. They are spaced far enough apart to allow focused observations and the efficient movement of the diamond between masters. The tray is white, since that is the traditional background color used at GIA and throughout the trade. From our experience, a white background is best for making comparisons of pale colors. Photo by Robert Weldon.

ly kept in the viewing box in a 12 in. (30 cm) long V-shaped nonfluorescent white plastic tray (figure 10), with the E master on the left. The portion of the tray on which the diamonds sit is 1 in. (25 mm) wide and the backing is $\frac{3}{4}$ in. (19 mm) high. This size creates a consistent background for the diamonds. The length of the tray allows enough room between diamonds for the grader to handle them, as well as to focus on color comparisons between specific pairs of

Figure 11. A standard “0/45” viewing geometry is used when color grading D-to-Z diamonds. The light source is above the tray at approximately “0” degrees, and the diamond is observed from a position approximately 12–15 in. (30–37.5 cm) away at an angle about 45° from the stone.



diamonds. With this arrangement, a grader can efficiently move through the grading process with an assigned quantity of diamonds without the added time of taking out and replacing the master stones.

While many diamond dealers and manufacturers take out only one or two reference diamonds at a time to compare to a diamond of unknown color, such a procedure is impractical for the production needs of a grading laboratory. It also may require that the observer rely on color memory in the decision making process. Studies have shown that color memory is not reliable for subtle color comparisons (Epps and Kaya, 2004), and having several master stones in the viewing environment at all times eliminates this problem.

Viewing Geometry. The visual complexity and often extremely subtle color of a polished diamond can make the grading of color very challenging. Therefore, the primary observation direction for color grading a diamond in the D-to-Z range is through the pavilion facets, with the diamond in the table-down position in order to reduce the complex, mosaic-like appearance seen face-up. The grader sits with his or her eyes approximately 12–15 in. (30.5–38 cm) from the diamond, closely adhering to a standard “0/45” geometry between the observer, the light source, and the diamond’s pavilion facets (figure 11). The tray holding the diamonds is positioned 8 in. (20 cm) beneath the fixed light source.

Figure 12. When grading D-to-Z diamonds, the observer rocks the tray over a small range in order to view the stone from nearly perpendicular to the pavilion facets to near-perpendicular to the girdle. This is necessary to avoid distracting reflections during color grading.

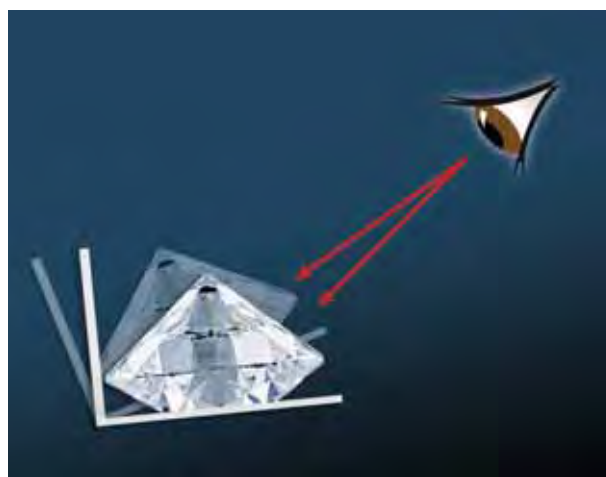




Figure 13. Fancy-shape diamonds have long played an important role in diamond jewelry. The color grading of fancy shapes is challenging due to the variations in proportions. GIA uses a standard viewing position for all fancy shapes to average the appearances encountered. The necklace consists of 44.06 carats of F-to-H oval diamonds; the J-color emerald-cut diamonds in the cuff links weigh 3.04 and 3.01 ct. Courtesy of Louis Glick & Co; photo by Harold & Erica Van Pelt.

During examination, the tray, while remaining on the upper shelf base of the viewing box, is rocked slightly—such that the line of sight varies from approximately perpendicular to the pavilion facets to near-perpendicular to the girdle (figure 12).

The visual comparison of round-brilliant diamonds to round-brilliant master stones eliminates one significant variable: shape. The situation is more complicated, however, when color grading fancy-shape diamonds (figure 13). Most fancy shapes can display up to three distinct amounts of color depending on their orientation in the table-down observation position. We have found that the most representative set-up for color grading fancy shapes is to orient them with their long and short axes at approximately 45° to the observer (figure 14). In this

position, the outline of the fancy shape most closely resembles that of the round brilliant (i.e., reduces shape comparison differences) and functions as the best visual “average” for the amount of color observed. It exhibits neither the most intense color appearance nor the “washed out” areas.

From our experience, it is difficult to distinguish subtle differences between the colors of two diamonds that are touching one another. Therefore, we place a diamond close to (no more than 1/5 in. or 5 mm) but not touching a master stone when making color observations. The diamond being graded should also be placed in the same line as the master stones, not in front of or behind them, so that they are all the same distance from the observer. Fancy-shape stones also should not be so close that their

Figure 14. When grading fancy shapes, the average appearance is best represented by placing the fancy shape with its long axis approximately 45° to the observer. This series of photos for a 1.20 ct emerald cut next to a GIA master stone illustrate why this “middle” position is used. On the far left, the emerald cut is positioned so the observer views the long side—its weakest color appearance. The photo on the far right illustrates the appearance seen when the grader looks through the end of the fancy cut, where the color appears strongest. The angled position used at the laboratory, which averages the color, is seen in the center. Other fancy shapes also best simulate the outline of the round when set in this position. Photos by Robert Weldon.





Figure 15. A fancy shape positioned with its long axis at 45° may visually overlap a master stone if placed too close to it (left), as seen with this 2 ct marquise. The fancy shape should be placed near the master stone, but without any overlap (right). Photo by Robert Weldon.

angled position causes them to overlap the master stone along the observer's line of sight (figure 15).

It is important to acknowledge that some years ago (in particular the 1970s and '80s), laboratory staff experimented with placing diamonds in different positions and at different distances from the light source in the color-assessment process (K. Hurwit, pers. comm., 2007). Whether the diamond was a round brilliant or a fancy shape, there were times when observations were made through the crown with the diamond face-up and through the pavilion with the diamond on its side, *in addition* to the primary direction: through the pavilion with the diamond table-down. In each of these positions, observations of color appearance were made through a wide range of viewing angles. Mentally averaging the appearances encountered through the combination of directions was used in an effort to ascertain differences between the subtle colors of a diamond and a master stone. Ultimately, it was determined that using multiple positions further complicates decision making and the repeatability of the color determination.

For consistent results across many observers and locations, the laboratory restricts the positions in which diamonds are observed. For round brilliant cuts in the D-to-Z range, color is graded table-down only. Because fancy shapes toward the lower end of the D-to-Z scale typically appear to have more face-up color than their round-brilliant counterparts, at or below Q a combination of table-down and face-up is used to balance the grade and acknowledge the more noticeable face-up color. At Z, face-up color determines whether a diamond is a fancy color.

Just as the diamond being graded and the master stone were put in a number of different positions in the past, the viewing conditions have varied, too. In the 1970s and 1980s, the color tray that fit over the well of the microscope for use with the microscope's overhead light was recommended to members of the trade who did not have a DiamondLite. Occasionally, staff members also used it for color grading. During

that same period, GIA's Gem Instruments division added a small recessed opening at the top front of the DiamondLite. When the cover to this opening was raised, a "color grader" tray could be placed in the opening (which was in front of the lamps). With this configuration, the light from the lamps was filtered through the plastic tray, thus minimizing the diamond's internal and surface reflections. Trade members and staff in the laboratory occasionally used this upper recessed tray area to observe color, similar to the way some *diamantaires* breathe on a diamond to "fog it" to minimize reflections.

The only location currently used for color grading at the GIA Laboratory is a V-shaped tray on the upper shelf in the viewing box (again, see figure 11). We do not alter the appearance of the diamond by filtering the light or breathing on the stone. All observations are made without magnification.

Determining the Diamond's Color Grade. GIA grades the overall color appearance of a diamond. Attention is not focused on specific areas, such as the center of the pavilion of a round brilliant or the long flat side of an emerald cut. By observing the overall appearance, the grader mentally blends all the visual sensations of the diamond.

Instead of trying to *match* the color of a diamond with a reference color, the GIA system involves placing or *bracketing* the color between pairs of master stones, which for most observers is an easier task. In general, the grading process is one of progressively narrowing the range until the diamond fits within a single grade (i.e., more color than the master stone on the left, and less color than the master stone on the right).

After the diamond to be graded has been wiped clean with a lint-free cloth, it is initially placed at one end (far left—the colorless end—by laboratory convention) of the tray on which the master stones are set in the viewing box. Using a pair of rubber-tipped tweezers, the grader moves the diamond along the set of master stones until it appears to be

one to two grades past the estimated color grade. It will, at this location, appear to have noticeably less color than the master stone to its left. The grader then moves the diamond back by placing it consistently to the right side of each master for comparison. When the diamond being graded appears to have less or the same amount of color as one master stone, and more color than the next master stone to its left, it has arrived at a single color grade range. Its grade is associated with the least colored of the two diamonds, since each master stone represents the highest (least colored) boundary marker in the range.

Some color grades in the D-to-Z scale may not appear to be different at first glance (for example, D, E, and F diamonds all appear virtually colorless). Therefore, it can be challenging for a grader to clearly place the diamond being graded between two master stones through the bracketing process (it may be located much closer to one of the masters). In this situation, it is common to identify the closest master stone, and then determine to which side of that master the diamond being graded should be placed. In making this determination, the grader places the diamond in one of two grade ranges that are separated by a master stone and then observes the diamond on each side of that master. This will result in one of a number of appearance relationships, the five most common of which are described in table 1 along with the corresponding grading decisions.

Master Eye Effect. The procedures detailed in table 1 were instituted to compensate for the phenomenon known as “master eye effect” (highlighted row in table 1) and the very subtle visual deviations in color

assessment it may cause. The effect is described as follows: When two diamonds are very similar in color appearance, the amount of color appears to reverse as the position of the diamonds is switched from left to right and right to left (Liddicoat, 1993). Much has been written about the dominance of one eye over the other in human binocular vision (see, e.g., Kromeier et al., 2006). What has long been described as the “master eye effect” in color grading is related to some degree to the difference in perception between the left and right eye. It is likely there are also psychological influences, such as the starting point used by a grader.

The effect of the master eye can be compounded in color grading by the production requirement of having a set of master stones in the field of vision when grading. The overall appearance of this set is that of a color gradation. If the master stones that form the color gradation are too close together, this can affect the grader’s perception of appearance relationships. To confirm this phenomenon, in the late 1990s we created a gradation of light-toned yellow color chips (simulating the D-to-Z range), and placed the chips in the viewing environment with one of them being a duplicate. Graders found that the undisclosed duplicate appeared to have less color than its twin when placed to the side of its twin next to chips with increasing color, and more when placed to the side of chips with lessening color (figure 16).

This tendency held true whether the gradation was arranged so the chips with less color were to the left or right of the observer. Recognizing this effect further strengthened the laboratory’s desire to

TABLE 1. Grading decisions for the five most common diamond vs. master stone appearance relationships.

Appearance of diamond as compared to closest master stone		Grading decision
Left side of master stone	Right side of master stone	
Slightly more color than master stone	→ AND noticeably less color than master stone	Receives higher grade than master stone
Same amount of color as master stone	→ AND less color than master stone	
Slightly more color than master stone	→ AND slightly (and to the same degree) less color than master stone	Receives same grade as master stone
Same or slightly more color than master stone	→ AND same or slightly less color than master stone	
Noticeably more color than master stone	→ AND slightly less color than master stone	

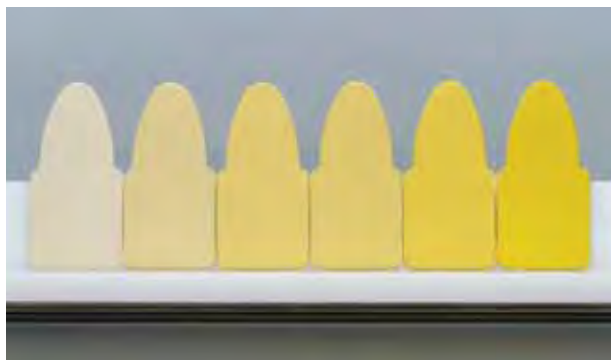


Figure 16. To better understand the effect of surrounding colors in making comparisons, color experiments were performed using standard color chips. In this photo, the third and fourth chips from the left are the same color. Graders found that the undisclosed duplicate appeared to have less color when placed to the side of its twin with increasing color and more when placed to the side with lessening color. This effect can be minimized in the grading process by spacing the color comparators farther apart on a long viewing tray. Photo by Jian Xin Liao.

transition to a longer viewing tray. Graders can now create much wider spacing between master stones to minimize the impact of the color gradation.

Additional Considerations for Color Grading. *Color Grading Diamonds that Differ Significantly in Size from the Master Stones.* Overcoming the visual effect of size differences between the diamond being graded and the master stone is an additional challenge even for the most experienced grader (figure

Figure 17. When grading diamonds significantly larger or smaller than those in the master set, the observer must look at the overall blend of color rather than the details. Here, a 10+ ct round brilliant is positioned next to an 0.70 ct J master. The best comparison process in this situation is for the experienced grader to observe the overall blend of the two diamonds simultaneously, rather than switching between the two diamonds, so that subtle color differences stand out. Photo by Robert Weldon.



17). To aid in making this determination, graders observe an overall blend of color, similar to that previously described for colored diamonds (King et al., 2005), rather than select visual details. Through experience, the grader also learns how to gaze simultaneously at both the master and the diamond being graded. In so doing, the blend of color in each diamond is easier to relate regardless of size.

Color Grading Fluorescent Diamonds. While some obviously fluorescent diamonds can appear different under differing conditions (Moses et al., 1997), our goal is to report the colors of all D-to-Z diamonds under one standard set of conditions. Therefore, fluorescent diamonds are graded using the same viewing environment and geometry as for other diamonds in the D-to-Z color range. In fact, all diamonds are color graded before they are checked for fluorescence strength, as we have noted that occasionally the color appearance of a diamond will change temporarily when exposed to UV radiation. As a result, color graders do not know the degree of fluorescence in a diamond before they assess its color.

Color Grading Diamonds with Eye-Visible Clarity Characteristics. While not common, the laboratory occasionally encounters diamonds with large, extensive, and/or colored inclusions that affect or obscure the bodycolor when observed under normal color grading conditions. In these instances, the color grade includes the effect of the inclusions. Noticeable inclusions become blended into the overall appearance such that, for example, dense areas of dark inclusions result in the diamond having a gray appearance (figure 18, left). If inclusions are restricted to a small area, their effect is limited (figure 18, right), because the diamond can usually be positioned so as to minimize the visual impact of the inclusions for grading purposes.

There are also times when the lab encounters diamonds with stains in fractures. If the stain is so prominent that it affects overall appearance, the lab will not grade the diamond because all or a portion of the stain might be removed by boiling in sulfuric acid, a procedure commonly used to alter the appearance of diamonds with surface-reaching fractures. Such a diamond will be graded only after the client has boiled it and the stain has been removed, as that is considered its permanent state.

Diamonds with dense clouds of tiny particles or whitish graining may appear translucent in the color grading process. If the transparency is greatly



Figure 18. When the grader observes the overall blend of color, the extensive inclusions in the diamond on the far left will become part of the observation and ultimately affect the final grade. When the included area is very limited, as in the diamond in the center, the stone is positioned (far right) to minimize the visual impact of the inclusions on the final grade. Photos by Jian Xin Liao.

affected, the diamond is graded as a colored diamond and described as Fancy white. At the laboratory, a master diamond is used for this comparison, but a simple method to help understand the approximate color-grade boundary is as follows: If the transparency is so affected that a grader cannot readily observe the pavilion facets through the table of the diamond using a 10× loupe under standard conditions, it is too translucent to grade on the D-to-Z scale and should be described as Fancy white. If it is not too translucent, it follows standard D-to-Z color grading procedures (figure 19). The movement of translucent diamonds off the D-to-Z scale is similar to the movement of light yellow diamonds past Z: In both cases, it is the degree of color, or translucency, seen table-up that determines whether the diamond enters the Fancy range. A translucent D-to-Z diamond may receive virtually any color grade.

Grading Mounted Diamonds. Prior to the 1980s, the laboratory graded mounted D-to-Z diamonds, reporting the grade in a two- to three-grade range. Over time, the laboratory decided to discontinue this practice and issue reports only on unmounted diamonds.

Currently, we examine mounted diamonds solely as part of a “confirmation process”—that is, to confirm it is the same diamond as one described on an existing report—within the laboratory’s Verification Service. Because the subtle color appearance of D-to-Z diamonds makes consistent color grading in mountings very challenging (since they can be affected by the color of the surrounding metal), the lab uses grade ranges (e.g., H to J) in these instances. For the Verification Service, the range is described only on “in-house” documents as part of the identification process required to match a diamond to a GIA report.

Color Grading Brown or Gray Diamonds in the D-to-Z System. From its inception, the D-to-Z system included near-colorless to light brown diamonds. Prior to and throughout the 1980s, the use of yellow master stones for brown diamond comparisons was a common procedure. At that time, the brown diamonds typically submitted for grading reports were in the E-to-J range. While there is a noticeable difference in hue, brown diamonds in this range share tone and saturation qualities with their yellow counterparts (for a discussion on the three attributes of color—hue,

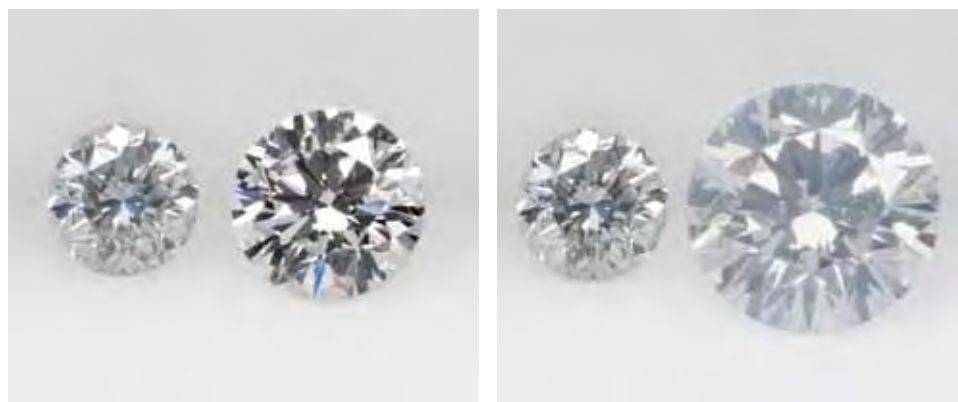


Figure 19. The smaller diamond appears obviously translucent next to the J master stone (left), but it is less translucent than the boundary Fancy white master (right). Therefore, it would be graded (table-down) on the D-to-Z scale. Photos by Robert Weldon.

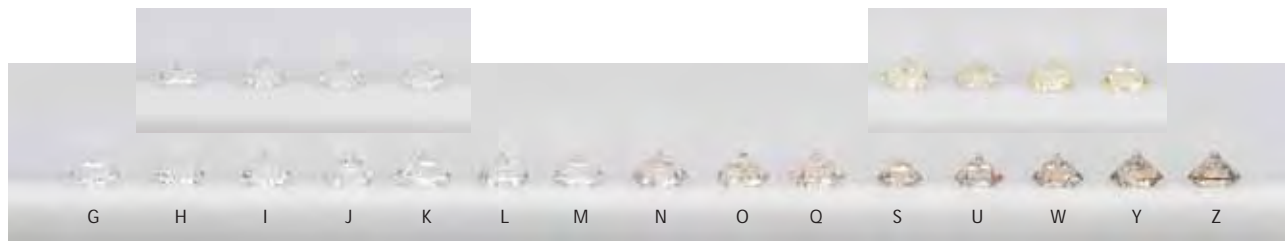


Figure 20. Historically, brown diamonds submitted to the lab for grading were most often located in the higher color grade range, similar to yellow masters (inset above left) in tone and saturation. In recent decades, the lab has seen greater numbers of darker brown diamonds. As a result, toward the lower end of the D-to-Z scale, graders noticed significant differences in color attributes between yellow (inset above right) and brown diamonds. To maintain consistency in the grading of these diamonds, GIA developed this master set of browns, which begins at G. Photos by Robert Weldon.

tone, and saturation—see King et al., 1994). This made the visual comparison to yellow masters compatible for brown diamonds in these letter grades.

With the influx of stones from Australia’s Argyle mine since the mid-1980s, there has been greater industry awareness and marketing of brown diamonds (Richardson, 1991). As a result, more brown diamonds have been submitted to the GIA Laboratory, not only in the near-colorless region but throughout the color grade scale. Accordingly, the laboratory created a master set of brown diamonds (figure 20). As these stones become darker, the differences in hue, tone, and saturation are more pronounced. This contributed early on to the laboratory’s decision to begin associating a word description with the letter grades of brown diamonds beginning at K (figure 21). Today, a *letter grade plus word descriptions* of “Faint brown,” “Very Light brown,” and “Light brown” are used for the grade ranges of K–M, N–R, and S–Z, respectively.

The color transition between brown and yellow diamonds is continuous, and the laboratory occasionally encounters diamonds with color appearances that are “in-between” the two different colors of the master sets (e.g., yellow-brown). It is important to choose the appropriate set of masters (i.e., yellow or brown) for the comparison process. This is usually accomplished by comparing the diamond being graded to both sets and selecting the one closest in appearance.

We recognize that others in the industry do not have D-to-Z scale brown master sets (and grading brown master stones is not a service the GIA Laboratory currently offers). Assessing the color of brown diamonds using only yellow master stones can be challenging. When doing so, the observer must remember to assess the overall depth of color—the combined effect of tone (lightness to darkness) and saturation (strength or weakness) of a color (King et al., 1994). Some observers try to grade just as they would yellow diamonds, and only look for saturation differences (the “amount” of yellow), which can

result in an incorrectly high determination compared to laboratory grading. If yellow master stones are the only ones available, the observer should assess the overall depth of color and equate it to the overall depth of the yellow master stone.

The reporting approach for gray diamonds is similar to—but not the same as—that used for browns. In the colorless to near-colorless range (E to J), they are graded using the D-to-Z scale letter grades. Beginning at K, though, gray diamonds receive a *word description only* of “Faint,” “Very Light,” or “Light” gray for the same letter grade ranges as for brown diamonds (King et al., 1994). Although gray diamonds are reported with only word terms in this range, historically they have not been considered a “fancy” color until they reach a description of “Fancy Light” (as with yellows and browns).

Color Grading at the Lower End of the D-to-Z Range. Color grading at the lower end of the scale (below N or O) can present special challenges for graders. As the color becomes more noticeable, so do the differences between color attributes. In determining the relationship of a diamond to a master stone, an observer must contend with subtle differences in tone (lightness or darkness) and hue (as opposed to the predominance of saturation in the decision making for other areas of the scale).

The difficulty in making grade distinctions between single color grades in this range limits the usefulness of all the individual color grades in the O-to-Z range. More important, we have found that such fine distinctions are not in demand among the laboratory’s clients; nor are they significantly useful to the trade for valuing these diamonds. We have informed clients that reporting color grades in this portion of the grading scale by using *grade ranges* is the best solution. The master stone locations used for laboratory reporting, are O, Q, S, U, W, Y, and the Z/Fancy Light boundary. Therefore, GIA grading reports will note a color as “S–T range” or “Y–Z range,” for example.

COLOR GRADE TERMINOLOGY BOUNDARIES

	Yellow	Brown	Gray	Other		
D	Letter Grade Only	Letter Grade Only		Colored Diamond Color Grade		
E					Letter Grade Only	
F						
G					Letter Grade Only	
H		Letter Grade Only				
I					Letter Grade Only	
J		Letter Grade Only				
K				Letter Grade + "Faint Brown"	"Faint Gray"	
L		Letter Grade + "Very Light Brown"	"Very Light Gray"			
M				"Very Light Gray"		
N						
O-P	Letter Grade + "Light Brown"	"Light Gray"				
Q-R			"Light Gray"			
S-T						
U-V	Colored Diamond Color Grade					
W-X						
Y-Z						
> Z	Colored Diamond Color Grade					

Figure 21. Shown here are the various boundaries at which colors transition off the D-to-Z scale, as well as terminology associated with the scale. After K, reports note a word description and letter grade for brown diamonds and a word description only for grays. Yellow, brown, and gray diamonds transition to the colored diamond color grading terminology after Z; all other colors transition at G.

As mentioned previously, round brilliants are graded table-down up to Z on the color grading scale, but face-up observation increases in importance when we are grading fancy shapes. From our experience, the majority of yellow fancy shapes graded Q or lower table-down appear to be one or more grades lower than this when observed face-up (figure 22). Historically, this led us to assign a final grade that averaged the two appearances when both diamonds fall on the D-to-Z scale. At the transition boundary between the D-to-Z scale and fancy colors, face-up appearance becomes the single factor that determines the color grade; that is, a diamond that has a stronger face-up color appearance than the Z/Fancy Light boundary master stone is considered a fancy color regardless of the color observed table-down.

(For a detailed discussion of the transition of yellow diamonds from the D-to-Z scale to the terminology for colored diamonds, see King et al., 2005.)

Over a period of months in the late 1990s, the laboratory researched ways to increase consistency of grading yellow fancy shapes in this part of the scale while acknowledging the relationship of the two observation positions. Working from the known face-up location of the Z/Fancy Light boundary, staff members made table-down and face-up comparisons for hundreds of fancy-shape yellow diamonds. These data were used to establish the relationship between the two observation positions. At that point, the laboratory selected a series of fancy-shape diamonds (figure 23) that would represent the face-up fancy shape boundary for the reported Light yellow grade

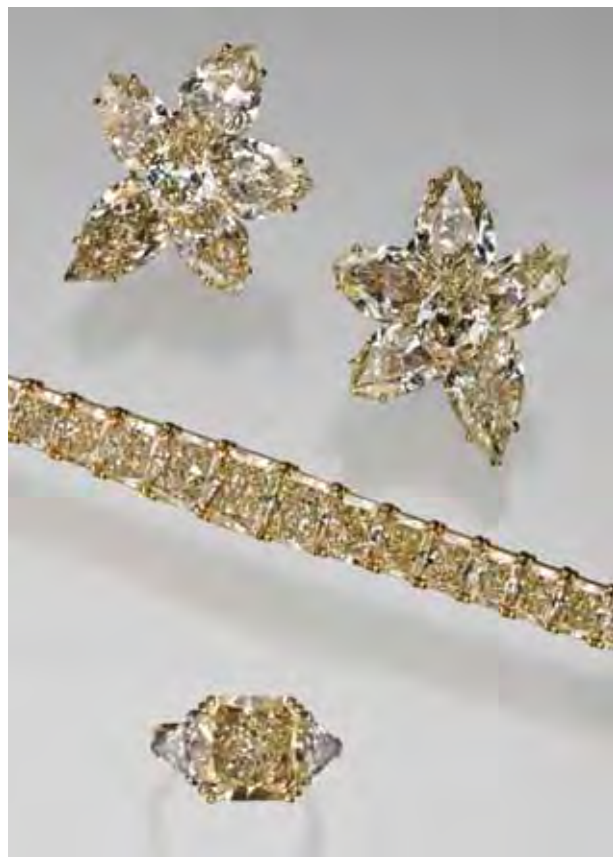


Figure 22. All the diamonds in these pieces are in the light yellow (S-to-Z) color range. At this end of the scale, face-up color becomes more noticeable, and can be used to good effect for yellow stones when mounted in yellow metal. The pear shapes in the earrings weigh a total of 53.92 ct, the diamonds in the bracelet total 42.16 carats, and the “starburst” cut in the ring weighs 8.92 ct. Courtesy of Louis Glick & Co.; photo by Robert Weldon.

ranges (S-T, U-V, W-X, and Y-Z). These diamonds supplement the round-brilliant masters, help expedite the grading process, and enhance consistency.

Transitioning from the D-to-Z Scale to Fancy Color Grades for Colors other than Yellow, Brown, and Gray. The occurrence of subtle colors other than yellow, brown, or gray is so rare that the presence of even slight tints is acknowledged in their color grading. When colors such as blue, pink, or green are equivalent to G or lower (i.e., the amount of color has moved out of the colorless range and into the near-colorless range), colored diamond color grading terminology is applied to describe that diamond (e.g., Faint pink or Faint blue [figure 24]). Figure 21 notes the location, in relation to the D-to-Z scale, where alternative terminology is applied for these colors as well as for brown and gray.

D-TO-Z INSTRUMENTAL COLOR MEASUREMENT

Colorimetry was introduced into gemology in England in the 1930s (“Measurement . . .,” 1933; “The standardization of colour,” 1933), but it was restricted to use with colored stones. Diamonds, with their often-subtle color differences, were more challenging. Robert Shipley Sr. envisioned the use of instruments for the color measurement of diamonds (Shipley, 1940) and, as mentioned earlier, introduced a visually comparative colorimeter in 1941. It was soon in full use at GIA for the grading of master stones. However, as Shipley Sr. recalled later (Shipley, 1958, p. 136), he was concerned because “the facets of the diamond were still pronounced, with the color varying over the observed portion of the stone. In other words, the facets being observed broke the color into a mosaic of varying intensities and this mixed pattern made it quite difficult to match the other half of the field [the portion of the wedge being viewed] with the diamond, since there was no single block of color to match against.”

In 1949, GIA instructor Joe Phillips developed an electronic colorimeter that employed a selenium photoelectric cell. Because it measured the relative transmission of yellow and blue light by a diamond, it was referred to as a distimulus (i.e., two stimuli) colorimeter. It was fairly effective but too expensive to produce commercially, and Phillips failed to resolve a number of other problems. While it was eventually abandoned, its design became the starting point for a small colorimeter developed by Robert Shipley Jr. several years later (see, e.g., GIA, 1962).

Shipley Jr. demonstrated his colorimeter at the 1956 AGS Conclave. Designed for use by AGS members in their stores, the new distimulus colorimeter had several limitations: It did not accurately grade stones with a greenish or brownish cast or those that were poorly cut. Large diamonds (over 5 ct) were also problematic (“Operating and maintenance instructions . . .,” n.d.; Sloan, 1956; GIA, 1962), as were highly fluorescent diamonds, since this instrument used an incandescent bulb with virtually no UV component. Even so, this electronic colorimeter was soon in use. Shipley Jr.’s colorimeter expanded the AGS color scale from VI to X and encompassed 11 AGS grades (AGS, 1965); however, it was not used for GIA grades (even though the 11 grades spanned the full 23-color D-to-Z color grading scale). The GIA Laboratory only used the electronic colorimeter to grade masters for AGS members (who used a 0 to 10 scale, not D to Z) and to check the calibration of colorimeters being supplied to AGS members by GIA.

By 1975, the costs and difficulties of repairing Shipley's colorimeters rendered them obsolete. Given the limitations of the instrument, GIA concluded it was not a suitable foundation for further developments in this area. Others in the industry did pursue such instrumentation, and Eickhorst patented a device using more advanced technology in 1974 (Eickhorst and Lenzen, 1974).

Over the course of the next 30 years, GIA researchers evaluated a number of color-measurement devices already in the marketplace that had been developed for various applications, including gemstones. They tested several colorimeters and spectrometers extensively and, for reasons such as lack of reproducibility or efficiency, concluded that none served the laboratory's purpose. In 1997, GIA made the decision to use its laboratory and research resources to develop a color measurement device of its own design for internal use. It sought a device that would mimic the visual D-to-Z color grading methodology as closely as possible.

Work started on this project in March 1998. In early 1999, the first instrument was constructed and put into use in the laboratory. For approximately one year, measurement data were collected in tandem with the visual grading results on thousands of diamonds. The statistical analysis of these data showed a good correlation between instrumental and visual color grades, and minor modifications to the device and measurement protocols continued to bring results even closer together. In addition, modulating the UV content in the light source allowed the laboratory to obtain reliable color measurement results for diamonds with obvious fluorescence that were very similar to those obtained with visual color grading. By mid-2000, the color grading accuracy of the device was similar to that of the laboratory graders, but with higher repeatability. Around this time, the laboratory began to use several of these devices to support the graders' opinions. This "instrument" opinion was not influential in the grading decision, but it helped support the visual grade determination and avoid errors. The process was started with stones below 2 ct and eventually expanded to larger sizes.

This approach was followed for the next year until the device's ability to perform accurate color grading had been validated. In 2001, following its application in the grading of tens of thousands of diamonds, we integrated the device as a "valid" opinion in the grading process, with visual agreement by one or more graders required to finalize the color grade of



Figure 23. The use of face-up masters in the light yellow grade range acknowledges the role of face-up color in grading fancy-shape diamonds at the lower end of the D-to-Z scale and enhances grading consistency. These represent, from left to right, S, U, W, Y, and the boundary between Z and Fancy Light yellow. Photo by Jian Xin Liao.

a particular diamond. Since then, the vast majority of diamonds passing through the laboratory have been graded by combining visual observation with instrumental color measurement. Note that this instrument is for the laboratory's internal use and is not available commercially.

SUMMARY AND CONCLUSIONS

Over the course of more than half a century, the D-to-Z diamond color grading system has become a critical component in the valuation of gem diamonds worldwide (figure 25). At the close of the background section, we noted that "using the same color grading terms does not constitute adhering to the conditions or methodology of the GIA system." We trust it is now clear that there is much more involved than the D-to-Z scale alone. The GIA system requires the use of standardized viewing conditions, calibrated references, and consistent

Figure 24. Colors other than yellow, brown, or gray are so rare that even subtle amounts are acknowledged. When a diamond has the same amount as—or more color than—the G master (i.e., moves out of the colorless to the near-colorless range) and shows a hue such as pink, blue, or green, it will be graded as a colored diamond—such as the Faint blue pear shape shown here between the F and G (yellow) masters. It appears to have more color than the G, to its right, so it would be graded on the colored diamond scale. Photo by Robert Weldon.





Figure 25. Color is so critical in the valuation of diamonds that diamond manufacturers must estimate the resulting color from the rough when calculating for the best yield. The octahedron pictured at top weighs 15.98 ct, while the macle weighs 22.33 ct. The faceted diamonds, ranging in color from D (the round on the left) to K (the oval), all weigh between 3.00 and 3.50 ct. Photo by Robert Weldon.

procedures to achieve sound, repeatable results. And it recognizes the importance of having standard policies and procedures not only for the majority of cases that are encountered but also for those seen less fre-

quently. Special approaches must be taken when the diamond being graded is significantly different from the master stones used in the laboratory. Larger diamonds, fancy shapes, those with a hue other than yellow, heavily included diamonds, and borderline fancy-color stones all require specific protocols to ensure the highest level of consistency and accuracy in the color grading process.

Technologies have evolved and will continue to evolve, so it is important to stay abreast of changes that may prove helpful in establishing color grades based on the original historic choice of those grade ranges. Some of the important advances have been the move from incandescent to fluorescent lighting in the viewing environment, the development of a viewing environment that maximizes the efficiency of the observer, and refinements in the system to accommodate increasing numbers of diamonds at the lower end of the scale. As it entered the 21st century, GIA developed color grading instrumentation to support the visual grading process.

Although daylight is the historical and universal standard for diamond observation, in reality no artificial light duplicates natural “daylight,” which itself changes with time and location. Nevertheless, we believe that a standard light source for diamond color grading should have key characteristics of daylight, including a UV component.

For GIA, any future updates in its diamond grading system must show a high correlation to past results in order to have merit. Nevertheless, we recognize that lighting technology and the understanding of human perception are constantly evolving, and believe that research is critical to maintaining the fundamental integrity of the system.

ABOUT THE AUTHORS

Mr. King (kking@gia.edu) is chief quality officer of the GIA Laboratory in New York City. Mr. Geurts is manager, Research and Development, at GIA Belgium in Antwerp. Mr. Gilbertson is research associate, and Dr. Shigley is distinguished research fellow, at the GIA Laboratory in Carlsbad, California.

ACKNOWLEDGMENTS

The authors thank Bert Krashes, former vice president of the GIA Laboratory (Gem Trade Laboratory at the time) for his historical perspective on color grading diamonds at GIA. Thomas M. Moses, senior vice-president at the GIA Laboratory in New York, provided guidance as well as current and past perspectives on color grading. Kelly Yantzer, manager of Systems Quality

Management at the GIA Laboratory in Carlsbad, assisted in the analysis of past and present laboratory color grading policies and procedures. Ilene Reinitz, project manager at the GIA Laboratory in New York, supplied a perspective on GIA lighting research over the years. Tim Thomas, GIA director of Instrumentation, provided information on the characteristics of standard light sources and best lighting practices. Peter De Jong, manager of Operations at GIA Belgium, provided overall insight on grading practices and, with GIA research scientist Troy Blodgett, information on prior light source testing conducted by GIA. Karin Hurwit, former senior staff gemologist with the GIA Laboratory, Carlsbad, kindly gave a historical overview of color grading methodology. Peter Hanselaer, CIE Division 1 representative from Belgium, provided information about CIE’s current activities.

REFERENCES

- AGS Research Service (1936) Notes on diamond grading. *Gems & Gemology*, Vol. 2, No. 4, pp. 77–78.
- American Gem Society [AGS] (1955) *Diamonds*. Los Angeles, CA.
- (1965) Diamond grading examination. Assignment 11 in *Selling and Merchandising*, AGS course materials, Los Angeles, CA.
- American Society for Testing and Materials [ASTM] (2003) Standard practice for visual appraisal of colors and color differences of diffusely-illuminated opaque materials. ASTM D1729-96, www.astm.org/standards/D1729.htm.
- A note on diamonds (1938) *Gems & Gemology*, Vol. 2, No. 10, p. 174.
- Approximate high asking price indications (1995) *Rapaport Diamond Report*, Vol. 31, No. 22, insert.
- At last—A recommended diamond display lamp—A daylight model (1938) *Guilds*, Winter 1938–1939, p. 9.
- Barton W. (1941) New devices grade gems. *Los Angeles Times*, June 29, p. A-8.
- Cattelle W. (1911) *The Diamond*. J. B. Lippincott, Philadelphia, PA.
- Chester C. (1910) *The Science of Diamond*. Chester & Bergman, Chicago.
- Christie's (2008) *Jewels: The Hong Kong Sale*. Auction catalog, December 2, Hong Kong.
- Collison W. (1947) The new standard Diamolite. *Gems & Gemology*, Vol. 10, No. 7, p. 431.
- Cowing M. (2008) A place for CZ masters in diamond colour grading. *Journal of Gemmology*, Vol. 31, No. 3–4 [in press].
- Dealers object to their diamonds having a jaundiced look (1894) *Jeweler's Circular*, March 7, p. 16.
- Diamond-grading instrument developed by GIA (1934) *Gems & Gemology*, Vol. 1, No. 4, AGS Campaign Supplement, p. 20.
- Eickhorst M., Lenzen G. (1974) *Method and Apparatus for Determining the Color of Cut Diamonds*. U.S. Patent 3,794,424, issued February 26.
- Epps H.H., Kaya N. (2004) Color matching from memory. In J. J. Caivano, Ed., *AIC 2004 Color and Paints*, Interim Meeting of the International Color Association, Porto Alegre, Brazil, November 3–5, pp. 18–21.
- Ferguson J. (1927) *Diamonds and Other Gems*. Publ. by the author, Los Angeles.
- Feuchtwanger L. (1867) *A Popular Treatise on Gems*, 3rd ed. Publ. by the author, New York.
- Gem talk (1981) *Jewelers' Circular Keystone*, September 1981, pp. 226–228.
- Gemological Institute of America [GIA] (1962) A system for diamond color grading. Assignment 19 in *Diamonds*, GIA course materials, Los Angeles.
- (1966) Diamond-grading, appraising and merchandising instruments. Assignment 35 in *Diamonds*, GIA course materials, Los Angeles.
- (1979) The art and science of color grading. Assignment 19 in *Diamonds*, GIA course materials, Santa Monica, CA.
- (1995) Grading color. Chapter 10 in *Diamond Grading*, GIA course materials, Santa Monica, CA.
- Gilbertson A. (2007) *American Cut—The First 100 Years*. Gemological Institute of America, Carlsbad, CA.
- Haske M. (2002) GIA GTL's color grading of fluorescent diamonds. www.adamsgem.org/giafluor.html [accessed December 14, 2007].
- Instrument research at laboratory continues (1937) *Guilds*, Spring and Summer, p. 2.
- International Commission on Illumination [CIE], International Electrotechnical Commission [IEC] (1987) *International Lighting Vocabulary*, 4th ed. Vienna, Austria.
- International Organization for Standardization [ISO] (2005) Viewing conditions: Graphic technology and photography. ISO 3664:2000, www.iso.org/iso/iso_catalogue/catalogue_tc/catalogue_detail.htm?csnumber=9117.
- King J.M., Moses T.M., Shigley J.E., Liu Y. (1994) Color grading of colored diamonds in the GIA Gem Trade Laboratory. *Gems & Gemology*, Vol. 30, No. 4, pp. 220–242.
- King J.M., Shigley J.E., Gelb T.H., Guhin S.S., Hall M., Wang W. (2005) Characterization and grading of natural-color yellow diamonds. *Gems & Gemology*, Vol. 41, No. 2, pp. 88–115.
- Kromeier M., Heinrich S.P., Bach M., Kommerell G. (2006) Ocular prevalence and stereoacuity. *Ophthalmic and Physiological Optics*, Vol. 26, No. 1, pp. 50–56.
- Liddicoat R.T. (no date) Untitled presentation manuscript. Richard T. Liddicoat Library and Information Center, Carlsbad, CA.
- (1993) *The GIA Diamond Dictionary*, 3rd ed. Gemological Institute of America, Santa Monica, CA.
- Mawe J. (1823) *A Treatise on Diamonds and Precious Stones*. Longman, Hurst, Rees, Orme, and Brown, London.
- Measurement of the colours of precious stones by means of the Guild Trichromatic Colorimeter (1933) *The Gemmologist*, Vol. 3, No. 26, pp. 39–44.
- Morton I. (1878) To South Africa for diamonds. *Scribner's*, Vol. 16, No. 4, pp. 662–675.
- Moses T.M. (1998) Letters: How GIA color-grades diamonds. *JCK*, Vol. 169, No. 12, pp. 21–22.
- Moses T.M., Reinitz I.M., Johnson M.L., King J.M., Shigley J.E. (1997) A contribution to understanding the effect of blue fluorescence on the appearance of diamonds. *Gems & Gemology*, Vol. 33, No. 4, pp. 244–259.
- On diamonds (1902) *The Connoisseur*, Vol. 4, September–December, pp. 248–252.
- Operating and maintenance instructions, American Gem Society electronic colorimeter (no date) Richard T. Liddicoat Library and Information Center, Carlsbad, CA.
- Richardson M. (1991) Australian miners peddle a browner shade of sparkle. *International Herald Tribune*, December 23, www.iht.com/articles/1991/12/23/shin.php.
- Roskin G. (1998) What GIA's fluorescence study ignored. *JCK*, Vol. 169, No. 9, p. 149.
- Schlossmacher K. (1949) The precise determination of the colors of gems, transl. by E. Kraus. *Gems & Gemology*, Vol. 6, No. 7, pp. 212–215.
- Sersen W.J., Hopkins C. (1989) Buying and selling gemstones: What light is best? *Gemmological Digest*, Vol. 2, No. 4, pp. 13–23.
- Shannon J. (1945) The GIA fluorescent unit. *Gems & Gemology*, Vol. 5, No. 3, pp. 254–256.
- Shipley R.M. (1938) New trade practice rules. *Gems & Gemology*, Vol. 2, No. 9, pp. 149–152.
- (1940) Color grades of diamonds. Section 32 in *Diamonds*, GIA course materials, Gemological Institute of America, Los Angeles.
- (1950a) A review of the diamond sections of the preceding courses. Assignment 201-2-4 in *Diamonds*, GIA course materials, Gemological Institute of America, Los Angeles.
- (1950b) The color of diamonds. Assignment 226 in *Diamonds*, GIA course materials, Gemological Institute of America, Los Angeles.
- (1955) Diamond-grading instruments. Assignment 2-37 in *Diamonds*, GIA course materials, Gemological Institute of America, Los Angeles.
- (1957) Final application of color, imperfection, proportion & finish grades to price. Assignment 2-31 in *Diamonds*, GIA course materials, Gemological Institute of America, Los Angeles.
- (1969?) Letter to Richard Liddicoat, June 10. Richard T. Liddicoat Library and Information Center, Carlsbad, CA.
- Shipley R.M., Liddicoat R.T. (1941) A solution to diamond grading problems. *Gems & Gemology*, Vol. 3, No. 11, pp. 162–167.
- Shipley R.M. Jr. (1941) Letter to Robert Shipley Sr., April 2. Richard T. Liddicoat Library and Information Center, Carlsbad, CA.
- (1958) Electronic colorimeter of diamonds. *Gems & Gemology*, Vol. 9, No. 1, pp. 136–143, 158.
- Shuster W. (2003) *Legacy of Leadership*. Gemological Institute of America, Carlsbad, CA.
- Sloan G. (1956) Letter to the Colorimeter Committee (Baumgardt, Broer, Donovan, Kaplan, Shipley Jr., Woodill, Muller, and GIA), October 13. Richard T. Liddicoat Library and Information Center, Carlsbad, CA.
- The standardization of colour (1933) *The Gemmologist*, Vol. 2, No. 23, pp. 380–381.
- Tashey T. (2000) True colors: Professional Gem Services takes a stand on the effect of fluorescence in color grading and appearance of white and off-white diamonds. *Cornerstone*, Fall, pp. 1, 3, 7.
- Tashey T. (2001) The effect of fluorescence on the colour grading of white and off-white diamonds. *The NCJV Valuer*, Vol. 19, No. 2, pp. 8–12.
- Tavernier J. (1676) *Les six voyages de Jean Baptiste Tavernier, Ecuier Baron d'Aubonne qu'il a fait en Turquie, en Perse, et aux Indes* [*The Six Voyages of Jean Baptiste Tavernier, Baron d' Aubonne, Made to Turkey, Persia, and the Indies*]. Gervais Clouzier et Claude Barbin, Paris.
- Wade F. (1915) Color and its affect [sic] on the value of diamonds. *The Jewelers' Circular*, August 4, pp. 49–53.
- Wade F. (1916) *Diamonds: A Study of the Factors that Govern Their Value*. G. P. Putnam & Sons, New York.
- Warner D. (2006) The Duboscq Colorimeter. *Bulletin of the Scientific Instrument Society*, No. 88, pp. 68–70.
- Wodiska J. (1886) *A Book of Precious Stones*. G. P. Putnam's Sons, New York.



RUBIES AND SAPPHIRES FROM WINZA, CENTRAL TANZANIA

Dietmar Schwarz, Vincent Pardieu, John M. Saul, Karl Schmetzer, Brendan M. Laurs,
Gaston Giuliani, Leo Klemm, Anna-Kathrin Malsy, Eric Erel, Christoph Hauzenberger,
Garry Du Toit, Anthony E. Fallick, and Daniel Ohnenstetter

Since late 2007, rubies and sapphires have been mined by hand methods from both eluvial and primary deposits at Winza in central Tanzania. The gem corundum is related to “dikes” of amphibolitic rocks that belong to the Paleoproterozoic Usagaran Belt. Based on crystal morphology, Winza corundum is subdivided into two types: prismatic-tabular-rhombohedral and dipyramidal. In general, medium red and dark (orangy) red top-quality rubies are rhombohedral. Pinkish red and purplish red rubies, as well as pink, purple, and blue (often strongly color zoned) sapphires are, for the most part, dipyramidal. The top-quality rubies are characterized by a distinct assemblage of long tube-, fiber-, needle-, or hair-like inclusions containing an orange-brown material (most likely limonite). The lower-quality material generally contains a larger amount of solid inclusions (mostly amphibole crystals), fissures, and growth features. Unique to corundum from this locality are bluish violet color zones oriented parallel to the prism and basal pinacoid, and occasionally also parallel to rhombohedral and dipyramidal faces. The relatively high Fe content of Winza rubies separates them from most other natural and almost all synthetic counterparts.

In early 2008, several very fine faceted rubies (e.g., figure 1) arrived in the market from a new deposit near the village of Winza in central Tanzania (Dimitri Mantheakis, pers. comm., 2008). These stones created considerable excitement, as the supply of fine unheated rubies had been scarce for years. In the ensuing gem rush, about 6,000 people had moved into the Winza area by July 2008. Although a few exceptional gems were recovered, for the most part the deposit has produced large quantities of ruby and pink-to-blue sapphire of much lower quality; very rarely, “padparadscha” sapphire is also found. Much of the material has been purchased and traded by Thai and Sri Lankan gem dealers who established buying offices in the nearby town of Mpwapwa. This report describes the mining and geology of the deposit, and provides a detailed gemological characterization of the rubies and sapphires.

Additional photos of the Winza mining area and photomicrographs of internal features are available in the *G&G* Data Depository (www.gia.edu/gemsandgemology). Also, more images and informa-

tion will be available on author VP's Winza web page at www.fieldgemology.org, beginning in mid-February 2009.

HISTORY

According to Dirlam et al. (1992), ruby was first discovered in Tanzania in the early 1900s near Longido, in the northern part of the country (figure 2). At Longido and other similar Tanzanian ruby-producing localities such as Lossogonoi, the corundum is found in “anyolite,” a rock composed of green zoisite and dark green to black amphibole.

In 1960, rubies and sapphires were discovered near the Kenyan border in the Uмба River valley (Hänni, 1987), where desilicated pegmatites intrude serpentinite.

See end of article for About the Authors and Acknowledgments.
GEMS & GEMOLOGY, Vol. 44, No. 4, pp. 322–347.
© 2008 Gemological Institute of America



Figure 1. Some exceptional rubies have been recovered since early 2008 from a new deposit at Winza, Tanzania. These ~5 ct and 11 ct faceted rubies are reportedly unheated, and are shown with a variety of rough samples from Winza. Courtesy of Van Cleef and Arpels, Piat, and the Gübelin Gem Lab (GGL); photo by V. Pardieu/GGL.

During the 1970s, rubies and spinels were found associated with marbles in primary or secondary deposits at two main areas in the Morogoro region of central Tanzania (Hänni and Schmetzer, 1991). The first area, located just east of the town of Morogoro near the village of Matombo, produced mainly during the 1980s. The second area is located to the south of Morogoro, near the mountain city of Mahenge. This area is quite large, and numerous ruby mining operations were known at Lukande, Mayote, Chipa, Epanko, Kitonga, and Kitwaro. The area is still being worked, but it is no longer as active as it was during the 1980s (Pardieu, 2005, 2007).

In the southern part of Tanzania, gem corundum was also found near Songea (in 1993) and Tunduru (in 1994; Milisenda et al., 1997), and these areas are still active today. However, mining declined after the discovery of the large gem placers at Ilakaka in Madagascar in 1999.

With the exception of some remarkable stones primarily from the Morogoro deposits, Tanzania was historically known to produce mostly cabochon-quality rubies or stones that required heat treatment (Dirlam et al., 1992). Therefore, the recent discovery of high-quality rubies at Winza is a welcome event for the Tanzanian gem trade.

Prior to the ruby rush, the Winza area was sparsely inhabited by maize farmers. The original discovery of ruby and sapphire there is shrouded in mystery, but some local residents report that gems were actually mined for years by a farmer who kept his activities secret. The farmer reportedly visited Dar es Salaam regularly to sell his stones. After the

farmer died, his young son continued his business but was not able to keep the secret. In November 2007, Tanzanian traders learned about Winza rubies and came to the area to mine. Local reports aside, we do know that mining activities have apparently taken place in the Winza area since at least the 1950s, as evident from a Mpwapwa district map published in that decade (and seen by one of the authors [VP] in Tanzania); it showed mine symbols near the location of the present corundum deposits. Another author (JMS) recalls that in the late 1960s, large quantities of well-crystallized opaque brown-gray corundum crystals measuring up to ~10 cm were produced from near Mvomero, which is located ~100 km east of Mpwapwa, but none of the material showed potential for gem use.

By December 2007, about 600 diggers and brokers from various mining areas and gem markets in Tanzania had moved to Winza to work the deposit for ruby and sapphire. In January 2008, one of the gem brokers (Abdul Msellem) told author VP about the new deposit. At the February 2008 Tucson gem show, Tanzanian dealer Dimitri Mantheakis informed author BML that more than 1,000 miners were active in a “gem rush” to the area.

In April 2008, author VP visited Winza with gemologist Jean Baptiste Senoble, and in June author BML visited the mining area with Dr. James Shigley of GIA Research. At the time of these two visits, about 5,000 miners were working the deposit. There were numerous brokers on-site, and several buying offices had been set up in the town of Mpwapwa. By July 2008, there were more than 100



Figure 2. The Winza deposit is located in central Tanzania, ~120 km south-east of Dodoma and 320 km west of Dar es Salaam. Other gem corundum localities in Tanzania include Longido, Lossogonoi, Morogoro, Mahenge, Tunduru, and the Uмба River valley.

foreign buyers (mostly Thai and Sri Lankan) in Mpwapwa and about 6,000 miners at Winza (A. Msellem, pers. comm., 2008). As of December 2008, the Tanzanian government was processing applications for 600 small-scale mining licenses (8 × 10 hectares each) in the Winza area (V. Komu, pers. comm., 2008).

LOCATION AND ACCESS

The Winza mining area is located 120 km (by air) from the capital city of Dodoma (again, see figure 2). From Dodoma, the small town of Mpwapwa is reached in about 2 hours by following a paved road for 48 km and a dirt road for 60 km. From Mpwapwa, a dirt road leads 85 km to Winza village (07°00'58" S, 36°21'54" E) and another 10 km to the mining area (07°05'03" S, 36°19'11" E). The travel time from Mpwapwa is 2.5–3 hours in a four-wheel-drive vehicle during the dry season (from approximately May to October). During the rainy season,

deep mud makes the road difficult to impassable, and it may take several days to reach Winza.

The mining area is sometimes referred to as “Mtakanini” (meaning “what do you want?” in Swahili) after the name of a nearby hill. Foreigners are not allowed to visit Tanzanian gem mining areas without proper authorization from government and local authorities.

GEOLOGIC SETTING

The Winza area belongs to the Paleoproterozoic Usagaran Belt (figure 3), a rock unit composed of highly metamorphosed basement rocks, metasediments that have undergone a lower grade of metamorphism, and felsic magmatic intrusives and volcanoclastic sediments that are nearly unmetamorphosed and undeformed. Structurally, the Usagaran Belt constitutes the eastern border of the Archean Tanzania Craton (see, e.g., Fritz et al., 2005).

The eastern parts of the Usagaran Belt were reworked during the Neoproterozoic East African Orogeny and have been designated the *Western Granulites*, while further to the east, a unit of younger Mesoproterozoic rocks composed of enderbite gneisses (metamorphosed igneous rocks of the charnockite series), schists, and marbles has been named the *Eastern Granulites* (Fritz et al., 2005). The Eastern and Western Granulites were metamorphosed simultaneously, and together they constitute the Neoproterozoic Mozambique Belt of Tanzania and Kenya.

Most of the known gem corundum occurrences in Tanzania and southeastern Kenya—including Longido, Uмба, the Mangari area, Morogoro, and Mahenge—belong to the granulite-facies Eastern Granulites, which was overprinted by a metamorphic event some 620–640 million years ago (Ma) at temperatures around 750–850°C and pressures in the range of 9.5–12 kbar (Appel et al., 1998; Moeller et al., 2000; Hauzenberger et al., 2004, 2007).

At the Winza deposit, gem corundum crystals occur in mafic rocks (of unknown age), which are hosted by 1800–2000 Ma basement rocks of the Usagaran Belt (Gabert and Wendt, 1974; Sommer et al., 2005). The main rock types are migmatitic and well-foliated gneisses, indicative of upper amphibolite to granulite facies conditions. The grade of metamorphism of East African gem corundum deposits within the Eastern Granulites appears similar to that of the Usagaran basement rocks at Winza.

Mining of the primary deposits has revealed

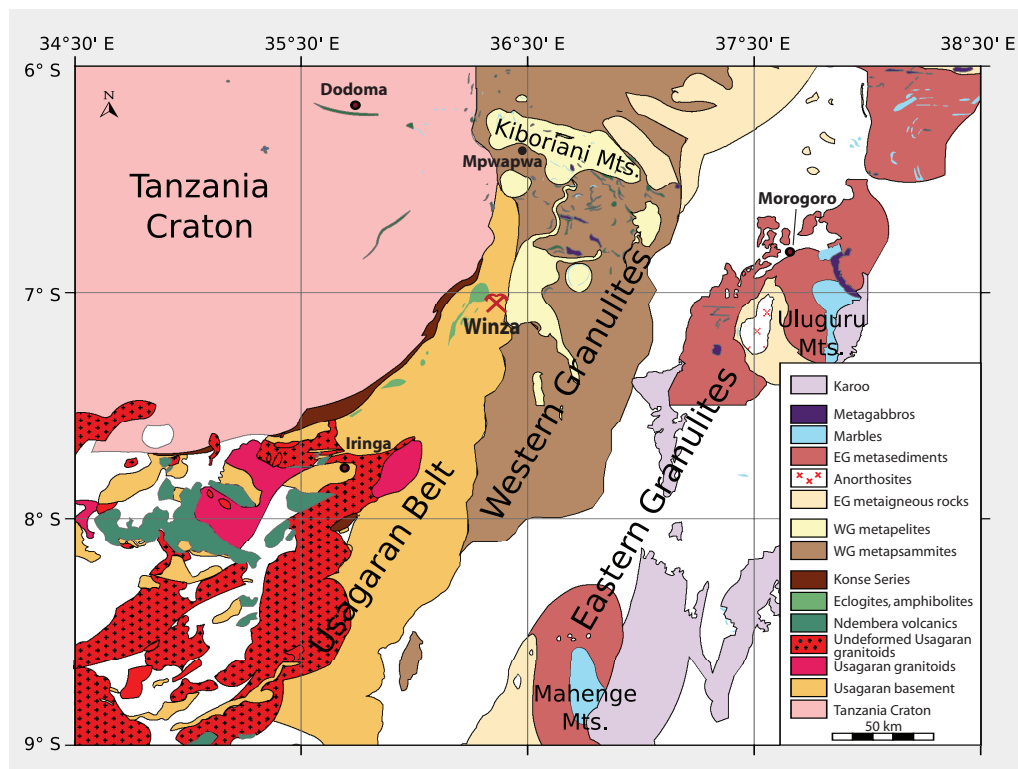


Figure 3. The Winza deposit is hosted by Usagaran basement rocks, not far from the Tanzania Craton. The basement is composed of a variety of highly metamorphosed rocks. Adapted from Fritz et al. (2005).

corundum crystals embedded within dark-colored amphibolite. Weathering of the primary deposits resulted in an overlying soil horizon (eluvial deposit) that also contains gem corundum.

MINING AND PRODUCTION

As of July 2008, mining in the Winza area was performed by several hundred small groups organized around a local miners' association. The miners constructed a settlement adjacent to the mining area, near a seasonal river (Mtindiri) that supplies water to wash the soil and for personal use. Both the eluvial and primary deposits have been worked (figure 4). The eluvial soil was excavated with picks and shovels, and taken to the river for washing. The soil was transported in bags by hand or on bicycles; a few operations also employed hand carts or pickup trucks. Although no mechanized mining was taking place, one of us (BML) saw a jiggling apparatus in the mining area that was awaiting installation.

The miners use small pumps and simple screens to wash the soil (figure 5), and then pick out the gems by hand. There is little or no water in the river during the dry season, so the miners dig pits in the river bed and build dams to create small pools for their washing activities.

Work on the primary deposits was initiated in March 2008. At the time of the authors' visits, tun-

nels up to 30 m deep had been excavated. Material was transported to the surface using buckets that were raised by windlasses or simply by pulling ropes

Figure 4. The eluvial and primary deposits at Winza (both shown here) have been mined by hand methods, and the gem-bearing material is then carried to the Mtindiri River for washing. This is typically done by hand, but a truck was also in use at the time this photo was taken in May 2008. Photo by B. M. Laurs.





Figure 5. The gem-bearing soil is washed using water from Mtindiri River. The miners dig pits in the riverbed to make small reservoirs, and the water is pumped through a network of hoses to the washing screens. Photo by V. Pardieu/GGL.

(figure 6). Local miners informed author VP that the best-quality rubies were recovered from the eluvial deposits, although author BML was told by a similar source that at least one exceptional stone was produced from one of the tunnels in the primary deposit. During both visits, the production from the primary deposits was reported to be lower compared to the

Figure 6. Ruby and sapphire mining in Winza is now concentrating more on the primary deposit located under the gem-rich soil. Mining takes place in pits that follow near-vertical amphibolite “dikes” (one is visible here between the two workers). Photo by V. Pardieu/GGL.



eluvial soil. As of October 2008, however, the eluvial deposits appeared to be mostly exhausted, but sapphires continued to be mined from a few tunnels in the primary deposit (A. Msellem, pers. comm., 2008).

Most of the Winza production is purchased at the mines by Tanzanian brokers, who typically sell the stones in Mpwapwa to foreign buyers. The buyers have constructed several offices and their advertisements are seen throughout Mpwapwa, making it reminiscent of the gem rush towns of Tunduru in southern Tanzania and Ilakaka in southern Madagascar.

Most of the Winza rough is brought to Bangkok and Colombo for distribution into the world market. Initially, heat treatment of Winza ruby was not very successful: Thai dealers reported that the stones turned orangy red without a significant improvement in color or clarity. Nevertheless, during the Gübelin Lab’s off-premises testing activities at the Hong Kong Jewellery & Watch Fair in September 2008, author DS identified the first heat-treated gem-quality rubies from Winza that were submitted by customers for certification by GGL. These stones (up to ~5 ct) displayed an orange modifying hue.

Although not abundant, some very clean and highly transparent rubies—which do not need heat treatment—have been discovered at Winza (again, see figure 1). Rough material of this quality has been mistaken as synthetic by some buyers because of its strong color and transparency. Synthetics are the main problem local buyers encounter when purchasing Winza stones in Tanzania (e.g., figure 7). Also of concern is the presence of other gem materials, such as pink-red spinel, in parcels of Winza ruby.

MATERIALS AND METHODS

For this study, we characterized 289 rubies and sapphires from Winza by a variety of techniques. A description of the samples and the methods by which they were tested is given in table 1.

At GGL, we used a Topcon refractometer, with a near-sodium equivalent light source, to measure refractive indices and birefringence. Specific gravity was determined by the hydrostatic method. The fluorescence behavior to standard 365 nm long-wave and 254 nm short-wave UV radiation was observed in a darkened room. Internal features were observed with standard gemological microscopes (Bausch & Lomb and Schneider Stemi 2000 with Zeiss optics). Mineral inclusions were analyzed using a Renishaw Raman 1000 spectrometer with an Ar⁺ (or green) laser at an



Figure 7. This pile of Winza ruby rough (left) formed part of a parcel offered by a Tanzanian gem broker; the small bright sample in the center turned out to be synthetic. The rough and cut samples in the right photo were seen in Dar es Salaam, and were reportedly mined from Winza. The two pieces on the left are synthetic (1.33 g rough and 1.55 ct cut), while those on the right are natural (3.89 ct cut and 0.52 g rough). Note the convincing color zoning in the rough synthetic piece. Photos by Jean Baptiste Senoble (left) and B. M. Laurs (right).

TABLE 1. Materials and methods used in this study of Winza gem corundum.

Sample group ^a	Heated?	Color	No. of samples in each group	No. of samples in each test								
				Morphology and growth structures	Standard gem properties	Internal features	Associated inclusions ^b	UV-Vis-NIR	FTIR	EDXRF	LA-ICP-MS	Isotope analysis
A1	No	Red, orange-red, purplish red, pinkish red, pink, purple, blue	1 matrix specimen	—	—	—	1 (EMPA), 1 (LA-ICP-MS)	—	—	—	—	—
A2	No		25 rough	25	—	25	3 (EMPA), 1 (XRD)	—	—	—	—	—
A3	No		70 (56+14) windowed	10	12	70	18 (Raman), 6 (LA-ICP-MS)	35	48	70	26	3
B	No	Red, orange-red, purplish red, pinkish red, padparadscha	60 faceted	20	8	60	5 (Raman)	11	11	60	20	—
C	No	Red, purplish red, orangy red	33 faceted	—	—	—	—	—	—	33	33	—
D	Yes	Orangy red	5 faceted	—	—	5	—	—	—	—	—	—
E	No/yes	Orangy red, purplish pink	3 pairs windowed	—	—	6	—	—	6	—	—	—
F	Yes	Orangy red	3 faceted	—	—	3	—	—	—	—	—	—
G1	No	Red, purplish red, purple, orangy red	25 matrix specimens	25	—	—	—	—	—	—	—	—
G2	No		50 rough	50	—	50	4 (SEM), 1 (XRD)	—	—	—	—	—
H	No	Purplish red to red	14 faceted	—	14	—	—	—	—	—	—	—

^a Notes:

- A1: Rock sample containing ruby/sapphire obtained by author JMS in Tanzania.
- A3: 56 samples were selected (based on color and transparency) from about 500 pieces of reportedly unheated rough obtained from miners or brokers in Mpwapwa and Arusha by one of the authors (VP) in April 2008. Fourteen samples were selected from rough material donated by various companies located in Bangkok, Colombo, and Idar-Oberstein. All samples were transparent and suitable for cutting. After two parallel windows were polished on each sample, they ranged from 0.32 to 8.71 ct.
- B: Most are from various companies in Thailand (-0.5–13.3 ct); includes >10 top-quality rubies submitted by GGL customers during and after the 2008 Basel Fair.
- C: Acquired from various companies in Thailand from April to June 2008 (-0.4–1.3 ct). All were represented as being from Winza, and their properties were consistent with the rough samples that were obtained in Tanzania by the authors.
- D: Examined microscopically by author DS in Bangkok in May 2008 (-0.5 ct each).
- E: Three untreated samples (-1.5–2.5 ct, orangy red and purplish pink) were each cut into two pieces, and then one piece from each sample was submitted for heat treatment in Bangkok in June 2008.
- F: Submitted to GGL gemologists for reports during the Hong Kong Jewellery & Watch Fair in September 2008 (-2–5 ct).
- G1 and G2: Obtained at the October 2008 Munich mineral fair.
- H: Submitted to the GIA Laboratory in Bangkok for reports (1.56–11.51 ct).

^b Analytic technique used for identification is shown in parentheses. Abbreviations: EMPA = electron microprobe analysis, LA-ICP-MS = laser ablation-inductively coupled plasma-mass spectrometry, Raman = Raman microspectroscopy, SEM = scanning electron microscopy (with energy-dispersive spectroscopy), XRD = X-ray diffraction.



Figure 8. The Winza rubies studied for this report include these samples (2.07–6.09 ct), which were examined at GIA's Bangkok lab in early 2008. All the stones proved to be unheated. Photo by Suchada Kittayachaiwattana.

excitation wavelength of 514 nm. Polarized ultraviolet-visible-near infrared (UV-Vis-NIR) absorption spectra were taken with a Perkin Elmer Lambda 19 spectrometer, in the range of 280–880 nm. Unpolarized mid-IR spectra (5000–1500 cm^{-1}) were collected using a Philips PU9624 Fourier-transform infrared (FTIR) spectrometer and a DRIFTS beam condenser, at a resolution of 4 cm^{-1} and with 200 scans.

Also at GGL, semiquantitative energy-dispersive X-ray fluorescence (EDXRF) chemical analysis was performed with a QuanX EC instrument (compare to Schwarz et al., 2000). It was operated using a special set of parameters optimized for the analysis of corundum with various conditions for voltage (six steps from 5–30 kV), lifetime (200–300 seconds), and filter type (no filter, cellulose, aluminum, palladium

of different thickness). Laser ablation–inductively coupled plasma–mass spectrometry (LA-ICP-MS) data—approximately four spot analyses per sample—were measured with a Perkin Elmer ELAN DRC-e single collector quadrupole mass spectrometer and a CETAC LSX-213 Nd:YAG laser ablation system. The Q-switched 213 nm laser was set to a 10 Hz pulse rate with an energy of ~30 mJ per pulse of 5-nanosecond duration. All analyses were performed as single-spot (100 μm) depth profiles. In addition to the 53 faceted and 26 windowed corundum samples analyzed by this technique, the minerals in one petrographic thin section (two pale pink corundum crystals, as well as garnet and amphibole from the matrix) were analyzed by both LA-ICP-MS and electron microprobe. Electron microprobe analyses were performed at the Eugen Stumpfl Electron Microprobe Laboratory, Universities of Graz and Leoben, Austria, with a JEOL JXA 8200 instrument. Analytical conditions consisted of an accelerating voltage of 15 kV and a 10 nA sample current; matrix corrections were made following the ZAF procedure.

At GIA in Bangkok, gemological properties were measured on 14 rubies (e.g., figure 8) using standard techniques.

Crystal morphology was studied by author KS by taking angle measurements of crystals/fragments using a contact goniometer and by angle measurement in the immersion microscope.

Growth structures were observed in rough, windowed, and faceted samples by microscopic techniques with the samples immersed in methylene iodide. Five black minerals that were attached to or exposed at the surface of these samples were analyzed by scanning electron microscopy with energy-dispersive spectroscopy (SEM-EDS) and X-ray diffraction.

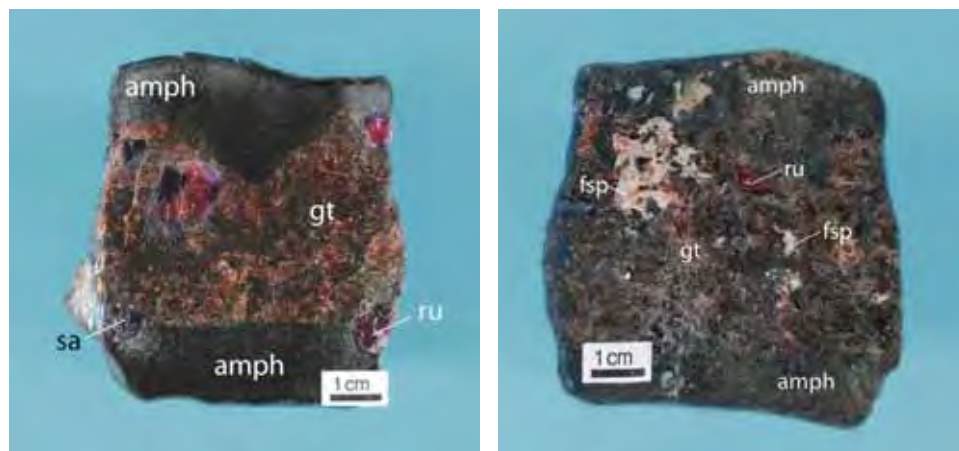


Figure 9. These slabs were cut from a Winza rock sample. The slab on the left consists of uniformly fine-grained amphibolite (amph) margins flanking orangy brown garnet (gt), ruby (ru), and sapphire (sa). The slab on the right also contains plagioclase feldspar (fsp). Photos by Patrick Lagrange.

TABLE 2. Crystal faces observed in rubies and sapphires from Winza, Tanzania.

Habit	Observed crystal form	Dominant face	Subordinate face	Miller index hkl ^a	Angle between c-axis and crystal face
Rhombohedral to prismatic	Basal pinacoid	<i>c</i>	—	(0001)	90°
	Second-order hexagonal prism	<i>a</i>	—	(1120)	0°
	Positive rhombohedron	<i>r</i>	—	(10 $\bar{1}$ 1)	32.4°
	Negative rhombohedron	<i>s</i>	—	(02 $\bar{2}$ 1)	17.6°
	Hexagonal dipyrmaid	—	<i>n</i>	(22 $\bar{4}$ 3)	28.8°
Tabular	Basal pinacoid	<i>c</i>	—	(0001)	90°
	Negative rhombohedron	—	<i>s</i>	(02 $\bar{2}$ 1)	17.6°
	Hexagonal dipyrmaid	<i>n</i>	—	(22 $\bar{4}$ 3)	28.8°
Dipyramidal	Basal pinacoid	<i>c</i>	—	(0001)	90°
	Positive rhombohedron	—	<i>r</i>	(10 $\bar{1}$ 1)	32.4°
	Negative rhombohedron	—	<i>s</i>	(02 $\bar{2}$ 1)	17.6°
	Hexagonal dipyrmaid	ϑ	—	(88 $\bar{1}$ 63)	7.8°
	Hexagonal dipyrmaid	<i>v</i>	—	(44 $\bar{8}$ 3)	15.4°
	Hexagonal dipyrmaid	—	<i>n</i>	(22 $\bar{4}$ 3)	28.8°

^a Based on morphological cell with *a:c* = 1:1.365.

Similar nontransparent-to-semi-transparent violet areas in nine rough and windowed samples from GGL were analyzed by electron microprobe (three samples) or LA-ICP-MS (six samples).

Oxygen isotope analyses of portions of three windowed GGL rubies (pink to red, deep red with blue banding, and deep red) were performed by author AEF in Scotland using a modification of the laser-fluorination technique described by Sharp (1990). Most analyses were run two or three times to check for isotopic heterogeneity and analytical artifacts. The method involved complete reaction of ~1 mg of powdered corundum, heated by a CO₂ laser, with ClF₃ as the fluorine reagent. The released oxygen was passed through an in-line Hg-diffusion pump before conversion to CO₂ on platinumized graphite. The yield was measured by a capacitance manometer, and the gas-vacuum line was connected to a dedicated VG Prism 3 dual inlet isotope-ratio mass spectrometer.

Three untreated samples (~1.5–2.5 ct, orangy red and purplish pink) were each cut into two pieces, and then one piece from each sample was submitted for standard heat treatment in Bangkok in June 2008.

MINERALOGICAL AND GEMOLOGICAL PROPERTIES

Host Rock Constituents. The matrix samples consisted of corundum crystals embedded within areas of coarse-grained orangy brown garnet that are hosted by granular dark green-black amphibolite (figure 9). This assemblage locally contains areas of plagioclase, with accessory spinel, mica, kyanite, and allanite.

Electron microprobe analyses of the amphibole identified it as aluminopargasite with a significant

amount of chlorine (0.8–1.0 wt.% Cl). The chemical composition varied slightly between the core and rim and within different areas of the sample. A representative chemical formula of an amphibole core is (Na_{0.39}K_{0.12})(Na_{0.17}Ca_{1.83})(Mg_{2.74}Fe_{0.59}²⁺Fe_{0.48}³⁺Al_{1.17})(Si_{5.97}Al_{2.03})O₂₂(OH_{1.72}F_{0.06}Cl_{0.22}). The host-rock garnet was found to consist of 34% grossular, 32% pyrope, 32% almandine, and 2% spessartine, with the chemical formula (Ca_{1.02}Mg_{0.96}Fe_{0.99}Mn_{0.1})(Al_{2.0})(SiO₄)₃.

Corundum Crystal Morphology. All the crystals studied showed some highly reflective planar faces, but most also had less reflective, not exactly planar, and somewhat inclined and rounded faces. The latter planes were apparently contact surfaces with other corundum crystals or associated minerals. This was carefully considered when the morphology of the sometimes extremely distorted crystals was determined. Some of the crystals had distinct growth striations on their crystal faces that were oriented perpendicular to the *c*-axis.

The corundum crystals showed a variety of habits. Some were elongated and mostly broken, whereas others were more equidimensional, essentially complete crystals. Occasionally, elongated forms also had end faces, but complete, well-terminated crystals were extremely rare. Four habits were recognized: rhombohedral (negative and positive), prismatic (long and short), tabular, and dipyramidal. The crystal forms observed for all habits are summarized in table 2. The top-quality rubies were rhombohedral, while the lower-quality corundum was characterized by different morphology.

The rhombohedral and prismatic types were gradational into one another. No intermediate samples,



Figure 10. Most of the rhombohedral Winza ruby crystals (here, up to 13×18 mm) showed negative rhombohedral (pseudo-octahedral) forms, consisting of *s* and *c* faces. Photo by K. Schmetzer.

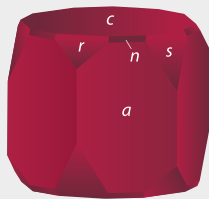
however, were observed between the rhombohedral-to-prismatic type and samples with dipyramidal habit. We saw only one tabular crystal, probably related to the positive rhombohedral type.

Surprisingly, most rhombohedral crystals consisted of the basal pinacoid *c* and the negative rhombo-

Figure 12. These Winza corundum crystals show prismatic (far left, 11×7 mm) and rhombohedral-prismatic (the other four, up to 14×14 mm) forms, which consist of various combinations of *c*, *a*, *s*, *r*, and *n* faces. Photo by K. Schmetzer.



Long Prismatic



Short Prismatic



Rhombohedral-Prismatic



Figure 11. Several of the ruby and sapphire crystals examined (here, up to 8×10 mm) had positive rhombohedral faces, or both positive and negative rhombohedral forms (*r* and *s*, respectively). Depending on the size of the basal pinacoid *c*, a platy habit may result. Photo by K. Schmetzer.

hedron *s* as dominant forms (figure 10), rather than *c* and the positive rhombohedron *r*. The latter habit, with *c* and *r*, is commonly observed in rhombohedral corundum from Mogok, Myanmar (Bauer, 1896; Melcher, 1902), and from Morogoro, Tanzania (Hänni and Schmetzer, 1991).

The negative rhombohedron *s* is extremely rare in corundum, though it was mentioned by Goldschmidt (1918) as a subordinate crystal form. To the best of our knowledge, *s* was not described previously as a dominant crystal form of corundum. The *r* and *s* forms can be distinguished by their different inclinations to the *c*-axis, which are 32.4° and 17.6° , respectively.

The angles formed by the basal pinacoid and the two rhombohedral forms were calculated as follows:

- Basal pinacoid *c* and positive rhombohedron *r*: $c^{\wedge}r = 122.4^\circ$, $r^{\wedge}r = 94.0^\circ$
- Basal pinacoid *c* and negative rhombohedron *s*: $c^{\wedge}s = 107.6^\circ$, $s^{\wedge}s = 111.3^\circ$

The two angles in corundum crystals with *c* and *s* faces are closely related to the characteristic angle of a spinel octahedron (109.5°). Therefore, this type of Winza corundum can also be described as pseudo-octahedral.

We observed only one Winza sample that showed just the *c* and *r* forms, but several intermediate samples with both *r* and *s* (figure 11). These crystals were often somewhat thick tabular (platy) in habit. Occasionally, the rhombohedral crystals also showed small hexagonal dipyramids *n*. In the one tabular sample, these faces were dominant (along with basal pinacoids) and the rhombohedral faces were subordinate.

In all the prismatic Winza crystals, in addition to the basal pinacoid *c*, the hexagonal prism *a* was dominant, while *s*, *r*, and *n* faces were subordinate. According to the relative size of the *c* and *a* faces, we observed long-prismatic and short-prismatic crystals (figure 12). We also saw samples with a habit intermediate between rhombohedral and short-prismatic, some with a complicated morphology (again, see figure 12).

In contrast, samples with dipyramidal habit had simple forms. Most broken crystal fragments showed only one dipyramidal face, either ϑ or less frequently ν . We also commonly observed *c*, occasionally in combination with small *r*, *s*, and *n* faces (figure 13). Interestingly, the dipyramidal Winza material also showed the rare negative rhombohedron *s*, but no sample with dipyramidal ϑ and ν faces in combination with the prism *a* was observed.

The forms described above can be recognized in faceted stones by examining them in immersion and performing growth structure analysis (see below).

Figure 13. The dipyramidal Winza ruby and sapphire crystals, such as those shown here (lower right is 7 × 13 mm), are dominated by ϑ faces, which are accompanied by various combinations of *c*, *r*, *s*, ν , and *n* faces. Photo by K. Schmetzer.



Figure 14. Note the homogeneity of color in this fine unheated 9.15 ct Winza ruby. Courtesy of Hakimi & Sons; photo by Robert Weldon.

Visual Appearance and Gemological Properties. On the basis of our faceted samples (as well as those seen in the trade), we know that Winza rubies and sapphires range from blue to red. Although some of the rubies show exceptional transparency, most Winza stones have some milkyiness due to fissures and mineral inclusions. Both rubies and sapphires commonly have distinct color zoning, often with blue (or, more rarely, yellow or colorless) domains. Fine, evenly colored, saturated red or blue stones are quite rare. Top-quality vivid red rubies are generally very homogeneous in color (figure 14), but they may contain small areas of narrow blue zones. Most of the rubies are pinkish to purplish red to dark (orangy) red with moderate saturation. The sapphires are pink, purple, and blue, typically with moderate saturation (e.g., figure 15). Only a very few blue sapphires (<5 ct) of good quality from Winza have been reported in the Thai market. Orange-pink padparadscha Winza sapphires are even rarer. Our heat-treated specimens were orangy red to orange-red. Some stones cut from Winza material (unheated and heated) show more than one color (e.g., figure 16).

The physical properties of some unheated samples are reported in table 3; there were no variations in their characteristics according to color.

Growth Features and Color Zoning. Growth planes were observed parallel to the dominant crystal faces in all morphological types. However, in most of the faceted samples examined, growth zoning was only seen parallel to the basal pinacoid *c*; rarely, it was parallel to several dominant faces (figure 17). Also uncommon was color zoning in completely red or pink samples (i.e., consisting of red or pink layers of various intensity; figure 18).



Figure 15. The faceted cushion cut (1.50 ct, courtesy of Mark Kaufman) and dipyramidal crystal (2.3 cm tall, courtesy of Werner Radl) provide attractive examples of sapphires from Winza; photo by Robert Weldon. The inset photos show color variations within a dipyramidal Winza sapphire crystal (1.3 cm tall, photo by Werner Radl) and in various faceted rubies and sapphires (0.61–1.69 ct; photo by K. Schmetzer).

The samples typically showed characteristic growth and color zoning consisting of bluish violet lamellae in otherwise uniformly colored red, pink, orange-pink, or pinkish violet corundum. These lamellae were observed occasionally in rhombohe-

Figure 16. Some Winza sapphires have been cut to show more than one color. These heat-treated samples weigh 0.88 and 1.03 ct. Courtesy of Michael Nemeth; photo by Robert Weldon.



dral and prismatic samples, and frequently in dipyramidal rubies and sapphires. Distinct lamellar zoning was easily seen—even with the naked eye—only in prismatic samples. Viewing perpendicular or oblique to the planes of these lamellae caused them to become transparent bluish violet. In contrast, when viewed parallel to the lamellar direction, the lamellae typically appeared black and nontransparent. Only in immersion, with proper orientation of the samples, did the fine lamellar nature of the color zoning become sharp in all samples (e.g., figure 19). Thus, such viewing conditions were necessary to resolve nonstructured color patches into fine lamellar patterns. In samples with bluish violet lamellae oriented parallel to several forms, the appearance of the color zones was rather complex (e.g., figure 20).

In prismatic crystals, the sharp bluish violet layers were typically oriented parallel to the dominant prism *a* (again, see figure 19). The pattern in rhombohedral and dipyramidal samples, however, was more complex. Viewed parallel to the *c*-axis, the dark bluish violet zone appeared confined to the outer rim of the crys-

TABLE 3. Physical properties of Winza corundum.

Property	Unheated ruby and sapphire
Color	Red, purplish red, pinkish red, orangy red Blue, pink, padparadscha
Dichroism (ruby) e-ray (or E c) o-ray (or E ⊥ c)	Orange to orangy red Purple-red to violet-red
RI	
n_o	1.767–1.771
n_e	1.758–1.762
Birefringence	0.008–0.010
SG	4.00–4.03 (average 4.02)
UV fluorescence	
Long-wave	Mostly weak to moderate; top-quality rubies strong to moderately strong
Short-wave	Very weak to weak; rarely, inert
Spectroscope	Typical chromium spectrum; in part, also Fe ³⁺ -related features
Internal features	<ul style="list-style-type: none"> • Long (typically curved) tube-, fiber-, needle- or hair-like inclusions of orange-brown color; common in top-quality red material, but not seen in pink, purple, or blue stones • Inclusion association: amphibole + garnet + apatite (rare) • Partially healed fissures composed of cavities containing mostly a polyphase filling of solid material • Fissures containing a grayish white to pale yellow substance resembling flux residues in synthetic rubies • Color zoning with thin bluish violet lamellae in both ruby and sapphire; various types of bluish violet layers parallel to the prism and/or the basal pinacoid • Rhombohedral twin planes, possibly with intersection tubules in one or more directions • Minute (exsolved?) particles

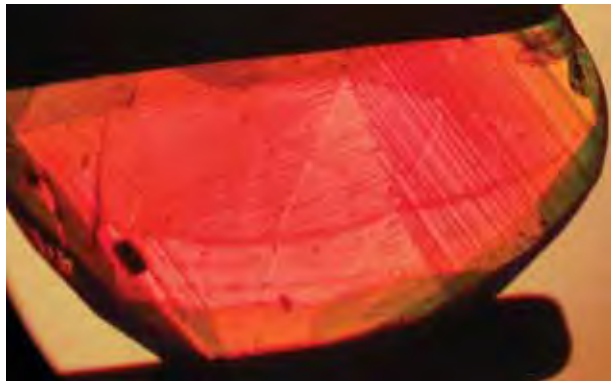


Figure 17. Multiple directions of growth zoning are rare in faceted Winza corundum. This stone has growth lines parallel to a (center of the sample), c (right portion), and a small zone parallel to n (left side). Photomicrograph by K. Schmetzer; immersion, magnified 40 \times and viewed \perp to the c-axis.

tals (figure 21, left; a similar crystal was documented by Choudhary, 2008). Viewed perpendicular to the c-axis, however, the bluish violet zones were seen to be localized within specific areas, separated by “normal” zones of ruby or sapphire (figure 21, center). On rotation, the intercalated “normal” layers may cause the bluish violet zones to appear as parallel layers oriented perpendicular to the c-axis (figure 21, right).

Nature of Dark-Colored Rims/Zones. Distinct bluish violet, almost black color zoning is common in Winza rubies and pink sapphires (Hänni and Krzemnicki, 2008; Krzemnicki and Hänni, 2008; Peretti 2008; Senoble, 2008). Abduriyim and Kitawaki (2008) mentioned that this color zoning is similar to the

Figure 19. Viewed parallel to the c-axis, this 13.8 \times 8.3 mm slab of prismatic Winza sapphire shows distinct bluish violet zones parallel to the hexagonal prism a. Photomicrograph by K. Schmetzer; immersion.

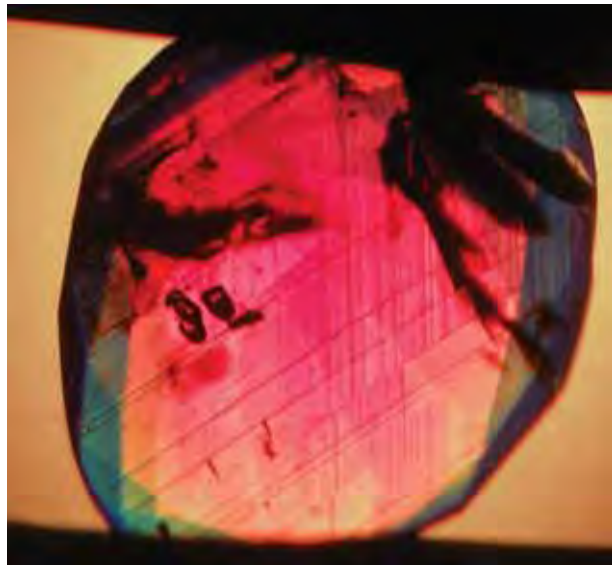


Figure 18. In this view perpendicular to the c-axis (which is horizontal) of a pink sample with layers of varying color intensity, growth patterns with color zoning are seen parallel to c and r. Photomicrograph by K. Schmetzer; immersion, magnified 50 \times .

pattern observed in rubies from Mong Hsu, Myanmar. To investigate whether such color zoning might be helpful for origin determination, as well as for separating faceted rubies and sapphires from their synthetic counterparts, the authors examined several samples of ruby and pink, pinkish orange, or pinkish

Figure 20. This sample shows complex color zoning, with bluish violet lamellae oriented parallel to the rhombohedra r and s, and also parallel to various hexagonal dipyrramids n. Photomicrograph by K. Schmetzer; immersion, magnified 50 \times and viewed approximately parallel to the c-axis.

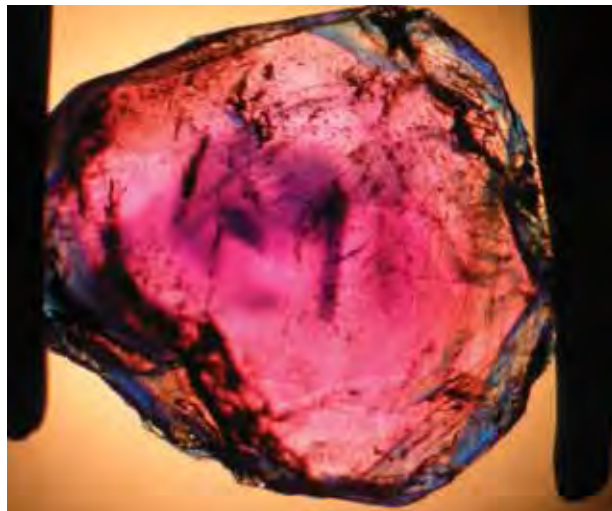




Figure 21. Viewed parallel to the *c*-axis, the 7-mm-wide dipyramidal corundum crystal on the left has a ruby core and a dark violetish blue (nearly black) rim. When another dipyramidal sample (center) is viewed perpendicular to the *c*-axis (which is horizontal in this photo), the bluish violet areas are restricted to small zones close to the rim. The rhombohedral sample on the right, which is also seen perpendicular to the *c*-axis (vertical in this photo), has bluish violet zones that appear as thin layers parallel to the basal pinacoid *c*. Photomicrographs by K. Schmetzer; center and right taken in immersion, magnified 50 \times .

violet sapphire with dark bluish violet- to black-appearing color variations (e.g., figure 22). Three different phases were identified:

1. Sapphire, which was black in reflected and transmitted light, but appeared bluish violet in thin slices or fragments (as described above).
2. Amphibole inclusions, which were black in reflected and transmitted light, but appeared green in thin areas. Such inclusions never revealed a fine lamellar or oriented pattern.
3. Black spinel rims on rubies with dipyramidal habit, but no black spinel was seen within the corundum crystals. Three chemical analyses gave a compositional range of $\text{Mg}_{0.5-0.6}\text{Fe}_{0.4-0.5}\text{Al}_2\text{O}_4$, which is intermediate between magnesium spinel and hercynite. Such rims are normally removed during the faceting process.

It was not always possible to distinguish between these three black-appearing phases without a detailed phase determination.

Twinning and Milky Domains. Rhombohedral twin planes (figure 23) were common. The samples typically contained one system of “intersection tubules,” but three-dimensional arrangements of these tubules were also observed (figure 24).

Very common in the sapphires were slightly milky domains in the form of clouds, bands, or “growth sectors” (figure 25). In general, their milky appearance was caused by the presence of very tiny gray pinpoint inclusions.

Inclusions. Elongate Needles. The most distinctive

features observed in Winza rubies were long tube-, fiber-, needle-, or hair-like inclusions (figure 26). These inclusions were especially common in the top-quality Winza rubies. The curved tubes were not observed in pink, purple, or blue samples. They were straight, slightly curved, bent, or even (rarely) spiral-like. They were filled with an orange-brown (probably polycrystalline) solid material, which generally did not give any useful signals when analyzed by Raman spectroscopy. A very large, slightly flattened tube exposed at the surface of a 0.60 ct faceted stone, however, showed an interesting mineral association. Several reflective (probably “unaltered”) sections of the tube provided a clear amphibole

Figure 22. These corundum crystals have dark bluish violet- to black-appearing translucent to opaque phases exposed at their surfaces. The dark areas in the two crystals on the left were found to be blue-violet sapphire, the sample in the center (9 \times 12 mm) contained black amphibole, and the two samples on the right had a rim of black spinel. Photo by K. Schmetzer.





Figure 23. Rhombohedral twin planes are common in Winza sapphires. Photomicrograph by V. Pardieu/GGL; magnified 40×, crossed polarizers.

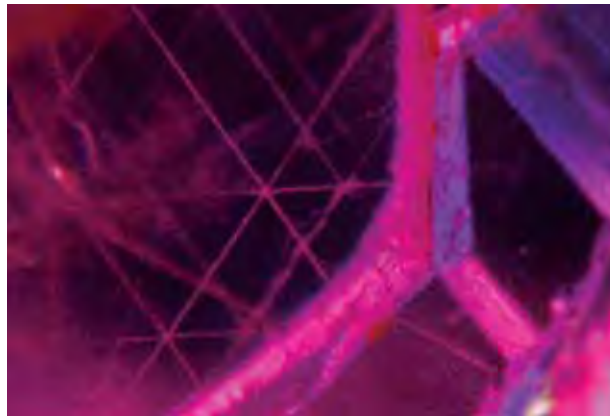


Figure 24. Intersections of the twin lamellae resulted in the formation of linear tubules—typically one system, but also three-dimensional networks as seen here. Photomicrograph by V. Pardieu/GGL; magnified 30×.

Raman spectrum, while brownish material between the reflective areas was identified as hematite.

Mineral Inclusions. Mineral inclusions were quite common. Compared to rubies/sapphires from many other localities, however, we identified (by Raman analysis or electron microprobe) only a small variety of mineral species in our samples: amphibole, garnet, apatite, and spinel.

By far the most common inclusion mineral observed was amphibole. It was very typical in the sapphires, but observed in only one (top-quality) ruby. The amphibole inclusions showed large variations in color, size, and shape. Many amphibole crystals were nearly colorless, while others were slightly green to dark green or brownish green to nearly black, and often showed strong pleochroism. For the most part,

the amphiboles displayed irregular, slightly rounded forms, but well-developed prismatic crystals also were common (figure 27). They occurred as single crystals or were clustered in groups or compact agglomerations. In some cases, they were accompanied by stress fissures in the host corundum.

The garnets were intense orange-yellow (figure 28); they were typically transparent and had well-developed or resorbed forms. Apatite was a very rare inclusion mineral (identified only in two of the top-quality rubies). It formed as colorless, transparent, prismatic, euhedral crystals that were not oriented crystallographically (figure 29). Spinel (Fe- and Mg-rich) was identified by electron microprobe as small inclusions in corundum, but it was not seen during

Figure 25. Winza sapphires commonly contain slightly milky domains caused by the presence of minute gray pinpoint inclusions. Photomicrograph by V. Pardieu/GGL; magnified 20×, fiber-optic illumination.



Figure 26. Probably the most characteristic features observed in some of the Winza rubies are long tube-, fiber-, needle-, or hair-like inclusions. These inclusions were especially common in the top-quality stones. Photomicrograph by V. Pardieu/GGL; magnified 40×.





Figure 27. Well-developed prismatic amphibole crystals are common in Winza corundum. The amphiboles do not show any preferred orientation in the corundum host; they can be considered as protogenetic inclusions. Photomicrograph by V. Pardieu/GGL; magnified 40 \times .

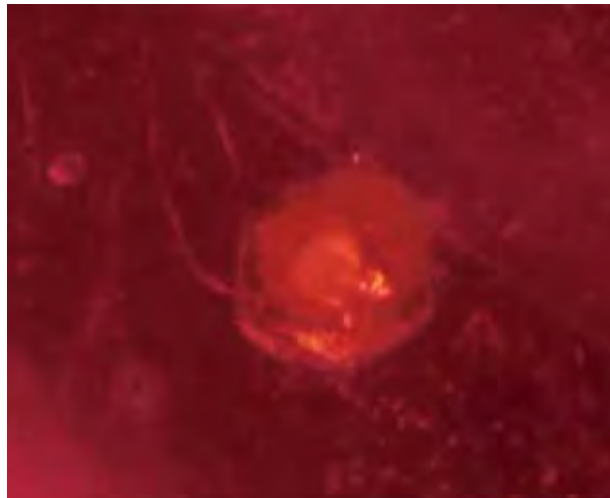


Figure 28. A well-formed orange-yellow garnet inclusion is present in this Winza ruby. Photomicrograph by V. Pardieu/GGL; magnified 40 \times .

the microscopic examination of the samples. It also formed dark rims surrounding dipyrarnidal rubies (see above). Opaque mineral grains displaying a grayish black metallic luster were tentatively identified as chalcocite (Cu_2S) by Raman analysis.

Uncommon in the sapphires were reflective particles that were generally accompanied by small, delicate, disk-like inclusions resembling the “thin films” more typical of basalt-related rubies (figure 30, left). Somewhat coarser particles were present in diffuse clouds or in stringer-like formations (figure 30, right).

Very rare were so-called comet tails associated with mineral inclusions (figure 31).

FTIR spectroscopy revealed the presence of various OH-bearing minerals, such as kaolinite, “limonite,” chlorite, and (very rarely) boehmite. These were observed on fissure planes and as components of the



Figure 29. Colorless transparent apatite crystals were seen in only two Winza rubies. Photomicrograph by V. Pardieu/GGL; magnified 40 \times .



Figure 30. Minute oriented reflective particles were seen in a few samples, generally accompanied by small disk-like inclusions reminiscent of “thin films” (left, magnified 30 \times). Less common are coarser particles present in diffuse clouds or stringer-like formations (right, magnified 80 \times). Photomicrographs by V. Pardieu/GGL; fiber-optic illumination.



Figure 31. A group of mineral inclusions (probably amphibole) is accompanied by a weakly developed "comet tail" in this Winza sapphire. Note also the pink-blue color zoning and (slightly diffuse) fine light blue growth bands. Photomicrograph by V. Pardieu/GGL; magnified 40 \times , fiber-optic illumination.

tube fillings. They also may be present in the form of submicroscopic "particles."

Fractures and Fluid Inclusions. Unhealed fissures were quite common in the commercial-quality material. These fissures were either strongly reflective (mirror-like) or they displayed a slightly frosted appearance caused by the presence of a gray or brown substance (e.g., oxihydrates, identified by FTIR).

Partially healed fissures were often present in medium- to low-quality rubies/sapphires. In general, they showed relatively coarse textures with highly reflective inclusions that were rounded or irregularly shaped; well-developed networks or fingerprint-like patterns were rare. Less common were healed fissures composed of cavities that for the most part were developed as negative crystals containing polyphase fillings with black (opaque), brown, and colorless (transparent, singly and doubly refractive) constituents (figure 32)

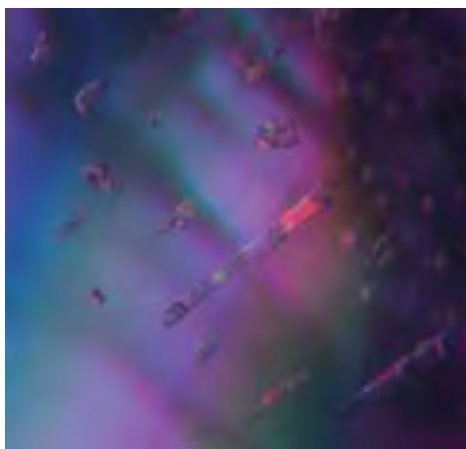
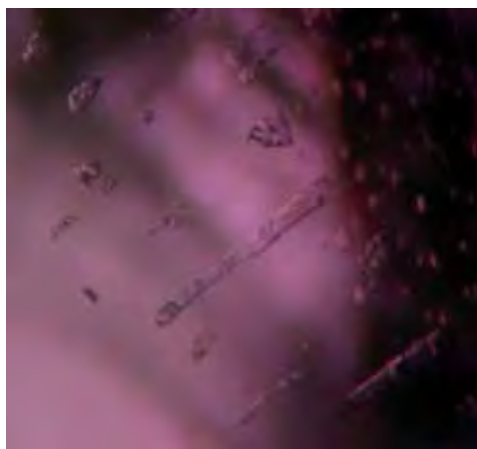


Figure 32. Partially healed fissures in some Winza rubies and sapphires were composed of negative crystals containing multiphase fillings with black-opaque and colorless-transparent (singly and doubly refractive) constituents. Photomicrographs by V. Pardieu/GGL; magnified 60 \times , brightfield (left) and cross-polarized (right) illumination.

that could not be identified by Raman analysis.

Many fissures appeared to be filled with a grayish white or pale yellow solid material (figure 33) that could not be identified. These inclusions may resemble the flux material common in some synthetic rubies.

CHEMICAL COMPOSITION

EDXRF analyses revealed that Winza rubies and sapphires showed a relatively uniform chemical composition. The chromophores Cr and Fe were present in significant concentrations. Cr concentrations fell into the common range for rubies (including the pinkish red and purplish red material) originating from most occurrences: ~0.10–0.60 wt.% Cr₂O₃. For the blue to purplish blue sapphires, Cr₂O₃ ranged from ~0.10 to 0.30 wt.%.

The Fe concentration in the rubies was relatively high, with more than 95% of the samples in the range of ~0.30–0.80 wt.% Fe₂O₃. In very few samples, Fe₂O₃ reached up to ~1 wt.%. Top-color Winza rubies were characterized by a combination of relatively low Fe₂O₃ (~0.30–0.40 wt.%) and relatively high Cr₂O₃ (~0.40–0.60 wt.%). Blue to purplish blue Winza sapphires had Fe₂O₃ concentrations of ~0.60–0.95 wt.%.

Winza rubies of the best color contained very little or no Ti (typically below the detection limit). For the other samples, TiO₂ concentrations were ~0.005–0.020 wt.%. The blue to purplish blue Winza sapphires typically contained ~0.01–0.03 wt.% TiO₂; the highest value found was ~0.045 wt.% TiO₂.

The V concentration of the rubies and sapphires was generally low, and in many samples it was below the detection limit of ~0.005 wt.% V₂O₃. Most common were V₂O₃ contents in the range of ~0.005–0.015

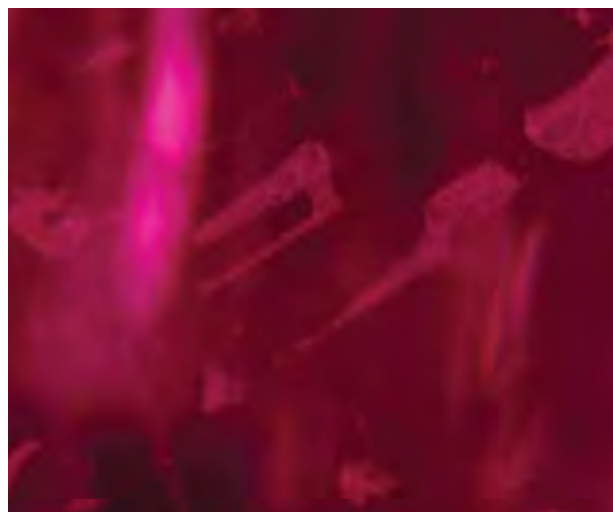


Figure 33. These irregularly shaped cavities are filled with a grayish white to pale yellow solid substance. Such inclusions may resemble the flux material observed in synthetic gems. Photomicrograph by V. Pardieu/GGL; magnified 60 \times .

TABLE 4. Electron microprobe analyses of two samples of pale pink Winza corundum.

Oxide (wt.%)	Wz1_Cor ^a	Wz2_Cor ^b
Al ₂ O ₃	98.80 \pm 0.44	98.50 \pm 0.18
Cr ₂ O ₃	0.07 \pm 0.02	0.05 \pm 0.02
Fe ₂ O ₃	0.36 \pm 0.06	0.39 \pm 0.06
TiO ₂	0.02 \pm 0.02	0.09 \pm 0.08
Total	99.25	99.03

^a 15 point analyses.

^b 6 point analyses.

wt.%; rarely, values up to ~0.02 wt.% were measured.

Ga content, for the most part, was below the detection limit (~0.005 wt.% Ga₂O₃). The highest Ga concentration found was ~0.01 wt.% Ga₂O₃.

Electron microprobe analyses of two pale pink corundum crystals in a rock thin section showed appreciable Fe and significant Cr, along with traces of Ti (table 4).

TABLE 5. Chemical composition by LA-ICP-MS of different colors of gem corundum from Winza, Tanzania (in ppmw).^a

Element	Red	N	Purple	N	Orange	N	Blue	N	Colorless	N
B	1.6 \pm 1.7	26	1.9 \pm 2.2	64	1.7 \pm 1.3	32	3.8 \pm 3.4	17	1.5 \pm 0.8	34
Na	3.1 \pm 8.1	40	4.7 \pm 18	68	5.0 \pm 19	37	2.5 \pm 5.5	15	0.88 \pm 2.4	23
Mg	39 \pm 36	54	39 \pm 33	120	36 \pm 20	59	45 \pm 36	30	26 \pm 25	55
Al	519900 \pm 2220	54	521300 \pm 2090	120	521500 \pm 2190	59	519500 \pm 1640	30	521900 \pm 1680	55
Si	4500 \pm 1210	54	4060 \pm 1650	120	3910 \pm 1450	59	4710 \pm 1180	30	3650 \pm 830	55
P	21 \pm 13	51	21 \pm 13	110	17 \pm 12	54	27 \pm 14	24	14 \pm 6.6	50
K	9.3 \pm 8.8	12	16 \pm 8.9	13	12 \pm 16	7	7.8 \pm 7.2	3	11 \pm 7.5	3
Ca	38 \pm 7	3	91 \pm 56	5	42 \pm 22	7	<40	0	25	1
Sc	0.060 \pm 0.0025	2	0.10 \pm 0.083	6	0.071 \pm 0.025	6	<0.12	0	0.060	1
Ti	63 \pm 63	51	120 \pm 170	110	88 \pm 110	56	280 \pm 380	30	61 \pm 64	55
V	2.5 \pm 2	54	2.1 \pm 1.4	120	2.1 \pm 1.5	59	3.1 \pm 1	30	1.8 \pm 1.3	55
Cr	2350 \pm 960	54	1390 \pm 640	120	1310 \pm 700	59	820 \pm 270	30	520 \pm 270	55
Mn	1.8 \pm 2.6	10	3.9 \pm 6.2	17	3.0 \pm 5.8	7	3.2 \pm 4.8	3	0.35 \pm 0.2	2
Fe	2370 \pm 670	54	2370 \pm 590	120	2430 \pm 670	59	3890 \pm 990	30	3070 \pm 890	55
Co	0.072 \pm 0.053	19	0.068 \pm 0.058	40	0.035 \pm 0.023	24	0.056 \pm 0.013	8	0.036 \pm 0.018	15
Ni	3.3 \pm 3.8	27	2.8 \pm 2.1	67	2.4 \pm 1.8	38	4.3 \pm 1.8	14	1.8 \pm 1.4	31
Cu	0.71 \pm 0.98	20	8.2 \pm 30	38	1.5 \pm 2.7	14	7.4 \pm 13	18	0.8 \pm 2.2	20
Zn	2.8 \pm 0.87	3	3.7 \pm 2.4	5	1.7	1	<1.7	0	1.5	1
Ga	21 \pm 6.5	54	25 \pm 11	120	23 \pm 6.6	59	28 \pm 5	30	21 \pm 7.7	55
Rb	0.034 \pm 0.033	10	0.081 \pm 0.078	12	0.11 \pm 0.12	8	0.094 \pm 0.13	3	0.034 \pm 0.048	4
Sr	0.94 \pm 2.4	13	3.0 \pm 11	20	2.8 \pm 6.6	8	1.0 \pm 2.1	5	0.017 \pm 0.0085	3
Zr	0.019 \pm 0.004	6	0.29 \pm 0.29	6	0.023 \pm 0.011	2	0.17 \pm 0.016	3	0.018	1
Nb	0.11 \pm 0.16	10	0.057 \pm 0.053	29	0.025 \pm 0.022	13	0.034 \pm 0.018	8	0.046 \pm 0.034	5
Sn	0.22 \pm 0.13	41	0.21 \pm 0.13	81	0.25 \pm 0.15	40	0.38 \pm 0.12	21	0.21 \pm 0.14	34
Cs	0.016 \pm 0.019	3	0.11 \pm 0.22	6	0.03 \pm 0.016	4	0.020 \pm 0.008	2	0.005 \pm 0.001	2
Ba	1.4 \pm 3.5	11	3.5 \pm 8.5	12	4.1 \pm 6.1	4	0.86 \pm 1.3	4	0.097 \pm 0.051	2
Ce	0.026 \pm 0.017	8	0.088 \pm 0.12	12	0.084 \pm 0.076	4	0.12 \pm 0.066	6	0.013	1
Ta	0.078 \pm 0.13	15	0.15 \pm 0.2	30	0.046 \pm 0.032	20	0.085 \pm 0.063	9	0.18 \pm 0.13	6
W	3.6 \pm 7.8	28	2.2 \pm 6.7	35	1.7 \pm 3.4	23	0.35 \pm 0.43	7	0.47 \pm 0.89	7
Pb	0.20 \pm 0.61	30	0.29 \pm 0.77	66	0.16 \pm 0.34	26	0.30 \pm 0.38	18	0.10 \pm 0.14	35

^a Notes: ppmw = parts per million by weight; < = value below the detection limit; N = number of values above the detection limit. Ablated material was carried to the ICP by He (5.0) carrier gas at a rate of 0.8 liters/minute (l/min). The plasma conditions of the ICP-MS were optimized to maximum intensity at U/Th ratio ~1 and Th/ThO ratio <0.5. This was achieved using the following parameters: plasma gas flow (Ar) 14.0 l/min, nebulizer gas flow (Ar) 0.85-0.9 l/min, auxiliary gas flow (He) 0.70-0.75 l/min, and RF power 1400 W. In the corundum matrices, the elements Be, B, Na, Mg, Al, Si, P, K, Sc, Ti, V, Cr, Mn, Fe, Co, Ni, Cu, Zn, Ga, Rb, Sr, Zr, Nb, Mo, Sn, Cs, Ba, Ce, Ta, W, Pb, Th, and U were measured quasi-simultaneously in each individual analysis.

LA-ICP-MS data for Winza corundum are reported in table 5. Generally, Si, Cr, and Fe were abundant, with concentrations above 500 ppm (0.05 wt.%). Traces of B, Na, Mg, P, Ti, V, Co, Ni, Cu, Ga, Sn, Ta, W, and Pb were commonly present. Na, Mg, Ti, Cr, V, and Fe were variable, while all other elements occurred in quite constant concentrations. A weak positive correlation was observed for the elements V and Ti.

SPECTROSCOPY

UV-Vis-NIR spectroscopy of Winza rubies revealed the well-known Cr^{3+} absorption bands at ~405–410 and 560 nm (figure 34, top). In addition, the spectra generally displayed a strong “background absorption” starting around 600 nm and increasing toward the UV edge. The absorption spectra of blue to purple-blue and padparadscha sapphires were, in general, combination spectra showing the Cr^{3+} absorption features together with a pronounced contribution of Fe^{3+} bands at 377/388 nm and 450 nm (figure 34, middle). More rarely seen was a combination of the Cr^{3+} features with the $\text{Fe}^{2+}\text{-Ti}^{4+}$ charge-transfer band of sapphire at around 700 nm (figure 34, bottom). The Cr “doublet” at 694 nm was visible in all spectra.

The FTIR spectra in the mid-infrared region between 5000 and 1500 cm^{-1} allow for the distinction of four main features (figure 35):

1. A more-or-less pronounced broad band with a maximum at ~3450 cm^{-1} was recorded in 41 of the 59 samples tested (spectrum A).
2. A prominent peak at ~3160 cm^{-1} —with accompanying peaks at ~3350, 3240, and 2420 cm^{-1} —was recognized in 38 samples (spectrum B). Most of the remaining samples showed a shoulder (sometimes very weak) at 3160 cm^{-1} . The 3160 cm^{-1} absorption was completely absent from only a very few samples. It is interesting to note that the “3160 group” (also named “3161-series”; Smith and Van der Bogert, 2006) was most prominent in the high-quality Winza rubies (i.e., in more than 90% of these stones).
3. An additional group of absorption peaks at ~3695, 3670, 3650, and 3620 cm^{-1} was rarely exhibited by high-quality rubies (spectrum C).
4. Distinct band groups in the 3560–3420 cm^{-1} region were detected in only three samples (spectrum D).

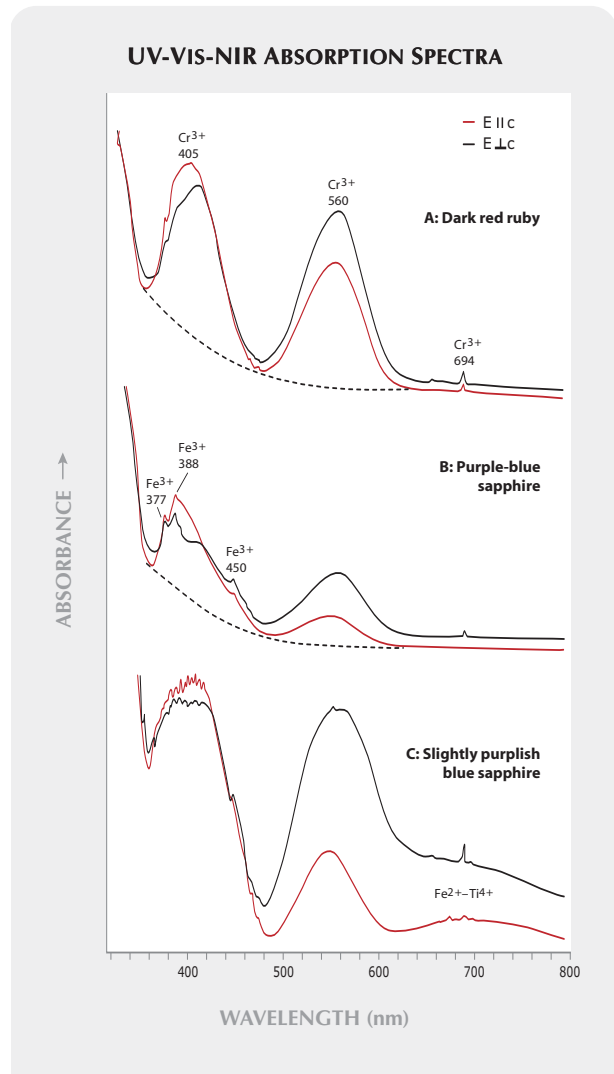


Figure 34. Polarized UV-Vis-NIR absorption spectra of Winza rubies show typical Cr^{3+} absorption bands at ~405–410 and 560 nm, as well as a strong “background absorption” (dotted line) in the UV region (A). The absorption spectra of blue to purple-blue sapphires from Winza generally show a combination of Cr^{3+} absorption features together with Fe^{3+} bands at 377/388 nm and 450 nm (B). Less common are combinations of the Cr^{3+} features with a $\text{Fe}^{2+}\text{-Ti}^{4+}$ charge-transfer band at ~700 nm (C, from a slightly purplish blue Winza sapphire).

The spectral features described above may be present in combination, with varying intensities of the different components (see, e.g., the combination of the band groups in the 3560–3420 cm^{-1} region and the 3160 cm^{-1} absorption in spectrum E, observed in a top-quality ruby). In two samples, weak peaks related to boehmite were detected at around 2100 and 1980 cm^{-1} (e.g., spectrum A).

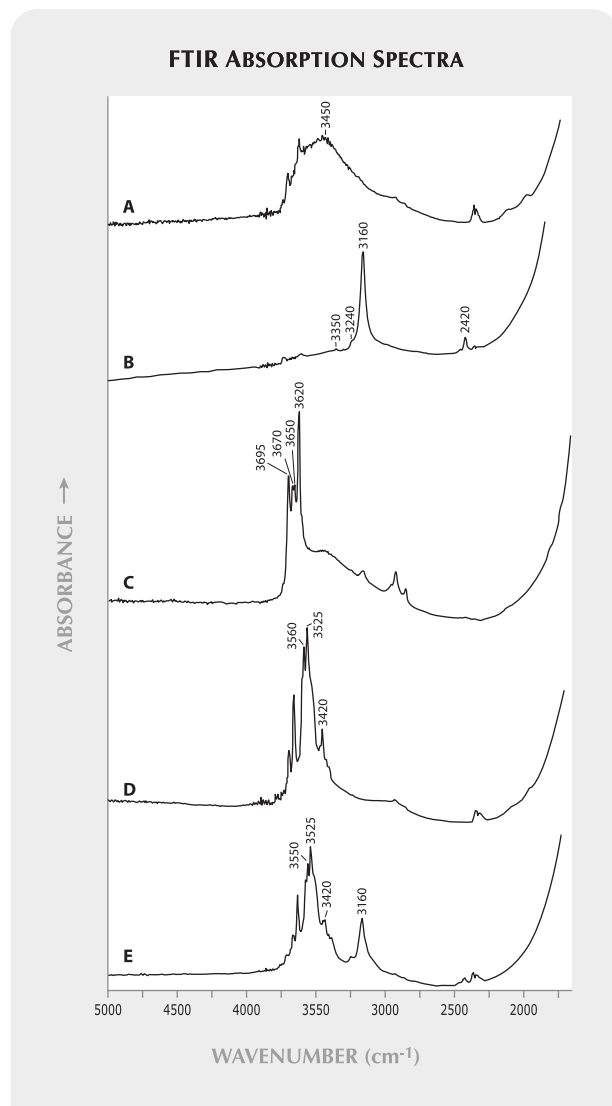


Figure 35. Unpolarized IR absorption spectra of Winza rubies showed four main features in the mid-infrared region between 5000 and 1500 cm^{-1} : (A) a broad band at $\sim 3450 \text{ cm}^{-1}$; (B) a prominent peak at $\sim 3160 \text{ cm}^{-1}$ often accompanied by peaks at ~ 3350 , 3240, and 2420 cm^{-1} ; (C) a group of absorption peaks at ~ 3695 , 3670, 3650, and 3620 cm^{-1} ; and (D) distinct bands in the 3560–3420 cm^{-1} region. These features may be present in combination and with varying intensities, as in spectrum E. In two samples, weak peaks related to boehmite were detected at around 2100 and 1980 cm^{-1} (e.g., spectrum A). Features seen at 2917, 2853, and 2349 cm^{-1} were caused by sample contamination.

OXYGEN ISOTOPE COMPOSITION

The oxygen isotope compositions obtained for three Winza rubies were $\delta^{18}\text{O} = 4.6\text{‰}$, 4.7‰ , and 4.9‰ (figure 36), giving a mean $\delta^{18}\text{O}$ of $4.7 \pm 0.15\text{‰}$. For information about the use of oxygen isotopes to charac-

terize corundum from different deposits, see Giuliani et al. (2007).

HEAT-TREATED SAMPLES

Heat-treated Winza rubies examined by one of the authors (DS) in Bangkok in May 2008 showed a distinct orangy red hue (as seen in the sample on the left in figure 16). The most striking internal feature was the presence of partially healed fissures displaying strong alteration patterns, with a drop-like or network-like melting appearance that is typical of intensely heat-treated rubies/sapphires. In part, these partially healed fissures were associated with altered mineral inclusions. Identical features were observed in the heat-treated rubies submitted to GGL for testing in Hong Kong in September 2008. The infrared spectra recorded for these samples did not show any features related to the presence of OH/H₂O (see Discussion below).

Comparison of the three pairs of unheated/heat-treated corundum showed that the orangy red sample did not change color. However, one of the purplish pink samples became intense red-orange after heat treatment. The second purplish pink sample developed an inhomogeneous color distribution, with orange and violet areas. All the unheated pieces showed the 3160 cm^{-1} absorption in varying intensity; these bands disappeared from the heat-treated samples.

DISCUSSION

Physical Properties. The measured refractive indices and specific gravity values from Winza (table 3) are consistent with those known for rubies and sapphires from all other localities. The morphology of the crystals is quite variable, and some of the samples have habits not seen previously in material from other ruby/sapphire deposits.

Microscopic Characteristics. *Growth Features and Color Zoning.* Although some Winza material may bear a superficial resemblance to Mong Hsu rubies, the orientation of the thin bluish violet lamellae within Winza corundum is completely different. Mong Hsu rubies typically have dark cores that are formed by bluish violet layers oriented parallel to rhombohedral and dipyrarnidal faces (Peretti et al., 1995). In the Winza samples, the bluish violet color zoning was oriented parallel to the prism and basal pinacoid, occasionally in combination with bluish violet layers oriented parallel to rhombohedral and dipyrarnidal faces. Such zoning has not been

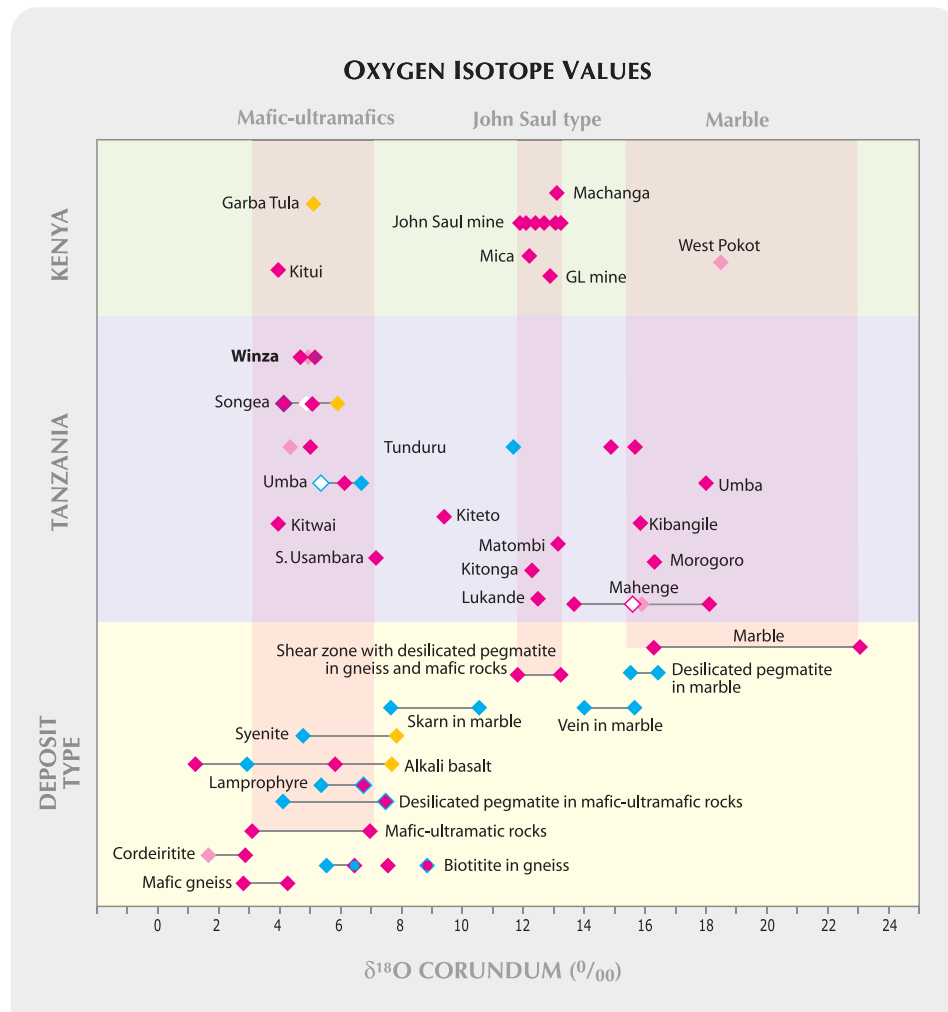


Figure 36. Oxygen isotope values for three rubies from Winza are shown with those for corundum from various types of primary and secondary deposits in Kenya and Tanzania. The data are reported in the conventional delta notation relative to V-SMOW (Vienna Standard Mean Ocean Water) equal to 0‰, and are compared with the oxygen isotopic ranges defined for various deposit types, after Giuliani et al. (2005, 2007). The symbol colors correspond to sample colors; white symbols represent colorless sapphires.

observed in gem corundum from other localities, to the best of the authors' knowledge.

Inclusions. Our findings are consistent with previous reports of inclusions in Winza corundum (Abduriyim and Kitawaki, 2008; GIT Gem Testing Laboratory, 2008; Hänni and Krzemnicki, 2008; Krzemnicki and Hänni, 2008; Pardieu and Schwarz, 2008; Smith et al., 2008).

Microscopic examination often can be used to distinguish Winza rubies/sapphires from those originating in other genetic environments or geographic localities. The following internal characteristics can be considered locality-specific for rubies/sapphires from Winza: (1) long tube-, fiber-, needle-, or hair-like inclusions of orange-brown color that are straight, slightly curved, bent, or rarely show a spiral-like appearance (restricted to medium red and vivid [orangy] red Winza rubies); and (2) a suite of mineral inclusions composed of amphibole + garnet + apatite + an opaque mineral (tentatively identified as chal-

cocite, based on Raman data); (3) any of various types of color zoning; (4) partially healed fissures composed of cavities displaying varying shapes (irregular, but also regular and developed as negative crystals) that contain a polyphase filling; (5) fissures containing a grayish white to pale yellow substance that often resembles flux residues in synthetic rubies; and (6) rhombohedral twin planes. The polyphase filling material of (4) shows various colors (black, brown, or colorless) and could not be identified. No Raman signal could be obtained for these fillers or those of (5).

The variety of mineral inclusions observed in Winza corundum is rather small compared to that seen in rubies and sapphires from other localities. The internal mineral association of a ruby or sapphire always reflects the nature of the host rock in which it crystallized. The association amphibole + garnet + plagioclase (+ kyanite identified as an accessory mineral) in the host rock indicates that the corundum formed in a metamorphic environment. Rubies from other localities reveal, in general, quite different

inclusion mineral associations (e.g., Henn et al., 1990; Hughes, 1997; Mercier et al., 1999; Simonet, 2000; Schwarz, 2001; and GGL database). Marble-hosted rubies from Myanmar's Mogok stone tract, for example, contain mostly rutile (needles and/or irregularly rounded opaque crystals of varying size), carbonates, sphene, zircon, apatite, garnet, graphite, spinel, sphalerite, pyrite, pyrrhotite, mica, olivine, pargasite, and anhydrite (the association "rutile + sphene + zircon" is probably locality-specific for rubies from Mogok).

Chemical Properties. SSEF (2008) reported Cr and Fe as the main trace elements, with "little" Ga, and Ti and V below the detection limit of their EDXRF instrument. Semiquantitative EDXRF analyses performed by GIT Gem Testing Laboratory (2008) indicated moderate contents of Cr (0.35–0.68 wt.% Cr_2O_3) and Fe (0.25–0.41 wt.% Fe_2O_3), very low to low amounts of Ti (55–192 ppm TiO_2) and V (from not detectable to 164 ppm V_2O_5), and low-to-moderate Ga contents (64–146 ppm Ga_2O_3). These values are in fairly good agreement with our data.

Comparison with Rubies from Different Genetic Environments. The chemical fingerprint of Winza rubies is quite different from that of rubies originating from marble-type deposits such as Mogok (figure 37A). The main difference is in the iron concentration: Rubies from marble host rocks typically have low iron contents. In Mogok and Mong Hsu rubies, for example, GGL data show that the Fe_2O_3 concentration is normally below ~0.05 wt.%. However, the lower Fe_2O_3 limit we found for Winza rubies is ~0.3 wt.%, and GIT Gem Testing Laboratory (2008) reported 0.25 wt.%. When comparing the Cr and Fe contents of Winza rubies with those of basalt-related rubies from the Thai/Cambodian border region, we found an almost complete overlap of the chemical data (see again figure 37A).

Comparison with Rubies Originating from Other African Deposits. Rubies from Songea, Tanzania, generally have low-to-moderate contents of Ti, V, and Ga—often below the EDXRF detection limit. The highest concentrations of these elements (from the analysis of ~30 samples; Schwarz, 2001) are ~0.03 wt.% TiO_2 , 0.05 wt.% V_2O_5 , and 0.05 wt.% Ga_2O_3 . The Cr content of Songea rubies normally varies between ~0.2 and 0.7 wt.% Cr_2O_3 (as compared to ~0.1 wt.% to ~0.6 wt.% [occasionally ~0.8 wt.% for top-quality] for Winza rubies). Songea rubies distinguish themselves by very high Fe contents (this is

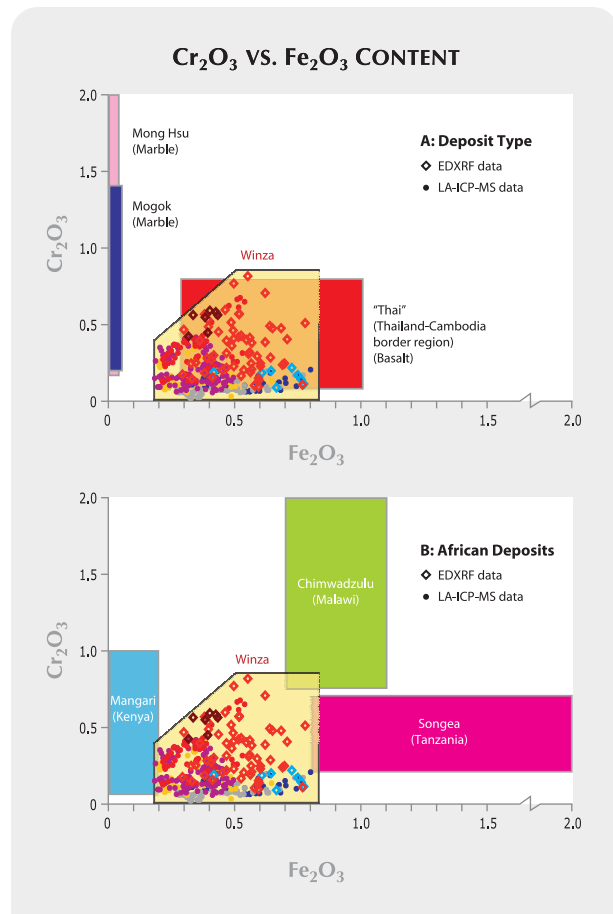


Figure 37. In a plot of Cr vs. Fe, more than 90% of the Winza rubies (red) and sapphires (other colors) fall into a population field extending from ~0.30 to 0.80 wt.% Fe_2O_3 and ~0.10 to 0.60 wt.% Cr_2O_3 . Top-quality Winza rubies fall into the upper left area of this field, while blue to purplish blue Winza sapphires are located near the lower right corner. In plot A, marble-hosted rubies from Mogok and Mong Hsu largely overlap one another, but they are completely separate from Winza. However, there is extensive overlap between stones from Winza and those of basalt-related rubies from the Thai/Cambodian border region. In plot B, Malawi rubies are distinguished by relatively high Cr contents. Mangari rubies typically have low Fe (mostly, <0.05 wt.% Fe_2O_3), but they may attain 0.2 wt.% Fe_2O_3 , while Malawi rubies vary from ~0.7 to 1.1 wt.% Fe_2O_3 . The highest Fe concentrations were found in rubies from Songea: ~0.8–2.0 wt.% Fe_2O_3 .

valid for the entire Songea corundum production, independent of the bodycolor)—~0.8–2.0 wt.% Fe_2O_3 —as compared to ~0.3–0.8 wt.% Fe_2O_3 for Winza rubies. As evident in figure 37B, there is minimal overlap between Songea and Winza in Cr and Fe.

Rubies from Kenya's Mangari region most commonly show ~0.005–0.15 wt.% Fe_2O_3 (very rarely up

to ~0.2 wt.%). This range, too, only very slightly overlaps the Fe content of Winza rubies (again, see figure 37B). The Cr contents of Mangari rubies fall mostly into the range of ~0.3–1 wt.% Cr₂O₃, which does overlap those from Winza.

The Fe and Cr contents of Malawi rubies are also quite different from those of Winza (again, see figure 37B), despite the fact that there are some similarities in their host-rock composition (Fe/Cr-rich amphibolite; Dill, 2005). Rubies from the Chimwadzulu Hill deposit have somewhat higher Fe contents (~0.7–1.1 wt.% Fe₂O₃) and a distinctly higher Cr concentration (~0.75–2 wt.% Cr₂O₃). GGL data indicate that rubies from both deposits have low Ti (generally <0.03 wt.% TiO₂), V (normally <0.02 wt.% V₂O₃), and Ga (often below detection limit; highest concentration found was ~0.01 wt.% Ga₂O₃).

There is very little LA-ICP-MS data for gem corundum available in the literature for comparison. Rankin et al. (2003) reported concentration ranges of Mg, Ca, V, Cr, Fe, Cu, and Ga for rubies originating from Longido (Tanzania) and Chimwadzulu Hill. Winza rubies and sapphires have Mg, Cr, Fe, and Ga concentrations that are equal to or slightly lower than the element concentration ranges reported by Rankin et al. (2003). Calcium, V, and Cu are much lower in Winza rubies and sapphires compared to stones from Longido and Chimwadzulu Hill.

Spectroscopy. The GIT Gem Testing Laboratory (2008) reported that the UV-Vis absorption spectra of Winza rubies typically show the Cr³⁺ bands and lines together with Fe³⁺ absorptions (377/387 and 450 nm) that would be expected for a ruby with high iron content.

The dominant absorption feature in chromium-colored corundum is the presence of intense bands related to Cr³⁺ at 405 and 560 nm. Additional spectral features observed for rubies are: (1) the so-called “background absorption,” which represents an increasing absorption toward the UV edge; and (2) the presence of Fe³⁺-related groups at ~375 nm and 450 nm. Rubies with low Fe contents (e.g., marble-hosted Mogok rubies and most rubies from Kenya’s Mangari region) typically show relatively “pure” Cr³⁺ spectra with variable, but low, UV absorption. The other “extreme” is provided by corundum from Songea. These rubies (and also sapphires of various colors) are characterized by very strong Fe³⁺-related features (Schwarz, 2001). Rubies from Malawi show, in general, spectra with combined Cr³⁺/Fe³⁺ absorption components.

Winza rubies and pink/purple sapphires, as well

as rubies from the Thai/Cambodian border region, show the chromium bands and a generally strong “background absorption,” which is influenced by several factors (figure 34A). Features related to Fe³⁺ are only weakly developed. Blue to purplish blue Winza sapphires display distinct Fe³⁺-related features (figure 34B), or they show the combination of Cr³⁺ bands and the Fe²⁺-Ti⁴⁺ charge-transfer absorption around 700 nm (figure 34C).

The padparadscha sapphire that was examined for this report owed its color to Cr³⁺/Fe³⁺ absorptions, rather than the combination of Cr³⁺ and color centers that are seen in “classic” padparadscha sapphires (i.e., from Sri Lanka). GIT Gem Testing Laboratory (2008) described three diagnostic patterns for OH-related peaks in the mid-IR absorption spectra of Winza rubies: Pattern A showed a broad absorption band from 3735 to 3000 cm⁻¹, centered around 3450 cm⁻¹, assigned to goethite. Pattern B showed absorption bands with approximate peaks at 3335, 3242, 3160, 3075, 2459, and 2420 cm⁻¹. Pattern C showed mixed absorption bands from patterns A and B.

Smith and Van der Bogert (2006) commented on the 3161 cm⁻¹ spectral feature (formerly described mainly in natural-color yellow sapphire from Sri Lanka). They indicated that, when present in high intensity, it appears to consist of at least six bands. This so-called 3161 series was attributed by past researchers to OH groups involved in charge-compensation with Si⁴⁺. Smith and Van der Bogert (2006) suggested that the 3161 series is actually due to structurally bonded OH associated with Mg²⁺. The average Mg contents measured in our samples were in the range of 30–65 ppm (table 5). The evaluation of whether this concentration is sufficient to support the “Mg-OH model” is beyond the scope of this article.

Balmer et al. (2006) reported that peaks at 3353 and 3242 cm⁻¹ are probably associated with the 3160 cm⁻¹ absorption. They could not confirm whether this group of peaks is related to goethite or to silanol groups (OH group attached to Si⁴⁺).

The FTIR spectra of the present study allow the following correlations:

1. All top-quality rubies containing the orange-brown tube/hair-like inclusions had the 3160 cm⁻¹ absorption as the dominant feature.
2. Only one sapphire showed a comparably prominent 3160 cm⁻¹ feature.
3. The 3160 cm⁻¹ absorption was present in almost all of the lower-quality samples, but it

appeared very weak or as a low shoulder when in combination with other bands.

4. Very few samples did *not* have the 3160 cm^{-1} feature.

These results imply that, although there is a strong correlation between the orange-brown tube/hair-like inclusions and a prominent 3160 cm^{-1} absorption, other factors must be taken into consideration. Since there is no clear correlation between other microscopic features and the presence/intensity of the 3160 cm^{-1} absorption band, the influence of sub-microscopic inclusions should be considered.

The characteristic group of four peaks with maxima at 3695, 3670, 3650, and 3620 cm^{-1} (spectrum C in figure 35) is typically attributed to kaolinite minerals (Beran and Rossman, 2006). This group was found in 17 samples (in four top-quality rubies, this group was weak, while in other samples it was, in part, quite strong).

According to A. Beran (pers. comm., 2008), the broad 3450 cm^{-1} absorption band (spectrum A in figure 35) is related to H_2O (submicroscopic inclusions or adsorptive humidity).

OH bands associated with the presence of chlorite-group minerals show typical absorption features in the range between 3560 and 3420 cm^{-1} (spectrum D in figure 35).

Geologic Origin. Observations by two of the authors (VP and BML) of primary deposits at Winza, as well as the examination of corundum-bearing host-rock specimens in the laboratory, showed a close association between corundum and cross-cutting layers or “dikes” of a garnet-bearing amphibolitic rock. Macroscopic observations by authors GG and DO of a sample obtained by JMS (figure 9) clearly showed that, according to its mineralogy, the dike-like body was mafic in composition before it was metamorphosed. Possible lithologies for the protolith include high-alumina gabbros (layered gabbros) or leucogabbros. The central part of the “dike” is composed of a metamorphic garnet + hornblende \pm plagioclase \pm corundum association. Metamorphic conditions estimated by using garnet-amphibole-corundum equilibria (winTWQ; Berman, 2007) showed that the metamorphic overprint was $800 \pm 50^\circ\text{C}$ and 8–10 kbar.

The color/growth zones of the corundum are commonly complex, which indicates crystal development during a number of stages characterized by variable Ti, Cr, and Fe availability.

Spinel that (rarely) overgrows or is included in

the corundum is Fe- and Mg-rich, whereas spinel from the host amphibole is Cr-rich, with up to 32 wt.% Cr_2O_3 (unpublished electron microprobe data of the authors). The presence of two chemically distinct spinel compositions indicates that two different generations are present. The Cr-spinel is probably a relict of the initial magmatic rock before the metamorphism, while the Fe- and Mg-rich spinel crystallized during the metamorphic stage that formed the corundum.

The amphiboles did not show any preferred orientation in the host corundum; they can be considered protogenetic inclusions reflecting the nature of the host rock. Amphibole inclusions showing various morphologies were commonly present. This is a strong indication that *all* the corundum morphologies originated from an amphibolite environment.

In the ternary Mg-Fe-Ti diagram that was established by Peucat et al. (2007) to distinguish magmatic from metamorphic sapphires, the chemical fingerprint of the Winza sapphires overlaps the border separating the metamorphic and magmatic population fields (figure 38).

Oxygen isotope values for three Winza corundum samples defined a consistent and restricted $\delta^{18}\text{O}$ range of $4.7 \pm 0.15\%$, indicating that they formed under comparable genetic conditions. This composition suggests two possible origins for Winza rubies (Giuliani et al., 2005, 2007): either in metamorphosed mafic-ultramafic rocks (worldwide $\delta^{18}\text{O}$ range of 3.2–6.8%, $n = 19$), or in desilicated pegmatites within mafic-ultramafic rocks such as plumasites (4.2–6.7%, $n=16$). We therefore conclude that the Winza rubies are of metamorphic origin, with a high-alumina meta-(leuco)gabbro as the protolith for the host rock.

Formation of the rhombohedral top-quality rubies with their exceptional combination of large size, intense color, and high transparency requires growth conditions different from those of the lower-quality corundum (characterized by a prismatic-tabular or dipyrarnidal morphology and the general presence of strong color zoning and abundant inclusions that reduce their transparency). An explanation for the (co-)existence of these two corundum types in the Winza area could be that they represent separate corundum “generations” formed at different geologic times or under locally different pressure-temperature (PT) conditions.

Separation from Synthetics and Heat-treated Natural Corundum from Other Sources. When the first Winza rubies appeared on the market, they were praised for

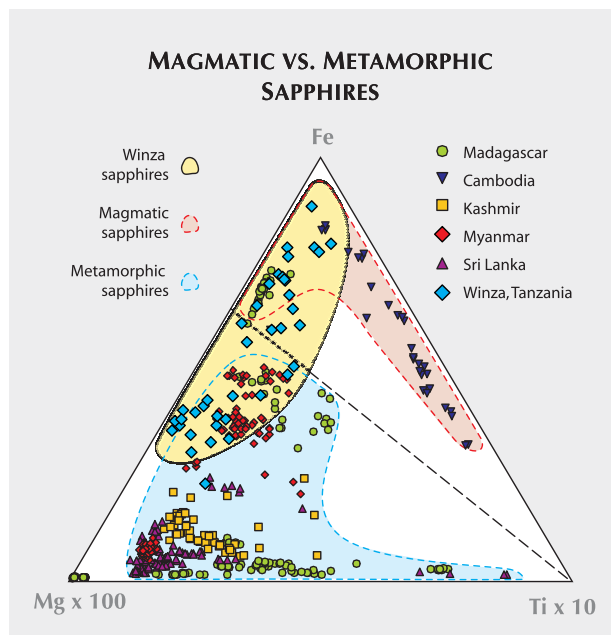


Figure 38. This ternary Fe-Mg-Ti diagram shows LA-ICP-MS data for blue sapphires originating from Winza and other deposits (all data points from GGL database). Peucat et al. (2007) defined two population fields for magmatic- and metamorphic-type blue sapphires. Note that the blue sapphires from Winza plot in a range overlapping both fields (this could indicate that melting processes might be involved, related to high-PT metamorphism). Modified from Peucat et al. (2007).

their exceptional color and clarity. At the same time, they caused suspicion and doubt, because the top-quality stones possessed such a high transparency and bright color that many dealers and gemologists who saw them for the first time thought they were synthetic. The identification and separation of Winza rubies from synthetics is generally quite easy—as long as the typical internal features described above are present. These are mineral inclusions such as amphibole, garnet, and apatite; orange-brown “tubes/needles/hairs”; and color zoning in various patterns. Only one inclusion feature could potentially cause confusion: Partially healed fissures consisting of irregularly shaped cavities filled with a grayish white to pale yellow solid material may resemble the flux components seen in some synthetics.

Another powerful tool for the separation of Winza rubies from synthetics (especially if characteristic inclusions are not present) is chemical fingerprinting, notably the Cr/Fe correlation. Elements such as Ti, V, and Ga are of little help because their contents are normally quite low in synthetic rubies/sapphires, as they are in the stones from Winza. The key element for the separation is Fe:

Contents in the range of ~0.3 to 0.8 wt.% Fe_2O_3 —which are typical of rubies/sapphires from Winza—are only rarely found in synthetic rubies. “High-iron” synthetic rubies are known from Douros (flux grown), Ramaura (flux grown), Gilson (flux grown), and Tairus (hydrothermally grown). In a detailed study by Schwarz et al. (2000), however, only very few synthetic rubies were found with Fe_2O_3 contents reaching the lower limit of the Winza rubies. These included some hydrothermal synthetic rubies and a very few flux synthetics grown by Douros (2 out of 35) and from the (experimental) production of Gilson (2 out of 27). Gilson synthetic rubies have not been produced and marketed commercially. In addition, all the flux synthetic samples examined by one of the authors (DS) showed healed fissures with typical flux patterns. Douros samples also distinguish themselves by high Ga concentrations (~0.04 to 0.1 wt.% Ga_2O_3). Practically all production from Tairus shows diagnostic internal features (especially pronounced growth structures). Therefore, chemical fingerprinting, when applied with other standard gemological tests, is an effective method for the separation of Winza rubies from synthetics.

The same is valid for the separation of heat-treated Winza rubies/sapphires from stones of other sources. Since heat treatment results in the alteration of fissure textures and solid inclusions, it tends to remove locality-specific internal features. Chemical fingerprinting is not affected by traditional heat treatment and can, therefore, be used in the same way as described for unheated stones. We believe that probably less than 1% of the faceted gems from Winza now on the market have been heat treated. This percentage may increase in the future if treaters are successful in applying heating techniques to pink, purple, or pinkish and purplish red starting material.

SUMMARY AND CONCLUSION

The arrival on the market of very fine cut rubies (e.g., figure 39) from a new deposit near Winza in central Tanzania was welcomed by the international gem trade, as the supply of top-quality rubies is scarce. It is difficult to predict if Winza will become a major source of fine rubies. Only time will tell. But if the area consistently produces fine stones and if a market is found for the lower-quality material, this mining region could become more than a gem rush.

Winza rubies and sapphires are hosted by metamorphic rocks of the Usagaran Belt. Observations of the associated mineral assemblages indicate that



Figure 39. The Winza area of central Tanzania is a new source of fine untreated ruby, such as the 3.18 ct center stone in this ring. Courtesy of The Collector Fine Jewelry, Fallbrook, California; photo by Robert Weldon.

the gem corundum is metamorphic in origin. The corundum is contained in “dikes” consisting mainly of the assemblage amphibole-garnet \pm plagioclase. Oxygen isotope data are consistent with an origin in metamorphosed mafic-ultramafic rocks.

The physical properties of Winza rubies and sapphires are quite constant, with RIs and SGs in the same range known for rubies and sapphires originat-

ing from other localities. However, Winza rubies and sapphires can be characterized by inclusion features that, in part, can be considered locality specific: long tube-, fiber-, needle-, or hair-like inclusions, containing an orange-brown, solid polycrystalline material (most likely limonite); amphibole crystals showing large variations in shape, along with garnet and possibly apatite and/or an opaque mineral; partially healed fissures containing cavities filled with a polyphase material; and fissures containing primarily a grayish white to pale yellow substance. These internal features provide confirmation of natural origin and are a very strong indication of the host stone’s locality of origin. Only the fissures with the grayish white to pale yellow substance may cause confusion, because they can resemble flux material in synthetic corundum. The specific type of bluish violet color zoning seen in rhombohedral and dipyrmidal samples has not been previously found in natural ruby or pink sapphire, to the best of our knowledge, so it is also useful for determining a Winza origin.

The chemical composition of Winza rubies and sapphires, which formed in association with amphibolites, is characterized by a relatively high Fe content. This separates them from most natural and almost all synthetic counterparts. Although there is extensive chemical overlap with rubies originating from the Thai/Cambodian border region, the latter display internal features that are totally different from the inclusions in Winza stones.

ABOUT THE AUTHORS

Dr. Schwarz (d.schwarz@gubelingemlab.ch) is research manager, Dr. Klemm is analyst, and Ms. Malsy and Dr. Erel are gemologists, at the Gübelin Gem Lab, Lucerne, Switzerland. Mr. Pardieu was a gemologist at the Gübelin Gem Lab at the time this article was prepared, and is now field gemologist at the GIA Laboratory in Bangkok. Dr. Saul is an independent geologist based in Paris. Dr. Schmetzer is a research gemologist residing in Petershausen, Germany. Mr. Laurs is editor of *Gems & Gemology* at GIA in Carlsbad, California. Dr. Giuliani is senior researcher in geology at the IRD (Institut de Recherche pour le Développement) and CRPG/CNRS, Nancy, France. Dr. Hauzenberger is associate professor of mineralogy and petrology at the Institute of Earth Sciences, University of Graz, Austria. Mr. Du Toit is manager of the Gemstone Identification Department at the GIA Laboratory in Bangkok. Dr. Fallick is geochemist at the Isotope Geosciences Unit, Scottish Universities Environmental Research Centre, Glasgow, Scotland. Dr. Ohnenstetter is petrologist at CRPG/CNRS.

ACKNOWLEDGMENTS

Mark and Eric Saul (Swala Gem Traders Ltd., Arusha, Tanzania), Jean Baptiste Senoble (Nomads Ltd., Bangkok), and Abdul Msellem (Arusha) are thanked for providing support during author

VP’s visit to Winza. Dimitri Mantheakis (Ruvu Gemstone Mining Ltd., Dar es Salaam, Tanzania) is thanked for guiding author BML’s visit to Winza, and also for donating samples of Winza ruby to GIA for examination. Field support and information were also provided by Vivian Komu (Ministry of Energy and Minerals, Dodoma, Tanzania). C.H. Lapidaries Ltd. Part. (Bangkok), Paul Wild OHG (Kirschweiler, Germany), and Mushan International (Colombo, Sri Lanka) kindly donated samples to the Gübelin Gem Lab for this study. Mingling Zeng performed UV-Vis-NIR, FTIR, and EDXRF at the Gübelin Gem Lab. We thank Dr. A. Beran and Dr. E. Libowitzky (Department of Mineralogy and Crystallography, University of Vienna, Austria) for supplying useful data and discussion on FTIR spectroscopy. George Bosshart (Zürich, Switzerland) kindly reviewed the gemological and analytical parts of this study. Dr. O. Medenbach and Dr. H.-J. Bernhardt (University of Bochum, Germany) kindly performed X-ray diffraction and electron microprobe analyses of some inclusions and associated minerals. The authors are also grateful to Günther Blass (Eschweiler, Germany) for X-ray diffraction and SEM analysis of associated minerals. The slabs in figure 9 were prepared by Cedric Demeurie (UHP, Nancy). Gem dealers Werner Radl (Mawingu Gems, Niederwörresbach, Germany), Mark Kaufman (Kaufman Enterprises, San Diego), Michael Nemeth (San Diego), and Hakimi & Sons (New York) kindly loaned Winza samples for examination.

REFERENCES

- Abduriyim A., Kitawaki H. (2008) New geological origin: Ruby from Winza of Tanzania. *Gemmology*, Vol. 39, Issue 8, No. 467, pp. 4–7 [in Japanese with English insert].
- Appel P., Möller A., Schenk V. (1998) High-pressure granulite facies metamorphism in the Pan-African Belt of eastern Tanzania: P-T-t evidence against granulite formation by continent collision. *Journal of Metamorphic Geology*, Vol. 16, pp. 491–509.
- Balmer W., Leelawatanasuk T., Atichat W., Wathanakul P., Somboon C. (2006) Update on FTIR characteristics of heated and unheated yellow sapphire. *GIT2006: 1st International Gem and Jewelry Conference*, Bangkok, December 6–7, p. 91.
- Beran A., Rossman G.R. (2006) OH in naturally occurring corundum. *European Journal of Mineralogy*, Vol. 18, pp. 441–447.
- Bauer M. (1896) Ueber das Vorkommen der Rubine in Birma. *Neues Jahrbuch für Mineralogie, Geologie und Paläontologie*, Vol. 11, pp. 197–238.
- Berman R.G. (2007) winTWQ (version 2.3): A software package for performing internally-consistent thermobarometric calculations. *Geological Survey of Canada, Open File 5462*, 41 pp.
- Choudhary G. (2008) Gem News International: An interesting zoned sapphire crystal from Winza, Tanzania. *Gems & Gemology*, Vol. 44, No. 3, pp. 270–272.
- Dill H.G. (2005) Geologie und Petrographie des Saphir- und Rubinvorkommens von Chimwadzulu Hill (W-Malawi). *Gemmologie: Zeitschrift der Deutschen Gemmologischen Gesellschaft*, Vol. 54, No. 1, pp. 7–20.
- Dirlam D.M., Misiorowski E.B., Tozer R., Stark K.B., Bassett A.M. (1992) Gem wealth of Tanzania. *Gems & Gemology*, Vol. 28, No. 2, pp. 80–102.
- Fritz H., Tenczer V., Hauzenberger C.A., Wallbrecher E., Hoinkes G., Muhongo S., Mogessie A. (2005) Central Tanzanian Tectonic Map (CTTM): A step forward to decipher pre-Pan-African and Pan-African structural events in the East African Orogen. *Tectonics*, Vol. 20, pp. 1–45.
- Gabert G., Wendt I. (1974) Datierung von granitischen Gesteinen im Dodoman- und Usagaran System und in der Ndembera-Serie (Tanzania). *Geologisches Jahrbuch*, Vol. B11, pp. 3–55.
- GIT [Gem and Jewelry Institute of Thailand] Gem Testing Laboratory (2008) Rubies from a new deposit in Tanzania. www.git.or.th/eng/eng_gem_and_jewelry_database/eng_lab_notes/2008/eng_ruby_from_tanzania.htm, June 5.
- Giuliani G., Fallick A.E., Garnier V., France-Lanord C., Ohnenstetter D., Schwarz D. (2005) Oxygen isotope composition as a tracer for the origins of rubies and sapphires. *Geology*, Vol. 33, pp. 249–252.
- Giuliani G., Fallick A.E., Rakotondrzafy M., Ohnenstetter D., Andriamamonjy A., Rakotosamizanany S., Ralantoarison Th., Razanatsheho M., Dunaigre Ch., Schwarz D. (2007) Oxygen isotope systematics of gem corundum deposits in Madagascar: Relevance for their geological origin. *Mineralium Deposita*, Vol. 42, pp. 251–270.
- Goldschmidt V. (1918) *Atlas der Krystallformen*, Vol. 5. Carl Winters Universitätsbuchhandlung, Heidelberg, Germany.
- Hänni H. (1987) On corundum from Umba Valley, Tanzania. *Journal of Gemmology*, Vol. 20, No. 5, pp. 278–284.
- Hänni H.A., Schmetzer K. (1991) New rubies from the Morogoro area, Tanzania. *Gems & Gemology*, Vol. 27, No. 3, pp. 156–167.
- Hänni H., Krzemnicki M. (2008) New rubies from Tanzania. *Gems & Jewellery*, Vol. 17, No. 3, pp. 8–9.
- Hauzenberger C.A., Bauernhofer A., Hoinkes G., Wallbrecher E., Mathu E. (2004) Pan-African high pressure granulites from SE-Kenya: Petrological and geothermobarometric evidence for polyphase evolution in the Mozambique Belt. *Journal of African Earth Sciences*, Vol. 40, pp. 245–268.
- Hauzenberger C.A., Sommer H., Fritz H., Bauernhofer A., Kröner A., Hoinkes G., Wallbrecher E., Thöni M. (2007) SHRIMP U-Pb zircon and Sm-Nd garnet ages from the granulite facies basement of SE-Kenya: Evidence for Neoproterozoic polycyclic assembly of the Mozambique belt. *Journal of the Geological Society*, Vol. 164, pp. 189–201.
- Henn U., Bank H., Bank F.H. (1990) Red and orange corundum (ruby and padparadscha) from Malawi. *Journal of Gemmology*, Vol. 22, No. 2, pp. 83–89.
- Hughes R. (1997) *Ruby and Sapphire*. RWH Publishing, Boulder, CO.
- Krzemnicki M., Hänni H.A. (2008) New Tanzania mine uncovers source of exceptional rubies. *InColor*, Spring 2008, pp. 46–47.
- Melcher G. (1902) Ueber einige kristallographische Constanten des Korund. *Zeitschrift für Kristallographie und Mineralogie*, Vol. 35, pp. 561–581.
- Mercier A., Debat P., Saul J.M. (1999) Exotic origin of the ruby deposits of the Mangari area in SE Kenya. *Ore Geology Reviews*, Vol. 14, pp. 83–104.
- Milisenda C.C., Henn U., Bank H. (1997) The new Tunduru-Songea gem fields, southern Tanzania. *26th International Gemological Congress*, Idar-Oberstein, Germany, September 27–October 3, pp. 37–39.
- Moeller A., Mezger K., Schenk V. (2000) U-Pb dating of metamorphic minerals: Pan-African metamorphism and prolonged slow cooling of high pressure granulites in Tanzania, East Africa. *Precambrian Research*, Vol. 104, pp. 123–146.
- Pardieu V. (2005) An update on ruby and sapphire mining in South East Asia and East Africa—Summer 2005. www.fieldgemology.org.
- Pardieu V. (2007) Tanzania, October 2007—A gemological safari. Part 1: Ruby, sapphire, moonstone, spinels, tsavorite, alexandrite: Gems from Central and South Tanzania. www.fieldgemology.org.
- Pardieu V., Schwarz D. (2008) Field report from Winza. *Rapaport Diamond Report*, Vol. 31, No. 26, pp. 173–175.
- Peretti A., Schmetzer K., Bernhardt H.-J., Mouawad F. (1995) Rubies from Mong Hsu. *Gems & Gemology*, Vol. 31, No. 1, pp. 2–26.
- Peretti A. (2008) New important ruby discovery in Tanzania: The Tanzanian “Winza”-(Dodoma province) rubies. *Contributions to Gemmology*, No. 7, April, www.gemresearch.ch/news/Tanzania/Tanzania.htm.
- Peucat J.J., Ruffault P., Fritsch E., Bouhnik-Le Coz M., Simonet C., Lasnier B. (2007) Ga/Mg ratio as a new geochemical tool to differentiate magmatic from metamorphic blue sapphires. *Lithos*, Vol. 98, pp. 261–274.
- Rankin A.H., Greenwood J., Hargreaves D. (2003) Chemical fingerprinting of some East African gem rubies by laser ablation ICP-MS. *Journal of Gemmology*, Vol. 28, No. 8, pp. 473–482.
- Schwarz D., Stern W., Zachovay M. (2000) Trace and minor element contents in synthetic rubies from different manufacturers. *31st International Geological Congress*, Rio de Janeiro, Brazil, August 6–17.
- Schwarz D. (2001) Sapphires and rubies from the Ruvuma (Tunduru and Songea), Lindi (Liwale) and Mtwara (Mbekenyer) districts in southern Tanzania. *28th International Gemmological Congress*, Madrid, Spain, October.
- Senoble J.B. (2008) An expedition to Tanzania’s new ruby deposits in Winza. *InColor*, Spring 2008, pp. 42–43.
- Sharp Z.D. (1990) A laser-based microanalytical method for the in-situ determination of oxygen isotope ratios of silicates and oxides. *Geochimica et Cosmochimica Acta*, Vol. 54, pp. 1353–1357.
- Simonet C. (2000) Géologie des gisements de saphir et de rubis. L'exemple de la John Saul mine, Mangari, Kenya. Ph.D. dissertation, University of Nantes, France.
- Smith C.P., Van der Bogert C. (2006) Infrared spectra of gem corundum. *Gems & Gemology*, Vol. 42, No. 3, pp. 92–93.
- Smith C.P., Beesley C.R., Quinn Darenius E., Mayerson W.M. (2008) Inside rubies. *Rapaport Diamond Report*, Vol. 31, No. 47, pp. 140–148.
- Sommer H., Kröner A., Hauzenberger C.A., Muhongo S. (2005) Reworking of Archaean and Palaeoproterozoic crust in the Mozambique Belt of central Tanzania as documented by SHRIMP zircon geochronology. *Journal of African Earth Science*, Vol. 43, pp. 447–463.
- SSEF Swiss Gemmological Institute (2008) New rubies from Tanzania. *SSEF Newsletter*, May, www.ssef.ch/en/news/news_pdf/SSEFnewsletter_may08.pdf.

THE WITTELSBACH BLUE

Rudolf Dröschel, Jürgen Evers, and Hans Ottomeyer

The 35.56 ct Wittelsbach Blue is one of the largest historic blue diamonds ever fashioned. It belonged to the Bavarian House of Wittelsbach and was displayed in the Treasury of the Munich Residence until it disappeared in 1931. It was secretly sold in 1951, “rediscovered” in 1961, and then sold again in 1964 to an undisclosed private buyer. In December 2008, the Wittelsbach Blue was sold at Christie’s London to jeweler Lawrence Graff for just over \$24.3 million, a record price for any diamond at auction. This article describes what is known about the Wittelsbach Blue since it was first reported in 1666, and the gemological information released to date on this diamond, which was recently graded Fancy Deep grayish blue. Investigations in the historical archives of Bavaria, Austria, and Spain revealed that there is no archival evidence to support many previous statements about this stone.

Due to their extreme rarity, blue diamonds, even more than colorless ones, have historically epitomized rank and wealth. Two of the largest known blue diamonds were once part of the crown jewels of European monarchies. The Hope diamond (now 45.52 ct) once belonged to the French royal family (Kurin, 2006), and the Wittelsbach Blue (now 35.56 ct, figure 1) was owned by the Bavarian royal family, the House of Wittelsbach.

Like the Hope, the Wittelsbach Blue is an intense steely blue. It is widely accepted that both originated from the Kollur mine in India’s Golconda District (Bauer, 1932; Balfour, 1987). According to its previously published history (e.g., Gaal, 1977; Bruton, 1981, Balfour, 1997; Morel, 2001; Christie’s, 2008a,b), the Wittelsbach Blue arrived in Vienna in 1666 as part of a dowry for a marriage into the House of Hapsburg. In 1722, it passed to the House of Wittelsbach in Munich, again as part of a dowry. It was mounted as a “symbol of dominion and power” (de Smet, 1963, p. 48) on the globe above the Bavarian Royal Crown around 1806 or 1807 (figure 2). During the 20th century, the Wittelsbach Blue was involved in a series of unusual events, which began in 1931 when the Wittelsbach Equity Foundation (German acronym WAF, for *Wittelsbacher Ausgleichsfonds*) tried in vain to sell it at the Christie, Manson & Woods auction house in London (Christie, Manson

& Woods, 1931). From the day of the auction through the next 30 years, the whereabouts of the Wittelsbach Blue were kept secret from the public. In 1951, the WAF secretly sold the Wittelsbach Blue, which was then “rediscovered” in 1961 by Antwerp diamond dealer Jozef Komkommer. In 1964, it was purchased by a private German collector whose identity was not revealed until recently.

During the authors’ investigations in the Bavarian State Archive in Munich, in the Austrian State Archives in Vienna, and in three Spanish historical archives in Madrid, Simancas, and Valladolid, it became evident that many of the accepted “facts” about the Wittelsbach Blue and its history that were published by Antwerp diamond specialist K. de Smet in his book, *The Great Blue Diamond, The Wittelsbacher, Crown Witness to Three Centuries of European History* (1963), and cited afterwards by many others, had no archival basis. Based on our comprehensive review of the available documents, we can now correct the historical record and report on the true, exciting history of the Wittelsbach Blue as it moved through Europe.

See end of article for About the Authors and Acknowledgments.
GEMS & GEMOLOGY, Vol. 44, No. 4, pp. 348–363.
© 2008 Gemological Institute of America



Figure 1. The Wittelsbach Blue (35.56 ct) is one of the largest and most famous blue diamonds in the world, with a known provenance that stretches back to the 17th century. Largely out of the public eye for more than 40 years, it was sold in December 2008, earning a record price for any diamond at auction. Photo courtesy of Christie's.

INDIAN ORIGINS

India was the world's only source of diamonds (Untracht, 1997) until about 1725 (Balfour, 1987), when the first Brazilian mines began to open (Legrand, 1981). Thus, all diamonds in Europe before that date, including the Wittelsbach Blue, must have had their origin in India (Harlow, 1998; Webster, 1994). Most of India's diamonds, and its largest, were found in a vast area on the eastern side of the Deccan plateau (Bharadwaj, 2002). Many of these diamond sources were located in the former kingdom of Golconda, which lay between the rivers Godavari in the north and Pennar in the south.

Jean Baptiste Tavernier (1605–89), the famed French diamond dealer, visited three mines in the Golconda region between 1630 and 1668, among them Coulour (also spelled *Kollur*). This famous mine was the source of several historic diamonds, including the Koh-i-Noor, the Hope, the Dresden Green, the Orlov, the Regent, and the Sancy (Kurin, 2006). According to Bauer (1932), it was also the source of “nice blue diamonds.” Balfour (1987, p. 112) wrote that the “Kollur mine, then, appears to be the only . . . known source of Type IIb natural blue diamonds” in India. The identity of the party who brought the Wittelsbach Blue (perhaps still in rough form) to Europe has been lost to the mists of history, but Tavernier is a possibility, given the timing of its arrival.

DOWRY OF AN EMPRESS

Madrid. In his book, de Smet (1963) reported the findings of “Dr. Klaus Schneider, Munich,” who was engaged by Jozef Komkommmer to investigate the history of the Wittelsbach Blue after he had purchased the stone in 1961 (Burgerwelzijn, 1962). Schneider—according to de Smet—was then a final-year doctoral student of history at Ludwig-Maximilian University

Figure 2. King Ludwig I of Bavaria (1786–1868) is shown here in 1826 in his coronation robes. The Bavarian crown with the Wittelsbach Blue is at his right. The crown and the right hand of the king (holding a scepter) rest on the Bavarian constitution. Painted by Joseph Karl Stieler (1781–1858), this portrait now hangs in the Neue Pinakothek museum in Munich. Courtesy of The Bavarian State Painting Collections, Munich.





Figure 3. Empress Margarita Teresa of Austria and her daughter Maria Antonia are shown here in this painting attributed to Jan Thomas at the end of the 17th century. Courtesy of the Kunsthistorisches Museum, Vienna.

(LMU) of Munich. (Interestingly, our inquiry at the LMU library in 2006 revealed that Klaus Schneider never completed his doctoral thesis, at least not at LMU or any other German university [see, e.g., *Jahresverzeichnis der Deutschen Hochschulschriften*, 1960–1970]. During 2006 and 2007, one of the authors [JE] conducted exhaustive efforts to locate Schneider and de Smet, without success.)

After investigations in the state archives of Bavaria and Austria during September and October of 1961, Schneider traveled to Spain early in 1962 to begin research in an unidentified Madrid archive (de Smet, 1963). Here, he said, he found the first mention of the Wittelsbach Blue “as early as 1664,” when King Philip IV (1605–1665) of the Spanish line of the House of Hapsburg, “ordered the treasurer to gather a dowry for his daughter,” Infanta Margarita Teresa (1651–1673; figure 3), “from new acquisitions of precious stones from India and Portugal. . . . It included a large blue diamond” (de Smet, 1963, p. 16). According to Schneider, he could find no addi-

tional information on the Wittelsbach Blue in Madrid, allegedly because “in the bloody years of the Spanish Civil War (1936–1939) the last existing documents were undoubtedly lost with the destruction of the Madrid archives” (de Smet, 1963, p. 17).

One of the authors (JE) visited Spain in November and December 2007 to seek some archival basis for Schneider’s statements. These investigations were performed with the support of five Spanish archivists in the General Archive of the Royal Palace in Madrid (which had no record of Schneider’s visit in 1962), in the Archivo General (General Archive) of Simancas, and in the Archivo de la Real Chancilleria (Archive of the Royal Chancery) of Valladolid. No documents could be found to support the contention that Philip’s treasurer had purchased a large blue diamond—or other stones from India and Portugal—“as early as 1664.” In addition, the archivists were unaware of any records being lost during the Spanish Civil War.

Our 2007 research also reviewed the invoices of the silver- and goldsmiths of the Spanish Court in the General Archive of the Royal Palace in Madrid from 1660 to 1669 for any mention of a large blue diamond, without success. Similarly, the invoices of court treasurers Baltasar Molinet, Antonio de León, and Agustín Spinola for 1660–1669, stored in the Valladolid archive, have no mention of a great blue diamond. One document in particular (found in file number 1816-19) seems to rebut de Smet’s contentions. This record dealt with Margarita Teresa’s trip to Vienna in 1666 to prepare for her marriage to Emperor Leopold I (Widorn, 1960). The document includes several quotes from goldsmith Luis de Saulca, who had set diamonds for Margarita Teresa’s mother, Queen Maria Anna (1634–96), and who would likely have been commissioned to set a stone such as the Wittelsbach Blue (J. Menéndez Trigos, pers. comm., 2007). Again, however, there is no mention whatsoever of such a diamond. Therefore, Schneider’s statements (de Smet, 1963) dealing with Spanish origins of the Wittelsbach Blue must be considered unsubstantiated. The only mention we could find of such a diamond as part of the dowry was in statements made by Margarita Teresa after she had reached Austria.

Vienna. Margarita Teresa married her uncle, Emperor Leopold I (1640–1705), in Vienna in 1667 (Widorn, 1960). Figure 3 shows the young Empress with her daughter Maria Antonia three years after the marriage. The marriage contract, dated December 18,

1663, and currently stored in the Austrian State Archive in Vienna (Marriage contract . . . , 1663), contains no mention of a large blue diamond, so the stone likely was not acquired before this date. In 1673, six years after the marriage, Margarita Teresa died. In her testamentary bequest (figure 4), she stated that her daughter, Maria Antonia, was her sole heiress (Widorn, 1960), with one exception: a precious ornament, which she had brought from Spain, was left to Leopold: “a great breast ornament with a great diamond in the midst.” Though the blue color is not mentioned, this diamond was most likely the future Wittelsbach Blue: No other large diamond is known to have been possessed by Margarita Teresa, and the court officials at the time would not necessarily have recorded the diamond’s color (I. Aguirre, pers. comm., 2008; G. Gonsa, pers. comm., 2008).

Schneider claimed that, on Leopold’s marriage to his third wife, Eleonora Magdalena, in 1676 (after the death of his second wife, Archduchess Claudia Felicitas, heiress of Tirol, that same year), he “was so enchanted by her beauty” that he gave the Empress “all the jewelry which he had inherited” from Margarita Teresa (de Smet, 1963, p. 18). Schneider also suggested (de Smet, 1963) that Empress Eleonora Magdalena gave the Wittelsbach Blue by testamentary bequest to her granddaughter, Archduchess Maria Amalia (1701–1756); he based this on docu-

Figure 4. The Testamentary Bequest of Margarita Teresa, dated March 23, 1673, appears to leave the Wittelsbach Blue to her husband Emperor Leopold I. The document reads, “In an Indian writing box. No 1. An ornament of diamonds from her Maj., the Empress brought from Spain; with thick and thin stones with some rhombs; this consists of the following pieces. A great breast ornament with a great diamond in the midst.” The color of the diamond is not mentioned. Courtesy of the Austrian State Archives, Vienna, HHStA FUK 1745, 1 and 2.

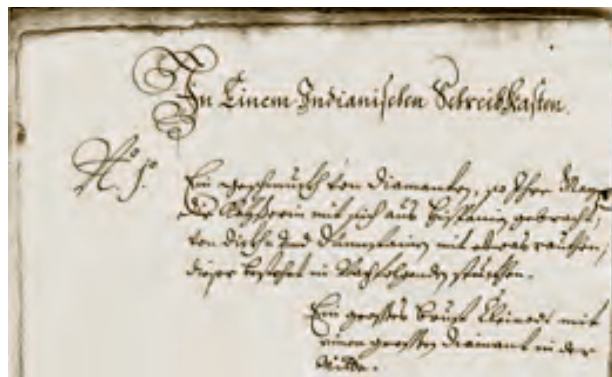


Figure 5. Archduchess Maria Antonia (seen in figure 3 as a toddler) is shown here at the age of 15. She married Bavarian Elector Max Emanuel in 1685, but was not happy with her husband and returned to Vienna in 1692. Painting by Benjamin von Block, 1684; courtesy of the Kunsthistorisches Museum, Vienna.

ments relating to the “Trousseau of Archduchess Maria Amalia.” However, investigations in the Austrian State Archive between August 2006 and July 2008 failed to uncover any records supporting Schneider’s claims.

Nor does Empress Eleonora Magdalena’s testamentary bequest, written between 1711 and 1720, make any mention of leaving the Wittelsbach Blue to Maria Amalia. During her lifetime, Eleonora Magdalena distributed her jewels to her daughters and also one piece to her son Joseph (Maria Amalia’s father), who had succeeded Leopold as Emperor in 1705, but she did not itemize gifts for her granddaughters. She left such decisions to her heirs. However, other documents in the Austrian State Archives may lead to a new explanation for the transfer of the Wittelsbach Blue to Maria Amalia.

Archduchess Maria Antonia (figures 3 and 5),



Figure 6. These portions of the General Inventory of Maria Antonia, dated September 22, 1685, indicate that she, too, owned a large diamond but with no mention of the color. They read: “General inventory of her Duchess Highness’s Jewelry, Silver, Clothing and Silk garments” (top); and (bottom) “Inventory of her Duchess Highness’s jewelry. A diamond jewel of thick and thin stones, which by her Maj. the Empress was brought from Spain, consists of the following pieces. A great breast trinket with a thick stone in the midst.” Note the similarity to the description in figure 4. Courtesy of the Austrian State Archives, Vienna, HHStA FUK 1777.

daughter of Margarita Teresa and Leopold, married Bavarian Elector Maximilian II Emanuel Wittelsbach (1662–1726) in July 1685. But it was not a happy marriage, and in early 1692, her husband left Munich to become governor of the Spanish Netherlands in the midst of the Nine Years War (1688–1697) and she returned to Vienna. According to Maria Antonia’s “General Inventarium” (General Inventory . . . , 1685; figure 6), prepared at the time of her marriage, she then possessed all the jewelry that her mother had brought from Spain in 1667 as her dowry. This 1685 document listed the large ornament with “a thick stone in the midst,”

using nearly identical language as in her mother’s 1673 bequest (figure 4), though still with no mention of the blue color. Although this ornament, again certainly the future Wittelsbach Blue, had been left to Leopold by Margarita Teresa, it seems clear that he passed it to his daughter for her dowry rather than giving it to Eleonora Magdalena as Schneider suggested.

This is further supported by Maria Antonia’s testamentary bequest of 1692 (figure 7), which stated that the gold jewelry her mother brought from Spain should stay at the Bavarian court. However, by the time of her death in December of that year, the “Bavarian court” no longer existed as such—Maximilian II Emanuel had by then moved his household to Brussels. Though he returned briefly in 1701, the War of the Spanish Succession, which began that year (and in which Bavaria and Austria fought on opposing sides), would largely keep him away from Munich until the Treaty of Utrecht in 1713. During all this time, Maria Antonia’s jewelry remained at the

Figure 7. Maria Antonia’s Testamentary Bequest, dated December 12, 1692, also indicates that she inherited some of the jewelry that her mother brought from Spain. It reads: “Yet I procure in memory of my beloved husband the diamond ornaments and the pearls around the neck and hands, which my beloved had given to me after the promise; then thirdly the Spanish ornaments set in gold that have to stay at all times at the Bavarian court and should never be disposed.” Courtesy of the Austrian State Archives, Vienna, HHStA FUK 1793/1-4.



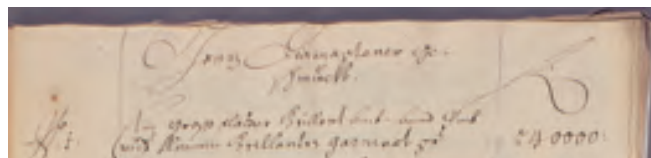
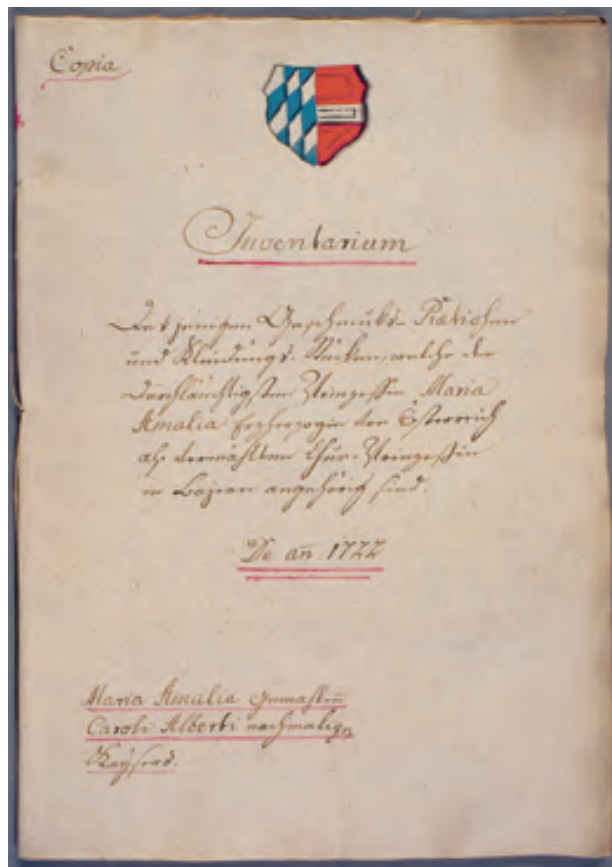


Figure 8. Inventory of the marriage contract between Maria Amalia and Crown Prince Charles Albert of Bavaria, dated 1722. The top of the contract shows a merger of the heraldic emblems of the Houses of Wittelsbach (blue and white) and Hapsburg (red and white). The cover (left) reads in part: “Inventory of the pieces of precious jewelry and clothes which belong to Her Highness Princess Maria Amalia, Archduchess of Austria as married Princess of Bavaria.” Above is the entry for the Wittelsbach Blue, reading “Whole diamond ornaments. No. 1: A large blue brilliant, encircled with small brilliants, price 240,000 guilders.” Courtesy of the Bavarian Secret House Archives.

Figure 9. In what is believed to be the oldest painting of the Wittelsbach Blue, Maria Amalia’s bridal portrait shows the large blue diamond as the centerpiece in her hair ornament. Detail from a painting by Frans van Stampart, 1722; courtesy of Lippold von Klencke, Castle Hämelschenburg.

Hapsburg court in Vienna, where it had been at her death, effectively under Emperor Joseph’s control. Thus, these documents may explain why the future Wittelsbach Blue became part of Maria Amalia’s dowry in 1722, when she, Emperor Joseph’s second daughter, married Bavarian Crown Prince Charles Albert (1697–1745).

CROWN JEWEL OF BAVARIA

Munich. Charles Albert was the son of Maximilian II Emanuel and his second wife, Princess Therese Kunigunde Sobieska. In the inventory of the marriage contract (figure 8), it was agreed that Maria Amalia would bring from Vienna to Munich “gems, jewels, and ornaments,” and that inventory documented for the first time “a large *blue* brilliant, encircled with small brilliants.” The official bridal portrait of Maria Amalia, painted in 1722 by Frans van Stampart (Glaser, 1976) and currently exhibited at Castle Hämelschenburg in Emmerthal, Lower-Saxony, shows Maria Amalia wearing a hair ornament set with a blue diamond that is clearly identifiable as the Wittelsbach Blue (figure 9). This painting is the oldest visual record of the diamond.





Figure 10. After her accession as empress in 1742, Maria Amalia wore the Wittelsbach Blue mounted in her crown (on the table to her right). This detail is from a picture painted in 1766, 10 years after her death. From the atelier of Georges Desmarées; courtesy of the Bavarian Palace Department.

After the 1742 coronation of her husband, Emperor Charles VII, now-Empress Maria Amalia wore the Wittelsbach Blue in a crown made to resemble the Ottonian imperial crown (Ottomeyer, 1979; figure 10; the Ottonian dynasty was a line of Holy Roman emperors during the 10th and 11th centuries).

Maria Amalia died in 1756 and in 1761 her son, Elector Maximilian III Joseph (1727–1777), had the Wittelsbach Blue mounted in a badge of the Order of the Golden Fleece, surrounded by large white and yellow diamonds (*Schatzkammer der Münchner Residenz*, 1937; Brunner, 1970, 1977; figure 11). This badge is currently displayed in the Treasury of the Munich Residence, though with the Wittelsbach Blue replaced by a glass imitation (Ottomeyer, 1979). A January 1774 inventory of all jewels stored in the Munich Treasury described the “Carat 36” Wittelsbach Blue as the most precious gem in the collection, with a value of 300,000 guilders (see the *G&G* Data Depository at www.gia.edu/gemsandgemology).

In January 1806, the kingdom of Bavaria was founded with Maximilian I Joseph as its first king. The new royal Bavarian crown (figure 12) prominently featured the Wittelsbach Blue in the orb under the cross, representing the heraldic blue color

of the House of Wittelsbach. It occupied this unique position from 1807 to 1931.

European crowns typically have a main stone that exceeds all other personal possessions of the ruler in size, color, and value. The Bavarian crown was a state symbol of a constitutional monarchy, and its legal possession was an outward sign of the legitimacy of the king. In Bavaria, the crown and other regalia, such as the sceptre, sword, orb, and the like, served as symbols of the sovereignty of the

Figure 11. Maria Amalia’s son, Elector Maximilian III Joseph, had the Wittelsbach Blue set in a badge of the Order of the Golden Fleece in 1761. The blue stone in this figure is a glass imitation. Altogether, 700 diamonds were used in the setting (many of which are small or not visible here). Photo by J. Evers.



new kingdom during the opening of parliament, the oath of each new King of Bavaria, and other state ceremonies (unlike the practice in other monarchies, the Bavarian crown was not used in coronations or worn by the king). Thus, the jewel on the top of the crown had a meaning beyond its material existence (Puhle, 2006).

The crown was designed in 1806 by Charles Percier, a famous Paris architect and designer for Emperor Napoleon I. Actual construction was by goldsmith Martin-Guillaume Biennais and his craftsmen. The jeweler Borgnis in Frankfurt served as an intermediary to match existing gems in the treasury with new acquisitions to complete the ring of pearls and the settings of various secondary stones (Ottomeyer, 1979; Erichsen and Heinemann, 2006).

The Munich Residence was the city palace of the Bavarian dukes, electors, kings, and emperors from 1508 to 1918. The Treasury of the Munich Residence, located on the ground floor in the eastern part of the Royal Palace (figure 13), is among the foremost of such collections in Europe (Heym, 1999). Until 1931, the most precious gem stored here was the Wittelsbach Blue. In a general bill ("Generalrechnung") from 1807, the Wittelsbach Blue was appraised at 300,000 florins, as much as all other royal ornaments combined (Ottomeyer, 1979).

DISAPPEARANCE AND REDISCOVERY

London. In 1918, at the end of the First World War, the Kingdom of Bavaria was replaced by the democratic Free State of Bavaria. After years of difficult negotiations, a contract was arranged in 1923 between the House of Wittelsbach and the Wittelsbach Equity Foundation (WAF). All former properties of the House of Wittelsbach, including the inventory of the Treasury of the Munich Residence, were transferred to the WAF to be displayed in public museums. In an appendix, it was stated that the sale of any property belonging to the WAF required the approval of the Bavarian state government. In 1931, the House of Wittelsbach and its head, Crown Prince Rupprecht, were faced with grave financial problems ("Verkauf . . .," 1931), so much so that the WAF decided to sell the Wittelsbach Blue and various other jewels through the auction house of Christie, Manson & Woods (later Christie's) in London (Christie, Manson & Woods, 1931). The Bavarian State Government, under minister president Dr. Heinrich Held, gave the required export permission for the Wittelsbach Blue. However, at



Figure 12. From 1807 to 1931, following the establishment of the Kingdom of Bavaria by Maximilian I Joseph in 1806, the Wittelsbach Blue sat at the top of the royal Bavarian crown. As with the badge in figure 11, it has since been replaced by an imitation made of blue glass. Photo by J. Evers.

the London auction on December 21, 1931 (figure 14), bidding failed to reach the reserve price, and the Wittelsbach Blue was not sold (Bruton, 1981). From the day of the auction until 1961, the whereabouts of the diamond were not publicly known.

Figure 13. The Royal Palace of the Munich Residence was built over 10 years, from 1823 to 1832. The Treasury of the Munich Residence is on the first/ground floor, to the right of the entrance as one goes into the building. It was home to the Wittelsbach Blue during most of the 19th and early 20th centuries. Photo by J. Evers.



Antwerp, Brussels, and Bruges. Acting in secret, the WAF sold the Wittelsbach Blue in Antwerp in 1951 to a merchant specializing in jewels and ornaments (Kuballa, 1964; Biehn, 1965). Baron Teuchert, speaking for the administration of the WAF, later stated that they did not know the name of this buyer because he was represented by an agent ("Der Blaue Wittelsbacher . . .," 1964). Later in 1951, the Wittelsbach Blue was resold to Antwerp diamantaire Romi Goldmuntz (Kuballa, 1964; figure 15), one of the world's most prominent diamond dealers (de Smet, 1963; "Er rührte . . .," 1972; Laureys, 2006).

Recently, Dr. Gerhard Immler, director of the Bavarian Secret House Archives, shared with one of the authors (JE) his research into the sales of precious art and gems by the WAF in the early 1950s. At the time, the WAF needed funds to repair damage to their properties that was sustained during World War II. The most direct method for obtaining these funds was by selling art in the WAF's collection. The responsible ministries and their leading secretaries, as well as the Bavarian minister president, supported the decision (G. Immler, pers. comm., 2006).

However, the financial situation of the WAF in the 1950s, as judged by statements made by mem-

Figure 14. In 1931, the Wittelsbachs were forced to put the Wittelsbach Blue (apparently once again mounted in the Golden Fleece ornament in figure 11) and numerous other items of jewelry up for auction. Shown here is the diamond's entry in the auction catalogue; it did not sell. Note that the carat weight as given here is incorrect.

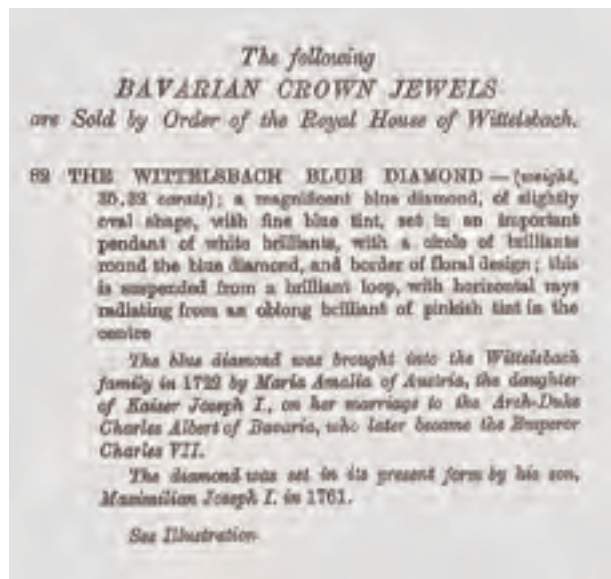


Figure 15. Romi Benjamin Goldmuntz (1882–1960) was one of the greatest diamond dealers in the world. In 1951, he purchased the Wittelsbach Blue in Antwerp, after it was sold in secret that year by the WAF. Photo by Beurs van Diamanthatdel.

bers of the House of Wittelsbach during a court case in 1962 ("Wer hat denn . . .," 1962), do not seem to bear out a dire need to sell the diamond. Then, the funds of the WAF were estimated to be DM 300–500 million. The value of the Wittelsbach Blue in 1951, based on events during the 1960s (see below) was probably about DM 1 million. Compared to the estimate of the WAF's total funds, an additional DM 1 million gained by selling the Wittelsbach Blue—the most precious piece of the Munich crown jewels—seems to be a very small improvement, even in a strained financial situation.

From April 17 to October 19, 1958, the Universal and International Exhibition (EXPO'58) was held in Brussels. Forty-seven Belgian jewelers, including Romi Goldmuntz and J. Komkommer & Son, displayed their gems at the Belgian Diamond

Industry pavilion (*Exposition Universelle et Internationale de Bruxelles*, 1958, 1961; *Official Guide . . .*, 1958). There, among other gems, Goldmuntz displayed the Wittelsbach Blue—without giving its name or origin. Nor was it known at the time that Goldmuntz was the owner of the large blue diamond. Further, though the Wittelsbach Blue was one of the largest and most historic blue diamonds in the world, not one of the millions of EXPO visitors—including diamond expert and later purchaser Jozef Komkommer—appeared to recognize it (de Smet, 1963).

After Goldmuntz's death in 1960, his heirs discovered the diamond in his gem collection, thinking it nothing but a large old-mine-cut stone. Not knowing the origin of the blue gem, in August 1961 they asked Antwerp jeweler Jozef Komkommer to recut it into a "pear-shape, emerald-cut or oval" (de Smet, 1963, p.7). However, contrary to de Smet's claims, Komkommer may not at first have realized what they had brought him. In a January 2008 interview with Jan Walgrave, former director of the Provincial Diamond Museum Antwerp, Komkommer's son Jacques claimed that he initially suggested a probable historic origin for the blue gem (J. Walgrave, pers. comm., 2008). Father and son compared characteristic data for historic diamonds in *The Diamond Dictionary* (Copeland et al., 1960), and in doing so quickly identified the unknown blue diamond as the missing Wittelsbach Blue. Together with some closely associated jewelers, Jozef Komkommer purchased the Wittelsbach Blue on August 28, 1961 (Burgerwelzijn, 1962; V. De Boi, pers. comm., 2007).

Soon thereafter, Komkommer contacted the Treasury of the Munich Residence—including Duke Albrecht of Bavaria, then head of the House of Wittelsbach, and Baron Teuchert of the WAF—offering to sell back the diamond. We do not know the price he quoted, but it has been reported as either DM 1.5 million (~\$375,000; "Der Blaue Wittelsbacher . . .," 1964) or DM 2 million ("Wer hat denn . . .," 1962). Whatever the price, Duke Albrecht refused the offer. Baron Teuchert, for his part, called the Wittelsbach Blue an "unproductive asset" not worth buying back ("Der Blaue Wittelsbacher . . .," 1964). He also then revealed where the diamond had been during 1931–1951: back in the WAF's safe in Munich.

Lucerne, Hamburg, and Düsseldorf. Spurned by the Wittelsbachs, Komkommer sought other buyers.

On August 14, 1963, during the International Lucerne Music Festival, he exhibited the Wittelsbach Blue at the Gübeline jewelry store, then overseen by famed gemologist Dr. Edward Gübeline. At the time, the Wittelsbach Blue was valued at about 2 million Swiss francs or around \$500,000. Publicity was high: Three local newspapers reported on the event ("Ein berühmter Steinerer . . .," 1963; "De Grote Blauwe Diamant . . .," 1963; "Der 'Wittelsbacher' in Luzern," 1963). Komkommer had hoped to sell the Wittelsbach Blue to one of the festival guests, but by mid-September had seen no success. However, while the stone was in Lucerne, Dr. Gübeline was able to conduct the first gemological examination of the diamond (see below).

In 1964, Hamburg jeweler Renatus Wilm recognized a chance to sell the Wittelsbach Blue to one of his countrymen (Kuballa, 1964, Biehn, 1965). Some "residual patriotism" led him to fear that this most important historic German gem could "drift to America," as had happened earlier with the Hope diamond. Komkommer and Wilm entered into a contract: Wilm would earn a \$50,000 finder's fee if he sold the Wittelsbach Blue by January 31, 1965, but Komkommer would get the same amount of money from Wilm should Wilm be unsuccessful (Kuballa, 1964; Biehn, 1965). To this end, Wilm exhibited the Wittelsbach Blue in his jewelry shops in Düsseldorf and Hamburg during October.

Wilm's efforts saw more success than those of Komkommer. At the end of 1964, he sold the Wittelsbach Blue and earned his \$50,000. The name of the buyer was not disclosed.

SOLD TO A PRIVATE PARTY

Antibes and Zurich. Here, the previously published history of the Wittelsbach Blue (e.g., Gaal, 1977; Bruton, 1981; Balfour, 1997; Morel, 2001) comes to an end, with the fate of the diamond after 1964 largely a mystery. In March 2006, we began our investigations to determine the name of the private purchaser in the digital archives of German newspapers and magazines. Our attention soon focused on Helmut Horten (1909–1987) of Düsseldorf, at one time the owner of one of Germany's largest department-store chains. One of the authors (RD) had first speculated on Horten's identity as the buyer of the Wittelsbach Blue in an article published in a small journal on Palatine topography in 1982 (Dröschel, 1982).



Figure 16. This photo of the Wittelsbach Blue was taken by Ernst Albrecht Heiniger and his wife Jeanne after years spent tracking down the diamond. The mounting was created in the 1960s by Harry Winston and was designed to reduce the visibility of the extremely large culet, and thus improve the overall appearance of the historic stone. Reprinted by permission of J. Heiniger.

The first reports connecting Horten with an unnamed 35 ct blue diamond were published in 1966. Horten had married in secret that year; his bride was a young secretary from Vienna named Heidi Jelinek, 32 years his junior (Bissinger and Lebeck, 1971a). Reports of the wedding appeared in the *Rheinische Post* (Diebäcker, 1966) and other publications (Adabei, 1966a,b) on August 3, 1966. Among other salacious details about the party at which Horten celebrated his second marriage, the article reported that Horten had presented his wife with a 35 ct blue diamond as a wedding gift. For *Rheinische Post* journalist Diebäcker, the article had severe consequences (J. Diebäcker, pers. comm., 2006). Horten withdrew all advertisements for his stores (in the order of DM1.5 million), demanding that Diebäcker be fired. Fortunately for Diebäcker, the publishers of *Rheinische Post* refused. (The two other articles—Adabei, 1966a,b—were published pseudonymously.)

A two-part 1971 article in *Stern* magazine (Bissinger and Lebeck, 1971a,b) provided more details of the Hortens' post-wedding party at Cap d'Antibes, France, which according to Diebäcker featured performances by the famed BlueBell Girls dancing troupe from Las Vegas, a ballet troupe from Tokyo, a dancing group from Oslo, and musicians from

Greece (Diebäcker, 1966). Reportedly, Helmut Horten presented the diamond to Heidi by simply pulling it from his trouser pocket in the midst of this gala. The 240 guests in attendance likely did not realize that the blue gem at the center of this scene was irreplaceable, once part of the Treasury of the Munich Residence.

Other popular journalists were also seeking the diamond. Academy Award-winning Swiss film producer Ernst Albrecht Heiniger (1909–1993; L. Piccolin, pers. comm., 2004) and his wife Jeanne were also avid gem photographers. *The Great Book of Jewels* (Heiniger and Heiniger, 1974) includes the story of their years-long search for the Wittelsbach Blue in the early 1970s.

The Heinigers had traveled thousands of miles to locate the gem without success. The diamond was nowhere to be found, and the name of the 1964 purchaser “was guarded with utmost secrecy” (Heiniger and Heiniger, 1974). Finally, after three years, they learned by chance that the Wittelsbach Blue was stored in a vault not far from their photo studio in the Zurich Bahnhofstrasse (G. Kling, pers. comm., 2007). Photographing the Wittelsbach Blue required lengthy negotiations and a costly insurance policy (Heiniger and Heiniger, 1974). In addition, they were required to sign documents stating that they would never reveal any information about the owner or the stone's location. The photo of the Wittelsbach Blue taken by the Heinigers is shown in figure 16.

A variety of other reports of the blue diamond appeared in German publications over the ensuing decades (e.g., Neuhauser, 1971; Zipser, 1991). Although no other blue diamond of this particular weight has ever been reported, none of these articles identified the stone as the missing Wittelsbach Blue. However, a brief 1979 article discussing the 70th birthday celebration of Helmut Horten (“70 Jahre H. Horten,”) finally confirmed the Hortens' ownership of the historic diamond. The article mentioned that, in 1966, Horten had presented Heidi with one of the greatest diamonds that ever adorned a woman: the famous “Wittelsbach Blue” (figure 17).

In March 2006, 27 years after this article appeared, one of the authors (JE) asked the *Welt am Sonntag* editor responsible for the 1979 report about its factual basis. He replied that the paper would not have published information on a stone like the Wittelsbach Blue from the private life of a person like Helmut Horten without his specific agreement.

The authors also contacted Jeanne Heiniger in September 2007 asking her to review the sections of this article dealing with the Hortens' ownership and the Heiningers' photograph of it. She answered by e-mail that "no addendum and no correction" were required (J. Heiniger, pers. comm., 2007). This is the second independent "source" for the Hortens' ownership.

St. Moritz and London. In November 2006, the authors received a report that the elusive Wittelsbach Blue had recently been displayed in a private exhibition at the Bulgari store in St. Moritz,

Figure 17. This brief article in the January 7, 1979 issue of the German national Sunday newspaper Welt am Sonntag, marks Helmut Horten's 70th birthday, and for the first time publicly links Horten and his wife with the Wittelsbach Blue.



Switzerland. This exhibition and a later one in Vienna were probably the first indications that Heidi Horten planned to sell the Wittelsbach Blue.

In November 2008, Christie's announced that the Wittelsbach Blue would be sold at auction in London on December 10, 2008 (Christie's, 2008a,b; Kratzer and Evers, 2008). This auction was conducted at Christie's headquarters—the same building where the Wittelsbach Blue was unsuccessfully offered nearly 80 years earlier. The winning bid was placed by London jeweler Lawrence Graff, who paid a hammer price of £16,393,250, or just over \$24.3 million and \$683,000 per carat (Christie's, 2008c). This is a record price for any diamond or piece of jewelry at auction. The WAF did not participate in the auction, but the authors have been told that it intends to negotiate with Graff to purchase the diamond (R. Borchard, pers. comm., 2008). However, no decisions in that respect had been made when this article went to press.

GEMOLOGICAL INVESTIGATIONS

During the short period in 1963 and 1964 between the rediscovery of the Wittelsbach Blue by Jozef Komkommer and its sale to Horten, a few diamond specialists had the opportunity to examine it. In addition to Dr. Gübelin, these included Finnish jeweler and diamond historian Herbert Tillander, who measured the cut, weight, and dimensions (Tillander, 1965). Hamburg jeweler Renatus Wilm, who had sold the Wittelsbach Blue to Horten in 1964, supported Tillander's findings. Most recently, the Christie's catalogue in which the diamond appears published a copy of the September 24, 2008, GIA Colored Diamond Grading Report on this stone (Christie's, 2008b, p. 126).

The rough diamond from which the Wittelsbach Blue was cut was probably a flat slab about 9 mm thick. This can be deduced from the broad proportions of the cut and the extremely large culet. Where the Wittelsbach Blue was cut and polished cannot be stated with certainty, but Paris (Morel, 1988), Lisbon and Venice (Tillander, 1995), and Bruges, Antwerp, and London (Bruton, 1981) have all been proposed in the literature. Jozef Komkommer reported the polish of the Wittelsbach Blue as being "uncommonly smooth, smoother than the work of the very best polishers of today" (de Smet, 1963, p. 8). Tillander also reported that the "appearance of this stone is particularly striking because of its unusually fine

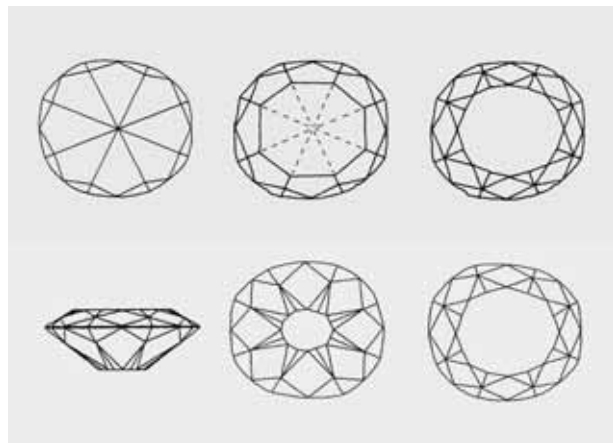


Figure 18. Tillander's sequence of drawings illustrates how the Wittelsbach Blue may have been developed from a variant of the pointed star cut (left). At center, the apex is replaced by a large table facet, after which star facets are added around the table (right). The complete facet diagrams are shown along the bottom. From Tillander, 1995.

polish and the absolute flatness of the facet surfaces" (Tillander, 1965).

In the GIA report, the cut of the Wittelsbach Blue is described as a "cushion modified brilliant." Like a modern brilliant cut, it shows excellent eightfold symmetry (figure 18). According to Tillander, it is basically a star cut (figure 18, top left) with its apex replaced by a table facet (figure 18, top center), so that the radially bisected girdle facets remained unchanged. Then, a brilliant cut was superimposed to complete the cut (figure 18, top right; Tillander, 1965). In addition to the main and girdle facets, the Wittelsbach Blue has double pavilion facets—perhaps unique for a historic diamond cut—with eight precisely developed facets around the culet (figure 18, bottom). According to Tillander (1995), it is the earliest known brilliant.

Photos of the stone and the GIA report indicate that over the years the knife-edge girdle was damaged in several places (figure 19). One can only hope that a future owner of the Wittelsbach Blue does not repolish it in order to remove this minor damage, as it would result in a loss of the stone's subtle original substance, identity, and historic form. However, a statement from Graff Diamonds shortly after the December 10 auction indicated that they intended to do just that, with the aim of making the diamond "flawless and a deeper color" (Reyburn, 2008).

As noted, the first gemological characterization of the Wittelsbach Blue as a type IIb diamond was performed in 1963 by Dr. Gübelin ("De Grote

Blauwe Diamant . . .," 1963). Balfour (1987) later reported that Gübelin observed red phosphorescence after exposure of the stone to short-wave ultraviolet radiation. Most blue diamonds display a chalky blue to green phosphorescence; only very rarely, as with the Hope diamond, do they exhibit red or orange-red (King et al., 2003; King et al., 1998). Gübelin also reported "strong semiconductivity" ("Ein berühmter Steinerner . . .," 1963; "De Grote Blauwe Diamant . . .," 1963). In a letter that accompanied the diamond grading report (Christie's, 2008b, p. 124), GIA confirmed that the 35.56 ct diamond was a type IIb with a moderate concentration of boron and that it had "bright and persistent red phosphorescence," similar to that present in the Hope diamond. It is also interesting to note that, like the Hope, the Wittelsbach Blue was color graded Fancy Deep grayish blue. The GIA report gave the clarity grade as VS₂ and the color as even. Polish and symmetry were "good," and—as noted by others—the girdle was extremely thin. Measurements revealed a 64% table, extremely large culet, and 38.8% total depth.

Figure 19. Over the centuries, the Wittelsbach Blue has sustained a certain amount of damage. The worst is to its knife-edge girdle, which suffered severe chipping over its three centuries of known history. Photo courtesy of Christie's.





Figure 20. Jozef Komkommer (1911–1980), whose recognition of the Wittelsbach Blue in 1961 (with the help of his son) saved it from recutting, is shown here examining the diamond with a loupe.

CONCLUSION

Helmut Horten died in Switzerland in November 1987. Heidi Horten, who has no children, is now the richest woman in Austria, with assets of € 3.7 billion (“Special report: The world’s billionaires,” 2008). Although she can use and increase the possessions of her former husband, she is not allowed to dispose of them in her will (Stern, 1971a; “Der Lotto-Gewinn des Jahres . . . ,” 1994). This may be the reason why she decided to sell the Wittelsbach Blue, which was her personal property, at the Christie’s auction.

During the 30 years between 1931 and 1964, the list of poor decisions dealing with the fate of the Wittelsbach Blue is remarkable. However, one man made the right decision for the Bavarian blue diamond, at the right moment: Jozef Komkommer, who refused to recut the Wittelsbach Blue into a more modern shape and thereby preserved its subtle essence, historical identity, and importance. The photo of Jozef Komkommer examining the Wittelsbach Blue in figure 20 serves as a small monument to a conscientious man.

ABOUT THE AUTHORS

Mr. Dröschel is a diamond historian in Idar-Oberstein, Germany. Dr. Evers (eve@cup.uni-muenchen.de) is a professor in the Department of Chemistry and Biochemistry, University of Munich. Dr. Ottomeyer is a professor at Humboldt University, Berlin and director general of the German Historical Museum, Berlin.

ACKNOWLEDGMENTS

The authors thank the following individuals for assistance in the preparation of this article: Mrs. W. Bartling, Hamburg; Mrs. Dr. H. Bauer, Kronen Zeitung, Vienna; Mrs. Dr. A. Baumeister and Dr. W. Alberg, Stadtmuseum Düsseldorf; Duke Franz of Bavaria, Munich; Manfred Bissinger, Hoffmann und Campe Verlag, Hamburg; Mrs. V. de Boi, Stedelijke Musea, Bruges; Ralf Borchard, Bavarian Radio, Munich; R. Burri, Zurich; S. Conrad, A. Neuhoff, Prof. Dr. T. M. Klapötke, and G. Oehlinger, Ludwig-Maximilian University, Munich; Mrs. K. Dannel, Airport Hamburg GmbH; J. Diebäcker, Duisburg; Dr. R. Dünki, Stadtarchiv Zürich; Mrs. L. Enderli, Fotostiftung Schweiz, Winterthur; Mrs. E. Heise, Neue Pinakothek, Munich; Dr. F. Falk, Schmuckmuseum Pforzheim; Mrs. D. Frost, Staats- und Universitätsbibliothek Bremen; J. Glasner and G. Reiprich, Bayerisches Hauptstaatsarchiv, Munich; Dr. G. Gonsa, Austrian State Archive, Vienna; Dr. S. Heym, Mrs. B. Wels, G. Graml, and J.

Breithoff, Bayerische Verwaltung der staatlichen Schlösser, Gärten und Seen, Munich; Mrs. A. Grüter and Mrs. M. Hug, Zentral- und Hochschulbibliothek, Lucerne; Th. Gübellin, Lucerne; Mrs. J. Gutwein, New York; Dr. O. von Habsburg, Starnberg; K. Hageresch, RotoSmeets, Bielefeld; Mrs. Jeanne Heiniger, California; Dr. G. Immler and A. Leipnitz, Geheimes Hausarchiv, Munich; L. von Klencke, Hämelschenburg; Mrs. Dr. G. Kling, Archiv Swiss PTT, Bern; Jacques Komkommer, Antwerp; G. Kruppenacher, Zürcher Hochschule der Künste, Zurich; Mrs. B. Kunze and B. Hinderer, Axel-Springer-Verlag, Berlin; Dr. E. Laureys, Mortsel, Mrs. L. Overstreet and Mrs. M. Rosen, Smithsonian Institution, Washington D.C.; L. Piccolin, Zurich, Mrs. P. Rielke and Mrs. R. Laukhuf, Hubert Burda Medien, Munich; Dr. K. Schütz, Mrs. I. Jung and A. Rührig, Kunsthistorisches Museum, Vienna; H. H. Serges, Serges Verlag, Solingen; T. Snoeren, Het Parool, Amsterdam; Mrs. L. Carillo Carminal, Biblioteca Nacional Madrid; Mrs. A. Huete, J. L. H. Elvira, A. A. Zimmerli, Palacio Real, Madrid; Mrs. I. Aguirre, Simancas and J. Menéndez Trigos, Valladolid; Dr. G. Steinhauser, Atom-Institut, Vienna; Mrs. Dr. U. Tillander-Godenhalm, Grankula; J. Walgrave, Provinciaal Diamond Museum, Antwerp; and R. Wolfensberger, Museum für Kommunikation, Bern. This article is dedicated to Prof. Dr. Dr. h.c. Heinrich Nöth, former President of the Bavarian Academy of Science, on the occasion of his 80th birthday.

REFERENCES

- Adabei (1966a) Hortens heimliche Heirat [Horten's private marriage]. *Abendzeitung*, August 3.
- Adabei (1966b) [no title]. *Express*, August 3.
- Balfour I. (1987) *Famous Diamonds*. William Collins Sons & Co., London, p.8.
- Balfour I. (1997) *Famous Diamonds*. Christie, Manson & Woods, London.
- Bauer M. (1932) *Edelsteinkunde*. Bernhard Tauchnitz, Leipzig.
- Ein berühmter Steinerne Gast an den Musikfestwochen [A famous stone as guest at the music festival] (1963) *Luzerner Neueste Nachrichten*, August 16.
- Bharadwaj M. (2002) *Great Diamonds of India*. India Book House Pvt., Nariman Point, Mumbai.
- Biehn H. (1965) *Juwelen und Preziosen [Precious Jewels]*. Prestel Verlag, Munich, pp. 366–368.
- Bissinger M., Lebeck R. (1971a) Die Helmut-Horten-Story [The Helmut Horten Story, part one]. *Stern*, March 28.
- Bissinger M., Lebeck R. (1971b) Wir leben nicht wie Lieschen Müller [The Helmut Horten Story, part two: We are not living like Lieschen Müller]. *Stern*, April 4.
- Der "Blaue Wittelsbacher" soll wieder nach München [The Blue Wittelsbach should come back to Munich] (1964) *Abendzeitung*, October 13.
- Brunner H. (1970) *Schatzkammer der Residenz München [Treasury of the Munich Residence]*, 3rd ed. Bavarian Administration of Castles, Gardens and Lakes, Munich.
- Brunner H. (1977) *Die Kunstschätze der Münchner Residenz [The Treasures of the Munich Residence]*. Edited by A. Müller, Süddeutscher Verlag, Munich.
- Bruton E. (1981) *Diamonds*. N.A.G. Press, London.
- Burgerwelzijn (1962) Waarom wordt blauwe diamant uit Gulden Vliestentoonstelling geweerd? [Why was the blue diamond excluded from the Golden Fleece Exhibition?]. *Burgerwelzijn*, July 14.
- Christie, Manson & Woods (1931) *Catalogue of the Bavarian Crown Jewels, the property of the Royal House of Wittelsbach, comprising Magnificent Brilliants and Emeralds which will be sold by Auction by Christie, Manson & Woods*. Printed by William Clowes and Sons, London.
- Christie's (2008a) The Wittelsbach Diamond: Unique royal history for sale at Christie's London in December. Press Release, November 3. <http://www.christies.com/presscenter/pdf/11042008/115110.pdf>.
- Christie's (2008b) *Jewels: The London Sale* (10 December 2008). Auction catalogue, Christie, Manson & Woods Ltd., London.
- Christie's (2008c) *Jewels: The London Sale*. Press release, auction result highlights, December 10, London.
- Copeland L.L., Liddicoat R.T., Benson L.B., Martin J.G.M., Crowningshield G.R. (1960) *The Diamond Dictionary*. Gemological Institute of America, Los Angeles.
- Diebäcker J. (1966) Hortens heimliche Hochzeit am Rhein [Horten's private marriage on the Rhine]. *Rheinische Post*, August 3.
- Dröschel R. (1982) Der Grosse Blaue Diamant, Wittelsbacher Hausdiamant [The great blue diamond, diamond of the House of Wittelsbach]. *Mitteilungen des Vereins für Heimatkunde im Landkreis Birkenfeld*, Vol. 56, pp. 42–45.
- Er rührte an den heiligen Gral dieser Nation [He touched the Holy Grail of the nation] (1972) *Spiegel*, No. 24, June 5.
- Erichsen J.K., Heinemann K. (2006) *Bayerns Krone 1806, 200 Jahre Königreich Bayern [Bavaria's Crown 1806, 200 Years Kingdom Bavaria]*. Bavarian Administration of Castles, Gardens and Lakes, Munich.
- Exposition Universelle et Internationale de Bruxelles [Universal and International Exhibition of Brussels]* (general catalogue) (1958). Puvrez, Brussels.
- Exposition Universelle et Internationale de Bruxelles* (1961) Les Participations Étrangères et Belges [Foreign and Belgian participants], Vol. 3. Etablissements Généraux d'Imprime, Brussels.
- Gaal R.A.P. (1977) *The Diamond Dictionary*, 2nd ed. Gemological Institute of America, Santa Monica, CA.
- General Inventory of Archduchess Maria Antonia, September 22 (1685) Austrian State Archives Vienna, (HHStA FUK 1777, vidimierte Abschrift vom 22 September 1685) GZBKA-2025771//0001-ÖSTA HHSTA/2007.
- Glaser H. (1976) *Kurfürst Max Emanuel, Bayern und Europa um 1700 [Elector Max Emanuel, Bavaria and Europe at 1700]*. Catalogue of the Exhibition in the Old and the New Castle Schleissheim, July 2–October 3, 1976, Vol. 2, Hirmer Verlag, Munich.
- De Grote Blaue Diamant, Der Wittelsbacher bei Gübelin [The great blue diamond, the Wittelsbacher, with Gübelin] (1963) *Luzerner Tagblatt*, August 16.
- Harlow G.E., Ed. (1998) *The Nature of Diamonds*. Cambridge University Press in association with American Museum of Natural History, New York.
- Heiniger E.A., Heiniger J. (1974) *The Great Book of Jewels*. New York Graphic Society, New York.
- Heym S. (1999) Bayerische Kronen und Juwelen [Bavarian Crowns and Jewels]. In G. Guadalupi, Ed., *Schätze der Welt, Meisterwerke der Goldschmiedekunst vom Alten Ägypten bis Cartier [Treasures of the World, Masterpieces of Goldsmith Art from Egypt to Cartier]*, Karl Müller Verlag, Erlangen.
- Jahresverzeichnis der Deutschen Hochschulschriften [Annual Index of German University Publications]* (1960–1970) Deutsche Bücherei, VEB Verlag, edited by the German Library, Leipzig.
- King J.M., Moses T.M., Shigley J.E., Welbourn C.M., Lawson S.C., Cooper M. (1998) Characterizing natural-color type Ib blue diamonds. *Gems & Gemology*, Vol. 3, No. 4, pp. 246–268.
- King J.M., Johnson E.A., Post J.E. (2003) Gem News International: A comparison of three historic blue diamonds. *Gems & Gemology*, Vol. 39, No. 4, pp. 322–325.
- Kratzer H., Evers J. (2008) Das Ringen um den blauen Wittelsbacher [The wrestling over the Wittelsbach Blue]. *Süddeutsche Zeitung*, November 5.
- Kuballa W. (1964) Der Stein, der aus der Krone fiel [The Gem that fell from the Crown]. *Süddeutsche Zeitung*, November 21/22.
- Kurin R. (2006) *Hope Diamond: The Legendary History of a Cursed Gem*. Smithsonian Books in association with Harper Collins, New York.
- Laureys E. (2006) Der Belgische Diamantsector [The Belgian diamond sector]. *Science Connection*, April 11, pp. 2–6.
- Legrand J. (1981) *Der Diamant, Mythos, Magie und Wirklichkeit [Diamond: Myth, Magic and Reality]*. Herder, Freiburg, Germany.
- Der Lotto-Gewinn des Jahres: Heidi Horten (3 Milliarden) [The lottery profit of the year: Heidi Horten (3 Billion)] (1994) *Bunte*, April 7.
- Marriage contract between Emperor Leopold I and Margarita Maria [Margarita Teresa] (1663) December 18. Austrian State Archives, Vienna FUK 1729,1-2.
- Morel B. (1988) *Les Joyaux de la Couronne de France [The Crown Jewels of France]*. Michel, Paris.
- Morel B. (2001) The diamonds of the European monarchies. In H. Bari and V. Sautter, Eds. *Diamonds, In the Heart of the Earth, in the Heart of Stars, at the Heart of Power*. Vilo International, Paris, p. 268.
- Neuhauser P. (1971) Horten und das 825 Millionen-Ding [Horten and the 825 Million object]. *Konkret*, October 7.
- Official Guide to the Universal and International Exhibition of Brussels* (1958) Desclée & Co., Tournai, Belgium.
- Ottomeyer H. (1979) *Die Kroninsignien des Königreiches Bayern [The Crown Insignia of the Kingdom of Bavaria]*. Verlag Schnell & Steiner, Munich.
- Puhle M. (2006) *Heiliges Römisches Reich Deutscher Nation. Von Otto dem Grossen bis zum Ausgang des Mittelalters [Holy Roman Empire of Germany. From Otto the Great to the End of the Middle Ages]*. Exhibition catalogue, Vol. 1.1, Pima, Magdeburg, Germany.

Reyburn S. (2008) Diamond sells for record \$24.3 million, defying slump. Bloomberg.com, December 10, www.bloomberg.com/apps/news?pid=20601088&sid=a5z_1QLCVudQ.

Schatzkammer der Münchner Residenz [Treasury of the Munich Residence] (1937) Bavarian State Administration of Castles, Gardens and Lakes, edited by H. Kreisel, University Book Printing, Dr. C. Wolf & Son, Munich.

70 Jahre H. Horten [70 Years H. Horten] (1979) *Welt am Sonntag*, January 9.

de Smet K. (1963) *The Great Blue Diamond, The Wittelsbacher, Crown Witness to Three Centuries of European History*. Standaard-Boekhandel, Antwerp-Amsterdam.

Special Report: The World's Billionaires (2008) www.forbes.com/lists/2008/10/billionaires08_The-Worlds-Billionaires-CountryOfCitizen.html [date accessed November 25, 2008].

Testamentary Bequest of Empress Margarita Teresa, March 23 (1673) Austrian State Archive Vienna, HHStA FUK 1745, 1 and 2, GZ2025771/0006-ÖSTA HHSTA/2006.

Testamentary Bequest of Archduchess Maria Antonia, December 12 (1692) Austrian State Archives Vienna, HHStA FUK 1793,1-4, GZÖSTA-2025771-0002-HHSTA/2007.

Tillander H. (1965) Six centuries of diamond design. *Journal of*

Gemmology, Vol. 9, No. 11, pp. 380–401.

Tillander H. (1995) *Diamond Cuts in Historic Jewellery*. Art Books International, London.

Untracht O. (1997) *Traditional Jewellery of India*. H. N. Abrams, New York.

Verkauf bayerischer Kronjuwelen [Selling of the Bavarian Crown Jewels] (1931). *Münchner Neueste Nachrichten*, November 29, p. 3.

Webster R. (1994) *Gems: Their Sources, Descriptions, and Identification*, 5th ed. Revised by P. G. Read, Butterworth-Heinemann, Oxford.

Wer hat denn Kaiser Karls Brilliant verkauft? [Who has sold the diamond of Emperor Charles?] (1962) *Quick*, May 6, pp. 30–32.

Der "Wittelsbacher" in Luzern [The "Wittelsbacher" in Lucerne] (1963) *Vaterland*, August 16.

Widorn H. (1960) Die spanischen Gemahlinnen der Kaiser Maximilian II, Ferdinand III, und Leopold I [The Spanish wives of Emperor Maximilian II, Ferdinand III, and Leopold I]. PhD Thesis, University of Vienna.

Zipser A. (1991) So angelte ich mir Frau Horten (5 Milliarden), Der Kuss auf den 5 Milliarden-Mund [So I fished for Mrs. Horten: The kiss on the DM 5 billion mouth]. *Bunte*, July 25.

VOTE & WIN!

Simply tell us which three 2008 articles you found most valuable, and you could win a 3-year subscription to

GEMS & GEMOLOGY.

Plus FREE copies of all three volumes of

The Dr. Edward J. Gübelin Most Valuable Article Award



A total value of
over \$300!

GEMS & GEMOLOGY®
IN REVIEW

Mark the articles in order of preference on the ballot card between pages 340 & 341. Then mail the card to arrive no later than **March 6, 2009** and it will be entered in a drawing for the grand prize.



EDITORS

Thomas M. Moses and
Shane F. McClure
GIA Laboratory

Fancy Dark Brown-Yellow Zoned Type IIa/IIb DIAMOND

Type IIb diamonds are very rare; type IIb diamonds in brown hues are even rarer. While zoned type IIa/IIb diamonds have been reported (see, e.g., Lab Notes: Fall 1993, p. 199; Summer 2005, pp. 167–168), they are also far from common. Therefore, the combination of properties exhibited by the diamond in figure 1, which was sent to the Carlsbad laboratory for a Colored Diamond Grading Report, is remarkable.

The 3+ ct pear shape was color graded Fancy Dark brown-yellow. No color zoning was visible with magnification, even when the stone was immersed in methylene iodide. Internal graining was colorless and weak. The diamond was inert to both long- and short-wave ultraviolet (UV) radiation from a standard gemological UV lamp, and exhibited no phosphorescence. When examined between crossed polarizers, it exhibited a dense “tatami” pattern, with strong localized strain surrounding a crystal (the only solid inclusion observed). The stone also exhibited feathers and indented naturals.

Editors' note: All items are written by staff members of the GIA Laboratory.

GEMS & GEMOLOGY, Vol. 44, No. 4, pp. 364–368.
© 2008 Gemological Institute of America

The mid-infrared (IR) spectra (figure 2) clearly showed the presence of two diamond types: IIa and IIb. When the pear shape was oriented such that the shoulder end was sampled, the resulting spectrum was typical of type IIa diamond with no absorption from boron or nitrogen impurities. However, when the point end was sampled, the spectrum exhibited bands at 2930 and 2801 cm^{-1} , which are characteristic of boron in type IIb diamond. This IIb spectrum was similar to that of a Fancy Dark greenish yellow-brown type IIb diamond examined at the New York laboratory in 2005 (again, see figure 2), though the boron peaks in the 2008 sample were less intense.

The ultraviolet-visible-near infrared (UV-Vis-NIR) spectra gathered from the present stone were typical of brown type IIa diamonds; absorption increased toward the blue end of the spectrum. This is in contrast to the visible spectra for blue type IIb diamonds, in which absorption increases toward the red end (A. T. Collins, “The colour of diamond and how it may be changed,” *Journal of Gemmology*, Vol. 27, No. 6, 2001, pp. 341–359).

In the DiamondView, the type IIa portions showed blue fluorescence and no phosphorescence, while the IIb regions exhibited much weaker blue fluorescence (figure 3) and short-lived weak blue/white phosphorescence. Boundaries between zones were irregular—in some places linear and in others jagged (figure 4, left). The IIa portions of the stone exhibited “mosaic” disloca-

tions (figure 4, right), which are typical in natural IIa and IIb diamonds (e.g., P. M. Martineau et al., “Identification of synthetic diamond grown using chemical vapor deposition [CVD],” Spring 2004 *Gems & Gemology*, pp. 2–25). Additionally, a “flame” or “wave” structure observed in the fluorescence of the IIb region was replicated in the phosphorescence for that region.

Since boron acts as an electron acceptor, type IIb diamond is classified as a semiconductor. When the electrical conductivity of the zoned diamond was

Figure 1. This 3+ ct Fancy Dark brown-yellow diamond was found to be distinctly type zoned (IIa and IIb).



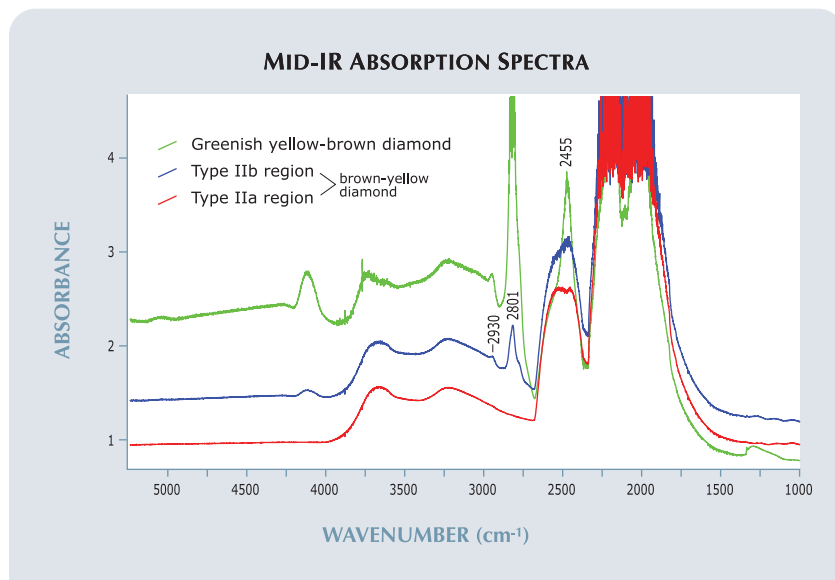


Figure 2. The mid-IR absorption spectra of the brown-yellow diamond in figure 1 indicate the presence of type IIa and IIb zones. Also shown for comparison is the spectrum of a greenish yellow-brown type IIb stone.

tested, the shoulder end (IIa) did not conduct, while the point end (IIb) was weakly conductive. This observation was not, in itself, conclusive, since type IIb diamonds are not homogeneously conductive, but it did correlate with the mid-IR and DiamondView results.

Photoluminescence (PL) spectra collected with a 488 nm laser revealed the presence of the 3H peak (503.5 nm), which has been reported before in type IIb diamonds (e.g., Fall 2004 Lab Notes, pp. 241–242). This peak occurred in

spectra from both regions of the stone, but it was stronger in the IIb region. Spectra collected using three other laser wavelengths indicated that the stone was of natural color. Raman spectroscopy (514.5 nm excitation) was used to try to identify the crystal inclusion, but no match could be found. This was unfortunate, since knowledge of the mineral might have provided valuable information pertaining to the origin of this exceptional diamond.

Karen M. Chadwick

Figure 4. The boundaries between the type zones are linear in some places and jagged in others (left); the type IIa regions in the diamond also show the subtle mottled appearance of “mosaic” dislocations (right).



Figure 3. This DiamondView image of the pavilion of the pear shape clearly shows the different type zones: moderate blue fluorescence for the type IIa region, and weak blue for the IIb zone.

HPHT-Treated CVD SYNTHETIC DIAMOND Submitted for Dossier Grading

Gems & Gemology has reported on synthetic diamonds grown by the chemical vapor deposition (CVD) method for several years (e.g., W. Wang et al., “Gem-quality synthetic diamonds grown by a chemical vapor deposition [CVD] method,” Winter 2003, pp. 268–283; P. M. Martineau et al., “Identification of synthetic diamond grown using chemical vapor deposition [CVD],” Spring 2004, pp. 2–25; and W. Wang et al., “Latest-generation CVD-grown synthetic diamonds from Apollo Diamond Inc.,” Winter 2007, pp. 294–312). CVD synthetic diamonds have been submitted to the GIA lab (e.g., Lab Notes: Spring 2008, pp. 67–69, and Summer 2008, pp. 158–159), but those samples were as-grown, even though high-pressure, high-temperature (HPHT) treatment of CVD synthetics is well known.

The 0.21 ct round brilliant in figure 5 was recently submitted for Diamond Dossier grading. Standard testing identified it as a CVD synthetic. It was graded near colorless (GIA does not use



Figure 5. This 0.21 ct CVD synthetic diamond was found to be HPHT treated.



Figure 6. The HPHT-treated CVD synthetic diamond shows weak birefringence in shades of gray, in contrast to the high-order interference colors previously documented in as-grown samples. Note the pinpoint inclusions. Field of view 1.73 mm.



Figure 7. DiamondView imaging of the synthetic diamond shows blue-green fluorescence with yellow-green striations, consistent with reports for HPHT-treated CVD synthetic diamonds.

letter grades on synthetic diamond reports) and VVS, with the clarity grade based on pinpoint inclusions. Between crossed polarizers, it exhibited weak birefringence in shades of gray (figure 6). In comparison, the as-grown sample described in the Spring 2008 Lab Note showed strong birefringence with high-order interference colors, consistent with the samples examined by Wang et al. (2007).

The sample was inert to long-wave UV radiation but fluoresced weak yellow to short-wave UV. In the DiamondView, it fluoresced blue-green, with yellow-green striations (figure 7), and exhibited weak blue phosphorescence. The fluorescence color was similar to the green luminescence of HPHT-treated nitrogen-doped CVD synthetic diamonds reported by Martineau et al. (2004), and it contrasted distinctly with the orangy pink to orangy red hues of the as-grown CVD synthetics described in the previous Lab Notes. The striations are growth phenomena, and are typical of CVD synthetic diamonds (see, e.g., Martineau et al., 2004).

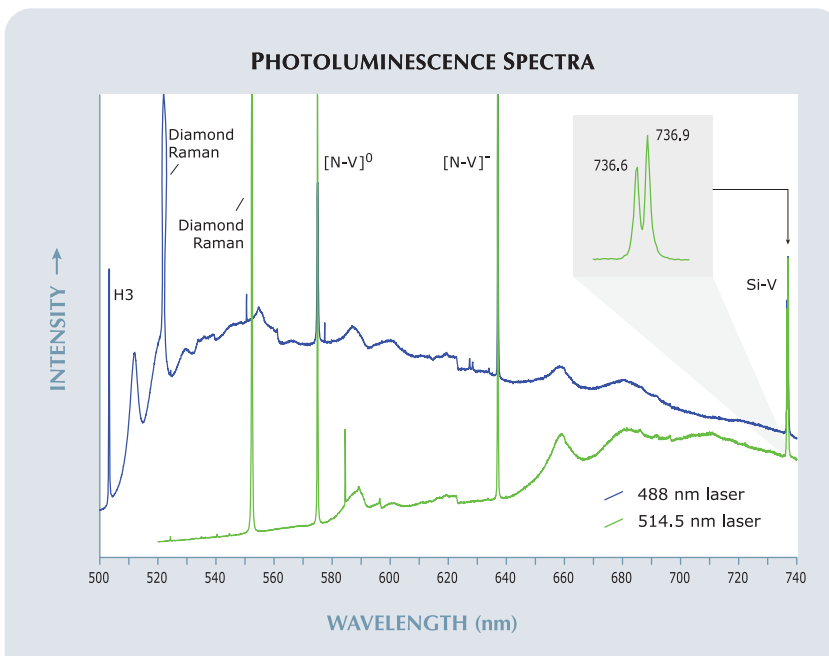
The mid-IR spectra established that the sample was type IIa. Neither of the hydrogen-related peaks at 3123 and 3107 cm^{-1} was detected. Martineau et al. (2004) stated that the former would be removed by HPHT treatment, while the latter could appear *after* HPHT treatment. A weak peak was observed at 1332 cm^{-1} , consistent with the near-colorless sam-

ples described by Wang et al. (2007).

Photoluminescence spectra collected at liquid-nitrogen temperature (~ 77 K) with 488 and 514.5 nm laser excitation (figure 8) exhibited a very

large peak doublet at 736.6/736.9 nm, due to the silicon-vacancy (Si-V) defect. Correspondingly, a very small doublet was recorded in the UV-visible spectrum at ~ 737 nm; the spectrum was otherwise featureless but with absorption rising toward the

Figure 8. The PL spectra (at 488 and 514.5 nm laser excitation) of the HPHT-treated CVD synthetic diamond show a very large Si-V doublet at 736.6/736.9 nm.



blue region, as is typical of a near-colorless type IIa diamond.

The Si-V defect was originally considered indicative of CVD synthetic diamonds; however, recent work has shown that the defect also exists in some natural colorless and near-colorless diamonds (C. M. Breeding and W. Wang, "Occurrence of the Si-V defect center in natural colorless gem diamonds," *Diamond and Related Materials*, Vol. 17, 2008, pp. 1335–1344). Large peaks were observed at 575.0 and 637.0 nm (the zero-phonon lines [ZPLs] of the nitrogen-vacancy centers [N-V]⁰ and [N-V]⁻, respectively), consistent with CVD synthetic diamond (see, e.g., Wang et al., 2003). In contrast to the as-grown CVD synthetic diamonds documented in the two earlier Lab Notes, the PL spectra for this diamond did not exhibit a 596.5/597.0 nm doublet. Again, this is consistent with the HPHT-treated CVD synthetic diamonds discussed by Martineau et al. (2004). The 488 nm spectrum did display a large peak at 503.1 nm—the H3 ZPL—associated with nitrogen. This is also consistent with the results of Martineau et al. (2004), and contrasts with the relative lack of H3 peaks in the near-colorless as-grown CVD synthetic diamond samples investigated by Wang et al. (2007). It appears that the H3 defect is introduced during HPHT annealing.

We have seen very few HPHT-treated CVD-grown synthetic diamonds in the laboratory, but the criteria discussed above allowed us to successfully identify this sample.

Karen M. Chadwick

QUARTZ with Secondary Covellite Dendrites

The discovery of some unusual dendritic inclusions in two transparent faceted quartz gems sent to the laboratory for examination helped us make a connection between two separate notes previously published in *Gems & Gemology*. The first of these (Spring 2005 Lab Notes, pp. 47–48) described thin hexagonal platelets of the copper sulfide covellite in colorless and smoky quartz,



Figure 9. Discovered in colorless quartz reportedly from Paraíba State, Brazil, this dendrite is grayish green in transmitted light (left). In reflected light (right), it shows strong metallic pink reflectance, suggesting it is covellite, which was confirmed by Raman analysis. Note the blue gilalite inclusions in the background. Field of view 4.39 mm high.

said to be from Minas Gerais, Brazil. The material was being marketed as "pink fire" quartz due to the intense pink reflectivity of the numerous tiny covellite inclusions. These appeared to be primary to the formation of the host, since they were not associated in any way with surface-reaching cracks. As is characteristic for thin crystals of covellite, these inclusions also appeared grayish green in transmitted light.

The second report (Fall 2005 Gem News International, pp. 271–272) dealt with inclusions of a blue-to-green mineral in quartz, which occurred as jellyfish-like radiating clusters. This mineral was identified as gilalite, a hydrated copper silicate. The quartz was stated to have come from the Brazilian state of Paraíba, and is often sold as "Paraíba" quartz.

Our recent examination of the two faceted quartz gems, which are reportedly from the same locality that produced the gilalite inclusions, proved interesting, as both contained obvious black-appearing dendrites that were green in transmitted light (figure 9, left), with a bright pink reflectance color (figure 9, right). This was the same reaction previously reported for

hexagonal platy covellite inclusions, which suggested that these dendrites were also covellite. Moreover, one of the gems contained inclusions of gilalite (identified by their appearance) as well, indicating the presence of copper in the system. The dendrites were situated along surface-reaching fracture planes, proof that they formed after the quartz had crystallized.

Since the broad edges of the inclusions had been polished through and were exposed at the surface, these dendrites made ideal targets for Raman microanalysis, which confirmed that they were covellite. Covellite is known to be a secondary copper mineral in copper deposits, so the discovery of these dendrites as fillings in quartz was not surprising, even though such secondary inclusions in quartz have not been reported before.

*John I. Koivula and
Karen M. Chadwick*

Induced Copper Contamination of TOURMALINE

In recent years, Gem Identification has received numerous requests to analyze tourmalines for the presence of copper,

since (justifiably or not) copper-bearing tourmalines generally command significantly higher prices in the marketplace than their non-cuprian counterparts. Such analyses are typically conducted on surface and near-surface areas of the faceted gems.

Since we are dealing with the detection of trace elements (in parts per million), we invariably face the problem of accidental or deliberate surface contamination. As the experiments described below indicate, this can be accomplished either by polishing a tourmaline on a copper lap, or by soaking the stone (faceted or in its rough state) in a concentrated solution of a copper salt such as copper sulfate. Accidental contamination from a copper lap is a very real possibility, since copper laps are often used to polish gems such as tourmalines.

To demonstrate the potential for this contamination, we started with two small (1–2 ct) faceted “watermelon” tourmalines and analyzed them by energy-dispersive X-ray fluorescence (EDXRF). Neither stone showed any copper peaks. We then rubbed the tourmalines 10 times in a circular motion against a flat copper lap, using moderate thumb pressure. When we repeated the EDXRF analyses, a clear signal for copper appeared.

At this point, we examined the tourmalines with a gemological microscope. We did not see any surface-reaching pits or cracks in the first tourmaline, only fine polishing lines. Nor did we see any evidence of copper on or in its surface.

The other stone had no eye-visible surface defects, but it did have a surface-reaching crack across the table that picked up minute amounts of microscopic copper when it was rubbed against the lap. In standard darkfield illumination, this contaminant was seen as thin black smudges that resembled the typical surface dirt often seen in such cracks (figure 10, left), but fiber-optic illumination revealed the metallic nature and copper color of the contaminant (figure 10, right). In light of these results, it seems clear that if copper laps are used to polish tourmalines, there is a possibility of accidental (or—though difficult to prove—deliberate) contamination.

This brings us to intentional contamination of tourmaline using concentrated copper salt solutions. The salt we chose for the experiment was copper sulfate, since chalcantite (the mineral name for naturally occurring copper sulfate) was readily available. We have no reason to believe that any other cop-

per salt in concentrated solution would not have worked just as well.

For this experiment, we selected another small (3 ct) faceted tourmaline with a few surface-reaching features—growth tubes and cracks—that did not detract significantly from its outward appearance. We also treated an ~7.5 ct piece of rough gem-quality tourmaline that had a nice greenish blue color that was not copper related.

Again, we first analyzed both samples using EDXRF; no copper was detected in either of them. Next, we warmed both samples in the light well of a gemological microscope and dropped them into the concentrated copper sulfate solution, which had been cooled in a refrigerator. This created a mild vacuum, which allowed the copper sulfate solution to enter any surface openings in the test subjects. After the solution had reached room temperature, we removed the tourmalines and hand-dried them with paper towels. Again, we repeated the EDXRF analyses.

Both tourmalines had absorbed enough copper solution to produce a visible copper signal on their EDXRF spectra. The copper peaks in the rough sample were not nearly as strong as the signal from the faceted stone, as expected. Although copper sulfate solution has an obvious blue color, no color from the solution was observed in either sample.

In analyzing tourmaline for copper, GIA uses a cleaning protocol that eliminates the potential for errors resulting from such contamination. These experiments underscore the importance of cleaning test samples thoroughly before analysis, and being aware of the very real possibility of surface contamination if unexpected elements are detected during analysis.

*John I. Koivula, Kevin G. Nagle,
and Philip A. Owens*

Figure 10. The crack across the table of this tourmaline readily picked up minute traces of copper when the stone was rubbed against a flat copper lap. In standard darkfield illumination (left), the copper looks like typical smudges of black dirt. However, with surface-incident fiber-optic illumination (right), the metallic nature and copper color of the contaminant are clearly seen. Field of view 0.9 mm.

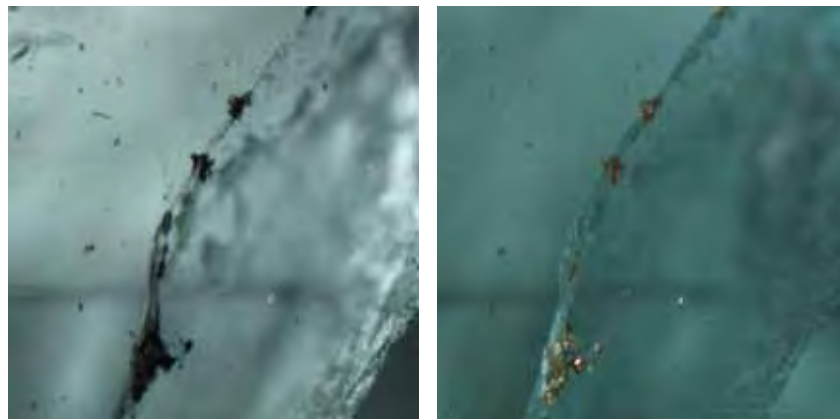


PHOTO CREDITS

Robison McMurtry—1 and 5; Karen M. Chadwick—3, 4, 6, and 7; John I. Koivula—9 and 10.



EDITOR

Brendan M. Laurs (blaurs@gia.edu)

CONTRIBUTING EDITORS

Emmanuel Fritsch, *CNRS, Institut des Matériaux Jean Rouxel (IMN), University of Nantes, France* (fritsch@cnrs-imn.fr)

Henry A. Hänni, *SSEF, Basel, Switzerland* (gemlab@ssef.ch)

Franck Notari, *GemTechLab, Geneva, Switzerland* (franck.notari@gemtechlab.ch)

Kenneth V. G. Scarratt, *GIA Laboratory, Bangkok, Thailand* (ken.scarratt@gia.edu)

COLORED STONES AND ORGANIC MATERIALS

Visit to andesine mines in Tibet and Inner Mongolia. Gem-quality plagioclase feldspar (labradorite) has been recovered for years from the U.S. state of Oregon (e.g., A. M. Hofmeister and G. R. Rossman, "Exsolution of metallic copper from Lake County labradorite," *Geology*, Vol. 13, 1985, pp. 644–647; C. L. Johnston et al., "Sunstone labradorite from the Ponderosa mine, Oregon," Winter 1991 *Gems & Gemology*, pp. 220–233). In 2002, red andesine-labradorite appeared in the gem market that was reportedly sourced from an unspecified locality in the Democratic Republic of the Congo (Spring 2002 GNI, pp. 94–95), but some believe that this material actually came from China. In late 2005, a red andesine called "Tibetan sunstone" was supplied by Do Win Development Co. Ltd. of Tianjin, China, reportedly from Nyima (actually Nyemo) in central Tibet (Winter 2005 GNI, pp. 356–357). Then, at the February 2007 Tucson gem shows, King Star Jewellery Co. (Hong Kong) and M. P. Gem Corp. (Kofu, Japan) introduced a similar red andesine from Tibet called "Lazasine." A large supply of red andesine allegedly from China was offered for sale as an official gemstone of the 2008 Summer Olympic Games in Beijing. Despite claims to the contrary, there has been widespread suspicion that the red Chinese andesines are diffusion treated. In fact, recent studies have proved the viability of diffu-

sion-treating such material (e.g., G. Roskin, "JCK web exclusive: The andesine report," posted November 12, 2008, www.jckonline.com/article/CA6613857.html).

In October–November 2008, this contributor visited two andesine deposits in the Chinese autonomous regions of Tibet and Inner Mongolia. The investigation was made possible by the cooperation of mine owners Li Tong of Tibet and Wang Gou Ping of Inner Mongolia, as well as trip organizers Wong Ming (King Star Jewellery Co.) and Christina Iu (M. P. Gem Corp.), who are partners in the Tibetan andesine mine. Also participating in the expedition were Masaki Furuya (Japan Germany Gemmological Laboratory, Kofu, Japan), David Chiang (BBJ Bangkok Ltd., Bangkok), and Marco Cheung (Litto Gems Co. Ltd., Hong Kong).

The Tibetan andesine mine we visited is located 70 km south of the region's second largest city, Xigazê (or Shigatse), in southern Tibet. This area is well south of the Nyima/Nyemo area (Lhasa region), and our guides were not aware of an andesine mine in that part of Tibet. We drove seven hours from the capital city of Lhasa to the mine, which lies at an elevation of more than 4,000 m. The site is divided into north and south areas with a total coverage spanning 3–4 km east-west and 5–7 km north-south. During our visit, fewer than 10 miners were digging pits in the south area, near a piedmont riverbed (located at the base of a mountain). Organized mining began there in January 2006 under the supervision of Li Tong. The work is done by hand, from April to November. According to the miners, red andesine was originally found in this area in the 1970s, and beads of this material first appeared in Lhasa's largest bazaar (Bakuo Street) in 2003.

The surface layer at the site consists of humic soil that is 0.5–3 m thick. The andesine is mined from an underlying layer consisting of greenish gray or dark gray sand/gravel in the south area (figures 1 and 2), and yellowish red or greenish gray soil in the north area. The andesine-bearing layers are apparently derived from Tertiary volcano-sedimentary

Editor's note: Interested contributors should send information and illustrations to Brendan Laurs at blaurs@gia.edu or GIA, The Robert Mouawad Campus, 5345 Armada Drive, Carlsbad, CA 92008. Original photos can be returned after consideration or publication.

GEMS & GEMOLOGY, Vol. 44, No. 4, pp. 369–379
© 2008 Gemological Institute of America



Figure 1. The andesine-bearing deposits in Tibet are exploited in a series of tunnels, with the miners using simple hand tools. Photo by A. Abduriyim.



Figure 2. Rounded crystals of Tibetan andesine are found in concentrations mixed with sand/gravel or soil. Photo by A. Abduriyim.

deposits (Qin Zang Gao Yuan [Tibet Highland] area geologic map, Chengdu Institute of Multipurpose Utilization of Mineral Resources, China Geological Survey, Chengdu, Sichuan Province, 2005). In the south mining area, a few tunnels penetrate several meters horizontally into the andesine-bearing horizons. In addition, a shaft was sunk several meters deep in the north area, but mining there was discontinued after the devastating Chengdu earthquake in May 2008. The andesine is concentrated in patches consisting of several to more than a dozen pieces (100–200 g total) mixed with sand/gravel or soil (again, see figure 2). These accumulations appear to have been concentrated across a wide area by water from seasonal snowmelt.

Alluvial transport has rounded the crystals, and most were found as translucent to transparent pebbles that were

<1 cm in diameter (figure 3), though the largest pieces reached 4 cm. Most were orangy red; deep red material was less common. Some had areas that were green or colorless, but we did not see any pieces that were completely brown, yellow, or colorless. The annual production from the region is estimated to be 700–800 kg, of which 30–50 kg are gem

Figure 3. The Tibetan andesine consists mainly of orangy red pebbles that are <1 cm in diameter. Photo by A. Abduriyim.



Figure 4. This horizon has produced andesine in the Guyang area of Inner Mongolia. Photo by Wong Ming.





Figure 5. These andesine pebbles (2–5 cm) were mined from the Inner Mongolian village of Shuiquan. Photo by A. Abduriyim.

quality. A visit to mountain peaks in the mining area revealed Jurassic volcanic rocks and detrital deposits; a volcanic origin is also the case for similar feldspar from Oregon.

The andesine from Inner Mongolia is mined from an alluvial deposit of sand/gravel in the Guyang area, north of Baotou city. The mine is situated in the Yinshan tectonic belt of Mesozoic-Cenozoic age (Inner Mongolia Guyang-Xiaoyutai area geologic map, Inner Mongolia Autonomous Region Geological Survey, Hohhot, 1982). Andesine has been recovered from a region measuring 20 km east-west and 5 km north-south. Humic topsoil overlies Tertiary (Pliocene) and Cretaceous sand/gravel; some areas also show layers of tuff or basaltic rock. The andesine is restricted to a light gray layer (locally iron stained) that is 1–3 m thick and lies several meters beneath the surface—down to more than 10 m—within the sand/gravel (figure 4). Organized mining has taken place near Shuiquan and Haibouzi villages, producing up to 100 tonnes annually. The andesine seen by this contributor commonly had high transparency and was somewhat rounded, except for broken pieces that showed well-developed cleavage surfaces. The stones were typically 0.3–5.5 cm in diameter, with 70–80% in the 1–2 cm range (figure 5). Most of the andesine was pale yellow. Colorless or deep yellow stones were uncommon, while other colors have not been reported from this area.

This field investigation confirmed that the Xigazê region of Tibet does indeed produce natural red andesine, while the Guyang area of Inner Mongolia is a source of pale yellow andesine that may be used as the starting material for diffusion treatment. Additional images from this expedition can be found in the G&G Data Depository at www.gia.edu/gemsandgemology.

Ahmadjan Abduriyim
(ahmadjan@gaaj-zenhokyo.co.jp)
Gemmological Association of All Japan – Zenhokyo
Tokyo, Japan

Gemological properties of andesine collected in Tibet and Inner Mongolia. While visiting andesine mines in Tibet and Inner Mongolia (see previous GNI entry), one of these contributors (AA) obtained several samples for gemological study that he witnessed being gathered by the miners. Ten pieces (up to 26.0 g; see, e.g., figure 6) from each region were polished with two parallel windows, and all were characterized for this report. It is currently impossible to unequivocally determine in the laboratory whether red andesine in the gem trade has been diffusion treated. This preliminary characterization was done to gather data on red samples that are known to be untreated, as well as pale yellow material that may be used as a starting material for diffusion treatment.

Figure 6. These are some of the samples of andesine obtained in Tibet (top, up to 5.4 g) and Inner Mongolia (bottom, up to 26.0 g, some partially polished) that were examined for this report. Photos by M. Kobayashi.



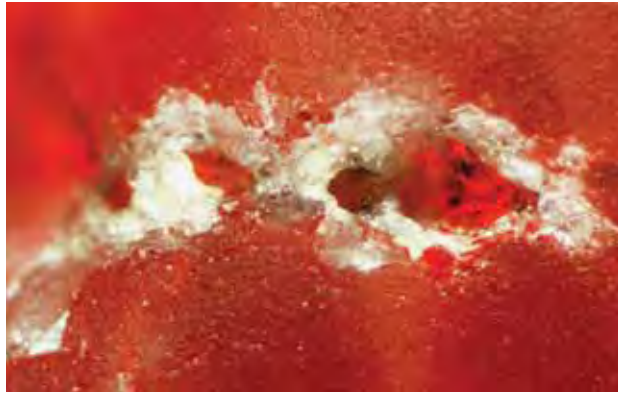


Figure 7. Surface etching was observed on some Tibetan andesine pebbles. Photomicrograph by A. Abduriyim; magnified 28 \times .

All the samples had a waterworn appearance, and some of the Tibetan pebbles also had embayed areas that appeared to have been created by chemical etching (figure 7). The pebbles from Inner Mongolia also were abraded, but they were more angular than the Tibetan samples and exhibited conchoidal fractures.

The Tibetan samples had the following gemological properties: color—brownish red to orange-red to red; pleochroism—weak; RI—1.550–1.561; birefringence—0.009; optic sign—biaxial positive; SG—2.69–2.72; fluorescence—orange to long-wave, and dark red to short-wave, UV radiation; and Chelsea filter reaction—red. The Inner Mongolian samples were pale yellow, but otherwise they exhibited almost identical properties except that they were inert to both long- and short-wave UV radiation, and they showed no reaction to the color filter.

Examination with a gemological microscope revealed that most of the Tibetan samples contained prominent twin lamellae and parallel lath-like hollow channels (figure 8, left), irregular dislocations (figure 8, right), and irregular color patches caused by milky turbidity from fine granular inclusions (figure 9). One of the polished samples displayed aventurescence due to the presence of native-copper platelets. The samples from Inner Mongolia contained parallel flat growth tubes (figure 10, left), as well as abundant linear fissures (figure 10, right) and fine twin

planes arranged parallel to a (010) direction. In some cases, the linear fissures caused a weak opalescence, and such stones cut *en cabochon* would be expected to show a weak cat's-eye effect. Cleavage planes were also well developed along one (010) direction.

Absorption spectra were measured with a UV-Vis spectrometer in the range 220–860 nm. The Tibetan andesine exhibited absorption from 320 nm toward shorter wavelengths, as well as a prominent broad band near 565 nm due to colloidal copper. In addition, a weak feature near 380 nm was due to Fe³⁺. Similar absorptions have been documented in red andesine that was reportedly from the Democratic Republic of the Congo and in red labradorite from Oregon (A. M. Hofmeister and G. R. Rossman, "Exsolution of metallic copper from Lake County labradorite," *Geology*, Vol. 13, 1985, pp. 644–647; M. S. Krzemnicki, "Red and green labradorite feldspar from Congo," *Journal of Gemmology*, Vol. 29, No. 1, 2003, pp. 15–23). Spectroscopy in the near-infrared region (800–2500 nm) revealed an absorption peak near 1260 nm that is caused by Fe²⁺.

The andesine from Inner Mongolia showed absorptions at 380, 420, and 450 nm. The 380 nm feature was strongest, while the broad band at 420 nm (presumably due to charge transfer between Fe²⁺ and Fe³⁺) was characteristic. A strong and broad absorption also was observed near 1260 nm.

Energy-dispersive X-ray fluorescence (EDXRF) chemical analysis of andesine from both Tibet and Inner Mongolia revealed very similar compositions, with 55–56 wt.% SiO₂, 26–27 wt.% Al₂O₃, 10 wt.% CaO, and 5.8–6.2 wt.% Na₂O. Trace elements such as K, Mg, Ti, Fe, and Sr were detected. The Tibetan stones also contained 0.06–0.10 wt.% CuO, but no Cu was detected in the Inner Mongolian samples. The chemical composition showed that all samples were andesine, with some plotting at the border with labradorite (An_{47–50}). Previous electron microprobe analyses of samples from Inner Mongolia showed they were labradorite, with a composition of An_{50–51} (or An_{52–53} if K is excluded; Y. Cao, "Study on the feldspar from Guyang County, Inner Mongolia and their color enhancement," Master's thesis, Geological University of China, 2006).

Laser ablation–inductively coupled plasma–mass spectrometry (LA-ICP-MS) analysis showed that samples from

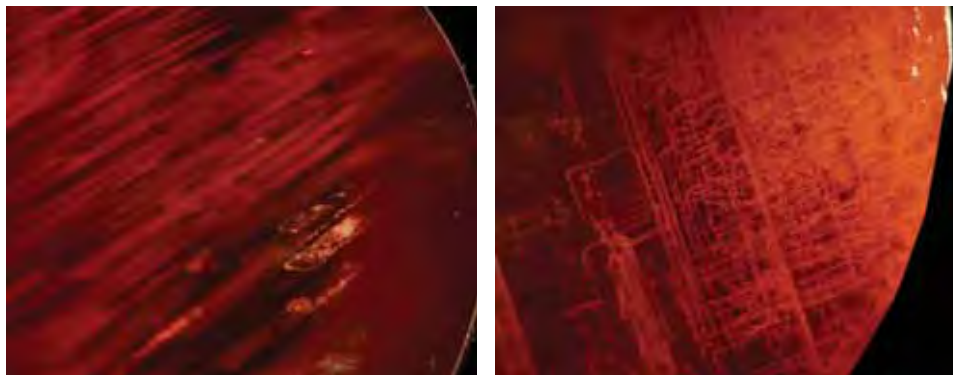
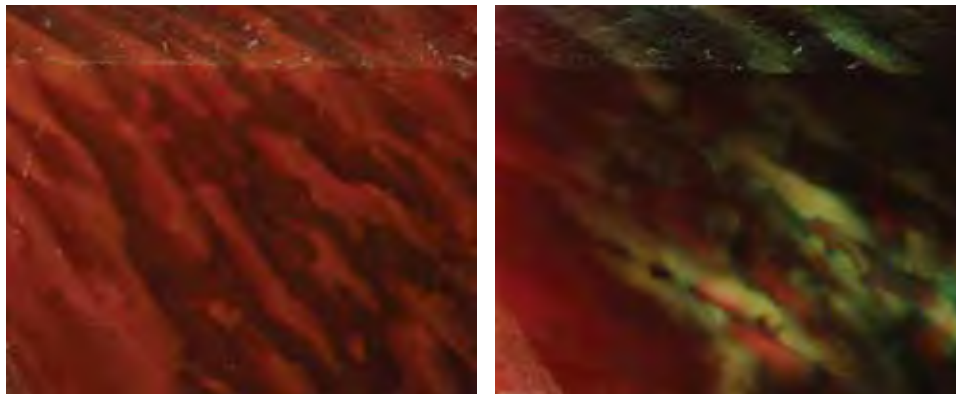


Figure 8. With magnification, twin lamellae and parallel lath-like hollow channels are seen in this orangy red andesine from Tibet (left, magnified 25 \times). Also present were distinctive dislocation features (right, magnified 20 \times). Photomicrographs by A. Abduriyim.

Figure 9. This Tibetan andesine exhibits concentrated areas of red and orange-red milky turbidity (left). When viewed with diffused light, some of these areas appear green or near colorless (right).

Photomicrographs by A. Abduriyim; magnified 25 \times .



both localities contained several trace elements: K (2200–3600 ppm), Fe (1000–3200 ppm), Sr (700–1000 ppm), Mg (330–620 ppm), Ti (400–510 ppm), Ba (120–160 ppm), Mn (20–40 ppm), Ga (20–30 ppm), Li (10–60 ppm), and Sc (5–15 ppm); B, V, Co, Zn, Rb, Sn, Ce, and Eu were <3 ppm each. No significant elemental difference was observed between Tibetan and Mongolian andesine, other than Cu content: 300–600 ppm in orangy red andesine, and <3 ppm in pale yellow andesine. In addition, Li was slightly dominant in Tibetan andesine.

Additional images from this study can be found in the G&G Data Depository at www.gia.edu/gemsandgemology.

Ahmadjan Abduriyim and Taisuke Kobayashi
Gemmological Association of All Japan – Zenhokyo
Tokyo, Japan

New find of vivid kunzite from Pala, California. In July 2008, several etched crystals of gem-quality kunzite were found at the historic Elizabeth R mine, located on Chief Mountain in the Pala District of San Diego County (see, e.g., Fall 2001 GNI, pp. 228–231). In mid-2008, Jeff Swanger (Escondido, California) purchased the mine from Roland Reed (El Cajon, California). Mr. Reed has continued to work the Elizabeth R while Mr. Swanger mines the neighboring Ocean View property, where he found a large gem pocket in 2007 (see Spring 2008 GNI, pp. 82–83).

Although this was not the first kunzite discovery at the Elizabeth R, these pieces had a particularly vibrant pinkish purple to pink-purple color that is seldom seen in natural-color kunzite (e.g., figures 11 and 12). Mr. Reed believes

they compare favorably to kunzite from the nearby Vandenberg mine, which produced colors that are considered among the finest found anywhere. Approximately 0.5 kg of top-grade material has been recovered, and the best pieces were sent for fashioning to Minas Gem Cutters of Los Angeles. So far 11 stones have been cut, and the two largest ones weighed 57 and 28 ct. The cut material is being sold through Pala International (Fallbrook, California).

The samples shown in figure 12 were examined microscopically by this contributor. The few internal features were typical for kunzite: elongated, tapered etch tubes; and two-phase (liquid and gas) inclusions—either alone, in parallel, or in a “fingerprint” pattern with irregular to rounded elongate shapes. No mineral inclusions were seen. One faceted stone contained very slight cleavage feathers on the pavilion, while the rough piece showed typical shield-shaped etch marks on its surface.

Kunzite is challenging to cut because of its cleavage, twin planes, and sensitivity to vibrations and thermal shock. It also has a reputation as an “evening” gem, since its color fades with prolonged exposure to light or heat. Kunzite can naturally show an attractive color, as in this new find from the Elizabeth R mine, or the purple-pink hue can be produced by irradiating (and annealing) pale or colorless spodumene. Most natural-color kunzite is light pink. This new production from Pala serves as a reminder that gem mining is still active in San Diego County, where kunzite was initially discovered more than 100 years ago.

Michael Evans (mevans@gia.edu)
GIA, Carlsbad

Figure 10. Dense concentrations of parallel growth tubes were common in the pale yellow andesine from Inner Mongolia (left). In some samples, linear fissures (right) caused weak opalescence. Photomicrographs by A. Abduriyim; magnified 20 \times .





Figure 11. These kunzite crystals (up to ~4.3 cm long) were recovered in July 2008 from the Elizabeth R mine in San Diego County. Photo by Mark Mauthner.



Figure 12. A number of fine faceted samples have been polished from the new Elizabeth R kunzite find. The crystal weighs 11.5 g and the cut stones are 12.47–19.32 ct. Photo by Robert Weldon.

Natural pearls of the Veneridae family. The best-known natural pearls from bivalves of the Veneridae (classified by Rafinesque, 1815) family are those from *Mercenaria mercenaria* (Linnaeus, 1758), also known as “quahog” pearls from the mollusk’s common name, northern quahog. These non-nacreous pearls range from “cream” white to brown, and from faint pinkish purple to dark purple, though some are pure white (e.g., figure 13). Like other natural pearls, quahog pearls are seldom perfectly round; in rare cases, circled quahog pearls occur (figure 14). *M. mercenaria* bivalves are found along the Atlantic coast of North America to the Yucatan Peninsula. The species also has been introduced along California’s Pacific coast.

However, *M. mercenaria* is not the only mollusk of the *Mercenaria* genus to produce pearls. White, “cream,” and sometimes brown non-nacreous pearls can be found in another species belonging to the same genus, *M. campechiensis* (Gmelin, 1791), or southern quahog. This species is found in the southern part of the *M. mercenaria* distribution area. *M. campechiensis* is slightly larger than *M. mercenaria*, and its interior surface lacks purple coloration; thus, it cannot produce purple pearls.

Nor are *Mercenaria* bivalves the only mollusks of the

Veneridae family that can produce beautiful pearls. In the Fall 2001 GNI section (p. 233), one of these contributors (EF) described an almost perfectly round purple pearl found along the coast of France in a mollusk from the *Venerupis* genus (Lamarck, 1818), *V. affinis decussata* (Linnaeus, 1758). This mollusk (known as “palourde” in French) is commonly harvested for its meat, which is considered a delicacy.

The interiors of *M. mercenaria* and *V. aff. decussata* shells, as well as the pearls associated with them, are similar in appearance (figure 15). The purple color is present at the shell margins, mainly around the muscle scars. Both pearls and shells display the same medium chalky whitish yellow fluorescence to long- and short-wave UV radiation, though it is weaker for the *V. aff. decussata*.

Raman spectroscopy of the samples in figure 13 (left

Figure 13. These two photos illustrate natural “quahog” pearls from the *M. mercenaria* mollusk. The white button-shaped sample (left image, far left) is ~10.5 × 7.8 mm (8.17 ct), and the brown button-shaped pearl in the right image is ~9.3 × 7.5 mm (5.03 ct). Courtesy of P. Lançon, Geneva; photos by Thomas Notari.





Figure 14. Note in these four baroque quahog (*M. mercenaria*) pearls that color variation in the bicolored samples is distributed along the pearls' rotational axis. All are circled except the second sample from the left, but its ovoid shape is still probably due to pearl rotation during formation. The bicolored sample on the left is $\sim 13.2 \times 11.2$ mm (11.62 ct). Courtesy of P. Lançon, Geneva; photo by Thomas Notari.

image) and figure 14, using 488, 514, and 561 nm laser excitations, showed that the purple color was due to a mixture of unsubstituted polyenic (polyacetylenic) compounds (figure 16). To our knowledge, the origin of the purple color of Veneridae pearls and/or inner shells has not been previously reported. Similar pigments have been

Figure 16. These Raman spectra for a purple quahog (*M. mercenaria*) pearl were taken at laser excitations of 488, 514, and 561 nm. In the region most "sensitive" to C=C stretching bonds (about 1500 cm^{-1} , see inset), variations in the position, shape, and relative intensities of the peaks are quite apparent. This suggests that the purple color is due to a mixture of unsubstituted polyenic (polyacetylenic) compounds and not to a single pigment. Raman spectra on colored samples from *V. aff. decussata* showed the same peaks. All the peaks are normalized to the main aragonite peak at 1086 cm^{-1} . The spectra are offset vertically for clarity.

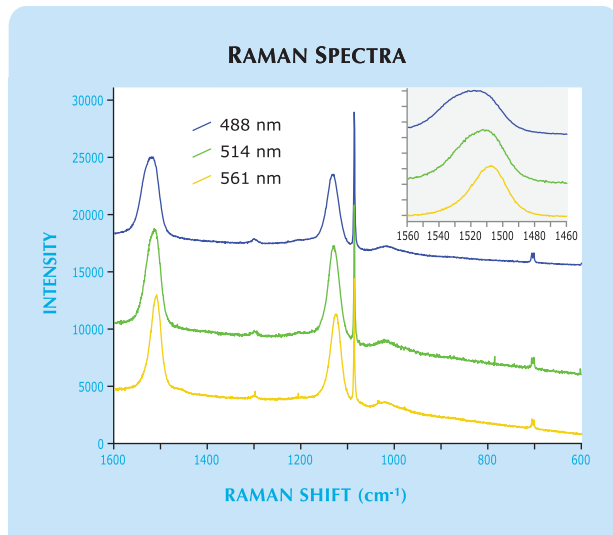


Figure 15. Though *V. aff. decussata* (inner shell, 4.5 cm) is found on the western coast of France and *M. mercenaria* (9.5 cm, courtesy of Antoinette Matlins, South Woodstock, Vermont) is found on the North American Atlantic coast, the two exhibit similar coloration. Photo by S. Karampelas.

observed in freshwater cultured pearls (S. Karampelas et al., "Identification of pigments in freshwater cultured pearls with Raman scattering," Fall 2006 *Gems & Gemology*, pp. 99–100).

M. mercenaria can reach 12 cm in diameter, while *V. aff. decussata* mollusks from the west coast of France do not exceed 7.5 cm. Thus, the latter mollusks produce smaller pearls (rarely up to 6 mm) compared to those from *M. mercenaria* (rarely up to 12 mm). It should be noted that "gem-quality" natural pearls from *V. aff. decussata* have been documented only once, whereas there have been numerous reports of gem-quality quahog pearls.

Stefanos Karampelas (s.karampelas@gubelingemlab.ch)
Department of Geology, University of Thessaloniki,
Greece;

Institut des Matériaux Jean Rouxel (IMN)
University of Nantes, France

Emmanuel Fritsch
Franck Notari

SYNTHETICS AND SIMULANTS

Synthetic citrine with abundant nail-head spicules. A necklace of transparent yellow faceted beads (figure 17) was sent to Gemlab for identification. Specular reflectance Fourier-transform infrared (FTIR) spectroscopy identified the material as quartz. FTIR spectra recorded in transmission mode were not definitive, but nevertheless were characteristic of synthetic citrine. The spectra contained an unusually intense water absorption centered at $\sim 3200\text{ cm}^{-1}$ (too strong to be resolved) and only a single sharp peak at 3580 cm^{-1} . In general, natural citrine has a much lower water content and shows more complex FTIR spectra.

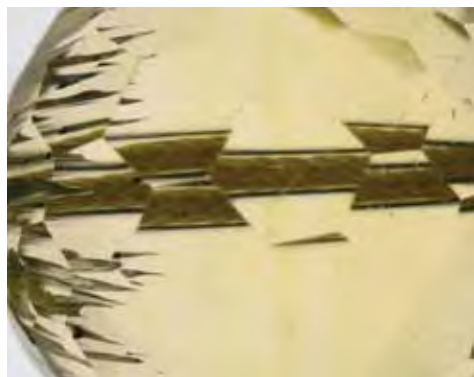


Figure 17. This necklace, submitted to the Gemlab Laboratory for identification, contained 49 faceted beads (~20 mm diameter) of what proved to be synthetic citrine. Photo by T. Hainschwang.

Microscopic examination revealed a most unusual inclusion scene: All of the beads were full of hollow growth channels (figure 18, left) and nail-head spicules (wedge-shaped, liquid-filled growth channels terminated by an inclusion on one end; figure 18, right). Nail-head spicules are characteristic inclusions in both synthetic beryl and synthetic quartz, though similar-looking inclusions have been described in some natural stones (G. Choudhary and C. Golecha, "A study of nail-head spicule inclusions in natural gemstones," Fall 2007 *Gems & Gemology*, pp. 228–235). Thus, isolated inclusions of this type do not necessarily offer proof of synthetic origin.

Nevertheless, the appearance of the nail-head spicules in these beads was typical for synthetic material, especially since the "heads" of the spicules contained "breadcrumb" inclusions (e.g., figure 19), the most characteristic and common inclusion in synthetic quartz. However, this contributor has never seen such a large number of these inclusions in any type of synthetic material. All of them

Figure 18. The inclusion scene in the beads consisted of hollow growth tubes (left) and nail-head spicules (right), which are often seen in synthetic quartz and beryl. Photomicrographs by T. Hainschwang; field of view is 18 mm (left) and 10.5 mm (right).



exhibited the typical wedge shape, and in most of them the liquid contained a gas bubble.

The inclusions, hollow cavities, and nail-head spicules were oriented parallel to the c-axis. In determining the optic axis direction, it was evident that none of the material was twinned—unlike most natural citrine, which is created by heat-treating natural amethyst that commonly contains Brazil-law twinning. The large, hollow cavities likely represent oversized nail-head spicules that were either exposed by the polishing process or reached the surface during the growth process. In some of these very large cavities, the breadcrumb inclusion was found at the narrow end of the channel (figure 20, left); in the others, it was absent (figure 20, right). These features, like the smaller nail-head spicules, can probably be attributed to rapid growth conditions.

The necklace, which had been sold to the client as natural quartz, was therefore identified as synthetic citrine. Despite this deception, the piece was a fantastic source of photomicrographs of nail-head spicules, which normally do not occur in such heavy concentrations.

Thomas Hainschwang

(thomas.hainschwang@gemlab.net)

Gemlab Laboratory for Gemstone Analysis and Reports

Balzers, Liechtenstein

Radiocarbon dating of "Neptunian" beads from Asia proves modern origin.

During the inaugural Macau Jewellery & Watch Fair in January 2008, this contributor purchased four baroque-shaped drilled beads of an unknown material that were sold as Neptunian beads. The brownish orange samples had white striae, and the brownish orange portions showed an appealing sheen (figure 21). When asked about their origin, the seller reported that the material was from fossilized conch shell found at an altitude of 5,000 m in the Himalaya Mountains. A brochure provided with the samples added that the beads had several medicinal uses.

In the laboratory, we found that the specific gravity of the beads was 2.78. Close examination showed that they had two folded layers, which is common for conch shell (figure 22). Raman spectroscopy identified the material (both the orange and white portions) as aragonite. EDXRF analysis

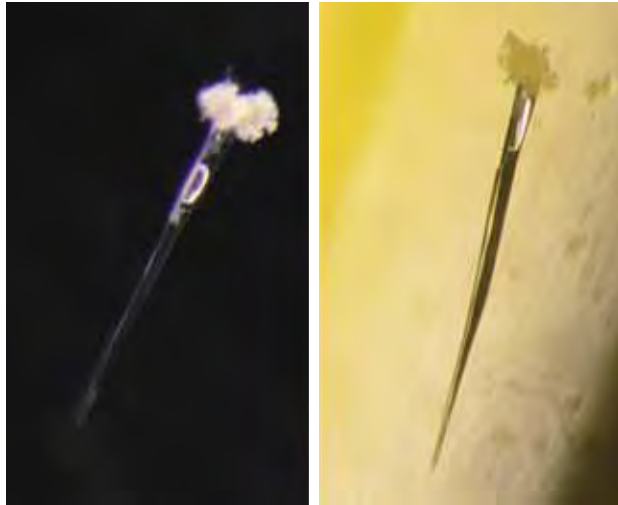


Figure 19. The nail-head spicules in the synthetic quartz beads, such as those shown here, consist of liquid-filled cavities that may contain a gas bubble and be terminated by a “breadcrumb” inclusion. Photomicrographs by T. Hainschwang; field of view is ~1 mm high for both.



Figure 20. Some of the surface-reaching hollow cavities in the synthetic citrine beads (e.g., as shown in figure 18) showed a breadcrumb inclusion at their narrow end (left) while others did not (right). Photomicrograph by T. Hainschwang; field of view is 5.4 mm high (left) and 4.1 mm high (right).

showed that Ca was the only major element, with traces of Sr present, as expected for aragonite from conch shell.

However, the material did not have the appearance of a fossil, so the author decided to apply a method rarely used in gemology: age determination by radioisotope. The Swiss Federal Institute of Technology (SFTT) in Zürich performed ^{14}C isotope measurement to calculate the age (radiocarbon dating can determine ages up to 30,000 years). To make the determination, the laboratory took 200 mg of powder from the drill hole of one of the beads.

A spectrum relating time with atmospheric radiocarbon content and the sample’s data is shown in figure 23. Because above-ground nuclear weapons testing in the 1950s substantially raised the concentration of ^{14}C in the atmosphere (and consequently in all living organisms), the testing produced two possible results (see P. J. Reimer et al., “Discussion: Reporting and calibration of post-bomb ^{14}C data,” *Radiocarbon*, Vol. 46, No. 3, 2004, pp. 1299–1304).

Figure 21. These baroque-shaped beads, marketed as fossilized Neptunian beads, proved to be recent shell material. The largest bead is ~17 mm long. Photo by H. A. Hänni, © SSEF.



The $^{12}\text{C}/^{14}\text{C}$ ratio of the sample intersected with the atmospheric ratio at 1957 and 1997. Clearly, the beads are far younger than the 35 million years claimed in the brochure.

Henry A. Hänni

Purplish blue synthetic quartz. Synthetic quartz has long been available in a wide range of colors, such as yellow, purple-violet, green, pink, colorless, parti-colored, and even blue. Recently, the Gem Testing Laboratory of Jaipur, India, had an opportunity to study a new and unusual “cobalt” blue synthetic quartz.

Figure 22. The beads consist of alternating layers of nacreous orange and non-nacreous white aragonite. Photo by H. A. Hänni, © SSEF; image width 16 mm.



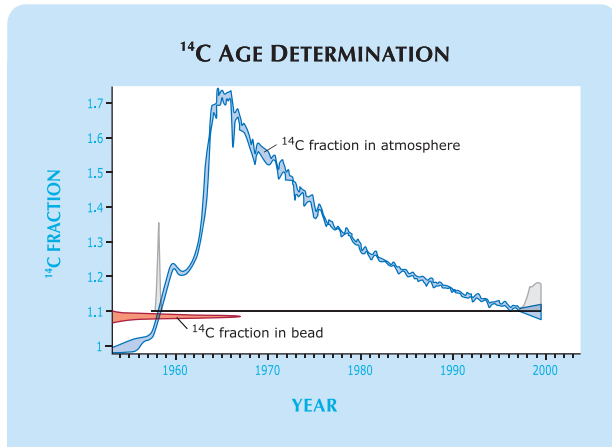


Figure 23. The ^{14}C distribution and the two maxima in gray indicate that the aragonite from a Neptunian bead originated in either 1957 or 1997. The Y-axis shows the $^{12}\text{C}/^{14}\text{C}$ ratio measured in the bead normalized to the $^{12}\text{C}/^{14}\text{C}$ ratio of the standard. Graph courtesy of G. Bonani and I. Hajdas, SFTT; © SSEF.

A purplish blue specimen weighing 73.08 g was submitted for identification. At first glance, the specimen appeared to be a cobalt glass because of its color (figure 24) and apparently frosted surface. However, we observed tiny circular growth features that were very similar to the “cobbled” surface seen in rough slabs of synthetic quartz. When the specimen was viewed from the side, a colorless zone with the appearance of a seed plate was evident, which led us to believe that the material was actually synthetic quartz.

The specimen displayed a clear anisotropic reaction when rotated in the polariscope, confirming that it was not

Figure 25. When the sample in figure 24 was viewed from the side, a seed plate was visible (white arrows) along with nailhead spicules that for the most part were restricted to the seed plate (red arrows). Also note the blue color zoning parallel to the seed; the diagonal features are surface-related optical effects. Photomicrograph by G. Choudhary; magnified 30 \times .

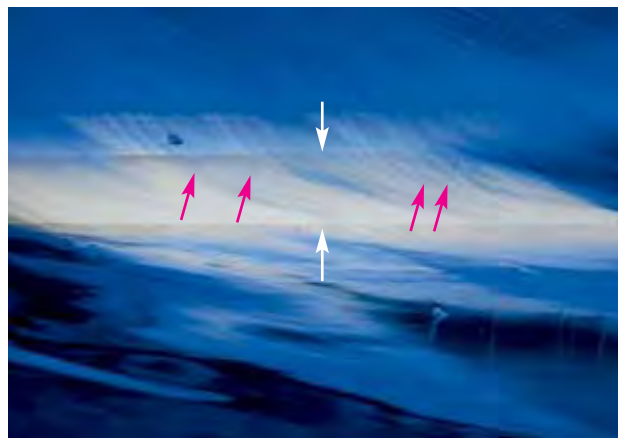


Figure 24. This bright “cobalt” blue specimen (73.08 g) proved to be synthetic quartz. Note the “cobbled” surface with circular growth patterns. Photo by G. Choudhary.

glass. A bull’s-eye optic figure—as expected for quartz—could not be resolved, due to the rough surfaces. With the desk-model spectroscope, however, we observed three strong bands in the green, yellow, and orange regions; this absorption pattern is typical of cobalt. The sample had a strong red reaction to the Chelsea filter, and was inert to long- and short-wave UV radiation.

Examination with magnification confirmed the presence of a seed plate. Also seen was color zoning parallel to the seed plate, as well as nail-head spicules along its length (figure 25). An interesting aspect was the location/orientation of the spicules. In general, nail-head spicules are oriented in one direction pointing away from the seed

Figure 26. At higher magnification, the spicules in the seed plate appeared to be oriented in different directions. The central colorless seed plate is separated from the synthetic quartz overgrowth by sharp planes on either side (see arrows). Photomicrograph by G. Choudhary; magnified 65 \times .





Figure 27. This 45.78 ct cabochon resembling chrysocolla proved to be dyed chalcedony. Photo by N. Ahmed, © Dubai Gemstone Laboratory.



Figure 28. Microscopic examination of the dyed chalcedony shows a greenish blue dye concentrated in fractures and cavities. Photomicrograph by N. Ahmed, © Dubai Gemstone Laboratory; magnified 20 \times .

plate, on both sides of the synthetic overgrowth. In this case, however, most of the spicules appeared to be in the seed plate rather than in the overgrowth material. At some viewing angles, the spicules appeared to be oriented in different directions (figure 26).

While the influx of interesting colors of synthetic quartz has given jewelers more options, proper disclosure remains essential.

Gagan Choudhary

TREATMENTS

Dyed chalcedony resembling chrysocolla. Historically, chalcedony has been dyed in a wide variety of colors, often to simulate various other gem materials. Recently, the Dubai Gemstone Laboratory received for identification a 45.78 ct greenish blue cabochon with areas of orangy brown (figure 27). At first glance, the semitranslucent-to-opaque stone resembled chrysocolla. An SG of 2.29 (determined hydrostatically) and a vague RI reading around 1.5 supported this initial impression (R. Webster, *Gems*, 5th ed., revised by P. G. Read, Butterworth-Heinemann, Oxford, UK, 1994, pp. 326–327). The stone did not exhibit strong reactions to long- or short-wave UV radiation, only a weak, patchy bluish green fluorescence to long-wave UV. The stone's Chelsea filter reaction was pinkish red.

Examination with magnification (up to 68 \times) did not reveal the minute chrysocolla inclusions present in chrysocolla chalcedony, although such inclusions are typically too small to see with a gemological microscope. However, microscopic examination did reveal that the

surface-reaching fractures and cavities had concentrations of a greenish blue dye (figure 28), which could be removed with acetone.

Colorless-to-milky chalcedony can easily be dyed with inorganic cobalt or copper salts to simulate chrysocolla (see A. Shen et al., "Identification of dyed chrysocolla chalcedony," Fall 2006 *Gems & Gemology*, p. 140). However, because of the stone's opacity, we did not obtain the characteristic absorption lines of chalcedony dyed with cobalt, and we were unable to perform UV-Vis-NIR spectroscopy to compare our data with those of Shen et al.

Nevertheless, all of these properties pointed to dyed chrysocolla or dyed chalcedony. Raman analysis is unable to differentiate between chrysocolla and chalcedony. However, EDXRF spectroscopy showed a major amount of Si and only traces of Fe, identifying the material as chalcedony. By contrast, chrysocolla is a hydrous copper silicate $[(\text{Cu,Al})_2\text{H}_2\text{Si}_2\text{O}_5(\text{OH})_4 \cdot n\text{H}_2\text{O}]$, and no Cu was detected in the sample. Therefore, the client was informed that the cabochon consisted of dyed chalcedony.

Nazar Ahmed (nanezar@dm.gov.ae)

Dubai Gemstone Laboratory
Dubai, United Arab Emirates

ANNOUNCEMENTS

Starting with this issue, the conference and exhibit calendars will only appear online at www.gia.edu/gemsandgemology. Please refer to this online resource for regular updates to these calendars.

For online access to GEMS & GEMOLOGY, visit:

gia.metapress.com

BOOK REVIEWS/GEMOLOGICAL ABSTRACTS 2008 ANNUAL INDEX

Beginning with this issue, the Book Reviews and Gemological Abstracts sections will be available only in electronic (PDF) format. These sections will be available free of charge both on the *G&G* web site (www.gia.edu/gemsandgemology) and as part of *G&G* Online (gia.metapress.com), and will be paginated separately from the rest of the issue. The year-end Index has also been moved online and is available on the *G&G* web site in the Indexes section.

These sections are also included in this full-issue PDF. Accordingly, the Table of Contents included in this file lists these additional sections, and thus differs from the Table of Contents in the print version. For these reasons, this PDF is *not* the official version of this issue—the “journal of record” for this issue is the combined print/online version that was released to subscribers. This full-issue PDF file is created for archival purposes in order to maintain continuity with previous issues.

BOOK REVIEWS

EDITORS

Susan B. Johnson
Jana E. Miyahira-Smith
Thomas W. Overton

Photoatlas of Inclusions in Gemstones, Volume 3

By E. J. Gübelin and J. I. Koivula, 672 pp., illus., publ. by Opinio Publishers, Basel, Switzerland [<http://publications.microworldofgems.com>], 2008. US\$299.00

Gemology now has its gemstone inclusion bible: the three-volume *Photoatlas of Inclusions in Gemstones*. Culminating 35 years of groundbreaking research, Volume 3 is the final “gem” in Dr. Edward J. Gübelin and John I. Koivula’s monumental achievement. The three books together are intended to be the most comprehensive visual reference library of gemstone inclusions available. Like the previous two volumes, this one is abundantly illustrated with high-quality photomicrographs that brim with information, clarity, and beauty.

The book is divided into three major parts. The first includes a preface by gemologist Edward Boehm, Dr. Gübelin’s grandson, and an introduction to using the *Photoatlas* library. The heart of the book is its second section, “Inclusions in Major Commercial Gems,” which deals with diamond, ruby, sapphire, and emerald. Each of these four chapters summarizes the different geologic processes that form or transport the gem, and the inclusions that characteristically result. As in Volume 2, the host material is clearly indicated in large type at the top of each page (e.g., “Inclusions in Sapphires”).

The section begins with diamond. Mineral inclusions in natural diamonds—peridotitic, eclogitic, and

deep-mantle—are discussed and well illustrated. The detailed examination of internal strain and “graining” patterns provides clues to distinguishing natural, treated, and synthetic diamonds. Inclusions in synthetic diamonds grown under high-pressure, high-temperature conditions are discussed and well illustrated (though not those grown by chemical vapor deposition), as are inclusions resulting from the full range of diamond treatments. The chapter concludes with identification of the main diamond substitutes: cubic zirconia and synthetic moissanite.

The ruby, sapphire, and emerald chapters cover inclusions in natural stones from all major localities. The authors often specify the particular mining region from which the inclusions originated and discuss the typical inclusions associated with the various modes of occurrence. Characteristic inclusions are organized according to genetic type. This is very valuable information, particularly for those who are interested in geographic origin. Also discussed are known treatments for each gem material and the inclusions that can identify them, as well as known synthesis methods and the characteristic inclusions they generate. Simulants such as assembled stones, synthetic overgrowths on natural stones, and glass are also discussed.

In the third section, “Inclusions in Rare and Unusual Gems,” 21 different gems—including axinite, benitoite, cordierite, danburite, ekanite, enstatite, fluorite, gypsum, pezzottaite, sapphirine, and taaffeite—are described and strikingly illustrated.

This section ends with a useful glossary and index.

Pioneered by the late Dr. Gübelin nearly 70 years ago, the study of internal features in gemstones, along with our current understanding of how and where certain minerals formed in the earth, enables gemologists to infer a great deal of information by simply viewing inclusions with magnification. By referring to the book’s exceptional photomicrographs, the experienced and diligent user of Volume 3 will frequently be able to ascertain the identity of individual inclusions and, in many cases, establish whether the stone is natural or synthetic. If the ruby, emerald, or sapphire is natural, the user may be able to determine the probable geographic origin and detect indications of treatment. The extensive further-reading list in each chapter provides easy access to additional information and photomicrographs. The scope of localities, treatments, and synthetics represented makes this book extraordinarily valuable to the gemologist, jeweler, and gem collector.

Admirers of beautiful art books will certainly appreciate all three of these volumes. The astute salesperson will also find occasions to use these photomicrographs to illustrate the unique beauty of inclusions in gems they are offering to a client.

With a total of 2,033 pages and more than 5,300 exquisite photomicrographs, the three-volume *Photoatlas* is the most remarkable achievement in the history of gemological literature. This reviewer cannot imagine that any serious gemologist would want to be without it, and

this volume in particular is highly recommended—it is an essential reference for anyone involved in the identification, research, or appraisal of diamonds, rubies, sapphires, and emeralds.

ROBERT E. KANE
Fine Gems International
Helena, Montana

Bulgari

By Amanda Triossi and Daniela Mascetti, 2nd ed. (revised and updated by Amanda Triossi), 320 pp., illus., publ. by Abbeville Press, New York [www.abbeville.com], 2007. US\$75.00

From their humble beginnings as traveling silversmiths in 19th-century Greece, the Bulgari family became a dynasty of internationally acclaimed fine jewelers. Dedication to excellence in design, materials, and fabrication vaulted the company to the iconic status it enjoys today. Patronized by royalty and the power elite, Bulgari is an Old World company that has remained on the cutting edge of fashion.

In 1996, Daniela Mascetti and Amanda Triossi coauthored the first edition of *Bulgari* (reviewed in the Winter 1998 *Gems & Gemology*, p. 303), in which they described the growth of this contemporary jewelry giant. Recently, Ms. Triossi gave the book an extensive revision. In this second edition, the visual design has been refined, the text has been updated, and more than 120 images have been added, including many press photos of the rich and famous wearing Bulgari jewelry.

In some chapters, there is little or no change from the first edition. Others—most notably “History of Bulgari,” “Evolution of the Bulgari Style,” and “Colour and Fabulous Gemstones”—have been updated to reflect changes in the family and their business structure, in new designs, and in the use of gemstones. The chapters on watches and perfumes

have also been expanded significantly, and a new chapter on accessories was added to show Bulgari’s further diversification during the 1990s into ties, scarves, leather goods, and eyeglasses.

Also useful would have been a timeline showing when the various jewelry styles and luxury items were introduced to the Bulgari product lines. An alphabetized glossary of the unique Bulgari styles—*tubogas*, *parentesi*, *pippoli*, *celtaura*, *gourmette*, and *B.zero1*, to name a few—would also have been very welcome. These are minor criticisms, however, when the book as a whole is considered. Overall, Ms. Triossi has done a superb job of revising the first edition to reflect the significant changes in the style and range of luxury products this remarkable company has undergone over the last decade, making this an important addition to the literature of jewelry history.

ELISE B. MISIOROWSKI
Leucadia, California

Guidebook to the Pegmatites of Western Australia

By Mark Ivan Jacobson, Mark Andrew Calderwood, and Benjamin Alexander Grguric, 356 pp., illus., publ. by Hesperian Press [www.hesperianpress.com], Victoria Park, Australia, 2007. US\$85.00

While the pegmatite districts of Western Australia and their mineral assemblages are known to many, information about them—particularly their locations—has been sketchy at best. Most were worked in the early 20th century, and some locales hadn’t been visited for decades. Because of the importance of these pegmatites to scientists and collectors, and a renewed interest in the industrial minerals they contain, the authors produced this field guidebook.

The bulk of this work is a listing of the many pegmatite districts and pegmatite-containing geologic areas of Western Australia. A major achievement of the book is the loca-

tion data, including detailed directions to the pegmatites and mines, as most of the previous literature offered only approximate locations. (The authors make it clear that their provision of directions to a given locality does not guarantee permission to visit. In some cases, they were unable to get permission themselves.)

Guidebook is a handsome hard-bound volume printed on high-quality paper. It contains 103 black-and-white photos and 76 maps. The introduction covers the history, mineralogy, classification, and mineral assemblages of these pegmatites. An immensely useful listing of the 120 minerals found in Western Australian pegmatites is provided. It includes not only the minerals but also their location(s), with some indicated as type localities. The following 10 chapters cover individual deposits within the major districts or geologic areas. Some of these locations are well known and have yielded significant commercial production (the Wodgina pegmatite field and the Greenbushes pegmatites, for instance). Others have provided mineral specimens for the collectors’ market (including emerald from the Poona pegmatite field and ferrocolumbite from the Giles columbite-beryl prospect in Spargoville). For each locality, be it a small prospect pit or a major operation, the authors provide an introduction and location data (some with GPS coordinates), as well as the history, geology, and mineralogy of the deposit. There are useful indexes for names, localities, and mineral species, plus an extensive reference list.

While the average gemologist might not have an urgent need for this book, pegmatologists and mineral collectors will find it invaluable. The fact that Western Australia’s pegmatites are not miarolitic (i.e., they do not have significant open pockets for freestanding crystals to form) has prevented them from achieving the kind of fame that the Pala District pegmatites of California enjoy. Nevertheless, collectible mineral specimens and some gems have been produced, and renewed interest will

likely lead to the discovery of more in the future.

MICHAEL EVANS
*Gemological Institute of America
Carlsbad, California*

OTHER BOOKS RECEIVED

Crazy About Jewelry! The Expert Guide to Buying, Selling and Caring for Your Jewelry. By Susan Eisen, 245 pp., illus., publ. by Full Circle International Publishing [www.crazyaboutjewelry.net], El Paso, TX, 2007. US\$16.95. This is the book you want your customers to read. Susan Eisen's enthusiasm for jewelry shines through her fun and functional work. There are a lot of good prac-

tical suggestions here, and though some in the industry might think her advice is simply common sense—such as not packing jewelry in your suitcase when you travel—I've heard of jewelry being lost in this manner countless times. Other chapters include "Redesigning Your Jewelry," "Medical Identification," "Cleaning It the Right Way," and "Knowing Your Jeweler." Ms. Eisen succeeds in relaying her advice in a casual, user-friendly manner, and the true-life stories from her career are both interesting and entertaining. Many of us will relate to her experiences, and the illustrations are colorful and attractive.

JANA E. MIYAHIRA-SMITH
*Gemological Institute of America
Carlsbad, California*

ERRATA

Two book reviews in the Fall 2008 issue, of *Amazonite: Mineralogy, Crystal Chemistry, Typomorphic Features and Infrared Reflection Spectrometry in Advanced Mineralogy, Gemology and Archaeometry*, both by Mikhail N. Ostrooumov, inadvertently misspelled the author's last name. In addition, the amazonite book was published by Polytechnics, St. Petersburg, not Nedra, Moscow.

Because of an oversight, Jared Nadler of Birmingham, Alabama, was omitted from the list of 2008 Challenge Winners in the Fall issue.

Gems & Gemology regrets the errors.



We've joined the revolution.

The *Online* revolution.

The Loupe, GIA's news magazine and your source for Institute and industry news, has joined the shift to online-only publishing. You'll love our new, easy-to-read format.

Make sure you don't miss a single issue. Log on to <http://LoupeOnline.gia.edu/subscribe> and enter your e-mail address. We'll send you a link to our latest edition.



GEMOLOGICAL ABSTRACTS

EDITORS

Brendan M. Laurs
Thomas W. Overton
GIA, Carlsbad

REVIEW BOARD

Edward R. Blomgren
Owl's Head, New York

Jo Ellen Cole
Vista, California

Sally Eaton-Magaña
GIA, Carlsbad

Eric A. Fritz
Denver, Colorado

R. A. Howie
Royal Holloway, University of London

Edward Johnson
GIA, London

Paul Johnson
GIA Laboratory, New York

David M. Kondo
GIA Laboratory, New York

Kyaw Soe Moe
West Melbourne, Florida

Keith A. Mychaluk
Calgary, Alberta

Francine Payette
East Victoria Park, Western Australia

James E. Shigley
GIA Research, Carlsbad

Boris M. Shmakin
Russian Academy of Sciences, Irkutsk, Russia

Russell Shor
GIA, Carlsbad

Elise Skalwold
Ithaca, New York

Jennifer Stone-Sundberg
Portland, Oregon

Rolf Tatje
Duisburg, Germany

COLORED STONES AND ORGANIC MATERIALS

Crystallization of biogenic Ca-carbonate within organo-mineral micro-domains. Structure of the calcite prisms of the pelecypod *Pinctada margaritifera* (Mollusca) at the sub-micron to nanometre ranges. A. Baronnet, J. P. Cuif [jean-pierre.cuif@u-psud.fr], Y. Dauphin, B. Farre, and J. Nouet, *Mineralogical Magazine*, Vol. 72, No. 2, 2008, pp. 617–626.

Atomic force microscopy (AFM) and transmission electron microscopy (TEM) were used to investigate the fine structure of calcite prisms in *Pinctada margaritifera* shell. AFM showed that the prisms were made of closely packed circular micro-domains (in the 0.1 μm range) surrounded by a dense cortex. TEM images and diffraction patterns revealed the internal structure of the micro-domains, each of which was enriched in calcium carbonate. Hosted in distinct regions of each prism, some of these domains were fully amorphous while others were fully crystallized as subunits of a larger calcite crystal. At the border separating the two regions, the micro-domains displayed a crystallized core and an amorphous rim, probably representing an arrested crystallization front. Compared to recent data concerning the stepping mode of growth of the calcite prisms and the resulting layered organization at the micron scale, these results offer unexpected insight into the modalities of biocrystallization. RAH

Emerald deposits and occurrences: A review. L. A. Groat [lgroat@eos.ubc.ca], G. Giuliani, D. D. Marshall, and D. Turner, *Ore Geology Reviews*, Vol. 34, No. 1/2, 2008, pp. 87–112.

This section is designed to provide as complete a record as practical of the recent literature on gems and gemology. Articles are selected for abstracting solely at the discretion of the section editors and their abstractors, and space limitations may require that we include only those articles that we feel will be of greatest interest to our readership.

Requests for reprints of articles abstracted must be addressed to the author or publisher of the original material.

The abstractor of each article is identified by his or her initials at the end of each abstract. Guest abstractors are identified by their full names. Opinions expressed in an abstract belong to the abstractor and in no way reflect the position of Gems & Gemology or GIA.

© 2008 Gemological Institute of America

Emerald is rare because unusual geologic and geochemical conditions are required to bring together sufficient amounts of Be (to make beryl) with Cr and/or V (the coloring agents). This article reviews the major emerald deposits of the world and presents chemical composition data for samples from each deposit.

In the classic model, Be-bearing pegmatites interact with Cr-bearing ultramafic or mafic rocks to form emeralds. In Colombian and certain other deposits, however, emeralds result from regional or tectonothermal metamorphic processes without magmatic activity. Various schemes have been proposed to classify emerald deposits, but not all have been useful in clarifying the actual conditions of emerald formation. Recent studies have demonstrated that emeralds crystallized under conditions where a combination of geologic mechanisms (magmatic, hydrothermal, and metamorphic) brought Be in contact with Cr and/or V in the right geologic setting.

In the field, emerald can be recognized by its color, hardness, and form, but it will not concentrate in heavy mineral fractions because of its relatively low SG. Exploration for emerald deposits is typically based on structural geology considerations and geochemical studies of soils and stream sediments in a target area. *JES*

The formation of precious opal: Clues from the opalization of bone. B. Pewkliang, A. Pring [pring.allan@saugov.sa.gov.au], and J. Brugger, *Canadian Mineralogist*, Vol. 46, No. 1, 2008, pp. 139–149.

The composition and microstructure of opalized saurian (Plesiosaur) bones from Andamooka, South Australia, were compared to saurian bones that were partially replaced by magnesian calcite from the same geologic formation, north of Coober Pedy, South Australia. The opalized bones were essentially pure SiO₂ (88.59–92.69 wt.%), with minor Al₂O₃ (2.02–4.04 wt.%) and H₂O (3.36–4.23 wt.%). No traces of biogenic apatite remained after opalization. During the formation of the opal, the coarser details of the bone microstructure were preserved down to the level of the individual osteons (~100 μm), but the central canals and boundary area were enlarged and filled with chalcedony, which postdates opal formation. The chemical and microstructural features are consistent with opalization occurring as a secondary replacement after partial replacement of the bone by magnesian calcite, and also with the opal forming first as a gel in the small cavities left by the osteons, with individual opal spheres growing as they settled within the gel. Changes in the viscosity of the gel provide a ready explanation for the occurrence of color and patch banding in opals. The indication that opalization is a secondary process after calcification in the Australian opal fields is consistent with a Tertiary age of formation. *RAH*

Nouvelles des travaux sur le béryllium et les saphirs bleus
[News on beryllium and blue sapphire research]. V.

Pardieu and L. Klemm, *Revue de Gemmologie*, No. 163, 2008, pp. 7–9 [in French].

The authors first give a brief history of the beryllium diffusion treatment of corundum. The presence of Be in *untreated* sapphire was first reported by P. Wathanakul and colleagues at the 2004 International Gemmological Conference, in a trapiche sapphire from Houay Xai in Laos. In mid-2006, F. Claverie and coauthors detected Be in untreated blue sapphires from Ilakaka, Madagascar. Twenty-eight blue sapphires obtained at the Ilakaka mines by one of the present authors were analyzed at the Gübelin Gem Lab, and 12 contained Be in local concentrations of 1–20 ppm. Complementary analyses at other labs (in Bangkok, Berne, and Lucerne) confirmed the findings.

Beryllium in untreated blue sapphires seems to be concentrated in comet-tail inclusions. These cloud-like inclusions also contained some Nb, W, Sn, and Ta. A correlation between these elements and Be could be useful for separating Be-diffused blue sapphire from untreated blue sapphire containing beryllium. The data might also serve as a chemical fingerprint for origin determination. *Guy Lalous*

Perlenzucht mit *Pinctada maxima* in Südost-Asien—ein Beispiel [Pearl culturing with *Pinctada maxima* in Southeast Asia—An example]. H. A. Hänni [gemlab@ssef.ch], *Gemmologie: Zeitschrift der Deutschen Gemmologischen Gesellschaft*, Vol. 56, No. 3–4, 2007, pp. 83–95 [in German].

This article describes modern pearl farming with *Pinctada maxima* oysters in Southeast Asia, using as examples two pearl farms in Bali and Irian Jaya. The oysters are cultured from fertilized eggs derived from carefully selected donor oysters. Hygienic standards are closely controlled during the entire growth process. These and other measures resulted in a good yield of high-quality pearls. After harvest, the oysters are not re-seeded; the meat is used for seafood and the shells for their nacre. The cultured pearls are processed, quality graded, and marketed in Australia. *RT*

Thortveitite: A new gemstone. R. Chapman [ross@gemsofaus.com.au], I. F. Mercer, A. H. Rankin, and J. Spratt, *Journal of Gemmology*, Vol. 31, No. 1/2, 2008, pp. 1–6.

A purple waterworn pebble of unknown origin was acquired in Bangkok in 2004, and it was cut into a strongly pleochroic, biaxial gemstone weighing 10.01 ct. It was identified as thortveitite (confirmed by Raman analysis), a scandium yttrium silicate that was previously unknown in gem quality.

Electron microprobe analysis revealed significantly higher concentrations of Sc and lower concentrations of Y than were reported in the literature for nongem thortveitite, which is normally opaque to translucent and found only as very small crystals. The unusual chemical composition suggested a possible synthetic origin, though the presence of three-phase inclusions in a planar array

indicated otherwise. Unlike quenched flux or melt inclusions, these features were composed of a gas bubble, brine, and cubic daughter crystal suspected to be halite; this suggested formation in a hydrothermal environment. The inclusions showed signs of exposure to heat, either in nature or in the laboratory. ES

Vaterit in Süßwasser-Zuchtperlen aus China und Japan [Vaterite in freshwater cultured pearls from China and Japan]. U. Wehrmeister [wehrmeis@uni-mainz.de], D. E. Jacobi, A. L. Soldati, T. Häger, and W. Hofmeister, *Gemmologie: Zeitschrift der Deutschen Gemmologischen Gesellschaft*, Vol. 56, No. 3–4, 2007, pp. 97–116 [in German].

Chinese and Japanese freshwater cultured pearls (beaded and non-beaded) were analyzed by Raman spectroscopy and LA-ICP-MS. The results showed that they consisted only of aragonite and vaterite, with no calcite. For the most part, the vaterite was concentrated near the center of the cultured pearls; less commonly, it occurred in small blemishes on the surface. Continuous growth structures transected both the aragonite and the vaterite areas. Low concentrations of Na and Sr were found in the vaterite, as well as relatively enriched Mg values, which allowed its distinction from aragonite by LA-ICP-MS.

The authors concluded that vaterite is a common phase in freshwater cultured pearls from China and Japan, and that it tends to concentrate near their centers. It was found in cultured pearls of high quality, as well as in lack-luster samples. RT

DIAMONDS

Kimberlite-hosted diamond deposits of southern Africa: A review. M. Field [matthew-field@btconnect.com], J. Stiefenhofer, J. Robey, and S. Kurszlaukis, *Ore Geology Reviews*, Vol. 34, No. 1/2, 2008, pp. 33–75.

This article reviews a century of scientific study of kimberlites in southern Africa and the diamonds and mantle-derived rocks they contain, which has increased our understanding of geologic processes and the conditions of diamond crystallization in the subcontinental lithosphere. The formation of kimberlite-hosted diamond deposits involves a lengthy and complex series of events, beginning with the growth of the diamonds in the mantle, followed by their removal and transport to the surface by kimberlite magmas. Age dating of mineral inclusions indicates diamond growth occurred several times during the earth's geologic history. Older diamonds—of Archean age—are mainly peridotitic, whereas younger diamonds originated from eclogitic, websteritic, or lherzolitic rocks, and their formation periods correspond in age with major tectono-thermal events in southern Africa.

Only about 1% of the kimberlite bodies discovered in southern Africa have been commercially exploited for dia-

monds, but among them are some of the world's richest mineral deposits. The bulk of this article is a review of 34 diamond mines in the region, including summaries of their geology and characteristics of their diamonds and mantle-derived rocks. The mines vary greatly in size, diamond grade, and value, as well as in their mantle-derived mineral suites. All the deposits are hosted by the Kalahari Craton, indicating that it provided the right environment for diamond growth and subsequent transport to the surface by kimberlite magmas. JES

Magnetic inclusions in diamonds. B. M. Clement [clementb@fiu.edu], S. Haggerty, and J. Harris, *Earth and Planetary Science Letters*, Vol. 267, No. 1/2, 2008, pp. 333–340.

Natural diamonds sometimes contain dark inclusions that are often described as being graphite or a sulfide mineral. In this study, the authors examined 11 near-colorless, slightly rounded octahedral diamond crystals (2–4 mm) with dark eye-visible inclusions (believed to be a sulfide) for possible remnant magnetism. All the samples were from the Orapa mine in Botswana. The dark inclusions were found to be single or multiple metallic black and opaque fracture systems, each of which contained a tiny grain (20–50 μm) of pyrrhotite. When released by crushing of the diamond, these tiny grains appeared “dirty-yellow.” Pyrrhotite has a greater differential expansion than diamond, and its presence caused the localized fracturing of the host crystal. The black material within the fractures had the same chemical composition as the associated inclusion. The shape and orientation of the pyrrhotite inclusions indicate that they formed at the same time as the host diamond. They were found to be capable of carrying strong and stable remnant magnetization.

These results suggest that with the availability of suitable samples, it may be possible to obtain information about the earth's geomagnetic field during key intervals of geologic time. Furthermore, specific details of the remnant magnetism would allow individual diamonds with pyrrhotite inclusions to be uniquely identified, even in cases where the inclusions are quite small (i.e., only a few microns in diameter). JES

Nanometre-sized mineral and fluid inclusions in cloudy Siberian diamonds: New insights on diamond formation. A. M. Logvinova [logv@nigmm.nsc.ru], R. Wirth, E. N. Fedorova, and N. V. Sobolev, *European Journal of Mineralogy*, Vol. 20, No. 3, 2008, pp. 317–331.

Nanometer-size isolated inclusions were studied in four cloudy octahedral diamonds from the Internationalaya pipe and one from the Jubileynaya mine, both in Yakutia. TEM, AEM, EELS, and HREM analyses of the samples were conducted, as well as line-scan and elemental mapping. All the crystals exhibited an octahedral habit with

opaque central cuboid cores that contained numerous nano-inclusions (30–800 nm). They were composed of multiphase assemblages that included silicates, oxides, carbonates, brines (KCl), and fluid bubbles. Distinguishable crystalline phases included a high-Mg silicate, dolomite, Ba-Sr carbonate, phlogopite, ilmenite, ferropericlase, apatite, magnetite, K-Fe sulfide (possibly djerfisherite), and kyanite. Carbonates identified by TEM from all the diamonds studied showed a general enrichment in incompatible elements such as Sr and Ba. Some elemental variations in the crystalline phases may be explained by fractional crystallization of the fluid/melt or the mixing of fluids with different compositions.

RAH

Using phosphorescence as a fingerprint for the Hope and other blue diamonds. S. Eaton-Magaña [sally.magana@gia.edu], J. E. Post, P. J. Heaney, J. Freitas, P. Klein, R. Walters, and J. E. Butler, *Geology*, Vol. 36, No. 1, 2008, pp. 83–86.

Little quantitative research exists on the phosphorescence properties of natural blue diamonds. This study used broadband UV radiation and a novel spectrometer system to examine the luminescence of 67 natural blue diamonds, including stones from the Aurora Butterfly and Aurora Heart collections, as well as the 45.52 ct Hope and the 30.62 ct Blue Heart.

The red phosphorescence of the Hope Diamond was once believed to be quite rare. This study showed that virtually all natural blue diamonds have red phosphorescence, however, the color is often masked by a concomitant luminescence in the green-blue region of the spectrum. Sixty-two of the 67 samples exhibited two phosphorescence peaks—at orange-red (~660 nm) and green-blue (~500 nm wavelengths). Significantly, the study demonstrated that because these two bands are nearly always present, the relative intensity of emissions and their decay kinetics (i.e., the ratio of peak intensities plotted against the half-life of the 660 nm peak) yields a unique “fingerprint” for each specimen. Phosphorescence analysis therefore provides a robust method to discriminate among individual blue diamonds using a relatively inexpensive, portable desktop spectrometer.

The authors also examined three blue synthetic diamonds and an HPHT-annealed gray-turned-blue natural diamond. All four exhibited the phosphorescence band at 500 nm but not the one at 660 nm, which suggests that phosphorescence spectroscopy might be an effective tool for discerning synthetic and HPHT-treated diamonds from natural blues.

Although the authors acknowledge there is insufficient evidence to completely describe the defect states, impurities, or energy-transfer mechanisms of phosphorescence, their findings suggest that the same donor-acceptor pair recombination mechanism is active in both natural and synthetic blue diamonds.

ERB

GEM LOCALITIES

Advances in our understanding of the gem corundum deposits of the West Pacific continental margins intraplate basaltic fields. I. Graham [i.graham@unsw.edu.au], L. Sutherland, K. Zaw, V. Nechaev, and A. Khanchuk, *Ore Geology Reviews*, Vol. 34, No. 1/2, 2008, pp. 200–215.

The continental margins of the western Pacific contain the world’s largest and richest deposits of gem ruby and sapphire. These deposits are genetically related to Late Mesozoic to Late Cenozoic basaltic volcanism, and today they are spread over a distance of more than 12,000 km, extending from Russia (Siberia) to Australia (Tasmania). The gem corundum consists of xenocrysts of magmatic and/or metamorphic origin trapped in the host basalt. The corundum is mined from placer deposits formed by weathering of the basalt.

Corundum suites from each origin type have distinctive trace-element geochemistry, mineral inclusions, crystallization ages, and formation conditions. Magmatic corundum appears to have crystallized under upper-mantle to mid-crustal pressure-temperature conditions (~700–1200°C), from melts of syenitic to nepheline syenitic composition. In contrast, the metamorphic corundum appears to have formed at slightly higher temperatures (~800–1300°C) and at depths ranging from the mantle to the lower crust. The conditions of corundum formation at the major deposits within the western Pacific continental margins are discussed.

JES

Afghan beryl varieties. L. Natkaniec-Nowak [natkan@uci.agh.edu.pl], *Journal of Gemmology*, Vol. 31, No. 1/2, 2008, pp. 31–39.

The author presents an in-depth characterization of three specimens of Afghan beryl from pegmatites at Ghursalak in Konar Province (aquamarine and morganite) and from the Panjshir Valley (emerald). INAA, XRD, ICP-AES, ICP-MS, and IR spectroscopic techniques were used to examine the beryls, and the results are summarized in accompanying tables. IR spectroscopy of the aquamarine and emerald indicated the presence of organic matter, probably bituminous material within structural channels. The author notes that while Afghanistan has not been a major gem producer for the world market, many important gems have been known from the region since Egyptian, Greek, and Roman times. Production is growing, and examples of fine material have appeared in markets worldwide.

ES

Age and origin of gem corundum and zircon megacrysts from the Mercaderes–Rio Mayo area, south-west Colombia, South America. F. L. Sutherland [lin.sutherland@austmus.gov.au], J. M. Duroc-Danner, and S. Meffre, *Ore Geology Reviews*, Vol. 34, No. 1/2, 2008, pp. 155–168.

Alluvial gem corundum has been known for several centuries from the Rio Mayo area of southwestern Colombia. Samples recovered from this area (some near colorless but most multicolored, 99% of them sapphire) exhibit features such as color zoning, polysynthetic twinning, and healed fractures, as well as various mineral inclusions (rutile, apatite, zircon, some plagioclase, and occasional allanite, which appears to be an inclusion unique to this locality). U-Pb dating of the zircon, allanite, and apatite inclusions suggested the corundum crystallized approximately 10 million years ago, placing the formation in the Miocene epoch. Corundum formation appears to be related to geologic events associated with the uplift of the northern portion of the Andes Mountains and accompanying volcanism. The article provides chemical composition data for both the corundum and the important mineral inclusions. *JES*

Black opaque gem minerals associated with corundum in the alluvial deposits of Thailand. S. Saminpanya [seriwat@hotmail.com] and F. L. Sutherland, *Australian Gemmologist*, Vol. 23, No. 2, 2008, pp. 242–253.

Black opaque spinel, pyroxene, and magnetite occur in gravels associated with corundum in the alluvial deposits of Denchai and Bo Phloi, Thailand. Raman spectra and XRD patterns have been used to unravel some of the misnomers surrounding these materials in the gem markets. The black spinel lies in the spinel-hercynite series, the black pyroxene is mostly augite, and the magnetite lies in the magnetite-ulvöspinel series. The details of their chemical composition suggest that these minerals did not originate in the same environment as the corundum or the basaltic host rocks. *RAH*

Gem corundum deposits of Madagascar: A review. A. F. M. Rakotondrazafy, G. Giuliani [giuliani@crpg.cnrs-nancy.fr], D. Ohnenstetter, A. E. Fallick, S. Rakotosamizanany, A. Andriamamonjy, T. Ralantoarison, M. Razanatsheho, Y. Offant, V. Garnier, H. Maluski, C. Dunaigre, D. Schwarz, and V. Ratrimo, *Ore Geology Reviews*, Vol. 34, No. 1/2, 2008, pp. 134–154.

Gem corundum is found at a number of localities in Madagascar, primarily in the central and eastern portions of this island nation. Ruby and sapphire formed at different stages and in distinct environments. The authors describe four main geologic settings:

1. primary deposits in magmatic rocks such as syenites, granites, and alkali basalts
2. primary deposits in metamorphic rocks such as granulites
3. primary deposits that resulted from alkaline metasomatism due to fluid circulation occurring along discontinuities in gneisses and granulites

4. secondary deposits derived from the erosion of surrounding rocks

The article provides an excellent review of the major ruby and sapphire deposits of Madagascar, including their geologic setting and age, host rocks, typical mineral assemblages, and inferred conditions of formation. *JES*

Greenish quartz from the Thunder Bay Amethyst Mine Panorama, Thunder Bay, Ontario, Canada. L. B. Hebert [labaker@gps.caltech.edu] and G. R. Rossman, *Canadian Mineralogist*, Vol. 46, No. 1, 2008, pp. 111–124.

The Thunder Bay Amethyst Mine Panorama is a major amethyst deposit on the western shore of Lake Superior in southern Ontario. Although most of the quartz is amethystine, loose pieces of yellowish green and green quartz have been found, and greenish gray quartz occurs *in situ* as part of a color-gradation sequence that includes colorless and smoky quartz along with chalcedony. Analysis of samples of all these colors show corresponding trends in the salinity and temperature of the quartz-forming hydrothermal solutions. The greenish material exhibits greater turbidity and more numerous fluid inclusions than the amethyst. Furthermore, differences in crystal growth rates also appear to have influenced the color of the quartz.

The authors conclude that the greenish gray coloration is not from the secondary heating of preexisting amethyst, but rather is another distinct radiation-induced color variety of quartz. This color resulted from specific chemical constituents in the hydrothermal solutions, the conditions of natural radiation exposure, and the incorporation of molecular water in the quartz, both as nano-scale and micro- to macro-scale fluid inclusions. The greenish gray material appears to have formed during the initial stages of mineralization, and these solutions underwent a decrease in salinity and quartz growth rate during quartz precipitation. *JES*

Opal-C, opal-CT, & opal-T from Acari, Peru. F. Caucia [caucia@crystal.uniipv.it], C. Ghisoli, I. Adamo, and M. Boiocchi, *Australian Gemmologist*, Vol. 23, No. 2, 2008, pp. 266–271.

Optical features, SG and XRD data, and IR spectroscopic features are described for 25 translucent-to-opaque volcanic opals from the Acari region of Peru. The XRD and IR results correspond with opal-C and opal-CT, with some samples being pure tridymite (i.e., opal-T). Opals displaying various colors and transparencies were classified according to their luster, and the relationship between luster and the presence of phyllosilicate phases within the opals was assessed. Andean opals with a vitreous but dull porcelain-like luster were opal-C and opal-CT that were free of phyllosilicates. *RAH*

Les pegmatites à beryl de la région d'Ambazac, Haute-Vienne [Beryl-bearing pegmatites from Ambazac, Haute-Vienne]. J. Patureau, *Revue de Gemmologie*, No. 164, 2008, pp. 12–16 [in French].

The massif of Haute-Vienne (north of Limoges, in the French Massif Central) consists of three types of leucogranite. The Saint Sylvestre leucogranite is the youngest (320 million years) and forms the Ambazac Mountains. This unit hosts numerous potassic pegmatites along with some sodalithic pegmatites. The potassic pegmatites are typically lenticular and are composed of K-feldspar, biotite, muscovite, and quartz, with apatite and beryl as accessory minerals. In the 19th and early 20th centuries, the pegmatites were actively exploited for K-feldspar (used in the porcelain industry of Limoges), piezoelectric smoky quartz crystals, and—most recently—uranium. Some gem-quality beryl was recovered, including goshenite, aquamarine, and heliodor. Of these, golden yellow to green-yellow heliodor has been the most abundant in recent decades. A few gemstones, including a 6.65 ct golden beryl, have been faceted from these finds. *FP*

INSTRUMENTS AND TECHNIQUES

Accelerating refractive rendering of transparent objects.

K. C. Hui [kchui@acae.cuhk.edu.hk], A. H. C. Lee, and Y. H. Lai, *Computer Graphics Forum*, Vol. 26, 2007, No. 1, pp. 24–33.

Ray tracing may be used to create photorealistic computer images of transparent gemstones and other objects. However, this technique requires a great deal of computation and is inherently slow. The authors propose a technique for the interactive rendering of transparent objects using a refractive rendering algorithm. There are two stages in the algorithm: pre-computation and shading. In the pre-computation stage, a ray-tracing process tailored to gemstone rendering is performed. A database is constructed for the storage of information such as the ray directions and the positions of the corresponding image points. In the next stage, these data are retrieved from the database for the shading of the transparent object, taking illumination into consideration. The time required for the pre-computation process is proportional to the number of polygons (p) composing the model, the image size (number of pixels, s), and the number of internal reflections (r). The performance of the shading process is determined by the light obstruction test and the illumination calculation, with a time complexity of p^2 and sr , respectively. Experimental results show that refractive rendering is significantly faster than ordinary ray-tracing techniques. *Dennis Zwigart*

Clarification of measurement of the RIs of biaxial gemstones on the refractometer. B. D. Sturman [darkos@rogers.com], *Journal of Gemmology*, Vol. 30, No. 7/8, 2007, pp. 434–442.

The author describes three rules for refractometer observations of biaxial gemstones that, if followed correctly, allow one to determine optic character and sign by simply recognizing observed patterns (without the need to construct graphs of RI measurements). All four possible biaxial patterns are discussed, and diagrams illustrate the behavior of gem materials on the refractometer based on calculated movements of shadow edges for different orientations of the optical elements and the facet being measured. The author notes that although one biaxial pattern is quite common and requires use of a polarizing filter to determine true beta, the other three are rare and may only show up at all because gem cutters sometimes use a large crystal face for the gemstone's table. *ES*

Determination of the optic axial angle in biaxial gemstones and its use in gemmology. B. D. Sturman [darkos@rogers.com], *Journal of Gemmology*, Vol. 30, No. 7/8, 2007, pp. 443–452.

Of the many concepts from optical mineralogy that have been applied to gemology, one that is little known is the use of optic axis angle to identify biaxial gemstones. This is especially helpful for differentiating between biaxial gemstones with similar or overlapping RIs (e.g., peridot vs. sinhalite). It can also distinguish between a uniaxial gem and a biaxial gem that has one optic axis oriented perpendicular to the table, which produces one variable and one constant shadow edge during rotation on a refractometer (e.g., tourmaline vs. actinolite). Along with background explanation, the author gives detailed examples and diagrams. Determination of the optic axis angle requires the same data needed to determine the optic sign, but the optic axis angle is a much more discriminatory constant for use in the identification of biaxial gemstones. *ES*

SYNTHETICS AND SIMULANTS

Gemmologische Kurzinformationen: Imitation für Feuerachat [Gemmological brief notes: Imitation of fire agate]. U. Henn [ulihenn@dgemg.com], *Gemmologie: Zeitschrift der Deutschen Gemmologischen Gesellschaft*, Vol. 56, No. 3–4, 2007, pp. 127–129 [in German].

Attractive beads sold as fire agate were proved to be heat-treated chalcedony (agate). The heating causes surface cracking that is somewhat reminiscent of fire agate, but the beads showed none of the surface iridescence or botryoidal structure that are typical of true fire agate. *RT*

Innovative composites 'Fusion.' G. Choudhary, *Gems & Jewellery*, Vol. 17, No. 2, 2008, pp. 20–22.

The author reports on some interesting gem assemblages, eye-catching composites marketed as "Fusion." The gems have concave pavilion facets, which improves their bril-

liance and overall appearance. Combinations include citrine and amethyst imitating ametrine, and topaz and amethyst resembling tanzanite. The composites vary from three to five pieces, giving an impression of multicolored stones.

Identification of these composites is straightforward. The presence of junction planes, which appear as sharp separations between the layers, is diagnostic. Spherical or flattened gas bubbles, dendritic flow patterns, and iridescence may all be present along the junction planes. In addition, the glues may fluoresce chalky blue to white under short-wave UV.

Guy Lalous

'Paraíba' tourmaline and similar looking materials. G. Choudhary and C. Golecha, *Gems & Jewellery*, Vol. 17, No. 1, 2008, pp. 16–18.

Paraíba tourmaline simulants are becoming more common in the marketplace. Materials such as apatite and glass have been joined by cubic zirconia and hydrothermal synthetic beryl; production of the latter two has reached a commercial scale. Short descriptions of these four simulants are presented, and their gemological properties are compared in a table. The authors describe a glass simulant with swirled color zoning, which at first glance displayed pleochroism reminiscent of that seen in tourmaline. All four simulants are easily separated from tourmaline through standard gemological testing.

ES

Single-crystal polarised-light FTIR study of an historical synthetic water-poor emerald. F. Bellatreccia, G. Della Ventura [dellaven@uniroma3.it], M. Piccinini, and O. Grubessi, *Neues Jahrbuch für Mineralogie Abhandlungen*, Vol. 185, No. 1, 2008, pp. 11–16.

Reexamination of a synthetic emerald grown in the late 19th century using a flux method showed its composition to be nearly stoichiometric and homogeneous except for significant variations in chromium (1.45–2.59 wt.% Cr₂O₃). Trace amounts of Ti, Mg, Fe, Zn, Na, K, and F were also noted. Despite the flux growth method, FTIR spectra in the OH-stretching region showed the presence of weak but significant H₂O vibrations. The polarized FTIR spectra collected with E_⊥c consisted of a sharp, intense band at 3463 cm⁻¹, whereas the E_∥c spectra consisted of two minor bands at 3643 and 3587 cm⁻¹. These bands were assigned to the ν₃ antisymmetric stretching and ν₁ symmetric stretching modes of type II water in the structural channels. These water molecules were probably associated with Li impurities in the mineral from the flux used for the synthesis. Using the molar absorption coefficient, the authors derived a water content of ~30 ppm.

RAH

TREATMENTS

Copper diffusion treatment of andesine and new mine of Tibet. *Gem Information*, Japan Germany Gemmological Laboratory, Vol. 37–38, 2008, pp. 1–8 [in

Japanese, abstracted from English translation].

Chinese andesine has attracted considerable attention due to rumors that an unknown treatment can reproduce the red color seen in some natural material. EDXRF data were collected for samples of pale yellow rough andesine before and after three stages of an unspecified treatment process performed in Thailand. These samples showed increasing CuO levels and deeper diffusion of red color with each stage of treatment. After the third stage, copper levels reached those recorded for andesine from the market.

Two pieces of pale yellow Mongolian rough underwent treatment (also unspecified) in China. Viewed in immersion, they showed less color at their surface and more color internally than the Thai-treated stones. The red color, when magnified, consisted of tiny reddish orange spots. Copper concentrations measured in these samples were also similar to those of andesine available in the market.

A new andesine deposit in a rugged mountainous area of Tibet was also described. Hand mining by locals during the summer has yielded stones with natural red and green hues, most of them <1 ct when cut. More information is needed to distinguish untreated Tibetan andesine from the treated stones.

ERB

Pearl treatments: How pearls, natural and cultured, are treated to enhance them, and how to detect the treatments. S. Kennedy, *Organic Gems*, No. 7, 2008, www.maggiecp.co.uk/subs/OG7%20Jan%2008/Pearl_Treatments.htm.

The article gives an overview of the primary pearl treatments encountered in the market. Most involve color enhancement, such as the use of silver nitrate staining to darken a pearl's appearance. The author also describes the filling of internal hollows in large pearls to enhance their weight. Both filling and silver nitrate staining are detectable by X-radiography. The author notes that some enhancements are still difficult to detect, such as yellow treated South Sea cultured pearls. Some practical knowledge of certain characteristics indicating treatment is provided. Two examples are the high likelihood of treatment in a matched string of brown Tahitian cultured pearls, and the fact that black is not a natural color for cultured pearls from freshwater mussels.

Annette Buckley

Surface treatment of gemstones, especially topaz: An update of recent patent literature. K. Schmetzer [schmetzerkarl@hotmail.com], *Journal of Gemmology*, Vol. 31, No. 1/2, 2008, pp. 7–13.

Following up on his 2006 *Journal of Gemmology* paper (covering the period 1996–2005), the author updates a list of patents pertaining to the surface treatment of gem materials. Although it is not known if any of the reported technologies have already been implemented, the author warns that that at least some will probably be applied in the future. Two types of surface treatment are identified and discussed: (1) processes not involving heat treatment

(i.e., coatings of wear-resistant material, coatings that cause an optical phenomenon, and coatings that form a diffractive optical element), and (2) processes involving heat treatment (i.e., heat treatment while in contact with a plate containing transition metals, and heat treatment following deposition of a coating). ES

MISCELLANEOUS

Development of an object-oriented classification model using very high resolution satellite imagery for monitoring diamond mining activity. E. Pagot [elodie.pagot@rc.it], M. Pesaresi, D. Buda, and D. Ehrlich, *International Journal of Remote Sensing*, Vol. 29, No. 2, 2008, pp. 499–512.

Satellite imagery has become a valuable tool in diamond exploration. This article details the development of a methodology for monitoring diamond mining activity from very high resolution satellite images using a multi-criteria “fuzzy” classification system. Previous investigations were based on medium-resolution sensors (e.g., Landsat TM data). In this study, two sets of satellite remote-sensing data were acquired four months apart and then processed using a “fuzzy sets” procedure. (“Fuzzy sets” are those in which elements have *degrees* of membership, rather than either belonging or not belonging to the set.) The authors discuss in detail the data-processing flow—image preprocessing methodology (geometric and radiometric corrections); image processing using multi-resolution segmentation and supervised fuzzy logic classification software; and the classification scheme that would eventually provide the object maps and statistics to assess the status of mining activity in the imaged areas (e.g., increasing, decreasing, or stable mining activity).

Of interest in one African diamond-producing zone was a large mechanized mine and small artisanal “hand-dug” sites that only required light manpower and equipment. The identification parameters for the mines (e.g., average size, aerial geometric shape, distance from rivers, water-clarity status, and excavation materials) were operationalized and became part of multi-temporal data sets.

The multi-criteria method showed an overall accuracy of 91% based on comparison with image datasets from standard manual photo interpretation. The authors conclude that the object-oriented interpretation model developed in the study proved successful in monitoring the level of diamond mining activity.

The advantages of using such image analysis include the wealth of additional information that can be derived from image objects, its robustness, its success in monitoring the level of diamond mining activity in inaccessible areas, and the complementing of maps with qualitative and quantitative information on mining activity for both small artisanal and large mechanized mines. ERB

Making diamonds work for development: An overview of initiatives. K. Hund, July 2008, www.madisondialogue.org/Hund_SRK_MadisonDialogue_v6_dbled.pdf.

There has been a proliferation of initiatives aimed at producing truly “clean,” “fair,” or “ethical” gold, diamonds, and other minerals, so that these resources can better contribute to sustainable development in the local communities where they are mined. These initiatives have been instigated and/or sustained by various stakeholders in the diamond business, as well as by governments, donors, NGOs, and other organizations. This paper analyzes nine initiatives designed to improve the lives of artisanal diamond miners and small-scale diamond cutters in various parts of Africa. Some have had better results than others, and the successes and failures are identified to provide lessons for the future.

Two initiatives in the Democratic Republic of the Congo are briefly described, though the report acknowledges that much more is happening there (e.g., diamond-oriented efforts by Congolese civil society organizations working on the social and environmental impacts of mining and forestry). The report also examines two company-led diamond fair trade initiatives: one by Finesse Diamonds, a U.S.-based De Beers shareholder, and the other by Target Resources, a London-based gold and diamond miner. Many other fair trade initiatives focusing on gems and gold offer lessons to be learned, but are beyond the scope of this paper.

A brief overview is provided of attempts by individual retailers worldwide to sell only diamonds that are ethically sourced. Many choose the safe option of Canadian stones, or even synthetic diamonds, yet these do not contribute to the development of diamond-producing countries in Africa.

Setting goals for standards and establishing guidelines is critical to establishing trust in fair trade principles. Seven organizations that are attempting to do so are analyzed. An overview of charity initiatives is given, many of which are using diamond industry profits to fund African development projects. As such, there is a difference between “diamond charity” and “development diamonds.” The report concludes with eight issues for discussion: the lack of clarity as to what constitutes an “ethical diamond,” the urgent need for monitoring, the difficulty of achieving overall aims, the ongoing lack of information exchange, the inability of many charities to address root problems, the need to collaborate, the fact that too many initiatives are top-down rather than bottom-up, and the failure to recognize existing internal structures that might be most effective.

The author provides a list of socially responsible diamond retailers and designers, as well as references and websites. An overview matrix of the different initiatives and what they aim to achieve is also included. EJ

Index

Volume 44

Numbers 1-4

SUBJECT INDEX

This index gives the first author (in parentheses), issue, and inclusive pages of the article in which the subject occurs for all feature articles, Notes & New Techniques, and Rapid Communications that appeared in Volume 44 of *Gems & Gemology*. For the Gem News International (GNI) and Lab Notes (LN) sections, inclusive pages are given for the item. The Winter 2008 Book Reviews section is available only as an online supplement, beginning with page S1. The Author Index (p. S18) provides the full title and coauthors (if any) of the articles cited.

A

Afghanistan

- afghanite and haüyne from Badakhshan (GNI)Sp08:79-80
- spodumene from (GNI)F08:277-279
- tourmaline and simulants purchased in Kandahar (GNI)Su08:187-188

Afghanite

- from Afghanistan (GNI)Sp08:79-80

Agate

- dendritic, from India (GNI)F08:262-263

Almandine, see Garnet

American Gem Society

- and color grading of D-to-Z diamonds (King)W08:296-321

Andesine

- from Tibet and Inner Mongolia—mining of (GNI)W08:369-371; properties of (GNI)W08:371-373

Aquamarine

- inclusions in (GNI)F08:275-276; (LN)Sp08:66
- separation from Maxixe-type and hydrothermal synthetic blue beryl (Adamo)F08:214-226
- trapiche (GNI)F08:275-276

Asterism

- in topaz from Brazil (GNI)Su08:182-183

Auctions

- of the Wittelsbach Blue diamond (Dröschel)W08:348-363

B

Ballerina Pearl Co., see Pearl, cultured

Beryl

- Maxixe-type (Adamo)F08:214-226
- orange, from India (GNI)Su08:167
- see also Aquamarine, Emerald

Beryl, synthetic

- hydrothermal blue (Adamo)F08:214-226

Bleaching

- of cultured pearls—to create “chocolate” color (Du Toit)F08:234-241; to create non-“chocolate” colors (LN)Su08:159-160

Book reviews

- Amazonite: Mineralogy, Crystal Chemistry, Typomorphic Features* (Ostrooumov, Platonov, and Popov)F08:286
- American Mineral Treasures* (Staebler and Wilson, Eds.)F08:284
- Bulgari* (Triossi and Mascetti)W08:S2
- Crazy About Jewelry! The Expert Guide to Buying, Selling and Caring for Your Jewelry* (Eisen)W08:S3
- The Diamond Handbook: A Practical Guide to Diamond Evaluation*, 2nd ed. (Newman)F08:284-285
- Diamond Ring Buying Guide*, 7th ed. (Newman)Su08:194
- Diamonds Are Waiting for You* (Holland)Sp08:99
- The Emerald Book* (Durlabhji, Fernandes, and Durlabhji, Eds.)Sp08:97-98
- Fleischer's Glossary of Mineral Species 2008* (Back and Mandarino)F08:286
- Gems & Minerals* (Landmann)F08:285-286
- Gems of the World* (Oldershaw)F08:285-286
- Gemstones: Enchanting Gifts of Nature* (Karanth)F08:286
- In Gold We Trust: Social Capital and Economic Change in the Italian Jewelry Towns* (Gaggio)Sp08:98-99
- Guidebook to the Pegmatites of Western Australia* (Jacobson, Calderwood, and Grguric)W08:S2
- Henry Dunay: A Precious Life* (Proddow and Fasel)Su08:192-193
- Infrared Reflection Spectrometry in Advanced Mineralogy, Gemology and Archaeometry* (Ostrooumov)F08:286
- Jewelry Savvy: What Every Jewelry Wearer Should Know* (Sliwa and Stanley)Sp08:98
- Laboratory Grown Diamonds*, 2nd ed. (Deljanin and Simic)Su08:194
- Late Antique and Early Christian Gems* (Jeffery Spier)Sp08:99
- Photoatlas of Inclusions in Gemstones, Volume 3* (Gübelin and Koivula)W08:S1

Rings: Jewelry of Power, Love and Loyalty (Scarbrick)Sp08:97

Russian Gemstones Encyclopedia (Bukanov)Su08:193

Safety Solutions (MJSAPress)Sp08:99

Southwestern Indian Jewelry: Crafting New Traditions (Cirillo)F08:286

Tables of Gemstone Identification (Dedeyne and Quintens)Su08:194

Traditional Jewelry of India (Untracht)F08:286

Verdura: The Life and Work of a Master Jeweler (Corbett)Su08:194

Volodarsk-Volynski: Mineralogy of the Volynian Chamber Pegmatites, Ukraine (Pavlishin and Dovgyi)Su08:193-194

Brazil

- star and cat's-eye topaz from (GNI)Su08:182-183

Brown, Grahame

- obituary (GNI)Sp08:94

Burma, see Myanmar

C

Calcareous concretions, see Pearl, non-nacreous

Calcite

- inclusions in grossular (LN)F08:259

California, see United States

Cathodoluminescence

- to identify yellow synthetic diamond melee (Kitawaki)F08:202-213

Chalcedony

- dyed to resemble chrysocola (GNI)W08:379

“Challenge,” see *Gems & Gemology*

Chatoyancy

- in lawsonite from California (GNI)Su08:171
- in peridot from a pallasitic meteorite (GNI)Su08:177
- in topaz from Brazil (GNI)Su08:182-183

Chemical composition

- of blue beryl, natural and synthetic (Adamo)F08:214-226
- of emerald from Norway

(Rondeau)Su08:108-122
of johachidolite from Myanmar
(Chadwick)F08:246-251
of ruby and sapphire from Tanzania
(Schwarz)W08:322-347
of tourmaline—copper contaminated
(LN)W08:367-368; from Mozambique
(GNI)F08:273-275; Paraiba-type
(Lauris)Sp08:4-31
see also Spectroscopy [various]; specific
gem materials

Chemical vapor deposition [CVD], see
Diamond, synthetic

China

Andesine-labradorite—red, possibly dif-
fusion treated (GNI)Su08:166-167;
from Tibet and Inner Mongolia
(GNI)W08:369-373

“Chocolate pearls,” see Pearl, cultured

Chrysocolla, see Chalcedony

Citrine, see Quartz

Clam pearl, see Pearl, non-nacreous

Clinochlore

chromium-rich (kämmererite), from
Turkey (GNI)Su08:168-169

Coating

of diamond, history of
(Overton)Sp08:32-55
and diffusion treatment of topaz
(Gabasch)Su08:148-154
of engraved black pearls
(GNI)Su08:174-175
of tanzanite (McClure)Su08:142-155

Colombia

emerald crystal in quartz from La Pita
(LN)F08:258
nomenclature for emeralds from
(Ringsrud)F08:242-245

Color, cause of

in diamonds, purple, from Siberia
(Titkov)Sp08:56-64
in emerald from Norway
(Rondeau)Su08:108-122
in feldspar-quartz-muscovite rock
(GNI)F08:266-267
in johachidolite from Myanmar
(Chadwick)F08:246-251
in Paraiba-type tourmaline
(Lauris)Sp08:4-31

Color change

in fluorite (GNI)F08:263
in sapphire with lead-glass filling
(GNI)Sp08:88

Color grading, see Diamond, color grading
of D-to-Z

Color zoning

in diamonds, purple, from Siberia
(Titkov)Sp08:56-64
in Paraiba-type tourmaline from
Mozambique (Lauris)Sp08:4-31
in ruby and sapphire from Tanzania
(GNI)F08:270-272;
(Schwarz)W08:322-347
in synthetic melee diamonds, yellow
(Kitawaki)F08:202-213

Colorimeter

use of, in color grading of D-to-Z dia-

monds (King)W08:296-321

Computer software

used in modeling of the Koh-i-Noor dia-
mond (Sucher)Su08:124-141

Conch pearl, see Pearl, non-nacreous

Conference reports

Gemological LA-ICP-MS User Group
(GNI)Sp08:90-91
International Pearl Convention
(GNI)Sp08:91-92
Scottish Gemmological Association
(GNI)Su08:188-189
Sinkankas Garnet Symposium
(GNI)Su08:188
Winter Conference on Plasma
Spectrochemistry 2008 (GNI)Sp08:90

Coral

and plastic composite (LN)F08:253

Corundum, see Ruby; Sapphire

Crookes, Sir William

and diamond irradiation
(Overton)Sp08:32-55

Cubic zirconia

used in modeling of the Koh-i-Noor dia-
mond (Sucher)Su08:124-141

Cultured pearl, see Pearl, cultured

**CVD [chemical vapor deposition]-grown
synthetic diamonds**, see Diamond,
synthetic

D

Danburite

yellow, from Tanzania (GNI)Su08:169-
171

Deepdene diamond

irradiation of (Overton)Sp08:32-55

Diamolite, see Instruments

Diamond

burned surface pattern on (LN)F08:256
color grading of D-to-Z (King)W08:296-
321
crystal with mixed growth
(GNI)Sp08:74-75
from Myanmar, new localities
(GNI)Sp08:82
type IIa, with strong phosphorescence
(GNI)Su08:164-165

Diamond, colored

black (LN)F08:254-255
brown-yellow, type-zoned (LN)F08:364-
365
brownish-greenish-yellow with dissolu-
tion features (LN)Sp08:66-67
orange, with 594 nm feature
(LN)Su08:156-157
pinkish brown (LN)F08:257-258
purple, from Siberia (Titkov)Sp08:56-64
reddish orange type Ib (LN)F08:255-256
Wittelsbach Blue (Dröschel)W08:348-
363
see also Deepdene diamond; Diamond,
synthetic; Diamond treatment

Diamond, inclusions in

bird-like feature (GNI)Su08:164
crystal formation resembling flying

saucer (LN)Su08:157-158
dissolution and growth features visible
with DiamondView (LN)Sp08:66-67
hydrogen cloud—in black diamond
(LN)F08:254-255; with mask pattern
(LN)F08:257
mantle suite, in pinkish brown
(LN)F08:257-258
olivine with cleavage fracture
(LN)F08:256
in yellow synthetic melee
(Kitawaki)F08:202-213

Diamond, synthetic

CVD—experimental, from LIMHP
(GNI)Su08:185-186; first sample sub-
mitted for GIA grading (LN)Sp08:67-
69; HPHT-treated sample submitted
for Dossier grading (LN)W08:365-
367; with traces of boron
(LN)Su08:158-159
melee, yellow—identification of
(Kitawaki)F08:202-213; in the mar-
ketplace (Keller)F08:201

Diamond treatment

glass filled, with subtle flash-effect col-
ors (LN)Su08:157
history of (Overton)Sp08:32-55
HPHT, of CVD synthetic
(LN)W08:365-367
irradiation produces color concentra-
tions (LN)F08:254-255
see also Diamond, synthetic

DiamondDock, see Instruments

DiamondLite, see Instruments

DiamondView instrument

and CVD synthetic diamond
(LN)Sp08:67-69, Su08:158-159,
W08:365-367
dissolution and growth features in dia-
mond revealed with (LN)Sp08:66-67
indicates two black diamonds cut from
the same crystal (LN)Fa08:254-255
and mixed-type IIa/IIb fancy-color dia-
mond (LN)W08:364-365
reveals strong phosphorescence in col-
orless diamond (GNI)Su08:164-165

Diffusion treatment

indication in “red andesine” from
China (GNI)Su08:166-167
and the surface coloration of topaz
(Gabasch)Su08:148-154

Diopside

inclusions—in rose quartz
(GNI)F08:276-277; in scapolite
(GNI)F08:277

Durability

of treated “chocolate” and natural
black Tahitian cultured pearls (Du
Toit)F08:234-241

Dyeing

of chalcedony to resemble chrysocolla
(GNI)W08:379

E

Editorials

“Challenges, Changes, and New

Directions" (Keller)W08:295
"A New Gemological Challenge:
Synthetic Diamond Melee"
(Keller)F08:201
"Ten Reasons Why You Should Attend
the 2009 GRC" (Keller)Su08:107
EDXRF, see Spectroscopy, energy-
dispersive X-ray fluorescence
Electron microprobe analysis, see
Chemical composition
"Elephant pearl," see Pearl, non-nacreous

Emerald

from Byrud, Norway
(Rondeau)Su08:108-122
filled voids in (LN)Sp08:69-70
gota de aceite and nomenclature of
Colombian (Ringsrud)F08:242-245
inclusion in quartz crystal (LN)F08:258
from North Carolina (GNI)Sp08:75-76

Enhancement, see Coating; Diamond treat-
ment; Dyeing; Heat treatment;
Treatment; specific gem materials

Errata

to list of 2008 *Gems & Gemology*
Challenge winners (F08:203)—
include Jared Nadler (W08:S3)
to "Sapphire with a double star"
(LN)W07:365—name of client omit-
ted (LN)Sp08:73
to two book reviews, *Amazonite . . .*
(Ostrooumov, Platonov, and
Popov)F08:286 and *Infrared*
Reflection Spectrometry . . .
(Ostrooumov) F08:286—author name
misspelled Oustoumov (W08:S3)

F

Faceting

of the Koh-i-Noor diamond
(Sucher)Su08:124-141
large number of facets on topaz
(GNI)Sp08:85-86

Fakes, see specific gem materials simulated

Feldspar

andesine-labradorite—from China, pos-
sibly diffusion treated (GNI)Su08:
166-167; from Tibet and Inner
Mongolia (GNI)W08:369-373
sodic plagioclase—blue-green, colored
by copper (LN)Su08:160-161; from
Tanzania and Kenya (GNI)Sp08:83-85
see also Rock

Filling, fracture or cavity

in diamond—history of
(Overton)Sp08:32-55; produces subtle
flash-effect colors (LN)Su08:157
in emerald and ruby (LN)Sp08:69-70
lead-glass, in color-change sapphire
(GNI)Sp08:88

Fluorescence, ultraviolet [UV]

of D-to-Z diamonds, impact on color
grading (King)W08:296-321
of johachidolite from Myanmar
(Chadwick)F08:246-251
see also DiamondView instrument;

specific gem materials

Fluorite

color-change, mistaken for garnet
(GNI)F08:263

Forsterite

colorless—from Myanmar
(GNI)F08:263-265; from Tajikistan
(GNI)F08:265-266

Fossils

"Neptunian" conch shell beads, repre-
sented as (GNI)W08:376-377

G

Garnet

almandine-spessartine from Tanzania
(GNI)Su08:165-166
color-change fluorite imitation of
(GNI)F08:263
see also Grossular; Spessartine

Gemological Research Conference 2009

postponement of (Keller)W08:295
reasons to attend (Keller)Su08:107

Gems & Gemology

"Challenge"—Sp08:95-96; winners and
answers F08:283
Edward J. Gübelin Most Valuable
Article Award Sp08:1-2
receives journalism and publishing
awards (GNI)F08:281

Geographic origin

of Paraíba-type tourmaline from
Mozambique (Laur)Sp08:4-31
of rubies and sapphires from Winza,
Tanzania (Schwarz)W08:322-347

GIA (Gemological Institute of America)

Laboratory

color grading of D-to-Z diamonds at
(King)W08:296-321

Glass

devitrified, inclusions in (LN)Sp08:70-
71
as filling in color-change sapphire
(GNI)Sp08:88-89
as filling in diamond, history of
(Overton)Sp08:32-55
imitation of rubellite (GNI)186-187
Libyan desert, archeological artifact
resembling (GNI)Su08:181-182

Gota de aceite, see Emerald

Grading reports, see Diamond

Graining

in diamond—(LN)Sp08:66-67; whitish,
effect on color grading
(King)W08:296-321
in synthetic diamond, CVD
(LN)Su08:158-159

Great Mogul diamond

compared to the Koh-i-Noor
(Sucher)Su08:124-141

Grossular

with calcite "melt" inclusion identified
by Raman (LN)F08:259

Growth structures

in corundum from Winza, Tanzania

(Schwarz)W08:322-347
dissolution and growth features in dia-
mond (LN)Sp08:66-67
see also DiamondView instrument

H

Haiyune

from Afghanistan (GNI)Sp08:79-80

Heat treatment

of Paraíba-type tourmaline from
Mozambique (Laur)Sp08:4-31
of ruby and sapphire from Tanzania
(Schwarz)W08:322-347
of synthetic sapphire, flame-fusion
(GNI)Sp08:87-88
of zircon (LN)Sp08:73
see also Diamond treatment;
Treatment

**High-pressure, high-temperature [HPHT]
synthesis**, see Diamond, synthetic

**High-pressure, high-temperature [HPHT]
treatment**, see Diamond treatment

History

of color grading of D-to-Z diamonds
(King)W08:296-321
of diamond treatment
(Overton)Sp08:32-55
of the Koh-i-Noor diamond
(Sucher)Su08:124-141
of the Wittelsbach Blue diamond
(Dröschel)W08:348-363

HPHT (high pressure, high temperature),
see Diamond, synthetic; Diamond
treatment

I

Imitations, see specific gem materials
imitated

Inclusions

in aquamarine—(Adamo)F08:214-226;
kelp-like (LN)Sp08:66; from Pakistan
and Namibia (GNI)F08:275-276
in beryl, Maxixe-type and hydrothermal
synthetic blue (Adamo)F08:214-226
calcite "melt," in grossular
(LN)F08:259
in danburite (GNI)Su08:169-171
dendritic, in agate (GNI)F08:262-263
in emerald—from Colombia
(Ringsrud)F08:242-245; from Norway
(Rondeau)Su08:108-122
in forsterite (GNI)F08:263-266
in glass, devitrified (LN)Sp08:70-71
nail-head, in synthetic citrine
(GNI)W08:375-376
in quartz—covellite dendrites
(LN)W08:367; green fluid
(LN)Su08:161; rose, from Madagascar
(GNI)F08:276-277
in ruby—crystals inside crystals
(LN)Su08:161-162; from Tanzania
(Schwarz)W08:322-347
in sapphire—pinpoints *en echelon*
(GNI)Su08:180-181; from Tanzania

- (Schwarz)W08:322-347; trapiche pattern in yellow (LN)F08:259-260
in scapolite, diopside (GNI)F08:277
in spessartine from Tanzania (GNI)Sp08:76-78
in spodumene from Afghanistan (GNI)F08:277-279
in synthetic fire opal (Choudhary)F08:228-233
in synthetic ruby, Verneuil (GNI)F08:279-280
in synthetic sapphire—(LN)Sp08:72-73; heat-treated flame-fusion (GNI)Sp08:87-88
in tourmaline—Paraíba-type from Mozambique (Laur)Sp08:4-31; of tourmaline (GNI)F08:272-273
in vanadinite (GNI)Su08:184-185
in zircon, heat-treated (LN)Sp08:73
see also Diamond, inclusions in
- India**
dendritic agate from Madhya Pradesh (GNI)F08:262-263
orange beryl from (GNI)Su08:167
- Infrared spectroscopy**, see Spectroscopy, infrared
- Inner Mongolia**
andesine from Guyang (GNI)W08:369-373
- Instruments**
DiamondDock, Diamolite, DiamondLite (King)W08:296-321
see also Cathodoluminescence; DiamondView instrument; Spectrometry [various]; Spectroscopy [various]
- Iridescence**
as indication of coating on tanzanite (McClure)Su08:142-155
- Isotope analysis**
oxygen, of ruby and sapphire from Winza, Tanzania (Schwarz)W08:322-347
- J**
- Jade**, see Jadeite
- Jadeite**
at Myanma Gem Emporium 1992-2007 (GNI)Sp08:89-90
U.S.-Myanmar import restrictions on (GNI)F08:280-281
- “Jambolite”**
feldspar-quartz-muscovite rock colored by copper minerals (GNI)F08:266-267
- Jeremejevitte**
59.58 ct, from Madagascar (GNI)Sp08:74-75
- Johachidolite**
from Myanmar (Chadwick)F08:246-251
- K**
- Kenya**
sodic plagioclase from Kioo Hill (GNI)Sp08:83-85
- update on the John Saul ruby mine (GNI)F08:267-269
- Koh-i-Noor diamond**
modeling of, by laser and X-ray scanning (Sucher)Su08:124-141
- Kunzite**
from Pala District, California (GNI)W08:373-374
- L**
- LA-ICP-MS**, see Spectrometry, laser ablation-inductively coupled plasma-mass
- Laser drilling**
of diamond, history of (Overton)Sp08:32-55
- Laser scanning**
to model the Koh-i-Noor diamond (Sucher)Su08:124-141
- Lawsonite**
from California (GNI)Su08:171
- Liddicoat, Richard T.**
role in developing the GIA system for color grading D-to-Z diamonds (King)W08:296-321
- Lighting methods**
for color grading of D-to-Z diamonds (King)W08:296-321
- Luminescence**, see Fluorescence, ultraviolet [UV]; Phosphorescence
- M**
- Madagascar**
59.58 ct jeremejevitte from (GNI)Sp08:74-75
rose quartz from Ihosy (GNI)F08:276-277
scapolite from Amboasary (GNI)F08:277
- Manganaxinitte**
blue, represented as tanzanite (GNI)Sp08:81
- Marketing and distribution**
at Myanma Gem Emporium 1992-2007 (GNI)Sp08:89-90
- Master stones**
used to color grade D-to-Z diamonds (King)W08:296-321
- “Mexifire,”** see Opal, synthetic
- Mica**
green (paragonite), from Pakistan (GNI)Su08:172-173
- Microscopic techniques**, see Inclusions
- Mining and exploration**
for beryl and quartz in Pala District, California (GNI)Sp08:82-83
for emerald in Byrud, Norway (Rondeau)Su08:108-122
for ruby and sapphire in Winza, Tanzania (Schwarz)W08:322-347
for tourmaline in Mozambique (Laur)Sp08:4-31
update on the John Saul ruby mine, Kenya (GNI)F08:267-269
- see also specific countries and specific gem materials
- Mogok**, see Myanmar
- Mongolia**, see Inner Mongolia
- Most Valuable Article**, see *Gems & Gemology*
- Mozambique**
tourmaline—from Muva (GNI)F08:273-275; Paraíba-type, from Mavuco (Laur)Sp08:4-31
- Myanmar**
forsterite from Mogok, colorless (GNI)F08:263-265
gem market—Myanma Gem Emporium 1992-2007 (GNI)Sp08:89-90; in Taunggyi (GNI)Sp08:82
johachidolite from (Chadwick)F08:246-251
new gem localities in (GNI)Sp08:82
ruby from Nanyaseik (GNI)F08:269-271
U.S. import restrictions on gems from (GNI)F08:280-281
- N**
- Nigeria**
tourmaline from, with tourmaline inclusion (GNI)F08:272-273
- Nomenclature**
gota de aceite and Colombian emeralds (Ringsrud)F08:242-245
of “Paraíba” tourmaline (Laur)Sp08:4-31
- North Carolina**, see United States
- Norway**
emerald from Byrud (Rondeau)Su08:108-122
- O**
- Obituaries**
Brown, Grahame (GNI)Sp08:94
Switzer, George S. (GNI)Su08:190
- Oligoclase**, see Feldspar
- Olivine group**
variation in properties according to composition (GNI)F08:263-265
see also Forsterite, Peridot
- Opal**
with synthetic-like growth pattern (GNI)Su08:173-174
- Opal, synthetic**
fire, marketed as “Mexifire” (Choudhary)F08:228-233
- Oxygen isotope analysis**
of ruby and sapphire from Winza, Tanzania (Schwarz)W08:322-347
- P**
- Pakistan**
green mica from (GNI)Su08:172-173
- Pallasite**, see Peridot
- “Paraíba” tourmaline**, see Tourmaline

Pearl, cultured

Ballerina “chocolate pearls,” durability of color in (Du Toit)F08:234-241
beadless—mantle-grown, from *Pinctada maxima* (GNI)Su08:175-176; twinned (GNI)Su08:176-177
black, engraved and coated (GNI)Su08:174-175
bleached, non-“chocolate” (LN)Su08:159-160

Pearl, non-nacreous

clam, and shell (LN)Sp08:71-72
conch, multicolored (LN)Sp08:72
“elephant pearl” imitation (GNI)Sp08:86-87
“quahog” (GNI)W08:374-375

Peridot

cat’s-eye, from meteorite (pallasite) (GNI)Su08:177
see also Olivine group

Phosphorescence

red, of the Wittelsbach Blue diamond (Dröschel)W08:348-363
see also Luminescence

Photography

used in modeling of the Koh-i-Noor diamond (Sucher)Su08:124-141

Plagioclase, see Feldspar

Plastic

composite of coral and (LN)F08:253

Q

“Quahog” pearl, see Pearl, non-nacreous

Quartz

citrine with eye-visible Brazil-law twinning (LN)F08:252-253
covellite dendrites in (LN)W08:367
emerald inclusion in (LN)F08:258
green fluid inclusions in (LN)Su08:161
rose, with inclusions, from Madagascar (GNI)F08:276-277

Quartz, synthetic

citrine (GNI)W08:375-376
purple-blue (GNI)W08:377-379
sold as tourmaline (GNI)Su08:187-188

R

Raman spectroscopy, see Spectroscopy, Raman

Rock

feldspar-quartz-muscovite, colored by copper minerals (GNI)F08:266-257

Rose quartz, see Quartz

Ruby

glass-filled—broad variety available at the Tucson shows (GNI)Sp08:74-75; with voids (LN)Sp08:69-70
inclusions within inclusions in (LN)Su08:161-162
from the John Saul mine in Kenya (GNI)F08:267-269
from Myanmar—Nanyaseik (GNI)F08:269-271; new localities (GNI)Sp08:82; U.S. import restric-

tions on (GNI)F08:279-280
from Winza, Tanzania—at BaselWorld (GNI)Su08:177-178; mining and exploration for (GNI)Su08:178-179; mining, geology, and gemological characterization of (Schwarz)W08:322-347

Ruby, synthetic

Verneuil, with natural-appearing inclusions (GNI)F08:279-280

Russia

diamond, purple, from Siberia (Titkov)Sp08:56-64

S

Sapphire

color-change, with lead-glass filling (GNI)Sp08:88
color zoning in (GNI)F08:270-272
inclusions in, *en echelon* pinpoints (GNI)Su08:180-181
from Myanmar, new localities (GNI)Sp08:82
rare-earth elements in (LN)Su08:162-163
from Winza, Tanzania—mining and exploration for (GNI)Su08:178-179; mining, geology, and gemological characterization of (Schwarz)W08:322-347; zoned crystal from (GNI)F08:270-272
yellow, with trapiche pattern (LN)F08:259-260

Sapphire, synthetic

green, with blue inclusions (LN)Sp08:72-73
heat-treated flame fusion (GNI)Sp08:87-88

Scapolite

from Madagascar, with diopside inclusions (GNI)F08:277

Serpentine

archeological artifact resembling Libyan desert glass (GNI)Su08:181-182

Shell

“Neptunian” conch beads (GNI)W08:376-377

Shiple, Robert M.

role in developing the GIA system for color grading D-to-Z diamonds (King)W08:296-321

Sodalite group, see Afghanite, Haiyine

Spectrometry, laser ablation—inductively coupled plasma—mass [LA-ICP-MS]

of andesine from Tibet and Inner Mongolia (GNI)W08:371-373
of danburite from Tanzania (GNI)Su08:169-170
of emerald from Norway (Rondeau)Su08:108-122
of johachidolite (Chadwick)F08:246-251
of Paraíba-type tourmaline from Mozambique (Laurs)Sp08:4-30
of ruby from Winza, Tanzania (Schwarz)W08:322-347

of sapphire—with a high concentration of rare-earth elements (LN)Su08:162-163; from Winza, Tanzania (Schwarz)W08:322-347
of tanzanite, coated (McClure)Su08:142-147

Spectroscopy, energy-dispersive X-ray fluorescence [EDXRF]

of andesine from Tibet and Inner Mongolia (GNI)W08:371-373
of forsterite, colorless (GNI)F08:263-266
of induced copper-contaminated tourmaline (LN)W08:367-368
of johachidolite (Chadwick)F08:246-251
of lead glass-filled color-change sapphire (GNI)Sp08:88
of ruby and sapphire from Winza, Tanzania (Schwarz)W08:322-347
of synthetic fire opal (Choudhary)F08:228-233

Spectroscopy, infrared

of aquamarine, Maxixe-type beryl, and hydrothermal synthetic blue beryl (Adamo)F08:214-226
of diamond—black (LN)F08:254-255; purple, from Siberia (Titkov)Sp08:56-64; zoned brown-yellow type IIa/IIb (LN)W08:364-365
of emerald from Norway (Rondeau)Su08:108-122
of opal, synthetic and natural fire (Choudhary)F08:228-233
of ruby and sapphire from Winza, Tanzania (Schwarz)W08:322-347
of synthetic diamond (Kitawaki)F08:202-213

Spectroscopy, photoluminescence

of CVD synthetic diamond—(LN)Sp08:67-69; experimental (GNI)Su08:185-186; HPHT-treated (LN)W08:365-367
of diamond—purple, from Siberia (Titkov)Sp08:56-64; type IIa, with strong phosphorescence (GNI)Su08:164-165
of forsterite (GNI)F08:263-265

Spectroscopy, radiance

of light sources used for diamond grading (King)W08:296-321

Spectroscopy, Raman

of devitrified inclusions in glass (LN)Sp08:70-71
of diopside—in rose quartz (GNI)F08:276-277; in scapolite (GNI)F08:277
of feldspar-quartz-muscovite rock colored by copper minerals (GNI)F08:266-257
of fluorite, color-change (GNI)F08:263
of forsterite (GNI)F08:263-266
of grossular and epidote in rose quartz (GNI)F08:276-277
of johachidolite from Myanmar (Chadwick)F08:246-251
of lepidolite inclusions in tourmaline (Laurs)Sp08:4-31
of multiphase inclusions in emerald from Norway (Rondeau)Su08:108-122

of olivine in pinkish brown diamond (LN)F08:257-258
of “quahog” pearls (GNI)W08:374-375
of sodic plagioclase inclusions in tourmaline (Laurs)Sp08:4-31
of triploidite inclusions in aquamarine (LN)Sp08:66

Spectroscopy, UV-Vis-NIR

of aquamarine, Maxixe-type beryl, and hydrothermal synthetic blue beryl (Adamo)F08:214-226
of beryl, orange, from India (GNI)Su08:167
of chromium-rich clinocllore (kämmererite) from Turkey (GNI)Su08:168-169
of diamond—orange, treated (LN)Su08:156-157; purple, from Siberia (Titkov)Sp08:56-64; reddish orange type Ib (LN)F08:255-256
of emerald from Norway (Rondeau)Su08:108-122
of manganaxinite (GNI)Sp08:81
of mica from Pakistan with Cr and V (GNI)Su08:172-173
of plagioclase feldspar from Tanzania (GNI)Sp08:83-85
of ruby and sapphire from Winza, Tanzania (Schwarz)W08:322-347
of synthetic diamond, brown CVD, with boron (LN)Su08:158-159
of tourmaline, Paraíba-type, from Mozambique (Laurs)Sp08:4-31

Spectroscopy, X-ray photoelectron (XPS)

of coated and diffusion-treated topaz (Gabasch)Su08:148-154

Spessartine

from Tanzania (GNI)Sp08:76-78
see also Garnet

Sphene

76.27 ct (GNI)Sp08:74-75

Spinel

from Tanzania (GNI)Sp08:74-75

Spodumene

from Afghanistan (GNI)F08:277-279
see also Kunzite

Switzer, George S.

obituary (GNI)Su08:190

Synthetics

see specific gem materials

T

Tahitian cultured pearl, see Pearl, cultured

Tajikistan

colorless forsterite from the Pamir Mountains (GNI)F08:265-266

Tanzania

almandine-spessartine from (GNI)Su08:165-166
danburite, yellow, from the Morogoro area (GNI)Su08:169-171
oligoclase from (GNI)Sp08:83-85
ruby and sapphire from Winza—mining and exploration for (GNI)Su08:178-179; mining, geology, and gemological characterization of (Schwarz)W08:322-347; zoned crystal from (GNI)F08:270-272
spessartine from Loliondo (GNI)Sp08:76-78
spinel from Mahenge (GNI)Sp08:74-75

Tanzanite

coated (McClure)Su08:142-155

Tibet

andesine from the Xigazê area (GNI)W08:369-373

Topaz

coating and diffusion treatment of (Gabasch)Su08:148-154
faceting of (GNI)Sp08:85-86
star and cat's-eye, from Brazil (GNI)Su08:182-183

Tourmaline

crystal with inclusion of tourmaline, from Nigeria (GNI)F08:272-273
glass imitation of rubellite (GNI)Su08:186-187
from Mozambique—Muva (GNI)F08:273-275; Paraíba-type (Laurs)Sp08:4-31
from Myanmar, new localities (GNI)Sp08:82
and simulants from Afghanistan (GNI)Su08:187-188
treatment by copper contamination (LN)W08:367-368

Trapiche

aquamarine (GNI)F08:275-276
sapphire, yellow (LN)F08:259-260

Treatment

of diamond, history of (Overton)Sp08:32-55
durability of color in treated “chocolate pearls” (Du Toit)F08:234-241
of synthetic ruby (GNI)F08:279-280
of tanzanite, coating (McClure)Su08:142-155
of topaz, coating and diffusion

(Gabasch)Su08:148-154

of tourmaline, Paraíba-type, from Mozambique (Laurs)Sp08:4-31
see also Bleaching; Coating; Diamond treatment; Diffusion treatment; Dyeing; Heat treatment; specific gem materials

Tucson Gem and Mineral shows

highlights of (GNI)Sp08:74-78

Turkey

Cr-rich clinocllore from (GNI)Su08:168-169

Turquoise

Persian, from Iran (GNI)Su08:183-184

Twinning, Brazil-law

eye-visible, in citrine (LN)Fa08:252-253

U

Ultraviolet, see Fluorescence

United States

emerald from North Carolina (GNI)Sp08:75-76
lawsonite from Marin County, California (GNI)Su08:171
Pala District, California—beryl and quartz from the Oceanview mine (GNI)Sp08:82-83; kunzite from the Elizabeth R mine (GNI)W08:373-374

V

Vanadinite

faceted yellow (GNI)Su08:184-185

W

Wittelsbach Blue diamond

history and characteristics of (Dröschel)W08:348-363

X

X-ray scanning

to model the Koh-i-Noor diamond (Sucher)Su08:124-141

Z

Zircon

heat-treated (LN)Sp08:73

Zoning, see Color zoning; specific gem materials

AUTHOR INDEX

This index lists, in alphabetical order, the authors of all feature articles, Notes & New Techniques, and Rapid Communications that appeared in the four issues of Volume 44 of *Gems & Gemology*, together with the full title and inclusive page numbers of each article and the issue (in parentheses). Full citation is given under the first author only, with reference made from coauthors.

A

- Abduriyim A., see Kitawaki H.
Adamo I., Pavese A., Prospero L., Diella V., Ajò D., Gatta G.D., Smith C.P.: Aquamarine, Maxixe-type beryl, and hydrothermal synthetic blue beryl: Analysis and identification, 214–226 (Fall)
Ajò D., see Adamo I.

B

- Beaton D., see Laurs B.M.
Befi R., see Laurs B.M.
Bertel E., see Gabasch H.
Bhandari R., see Choudhary G.
Breeding C.M., see Chadwick K.M., Du Toit G., Laurs B.M., Titkov S.V.

C

- Carriere D.P., see Sucher S.D.
Chadwick K.M., Breeding C.M.: Color variations and properties of johachidolite from Myanmar, 246–251 (Fall)
Choudhary G., Bhandari R.: A new type of synthetic fire opal: Mexifire, 228–233 (Fall)

D

- Diella V., see Adamo I.
Dröschel R., Evers J., Ottomeyer H.: The Wittelsbach Blue, 348–363 (Winter)
Du Toit G., Shen A.H., Breeding C.M.: The color durability of “Chocolate Pearls” by Ballerina Pearl Co., 234–241 (Fall)
Du Toit G., see also Schwarz D.

E

- Erel E., see Schwarz D.
Evers J., see Dröschel R.

F

- Fallick A.E., see Schwarz D.
Falster A.U., see Laurs B.M.
Fritsch E., see Rondeau B.

G

- Gabasch H., Klauser F., Bertel E., Rauch T.: Coloring of topaz by coating and diffusion processes: An X-ray photoemission

study of what happens beneath the surface, 148–154 (Summer)

- Gatta G.D., see Adamo I.
Geurts R.H., see King J.M.
Gilbertson A.M., see King J.M.
Giuliani G., see Schwarz D.
Groat L., see Rondeau B.

H

- Hauzenberger C., see Schwarz D.

K

- Keller A.S.: “Challenges, Changes, and New Directions,” 295 (Winter)
A new gemological challenge: Synthetic diamond melee, 201 (Fall)
Ten reasons why *you* should attend the 2009 GRC, 107 (Summer)
King J.M., Geurts R.H., Gilbertson A.M., Shigley J.E.: Color grading “D-To-Z” diamonds at the GIA Laboratory, 296–321 (Winter)
Kitawaki H., Abduriyim A., Okano M.: Identification of melee-size synthetic yellow diamonds in jewelry, 202–213 (Fall)
Klauser F., see Gabasch H.
Klemm L., see Schwarz D.

L

- Laurs B.M., Zwaan J.C. (Hanco), Breeding C.M., Simmons W.B. (Skip), Beaton D., Rijdsdijk K.F., Befi R., Falster A.U.: Copper-bearing (Paraiba-type) tourmaline from Mozambique, 4–30 (Spring)
Laurs B.M., see also Schwarz D.

M

- Malsy A.-K., see Schwarz D.
McClure S.F., Shen A.H.: Coated tanzanite, 142–147 (Summer)
Mineeva R.M., see Titkov S.V.

N

- Nordrum F.S., see Rondeau B.

O

- Ohnenstetter D., see Schwarz D.
Okano M., see Kitawaki H.

- Ottomeyer H., see Dröschel R.
Overton T.W., Shigley J.E.: A history of diamond treatments, 32–55 (Spring)

P

- Pardieu V., see Schwarz D.
Pavese A., see Adamo I.
Peucat J.-J., see Rondeau B.
Prospero L., see Adamo I.

R

- Rauch T., see Gabasch H.
Rijdsdijk K.F., see Laurs B.M.
Ringsrud R.: *Gota de aceite*: Nomenclature for the finest Colombian emeralds, 242–245 (Fall)
Rondeau B., Fritsch E., Peucat J.-J., Nordrum F.S., Groat L.: Characterization of emeralds from a historical deposit: Byrud (Eidsvoll), Norway, 108–122 (Summer)

S

- Saul J.M., see Schwarz D.
Schmetzer K., see Schwarz D.
Schwarz D., Pardieu V., Saul J.M., Schmetzer K., Laurs B.M., Giuliani G., Klemm L., Malsy A.-K., Erel E., Hauzenberger C., Du Toit G., Fallick A.E., Ohnenstetter D.: Rubies and sapphires from Winza, central Tanzania, 322–347 (Winter)
Sergeev A.M., see Titkov S.V.
Shen A.H., see Du Toit G., McClure S.F.
Shigley J.E., see King J.M., Overton T.W., Titkov S.V.
Simmons W.B. (Skip), see Laurs B.M.
Smith C.P., see Adamo I.
Sucher S.D., Carriere D.P.: The use of laser and X-ray scanning to create a model of the historic Koh-i-Noor diamond, 124–141 (Summer)

T

- Titkov S.V., Shigley J.E., Breeding C.M., Mineeva R.M., Zudin N.G., Sergeev A.M.: Natural-color purple diamonds from Siberia, 56–64 (Spring)

Z

- Zudin N.G., see Titkov S.V.
Zwaan J.C. (Hanco), see Laurs B.M.